UNIVERSITY OF CALIFORNIA, SAN DIEGO

The intersection of degradation, replication, and DNA repair in virus-host interactions

A dissertation submitted in partial satisfaction of the

requirements for the degree Doctor of Philosophy

in

Biology

by

Rachel Anna Schwartz

Committee in charge:

Professor Matthew D. Weitzman, Chair
Professor Randolf Hampton
Professor Richard Kolodner
Professor Lorraine Pillus
Professor Deborah Spector

2008

The dissertation of Rachel Anna Schwartz is approved, and it is acceptable in quality and form for publication on microfilm:

Chair

University of California, San Diego

2008

DEDICATION

I dedicate this work to three incredibly important people in my life. First, this thesis is for my parents--you always made me believe I could achieve whatever I wanted in life. Because of you, I never doubted myself. This work is also dedicated to Sergio Duron. You are my pillar, my center of gravity, my home.

TABLE OF CONTENTS

LIST OF FIGURES

Chapter 1

Chapter 2

Chapter 6

Appendix

LIST OF TABLES

Chapter 3

Chapter 4

ACKNOWLEDGEMENTS

I thank Matthew Weitzman for the opportunity to work in the lab and patience over the years, and all the past and present members of the Weitzman lab for their friendship, guidance, and support during my scientific training. I especially thank Christian and Caroline for all of their mentoring.

I am extremely grateful to co-authors and co-workers Christian Carson, Travis Stracker, Darwin Lee, Caroline Lilley, Geoffrey Cassell, Sarah Adam, Alejandro Palacios, Mauro Giacca, Seema Lakdawala, Matthew Russell, Chrissy Schuberth, and Heather Eshleman for their contributions to the papers and projects documented in this dissertation. I am also grateful to Mauro Giacca and Alejandro Palacios for collaborating on the AAV-MRN project.

Figure 7C in Chapter 1 is reprinted from material as it appears in Nature 2002. Stracker TH, Carson CT, Weitzman MD, Adenovirus oncoproteins inactivate the Mre11-Rad50-NBS1 DNA repair complex, 418:348-352. This material is from the dissertation author's lab and is used solely for background information.

Some data in Chapter 2 is a reprint of the material as it appears in EMBO J. 2003. Carson CT, Schwartz RA, Stracker TH, Lilley CE, Lee DV, Weitzman MD, The Mre11 complex is required for ATM activation and the G2/M checkpoint, 22:6610-20. The dissertation author was a researcher and an author of this paper.

Chapter 3, in full, has been submitted for publication for material as it may appear in J Virol. 2008, Schwartz RA, Lakdawala SS, Eshleman HD, Russell MR, Carson CT, and Weitzman MD, Distinct requirements of the adenovirus E1b55K protein for degradation of cellular substrates. The dissertation author was the primary researcher and author of this paper.

Some of the data in Chapter 7 is a reprint of the material as it appears in J Virol. 2007. Schwartz RA, Palacios, JA, Adam, SA, Cassell, GC, Giacca, M, Weitzman MD, The Mre11/Rad50/Nbs1 complex limits adeno-associated virus transduction and replication, 81(23):12936-12945. The dissertation author was the primary researcher and author of this paper.

I am grateful to the UCSD CMG Training Grant and the ARCS Foundation for their financial support during my graduate training.

I thank the members of my graduate committee: Matthew Weitzman, Susan Forsberg, Randy Hampton, Richard Kolodner, Lorraine Pillus and Debbie Spector for their guidance and scientific discussions over the years.

I am also grateful to the Hunter Lab, the Verma Lab, the Lundblad Lab, Zhongsheng You, Matt Penfield, Cindy Doane, Jamie Simon, and Liz Grabowski for their advice, expertise, and reagents.

I thank all the friends I have made here in San Diego and the ones transplanted from Illinois for wonderful memories over the years.

VITA

2008	Ph.D., University of California, San Diego
2001-2008	Teaching Assistant/Graduate Student Researcher Division of Biology, University of California, San Diego
1999-2001	Research Specialist, W.M. Keck Center for Comparative and Functional Genomics, University of Illinois, Urbana-Champaign
1999	B.Sc*. magna cum laude,* Department of Cell and Structural Biology, University of Illinois, Urbana-Champaign
1998-1999	Undergraduate Researcher, Department of Cell and Structural Biology, University of Illinois, Urbana-Champaign
1996-1997	Howard Hughes Undergraduate Research Felllow, Department of Veterinary Immunology, University of Illinois, Urbana-Champaign

PUBLICATIONS

Schwartz RA, Lakdawala SS, Eshleman HD, Russell MR, Carson CT, Weitzman MD. Distinct requirements of the adenovirus E1b55K protein for degradation of cellular substrates. Journal of Virology. 2008 Submitted.

Lakdawala SS, Schwartz RA, Ferenchak K, Carson CT, McSharry BP, Wilkinson GW, Weitzman MD. Differential requirements of the C-terminus of Nbs1 in suppressing adenovirus DNA replication and promoting concatemer formation. Journal of Virology. 2008 Submitted.

Cervelli T, Palacios JA, Zentilin L, Mano M, Schwartz RA, Weitzman MD, Giacca M. Processing of recombinant AAV genomes occurs in specific nuclear structures that overlap with foci of DNA damage response proteins. Journal of Cell Science. 2008 121(Pt3):349-57.

Schwartz RA, Palacios JA, Adam SA, Cassell GC, Giacca M, Weitzman MD. The Mre11/Rad50/Nbs1 complex limits adeno-associated virus transduction and replication. Journal of Virology. 2007 81(23):12936-12945.

Lilley CE, Schwartz RA, Weitzman MD. Using or abusing: viruses and the cellular DNA damage response. Trends in Microbiology. 2007 15(3):119-126.

Weitzman MD, Carson CT, Schwartz RA, Lilley CE. Interactions of viruses with the cellular DNA repair machinery. DNA Repair. 2004 3(8-9):1165-73.

Sanchez V, McElroy AK, Yen J, Tamrakar S, Clark CL, Schwartz RA, Spector DH. Cyclin-dependent kinase activity is required at early times for accurate processing and accumulation of the human cytomegalovirus UL122-123 and UL37 immediate-early transcripts and at later times for virus production. Journal of Virology. 2004 78(20):11219-11232.

Carson CT, Schwartz RA, Stracker TH, Lilley CE, Lee DV, Weitzman MD. The Mre11 complex is required for ATM activation and the G2/M checkpoint. EMBO J. 2003 22(24):6610-20.

Zuckermann FA, Husmann RJ, Schwartz R, Brandt J, Mateu de Antonio E, Martin S. Interleukin-12 enhances the virus-specific interferon gamma response of pigs to an inactivated pseudorabies virus vaccine. Vet Immuno. Immunopathol. 1998 63(1-2):57-67.

ABSTRACT OF THE DISSERTATION

The intersection of degradation, replication, and DNA repair in virus-host interactions

By

Rachel Anna Schwartz

Doctor of Philosophy in Biology

University of California, San Diego 2008

Matthew D. Weitzman, Chair

Viruses are highly evolved entities that target key cellular pathways in order to promote their own reproduction. However, host cells encode a number of defenses that obstruct productive infection, and viruses must either employ these to their advantage or disable them. A growing body of research is indicating that viruses must contend with cellular DNA damage response pathways that can affect virus replication. Adenovirus (Ad) is a DNA virus encoding proteins that defend against host DNA repair functions. Infection of cells with an E4 deleted Ad induces a cellular DNA damage response mediated by ATM and ATR, and mutant viral genome concatemerization. The

adenoviral E1b55K/E4orf6 complex prevents these activities, and degrades a number of cellular factors, including p53, the Mre11 complex (MRN), and DNA Ligase IV. We examined the mechanism of E1b55K/E4orf6 mediated degradation of substrates and found that these events were separable. Intriguingly, analysis of cellular factors involved in down-regulation of targets suggested that E1b55K/E4orf6 might assemble distinct ubiquitin ligases. We also defined some of the viral requirements for degradation, and described a set of E1b55K mutants that can distinguish between substrates. Using these E1b55K separation-of-function mutants, we examined the consequences of substrate degradation on cellular responses. Through these experiments, we found that MRN is critical to mounting a DNA damage response to mutant Ad infection and exogenous DNA damage. While down-regulation of MRN can prevent mutant viral genome concatemerization, DNA Ligase IV degradation can also compensate. These E1b55K/E4orf6 activities had additional consequences for the small DNA virus, adeno-associated virus (AAV). Adenoviral proteins, including E1b55K/E4orf6, provide helper functions for AAV production. We found that MRN is a barrier to AAV replication, and its degradation is a critical helper activity of E1b55K/E4orf6. Interestingly, AAV and Ad co-infection induces a DNA damage response independent of MRN, which is degraded by Ad. Unlike an E4-deleted Ad infection, which triggers ATM and ATR, our data shows that a subset of signaling events during Ad and AAV co-infection are dependent on DNA-PK. Our experiments also indicate

that DNA-PK has a role in AAV transduction and replication, and that this PIKK might be influenced by MRN. The work presented in this dissertation elucidates functions of the adenoviral E1b55K and E4orf6 proteins in both the adenovirus and AAV lifecycles. Our results also demonstrate how these viral proteins affect the cellular machinery for protein degradation and DNA repair. Our data prove that adenovirus and AAV provide powerful model systems to gain insight into these cellular pathways.

Chapter 1. Introduction

Viruses as model systems to study the cellular DNA damage response

A growing body of literature suggests that viruses interact with cellular DNA repair factors during the course of establishing productive infections (203, 322, 365). Viral nucleic acid is produced in abundance during replication, and may form aberrant structures not usually seen during host cell reproduction. Viral DNA may therefore be recognized by host DNA damage response factors, and trigger signaling cascades and repair functions. Among the viruses that have now been shown to elicit DNA damage signaling cascades are herpes simplex virus-1 (HSV-1) (202, 372) and HSV-2 (319), human cytomegalovirus (HCMV) (219), Epstein-Barr virus (EBV) (185), polyomavirus (79), simian virus 40 (SV40) (261, 317), and human immunodeficiency virus-1 (HIV-1) (189, 194, 291). This cellular reaction could conceivably interfere with viral replication, so the virus must counter with some type of defense. Viruses which employ proteins that bind or mislocalize potentially detrimental cellular factors include adenovirus (51, 98, 335, 392), HSV-1 (371), JC virus (81), and many others (203). A large number of viruses also encode strategies to induce specific destruction of cellular factors by harnessing the ubiquitin/proteasome system (203, 272), including adenovirus (8, 365), HSV-1 (114, 266), Kaposi's sarcoma herpes virus (KSHV) (46), human papilloma virus-16 (HPV-16) (16, 32, 167, 305), HIV-1 (208, 397), and

SV40 (406). On the other hand, viruses may utilize the cellular DNA damage response machinery to benefit the viral lifecycle. HSV-1, polyomavirus, and SV40 appear to require damage signaling for replication (79, 202, 317), while retroviruses need repair proteins for integration (80, 193). An increasing amount of research in this field is suggesting that many viruses harbor strategies to defend against *and* utilize host DNA repair components (203). Since viruses are highly evolved, they tend to target key cellular pathways to promote their lifecycles. Therefore, they provide useful tools to study the cellular DNA damage response machinery.

The cellular response to DNA damage

Cells encode a vast network of molecules designed to detect and repair all kinds of DNA damage. While experimental systems utilize exogenous sources such as gamma or UV irradiation, or chemical clastogens to induce DNA damage, lesions can also be induced during normal cellular homeostasis. Reactive oxygen intermediates may cause base damage to DNA, thus stalling replication forks. DNA single-strand or double-strand breaks (DSBs) may also be purposely introduced by the activity of topoisomerases during replication, Spo11 and DNA repair enzymes during meiotic recombination (287), or the Rag proteins during VDJ recombination (201). DSBs are particularly dangerous because both DNA strands are

compromised, and genomic instability can arise from the inability to fix these lesions. However, numerous cellular mechanisms act to ensure the fidelity of repair. During a generalized response to DNA double-strand break (DSB) (see Figure 1), the lesion and local chromatin changes are detected by sensors, which act with transducers to rapidly initiate a signaling cascade that is amplified by the activation of effectors. The effectors coordinate numerous events within the cell to promote DNA repair by either non-homologous end-joining (NHEJ) or homologous recombination (HR).

Activation of effectors is particularly important to initiating checkpoints that halt cellular progression through the cell cycle to allow time for repair before division. DNA damage induces three major checkpoints in mammalian cells: the G1/S transition, the intra-S phase checkpoint, and the G2/M transition (47, 297). The G1/S transition inhibits S phase entry by restricting origin firing when cells are damaged in G1. The intra-S phase checkpoint also down-regulates origin activity when DSBs or replication fork stresses occur in S phase, the latter is sometimes referred to as the replication checkpoint (13). G2/M checkpoint prevents cells from entering mitosis with DNA damage incurred in G2 or other cell cycle phases (see Chapter 2 for further discussion). In addition to these checkpoints, extensive damage may also cause prolonged cell cycle arrests, senescence, or apoptosis (175). However, escape from these checkpoints could allow the accumulation of

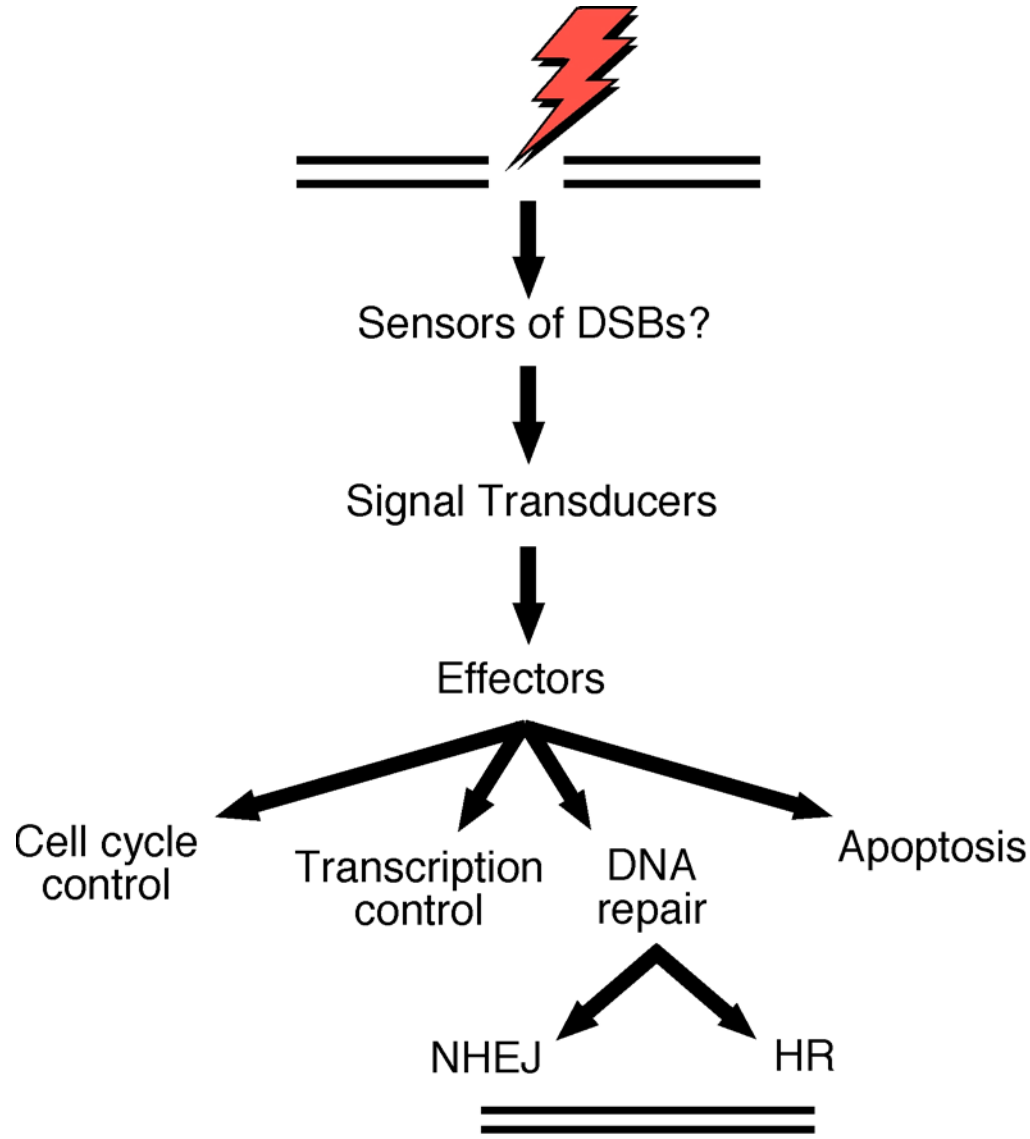

Figure 1. Overview of the cellular response to DNA damage. After a lesion is incurred, sensors stimulate transducers to activate a signaling cascade that is amplified by the activation of effectors. Effectors are responsible for activating cell cycle checkpoints that allow time for repair, and coordinating other cellular activities to promote DNA repair by homologous recombination (HR) or non-homologous end-joining (NHEJ).

heritable mutations that promote transformation. Supporting this, humans and mice lacking certain transducers and effectors have high incidences of cancer (175), and oncogene-induced aberrant cell division promotes accumulation of DNA damage that can lead to transformation (143). These observations underscore the importance of the damage response in coordinating checkpoints to promote repair.

At the center of the damage response are two PI3-kinase related kinases (PIKKs), ATM and ATR, with kinase activity directed towards proteins rather than lipids (2). ATM is central to transducing the damage response to DNA DSBs (1, 10), although chromatin perturbations in the absence of DSBs also activate ATM (9, 172). Insights into ATM activities in human cells have come from patients with ataxia-telangiectasia (A-T), and have demonstrated the importance of ATM in the response to DSBs and maintenance of genome stability. Among the phenotypes A-T patients exhibit, immunodeficiencies, radiation sensitivity, and predisposition to cancer are just a few that indicate a defective response to DSBs (68). A-T cells lack detectable levels of ATM protein, and display sensitivity to irradiation (IR), defects in G1, intra-S, and G2/M cell cycle checkpoints, and substrate phosphorylation (10).

ATR responds to replication fork stresses and lesions that contain single-stranded DNA (ssDNA) (1, 10, 411). In contrast to ATM, ATR is essential and null mutants are embryonic lethal (38, 83). However, functions of

ATR have been studied in human cell lines expressing kinase-dead ATR (254), cells derived from patients with Seckel syndrome (259), which have a splicing defect in ATR mRNA that reduces protein levels, and cells with conditional disruption of ATR (39, 74). These and other systems indicate the importance of ATR to normal DNA replication, and S phase and G2/M checkpoints. Without ATR, cells accumulate damage in S phase that likely contributes to lethal genomic instability (311).

ATM and ATR phosphorylate a variety of protein effectors to transduce the damage signal, activate cell cycle checkpoints, and coordinate DNA repair. The PIKKs show a preference for SQ/TQ motifs (178), and a recent proteomics screen examining the damage dependent phosphorylation of these protein motifs indicated that ATM and ATR may have over 700 substrates (231). Although common targets include Nbs1, BRCA, Chk1, Chk2, RPA32, SMC1, p53, and the histone H2A variant, H2AX, phosphorylation by either ATM or ATR is often stimulus specific (85), as indicated by studies using the mutant cell lines described above or those employing siRNA. Intriguingly, recent reports are suggesting that ATM and ATR activate one another in mammalian cells, and do not simply exist in parallel pathways. For example, ATR activation occurs in S or G2 phase cells in response to DSBs, and requires ATM and DNA processing (3, 164, 242). Another study suggests that ATR mediates ATM activation in response to UV and HU (334). Cross-talk

may ensure proper activation of checkpoints and DNA repair pathways, depending on the cell cycle phase and the presence of suitable repair templates.

Research efforts have elucidated many early steps in the DNA damage response and activation of ATM and ATR (Figure 2). In human cells, activation of ATM after damage involves intermolecular autophosphorylation of dimers to release active ATM monomers that can phosphorylate substrates (9, 19). Three autophosphorylation sites have now been identified on serines 367, 1893, and 1981 (9, 19, 183), and are important to promoting genome stability and triggering cell cycle checkpoints in human cells (183). In mouse models and in vitro, however, autophosphorylation of serine 1981 is dispensable for ATM activity (196, 269). Full activation of ATM occurs on DNA flanking sites of damage (9, 395, 396), and a number of events amplify and transduce the damage signal (Figure 2). DSBs occur in the context of chromatin, and the rapid phosphorylation of H2AX (γH2AX) by ATM is required for reinforcement of the damage signal rather than its initial recognition (53). γH2AX promotes recruitment of mediator proteins, such as MDC1, that engage adaptor proteins like Nbs1, 53BP1, and BRCA1 at the site of damage (15, 216, 331). MDC1, 53BP1, and BRCA1 are also required for the phosphorylation of some effectors after DNA damage (92, 124, 214, 356).

Figure 2. Simplified models of DNA damage response pathways mediated by ATM and ATR. (A) Simplified schematic of an ATM induced damage response after a DNA double-strand break (DSB). A DSB occurring in chromatin (nucleosomes represented by blue squares) induces MRN and ATM localization to the site of damage where MRN facilitates ATM autophosphorylation, monomerization, and activation (see text for further details). Ku proteins (see Figure 4) may also localize at a break early with MRN and ATM. ATM phosphorylates histone variant, H2AX, and this stimulates the recruitment of mediator MDC1, which is also phosphorylated. MDC1 reinforces ATM and MRN at the lesion, and facilitates recruitment and phosphorylation of other substrates such as BRCA1, 53BP1, Chk2, and Nbs1. Chromatin remodeling around the lesion also occurs in addition to spreading of the H2AX signal megabase distances either side of the break. DSBs in S or G2 phase cells are also processed to produce ssDNA that activates ATR. ATM activation can occur in response to UV and HU in a manner that requires ATR. **(B)** Simplified schematic of ATR activation after damage at a replication fork. If DNA damage at fork stalls replication, the MCM complex unwinds DNA ahead of the fork, producing ssDNA/dsDNA junctions and long regions of ssDNA coated by RPA (peach circles). RPA-coated ssDNA recruits the ATR-ATRIP complex and promotes 9-1-1 loading at the ssDNA/dsDNA junction by Rad17. These protein complexes may stimulate ATR/ATRIP activity and their phosphorylation of 9-1-1 and Rad17. RPA is also phosphorylated. TopBP1 and Claspin are recruited and phosphorylated by ATR/ATRIP, and these interactions are required for the kinase activity of ATR directed towards Chk1. The Tipin/Timeless complex may also be required for ATR signaling events. Although chromatin is not depicted here, ATR can phosphorylate H2AX. MRN localizes to replication forks through multiple interactions, playing roles in fork stability and checkpoint induction. Damage at the fork also triggers post-translational modifications of RFC and PCNA, and phosphorylation of the MCM complex. A DSB at a replication fork may also elicit ATM activation as depicted in (A) (dashed arrow).

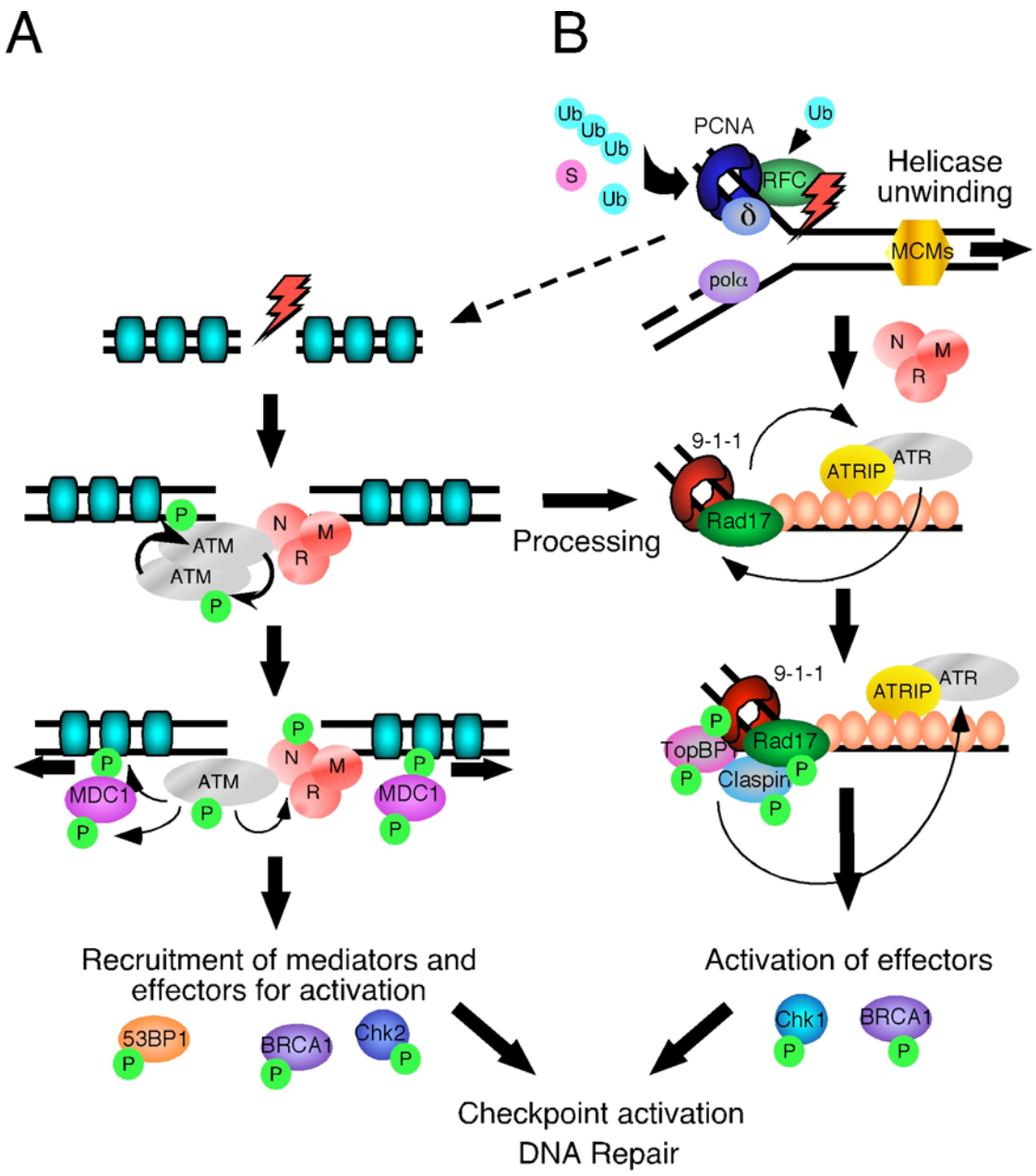
A
B
Ub
Ub
Ub
S
Ub
PCNA
Ub
RFC
δ
Helicase
unwinding
MCMs
polα
N
M
R
9-1-1
ATRIP
ATR
Rad17
P
ATM
ATM
N
M
R
P
Processing
9-1-1
ATRIP
ATR
P
TopBP1
Rad17
P
P
Claspin
P
P
MDC1
P
ATM
P
N
M
R
P
MDC1
P
Recruitment of mediators and
effectors for activation
Activation of effectors
53BP1
P
BRCA1
P
Chk2
P
Chk1
P
BRCA1
P
Checkpoint activation
DNA Repair

Replication fork stress and DNA intermediates with ssDNA activate ATR. Unlike ATM, ATR does not appear to be dimerized in cells, but rather, constitutively associated with ATRIP (74) through a common PIKK recruitment domain found in Nbs1, ATRIP, and Ku80 (116, 396). Interestingly, substrates with ssDNA/dsDNA junctions and long stretches of ssDNA have emerged as potent ATR activators (reviewed in (411)). RPA coats ssDNA produced after stalling of replication forks or DNA processing (118), and serves to independently recruit ATR-ATRIP, the Rad17 complex, and the Rad9/Rad1/Hus1 (9-1-1) complex (108, 224, 412) (Figure 2). Full activation of ATR and phosphorylation of effectors like Chk1 requires Rad17 and 9-1-1, in addition to mediators Claspin and TopBP1 (149, 186-188) and the Tipin/Timeless complex (65, 394). Similar to ATM signaling, a subset of ATR phosphorylation events also requires the adaptor, BRCA1 (124).

The Mre11 complex (MRN), composed of Mre11, Rad50, and Nbs1 (Xrs2 in yeast), is a conserved complex that is also critical to DNA damage sensing, signaling, and repair (78, 338). Like ATR, MRN is essential in mammalian systems (217, 384, 409). However, functions of the complex have been studied using a variety of systems, including cells from patients with the rare disorders Nijmegen breakage syndrome (NBS) and Ataxia-telangiectasia like disorder (A-TLD) (49, 330). These patients have hypomorphic mutations in the genes encoding Nbs1 and Mre11, respectively, and exhibit phenotypes

similar to A-T (90, 344). Cells from these patients show genetic instability, sensitivity to irradiation, and some checkpoint defects, though not as profound as A-T cells, likely due to their hypomorphic nature (49, 330).

Mre11, Rad50 and Nbs1 have a number of domains crucial to their functions (see Figure 3 for details). Together, the complex forms a molecular bridge that can tether DNA ends together through the Rad50 zinc hook (155) (see Figure 3B) in order to promote repair (212, 318, 374). The recently described Rad50 adenylate kinase activity was also found to be critical for tethering and repair (22). Additionally, MRN exhibits DNA unwinding, 3' to 5' exonuclease, and endonuclease activities in vitro on a variety of DNA substrates (78). The Mre11 endonuclease activity is required for the cleavage of hairpins (213) and Spo11 protein-bound DNA at meiotic DSBs in yeast (239). Although MRN is also required for processing DSBs (162, 211, 243), it is unclear whether the nuclease activity is actually required for this (34, 164, 239, 351). Recently, MRN was reported to associate with CtIP (Ctp1 or Sae1 in *S. pombe* or *S. cerevisiae*, respectively) to promote resection of DSBs and HR in S and G2 phase (205, 303), but how these proteins coordinate their nuclease activities (213, 232, 277) in mammalian cells remains to be determined.

In addition to its biochemical activities, MRN is crucial to DNA damage signaling through ATM and ATR. In work our lab contributed to (discussed in

Figure 3. The Mre11 complex. (A) Schematics of important domains in Mre11, Rad50, and Nbs1. The N-terminus of Mre11 has four conserved phosphoesterase motifs (N1-N4) and exhibits 3'-5' exonuclease and endonuclease activity against a variety of DNA substrates. Mre11 also has two DNA binding domains and a glycine-arginine rich methylation domain (GAR domain). Indicated in red are the two mutations found in A-TLD3 (N117S) and A-TLD1 (R633 stop) cells, respectively. Mre11 binds both Nbs1 and Rad50. Nbs1 has an N-terminal FHA domain and BRCT domain, followed by another putative BRCT domain. These domains are critical for phospho-protein interactions, and may reinforce Nbs1 interaction at sites of damage through γH2AX association. Two phosphorylation sites (Ser278 and Ser343) on Nbs1 are required for intra-S phase checkpoints. The Mre11 binding domain and ATM recruitement domain are located at the C-terminus. In red is the most common mutant allele found in NBS cells, which results in the expression of a truncated protein ending at aa 218. Lymphoblasts from NBS patients with this allele produce a trunctated p70 protein beginning from an internal translation site just down-stream of aa 218. Rad50 is similar to structural maintenance of chromosomes (SMC) proteins. It has Walker A and B motifs at either end of the protein, and coiled-coil domains that interact to juxtapose the A and B motifs, forming a functional ATPase. Two cysteine residues reside in the hinge region and coordinate a zinc molecule with two cysteines from another Rad50 molecule to form a zinc hook. These interactions facilitate DNA tethering (see B). **(B)** Model depicting DNA tethering by the Rad50/Mre11 complex. Dimers of Rad50 (green) and Mre11 (blue) bridge broken ends of DNA. The hinge regions of Rad50 form a zinc hook domain whose cysteines coordinate zinc (pink circle) to promote inter-molecular association. Walker A and B motifs in Rad50 are represented by green globular domains "A" and "B". Mre11 interacts with Rad50 near the area between the ATPase domain and the coiled-coil region. Nbs1 is omitted for simplicity.

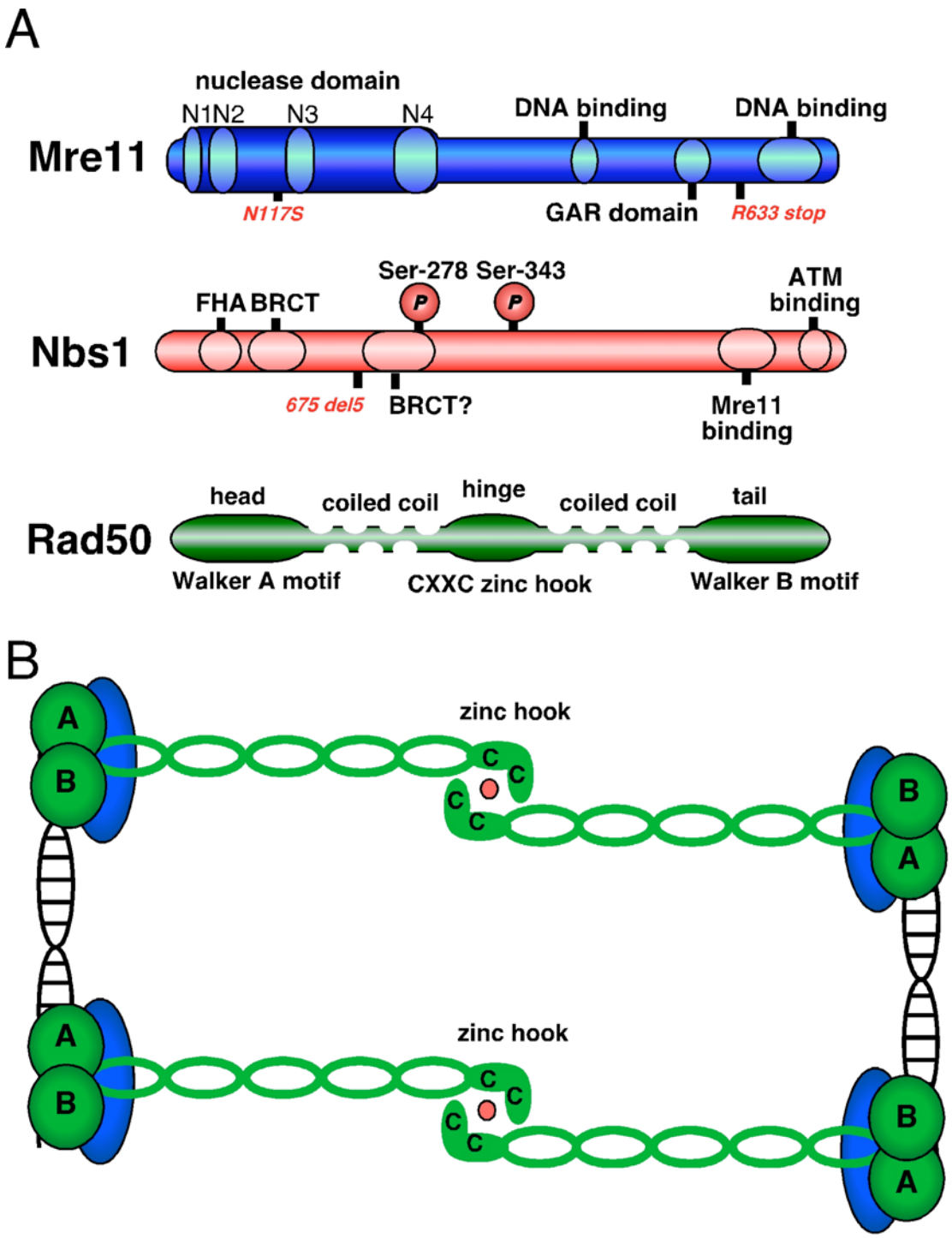
A
nuclease domain
N1N2
N3
N4
DNA binding
DNA binding
Mre11
N117S
GAR domain
R633 stop
Ser-278
Ser-343
ATM
binding
FHA
BRCT
P
P
Nbs1
675 del5
BRCT?
Mre11
binding
head
coiled coil
hinge
coiled coil
tail
Rad50
Walker A motif
CXXC zinc hook
Walker B motif
B
zinc hook
A
B
C
C
C
C
B
A
zinc hook
A
B
C
C
C
C
B
A

Chapter 2), MRN was shown to be required for ATM activation after DSB induction (50, 197, 351)(also reviewed in (195)). In vitro studies have shown that MRN makes multiple contacts with ATM, stimulating its autophosphorylation and monomerization, ATM substrate interaction, and kinase activity (196, 197). Full ATM activation requires all three MRN members, and the DNA unwinding and tethering activities of MRN (75, 196). More recent studies have shown that the C-terminus of Nbs1 contains a conserved PIKK interacting motif found in Ku80 (see below) and ATRIP (116, 396). While this domain is required for ATM activation and its presence at sites of damage in multiple systems (55, 116, 244, 396), it appears less important in mouse models (88, 337). ATR induction after DSBs requires ATM activity and MRN/CtIP dependent DNA processing to produce ssDNA in S and G2 cells for HR (3, 164, 205, 242, 243, 303). MRN is also necessary for ATR activity in response to low doses of other types of damage, like UV and hydroxyurea (164, 242, 262, 333, 408).

Since MRN mediates early activation of ATM and ATR in response to DSBs, MRN has been suggested to play a role in DNA damage sensing (271). This finding is supported by the rapid relocalization of MRN to sites of DNA damage (14, 164, 227, 235), and its presence at cellular replication forks (226, 236). Although MRN may be a putative sensor, the complex is also a target of both ATM and ATR. Nbs1 is phosphorylated by both kinases, and serines 278

and 343 are required to activate the intra-S phase checkpoint (117, 204, 262, 380, 405). Mre11 and Rad50 are also phosphorylation targets (76, 231), but the physiological relevance of their modification remains to be determined.

Within mammalian cells, two main DNA repair pathways are utilized in response to DSBs: NHEJ or HR. Interestingly, cell cycle factors and the lesions themselves appear to regulate DNA processing and repair choice (11, 33, 286, 320, 382). In S phase and G2 when a sister chromosome is available as a template, the Rad52 epistasis group mediates HR (reviewed in (341)), and the outcome is error-free DNA repair (for reviews see (340, 381)). NHEJ can function in all phases of the cell cycle, but is particularly important in G0 and G1 when cells lack a sister chomosome template. The NHEJ pathway (200, 201) is represented in Figure 4, and minimally includes the DNA-PK complex, which binds and tethers DNA, and XRCC4, DNA Ligase IV, and XLF/Cernunnos (4, 40), which ligate ends together. NHEJ can be adapted to repair more complicated lesions through the activity of additional processing proteins at the expense of accurate repair (see Figure 4). However, the costs of small sequence alterations still outweigh the cellular consequences of genomic instability. Interestingly, this mutagenic pathway is capitalized on during VDJ recombination to generate diversity at DNA junctions (201).

DNA-PKcs (the catalytic subunit of DNA dependent protein kinase) is a third PIKK involved in the DNA damage response with an important role in

Figure 4. Non-homologous end-joining. A simplified schematic of non-homologous end-joining (NHEJ) is depicted. After a lesion is incurred, Ku70 and Ku86 rapidly bind DNA ends. The complex has an internal channel that can accommodate DNA, and translocates inward on the DNA strand after binding. The Ku complex is thought to undergo a conformational change that increases its affinity for DNA-PKcs, allowing its recruitment and tethering of DNA ends. If complicated lesions require processing before ligation, Artemis, MRN, and/or polymerases μ or λ (pol) may associate with DNA-PKcs to clean up the DNA ends in an error-prone manner. Phosphorylation of Artemis by DNA-PKcs promotes its endonuclease activity. After processing, XRCC4/DNA Ligase IV and XLF (Cernunnos) ligate the DNA ends. Processing may lead to alteration of primary sequence (blue). DNA-PKcs auto-phosphorylation is required for NHEJ and may occur in trans. DNA-PKcs mediated phosphorylation of XRCC4 and the Ku proteins were omitted for simplicity since the physiological relevance is unclear.

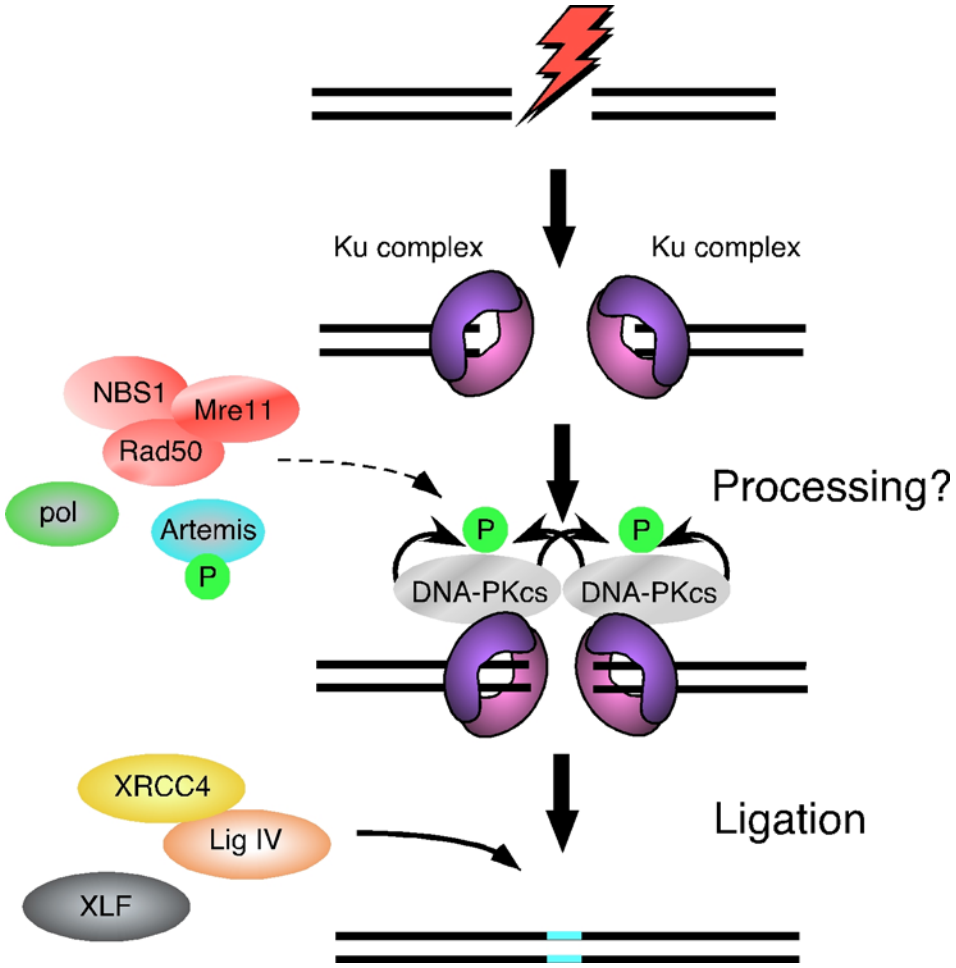
Ku complex
Ku complex
NBS1
Mre11
Rad50
pol
Artemis
P
Processing?
P
P
DNA-PKcs
DNA-PKcs
XRCC4
Lig IV
XLF
Ligation

NHEJ, as demonstrated by the repair defects of deficient rodent and human cells (42, 142). The DNA-PK holoenzyme is composed of DNA-PKcs and the DNA binding Ku70/Ku86 heterodimer, although DNA-PKcs is not constitutively associated with Ku (71). Supporting this, the Ku proteins have some distinct activities compared to DNA-PKcs (100, 142), even though Ku deficient cells also exhibit defects in NHEJ (100, 142). The holoenzyme complex forms after the Ku proteins bind DNA ends and presumably change conformation to recruit DNA-PKcs (see Figure 4) (reviewed in (42)). Ku80 encodes a C-terminal PIKK recruitment domain, like ATRIP and Nbs1, which is required for DNA-PKcs interaction (116). Recent live cell imaging studies support this, and show rapid Ku-dependent relocalization of DNA-PKcs to sites of damage (177, 225, 349) with faster kinetics than HR protein recruitment (177). Although the mechanisms are not completely clear, retention and activity of DNA-PK at sites of breaks may depend on the type of damage, the phase of cell cycle, and DNA-PKcs kinase activity (see below) (11, 33, 85, 320).

Although DNA-PKcs can tether DNA ends together (84, 327), it also exhibits DNA-stimulated kinase activity that is required for repair (reviewed in (71, 85, 368)). DNA-PKcs autophosphorylates itself on two major serine/threonine clusters, and this activity is thought to regulate DNA processing and DNA repair pathway choice (77, 91, 320, 368). In addition, DNA-PKcs kinase activity is directed towards a number of targets. DNA-PKcs

phosphorylates Artemis during VDJ recombination, and promotes its endonuclease activity for hairpin opening (133, 220, 256). These two proteins are also required for the NHEJ mediated repair of a subset of DSBs (286) that presumably need processing. Other substrates include RPA32, XRCC4, the Ku proteins, WRN, p53, H2AX (71), but the physiological relevance of their modifications by DNA-PKcs in cells remains elusive. For example, the DNA-PKcs phosphorylation sites on XRCC4 and the Ku proteins are not required for repair (99, 398). Additionally, ATM and ATR phosphorylate many of these substrates after damage (71), including Artemis (133, 286, 402). In the case of H2AX, DNA-PKcs mediated phosphorylation only occurs in the absence of MRN and ATM (116, 332), so it is unclear whether DNA-PKcs is compensating for loss of ATM activity or whether DNA-PKcs is activity suppressed. However, the fact that DNA-PKcs cannot phosphorylate H2AX when a specific small molecule inhibitor inactivates ATM suggests the latter possibility (116, 153). Since most genotoxic reagents currently used to study damage responses activate ATM and ATR, it is difficult to establish the contribution of DNA-PKcs mediated substrate phosphorylation to damage signaling.

While a great deal of progress has been made regarding the roles of MRN, ATM, and ATR in the early events of the DNA damage response, many important questions remain. MRN has a number of DNA processing abilities, however, we do not completely understand how they impact damage signaling

and DNA repair. MRN is also required for ATM and ATR activation, at least after certain types of damage, but we do not know how MRN impacts DNA-PK activity. Likewise, it is unclear how ATM and ATR coordinate with DNA-PK to promote signaling and repair functions. Finally, we are only just beginning to understand how chromatin is modified and may trigger signaling events during DNA damage, and what roles alternative post-translational modifications (see below) play in the damage response.

Post-translational modifications by the cellular ubiquitination machinery

Maintaining tight control of protein functions is critical to proper cellular homeostasis. The cell encodes numerous strategies that dictate when and where a given protein is expressed, and how it should operate. At the post-transcriptional level, covalent modification of proteins can regulate activity through several mechanisms. Phosphorylation, hydroxylation, methylation, acetylation, and glycosylation can change cellular localization or interaction with other proteins or DNA. Alternatively, attachment of ubiquitin or other ubiquitin-like proteins (UBLs) to a given substrate may alter its function (176). Ubiquitin is a 76 aa protein that can mark targets for destruction or regulate substrate activities through non-proteolytic means (129). All UBLs share structural features with ubiquitin and are attached to their targets in a similar manner (see below) (106, 176). The list of UBL family members and the

diverse pathways they regulate is growing (176). Interestingly, a great deal of cross-talk occurs between post-translational modification pathways, and often, one modification stimulates or regulates another (160).

Ubiquitin is covalently attached to a target through a series of enzymatic reactions (see Figure 5A for details). E1, E2, and E3 cellular enzymes activate ubiquitin and catalyze its transfer to the substrate. Although alternate ubiquitination sites have been reported (45), a lysine residue usually receives the ubiquitin linkage (129, 176). Mammalian cells encode two known E1s (129, 165), a larger subset of E2 enzymes, and a tremendous number of E3 ligases, which give specificity to the ubiquitination of targets (129). E3 ligases are primarily classified into two categories, depending on the presence of HECT domains or RING motifs (129, 176) (Figure 5). The major distinction between these E3s is whether ubiquitin is conjugated to the E3 before transfer to the substrate (HECT domain ligases) or not (RING motif ligases) (129, 176).

The Cullin-RING ligases (CRLs) constitute the largest superfamily of RING E3 ligases (272). CRLs are modular (see Figure 6) and anchored by one of seven Cullin subunits (Cullin 1, 2, 3, 4a, 4b, 5, and 7). The N-terminal domain of the Cullin binds adaptor proteins, while the C-terminal domain binds a RING protein (either Rbx1 or Rbx2), which is responsible for docking the E2 and catalyzing ubiquitin transfer (272). Different Cullin proteins have preferences for certain adaptors and RING proteins. Cullin 1 associates with

Figure 5. The cellular ubiquitin pathway. (A) Schematic of ubiquitin conjugation of substrates. A conjugatable ubiquitin (Ub) molecule (gray circle) with a free C-terminal glycine is activated by an E1 ubiquitin-activating enzyme (blue) and ATP. A high energy Ub-AMP bond is formed which is subsequently attacked by the E1 catalytic cysteine residue to form a thioester linkage between Ub and the E1. The Ub molecule is then transferred to the E2 enzyme (green), which also forms a thioester linkage between the catalytic cysteine and Ub. The Ub moiety can then be transferred to the ε-amino group of a lysine residue within substrate (red) via E3 (yellow) activity. Two major classes of E3 enzymes differ slightly in Ub conjugation. HECT (homology to the E6-AP C-terminus) ligases form a thioester bond with Ub before transferring Ub to the target protein. RING (really interesting new gene) based ligases coordinate the E2 and substrate to facilitate Ub transfer without forming a thioester linkage. Similar enzymatic reactions also occur for other ubiquitin-like proteins, such as SUMO. DUBs are omitted for simplicity. Adapted from {Kerscher, 2006 #221}. **(B)** Potential outcomes of substrate ubiquitination. Depending on the E2 and E3 enzymes utilized, substate ubiquitination can result in mono-ubiquitination or multiple mono-ubiquitination, or poly-ubiquitination. Poly-Ub conjugates can also be linked to one another through 7 different lysine linkages, most commonly lysine 48 (K48) and lysine 63 (K63). While lysine 48 poly-ubiquitin chains primarily target a substrate for proteasome-mediated degradation, mono-ubiquitination and K63 poly-ubiquitination usually do not and are involved in signal transduction and localization.

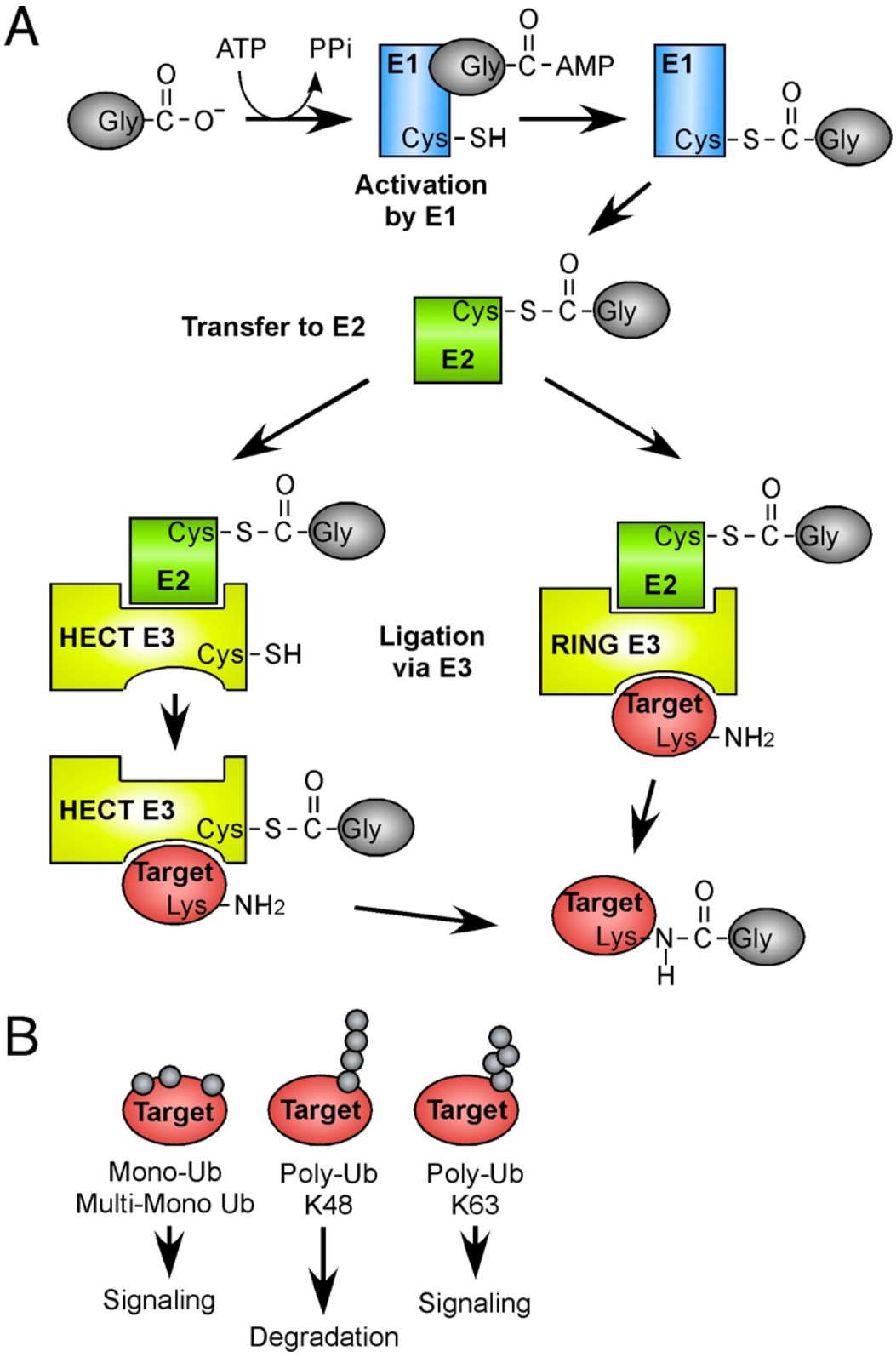
A
ATP
PPi
Gly
E1
Cys
SH
AMP
Activation
by E1
Transfer to E2
E2
HECT E3
Ligation
via E3
RING E3
Target
Lys
NH2
B
Target
Mono-Ub
Multi-Mono Ub
Poly-Ub
K48
Poly-Ub
K63
Signaling
Degradation
Signaling

the Skp1 adaptor protein in SCF (Skp1-Cullin-F-box protein) ligases (Figure 6A), while Cullins 2 and 5 bind Elongins B and C (Figure 6B) (272). Additionally, although the two related RING proteins exhibit approximately 50% identity (169, 260) and can both interact with multiple Cullins (260), Cullin 2 may actually prefer Rbx1 while Cullin 5 associates with Rbx2 (170). The molecular basis for these preferences is currently unclear.

Adaptor proteins such as Skp1 and Elongin C bind sequences within substrate receptors called F-boxes and BC boxes, respectively (272) (see Figure legend 6 for detail). BC boxes have a consensus motif of (A,P,S,T)LXXXCXXX(A,I,L,V) and often, a down-stream hydrophobic sequence that somehow regulates association with either Cullin 5 (Cul 5 box) or Cullin 2 (Cul 2 box) (170, 222). BC box and F-box containing receptor proteins recruit the cellular target for ubiquitination, usually through another protein interaction motif such as a WD40 domain (272). The combination of these distinct modules and receptor proteins gives CRLs their substrate specificity.

Different sets of E2 and E3 enzymes dictate whether proteins become mono- or poly-ubiquitinated, and which lysine linkages within ubiquitin are utilized (67, 106, 129). Covalent modification of a substrate with lysine-48 linked ubiquitin chains usually targets it for destruction by the proteasome (Figure 5B) (129). In this case, the cell can regulate function by altering the

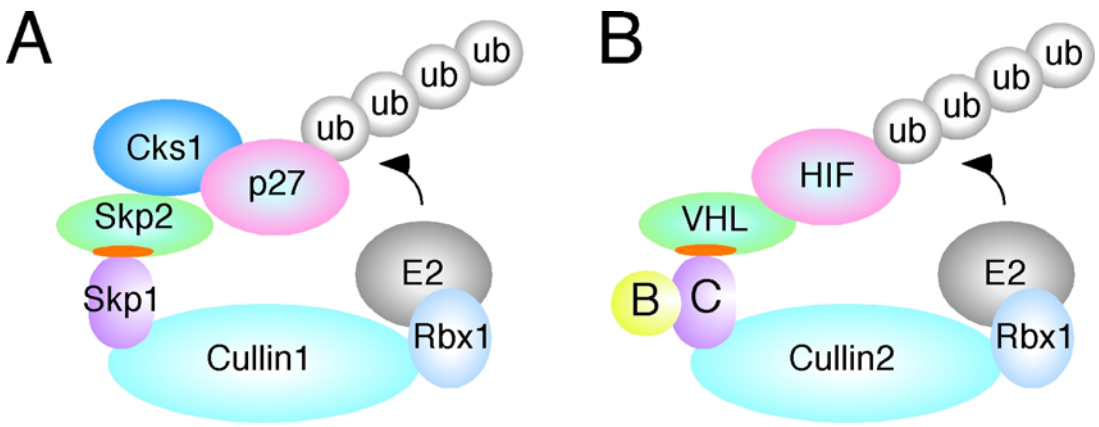

Figure 6. Schematic of modular Cullin-containing ubiquitin ligases. (A) A simplified figure of an SCF^{skp2} ubiquitin ligase based on the published crystal structure. Here Cullin 1 binds Rbx1 and adaptor protein Skp1. Skp 1 is linked to the F-box protein Skp2, which binds the substrate, p27. Cks1 is required for p27 degradation. The F-box in Skp2 is highlighted in orange. The arrow represents transfer of ubiquitin directly to the substrate. **(B)** A model of the von Hippel-Lindau (VHL)-containing CRL. Here Cullin 2 binds Rbx1 and adaptor proteins Elongins B and C. Elongin C is linked to VHL by a BC box motif (orange). VHL binds hyrdoxylated HIF1α for ubiquitination and proteasome mediated degradation.

concentration of a given protein. In many circumstances, a specific pool of a protein is targeted due to another post-translational modification such as phosphorylation (129, 160, 176, 272). For example, during the DNA damage response, phosphorylated Chk1 is degraded and may help down-regulate the DNA damage response (403). Induction of the intra S phase checkpoint requires Chk1 or Chk2 phosphorylation of Cdc25A for its degradation by the $SCF^{\beta\text{-}TRCP}$ ubiquitin ligase (44, 166). While lysine-48 linked ubiquitin chains can lead to degradation, mono-ubiquitination and lysine-63 polyubiquitination have alternate functions, such as signaling (129, 151). After certain types of DNA damage, PCNA may become mono- or poly-ubiquitinated on the same lysine residue to promote either error-prone or error-free DNA repair, respectively (82, 237). In yeast, this same lysine may also be SUMOylated to prevent aberrant HR at replication forks (273). MDC1 recruits RNF8 and ubc13 to DSBs where they ubiquitinate histones, which in turn provides a platform for 53BP1 and BRCA1 association (159, 180, 223, 355). Since RNF8 and ubc13 catalyze lysine-63 linked ubiquitin chains (158, 275), this histone signal may be important for 53BP1 and BRCA1 association. Although other lysine-linked poly-ubiquitin chains have been identified, their functions are currently not well understood (129, 176). A large family of enzymes with de-ubiquitinating activity, called DUBs (257), can also modulate target modification by removing ubiquitin or UBLs to help regulate function.

The importance of the ubiquitin-proteasome system is illustrated by the many pathways it regulates, and disrupted activity is often associated with numerous diseases (140, 154). Additionally, a large number of pathogens disrupt or dysregulate the ubiquitin system in order to commandeer this machinery (12, 203, 272). While much has been learned about ubiquitin and UBL modification of substrates, many unanswered questions remain, particularly with regard to E3 ligases. Although an enormous number of E3s have been identified through proteomic approaches, the substrates and pathways affected by these are largely unknown. Crystallography studies have also provided important insights into cullin-containing ligase structures, however, it is still not clear how these multi-component enzymes are assembled and regulated. Finally, we are only beginning to elucidate the mechanisms pathogens use to target or hijack ubiquitin pathways.

Adenovirus

Adenoviruses (Ad) are a family of lytic viruses that replicate in the nuclei of infected cells (313). They infect a wide variety of mammalian and avian hosts, and are classified into subgroups based on antibody-mediated neutralization profiles. The serotypes that infect humans are associated with acute respiratory infections (not the common cold), conjunctivitis, and infantile gastroenteritis (313). Interestingly, although adenoviruses have never been

associated with cancer in humans, certain subgroups exhibit strong oncogenic potential in newborn hamsters, and all serotypes can transform primary cells in culture (109, 313), providing a strong viral model with which to study cellular transformation (see Chapter 7 for further discussion).

Adenovirus serotype 5 (Ad5) is one of the most well-studied members, and part of serogroup C. Like all adenoviruses, it has a linear double-stranded DNA genome that is approximately 36kB in length (Figure 7A). Inverted terminal repeats (ITR) are located at the 3' and 5' ends of the genome and serve as origins of replication (Figure 7A). Covalently attached to the 5' ends of the genome are the terminal proteins, which prime viral DNA replication (Figure 7B) (209, 313). The Ad genome encodes a series of viral gene products expressed in a temporal manner during infection. Multiple mRNAs are produced from each region by alternative splicing and alternate polyA usage (313). Early genes (E, see Figure 7A) are transcribed shortly after translocation of the viral DNA to the nucleus. Expression of the early regions begins from the ends of the genome, starting with the E1 and E4 regions, and proceeds inward. The proteins from the E2 region, which include the ssDNA binding protein (DBP), the viral polymerase, and the pre-terminal protein, are required for replication (Figure 7B). Other early products, especially those from the E1 and E4 regions, modulate the host environment to promote viral

Figure 7. Adenovirus replication and concatemer formation. (A) Simplified schematic of the adenovirus genome. The double-stranded DNA virus is 36kB in length. Arrows above and below the genome represent early (E) and late (L) regions of gene expression. VA RNAs (white arrowhead) are small RNAs that protect against interferon-induced cellular responses. Expression of VA RNAs begins early and increases throughout the viral lifecycle. The green ends of the genome represent inverted terminal repeats (ITRs) of approximately 100-140bp that serve as origins of replication. TP refers to the mature terminal protein covalently attached to the 5' ends of the genome. The viral introns and delayed early genes, IX and IVa2, have been omitted for simplicity. **(B)** Adenoviral DNA replication. TP as in (A), pTP is the pre-terminal protein produced during the early phase of gene expression. Replication is initiated when the pTP and the Ad polymerase bind the ITR in a sequence dependent manner. Priming results from the covalent attachment of pTP to a molecule of dCMP, forming the first 5' residue of the Ad genome. Elongation requires the Ad polymerase, DBP and other cellular factors. Type I replication results in strand displacement, producing a duplex genome that may re-initiate type I replication, and a single strand that circularizes via the ITR sequences. Type II replication on this genome occurs with the same ordered events as with type I replication, producing a duplex of viral DNA. Cleavage of pTP to produce the mature TP occurs during late stage packaging of viral DNA. For simplicity, the Ad DNA polymerase, DBP, and other cellular factors have been omitted. **(C)** An E4-deleted adenovirus is concatemerized during infection. HeLa cells were infected with wild-type Ad5 or E4-deleted mutant *dl*1004 (both at MOI of 25) for 30 hours before harvesting for analysis of viral DNA by pulsed-field gel electrophoresis. Viral DNA was visualized on the gel by staining with ethidium bromide (right), or after southern blotting with a probe to Ad DNA (left). Arrowhead represents the linear monomeric adenoviral genome. (C) was reprinted from (335).

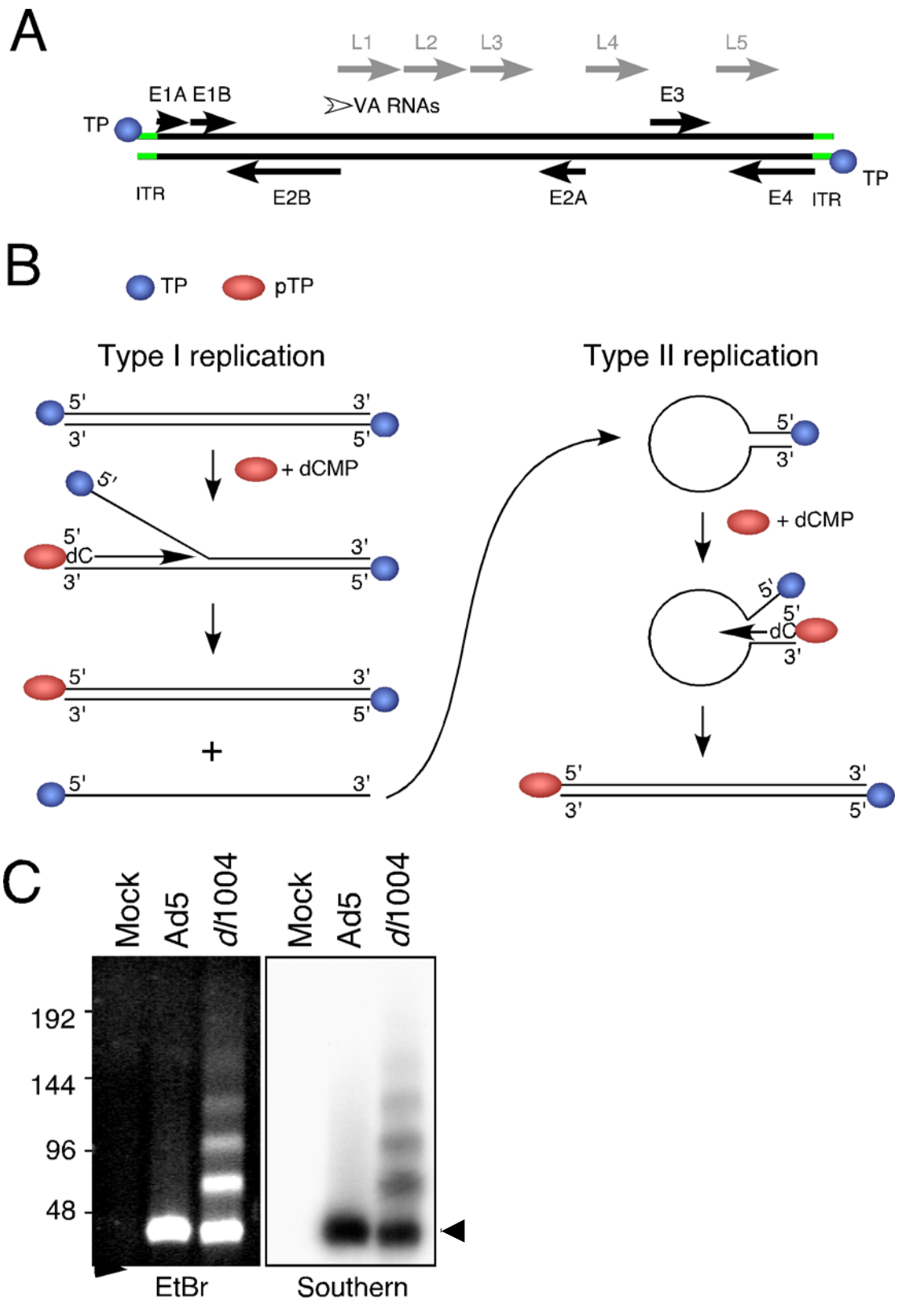
A
L1
L2
L3
L4
L5
E1A E1B
VA RNAs
E3
TP
TP
ITR
E2B
E2A
E4
ITR
B
TP
pTP
Type I replication
Type II replication
5'
3'
+ dCMP
dC
+
C
Mock
Ad5
d/1004
Mock
Ad5
d/1004
192
144
96
48
EtBr
Southern

replication and prevent host defenses (18, 313, 364, 367) (see Chapters 2-4 for further discussion).

After replication has begun, the viral transcriptional profile shifts. Early and delayed-early viral gene products that continue to modulate the host cell and promote viral late gene expression are produced (313). The late regions (Figure 7A, L1-L5) encode structural proteins responsible for packaging the viral DNA. Concomitant with late viral gene expression, is the shut-down of host gene expression. This is mediated by the inhibition of cellular mRNA export, likely due to preferential viral mRNA export (123), and the impediment of host mRNA translation. The lytic lifecycle ends with newly encapsidated virions bursting from the host cell. In immortalized cell lines such as HeLa, the Ad lifecycle takes approximately 24 hours. In primary cells, though, this cycle is extended, particularly the early phase (131, 313).

Genetic studies utilizing mutant adenoviruses have provided insights into the functions of the early gene products. E4 deletion mutants have severe defects in viral DNA replication, viral mRNA transport, host cell shut-off, and viral late protein production (reviewed in (18, 123, 313, 364, 367)), although some of these phenotypes are overcome at high multiplicities of infection (157). E4orf6 and E4orf3 were shown to act in a partially redundant manner to promote these steps in the viral lifecycle (36, 144, 157, 362). E1b deletion mutants have similar deficiencies to E4 deletion mutants in viral mRNA export

and late protein synthesis (6, 7, 35, 198, 274). The analysis of double mutants suggested that E1b55K/E4orf6 and E4orf3 function in parallel pathways to promote these activities (35, 36, 157, 314, 362). Supporting this, E1b55K was found to complex with E4orf6 during infection (302), and E4orf6 or E4orf3 is required for nuclear E1b55K localization (136, 181). Additionally, E4orf3 deletion alone confers no visible defects during the Ad lifecycle (36, 157), but it is required for efficient virus replication in the absence of E1b55K or E4orf6 (35, 314, 315). Although it is clear from these observations that E4orf3 and a complex of E1b55K/E4orf6 perform similar critical functions during Ad infection, the mechanisms through which they act are only beginning to be understood.

Adenovirus and the cellular DNA damage response machinery

The linear double-stranded genome of adenovirus and its replication intermediates (Figure 7A and 7B) could be potential substrates for the cellular DNA damage response machinery. The first indication that adenovirus was targeted by host DNA repair factors came from examining the replication of an E4-deleted adenovirus. In addition to the defects described above, E4-deleted adenoviruses exhibit concatemerization of mutant viral genomes (Figure 7C), with heterogeneous processed genome junctions (360). This phenotype is not seen during WT Ad infection (Figure 7C) (360), suggesting that E4 proteins

inhibit this process. Indeed, expression of either E4orf3 or E4orf6 was sufficient to prevent concatemerization in trans (360), but the mechanism was not understood.

Examination of concatemer formation in mutant cell lines infected with an E4-deleted Ad indicated that the host cell NHEJ machinery was responsible. Our lab found that in addition to DNA-PK (30), DNA Ligase IV and the MRN complex were required (335). Interestingly, mutant viral genome concatemerization was dependent on the nuclease activity of Mre11 (335). Given the processing of Ad genome junctions in concatemers (360) and the similarity in structure to Spo11-bound DSBs in yeast, we proposed that terminal protein-bound Ad genomes were substrates for Mre11 nuclease activity (335).

We also found that Ad E4 proteins had two strategies to inactivate MRN, preventing concatemerization (335). E4orf3 mislocalizes MRN into track-like structures, similar to its effects on the promyelotic leukemia ND10 protein, PML (51, 98). E4orf6 acts together with E1b55K to target MRN for proteasome-dependent degradation. E4orf6 and E4orf3 can also bind DNA-PKcs (30), and this was proposed to prevent concatemerization (30). However, although E4orf6 alone blocks cellular DNA repair (30, 147), E4orf6 in the absence of E1b55K and E4orf3 does not inhibit concatemer formation

(335). Furthermore, E4orf3 mutants unable to prevent concatemerization still bind DNA-PKcs (112), suggesting these events are separable.

In addition to MRN, E1b55K/E4orf6 also degrades the tumor suppressor, p53 (137, 238, 251, 282, 292, 329). The viral complex is thought to recruit cellular E3 ligase factors, Cullin 5, Rbx1 and Elongins B and C to promote degradation (146, 281). Recently, these viral proteins were also found to degrade DNA Ligase IV (8), providing another potential mechanism to prevent concatemerization. Although E1b55K associates with a number of proteins it does not degrade, such as SSBP2, NuMA, and mSin3A (122, 146, 221, 279), the contribution of these E1b55K interactions to the viral lifecycle are still unclear. Additionally, most of the viral functions of E1b55K/E4orf6 are attributed to the degradation of substrates (25, 72, 378). Therefore, understanding how the E1b55K/E4orf6 complex functions as a ubiquitin ligase to target its substrates is critical to elucidating not only its contributions to the adenoviral lifecycle, but also to understanding how viruses commandeer the host machinery for their advantage.

Adeno-associated virus

Adeno-associated virus (AAV) is a small DNA virus that was discovered as a contaminant of adenovirus preparations. Infection with AAV is not associated with any known pathogenesis. However, AAV has been the subject

of a great deal of research because of its application in gene therapy studies. AAV has an interesting biphasic lifecycle, with both lytic and latent stages (Figure 8) that depend on the host cell environment (241). AAV is classified as a dependovirus, since productive replication requires a helper virus and the cellular DNA replication machinery. In the absence of helper virus, AAV can site-specifically integrate into a region on chromosome 19, called AAVS1, and remain latent (105, 241) (see Chapter 7 for further discussion).

The AAV genome is 4.6kB and composed of primarily ssDNA with ITRs at either end (Figure 9) (357). Wild-type (WT) AAV minimally encodes four Rep gene products (discussed further in Chapter 6), involved in viral replication and packaging, and three Cap gene products, which are structural (Figure 9A) (241). The ITRs form double hairpin structures that provide priming for replication (Figure 9), and are required for integration and packaging. Recombinant AAV (rAAV) vectors consist of transgenes flanked by the ITRs, replacing the viral Rep and Cap genes (Figure 9B). A number of features make rAAV vectors attractive for gene therapy purposes, including ease of manipulation and ability to transduce non-dividing cells (130, 138, 299). No viral genes are expressed from rAAV vectors, and transduction is therefore regulated by host cell factors (130, 138, 299).

Ad, HSV-1, HCMV, HPV and vaccinia virus can all provide helper activities to promote AAV production (241, 357). In the case of Ad, a well-

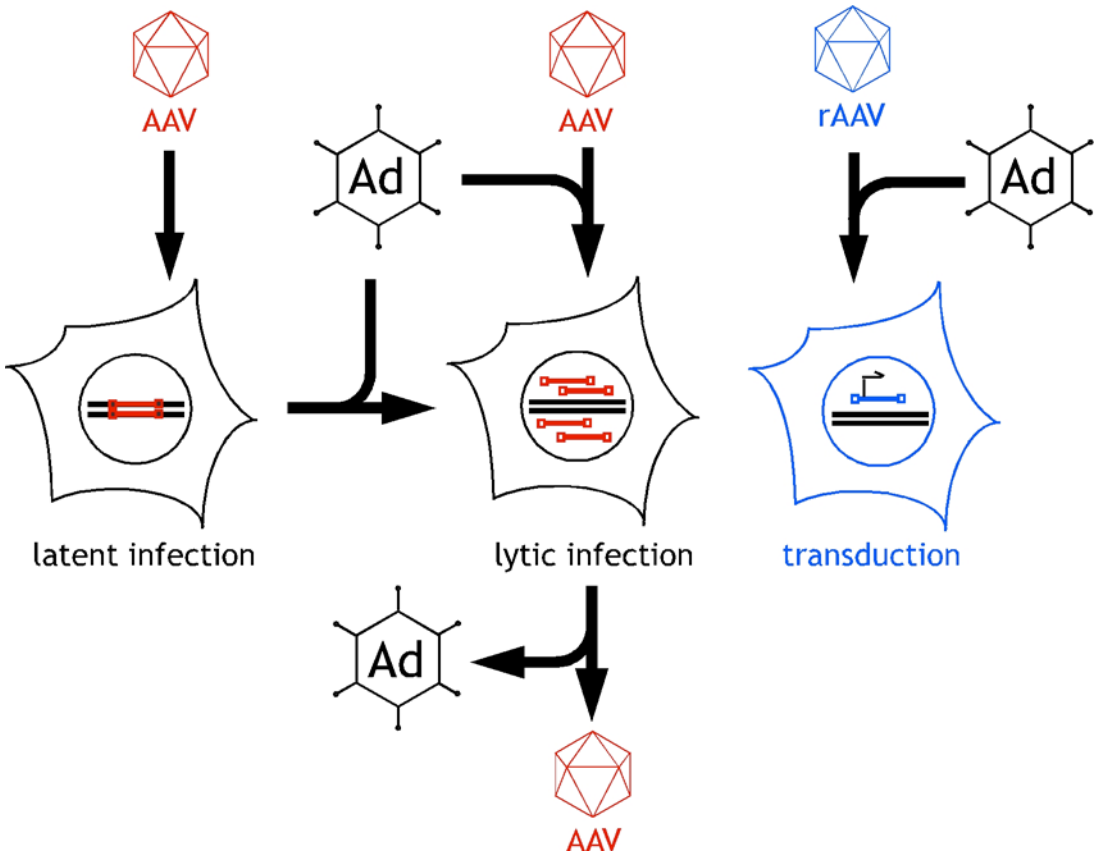

Figure 8. Schematic of the AAV lifecycle. Wild-type (red) or recombinant AAV (blue) viruses can infect host cells. For wild-type virus, lytic or latent infection depends on the presence of a helper virus, such as adenovirus (Ad). Lytic infection results in the production of both viruses. Limited AAV replication can also occur in the absence of helper viruses with genotoxic agents. Latent infection occurs in the absence of helpers and primarily results in the site-specific integration of the AAV genome into a site on chromosome 19. Expression of gene products during recombinant AAV transduction is also greatly enhanced by helper virus. No replication of AAV occurs in transduction and gene expression can last for extended periods of time. Genomes can integrate, but rarely and not in a site-specific manner, and are often maintained in an episomal state.

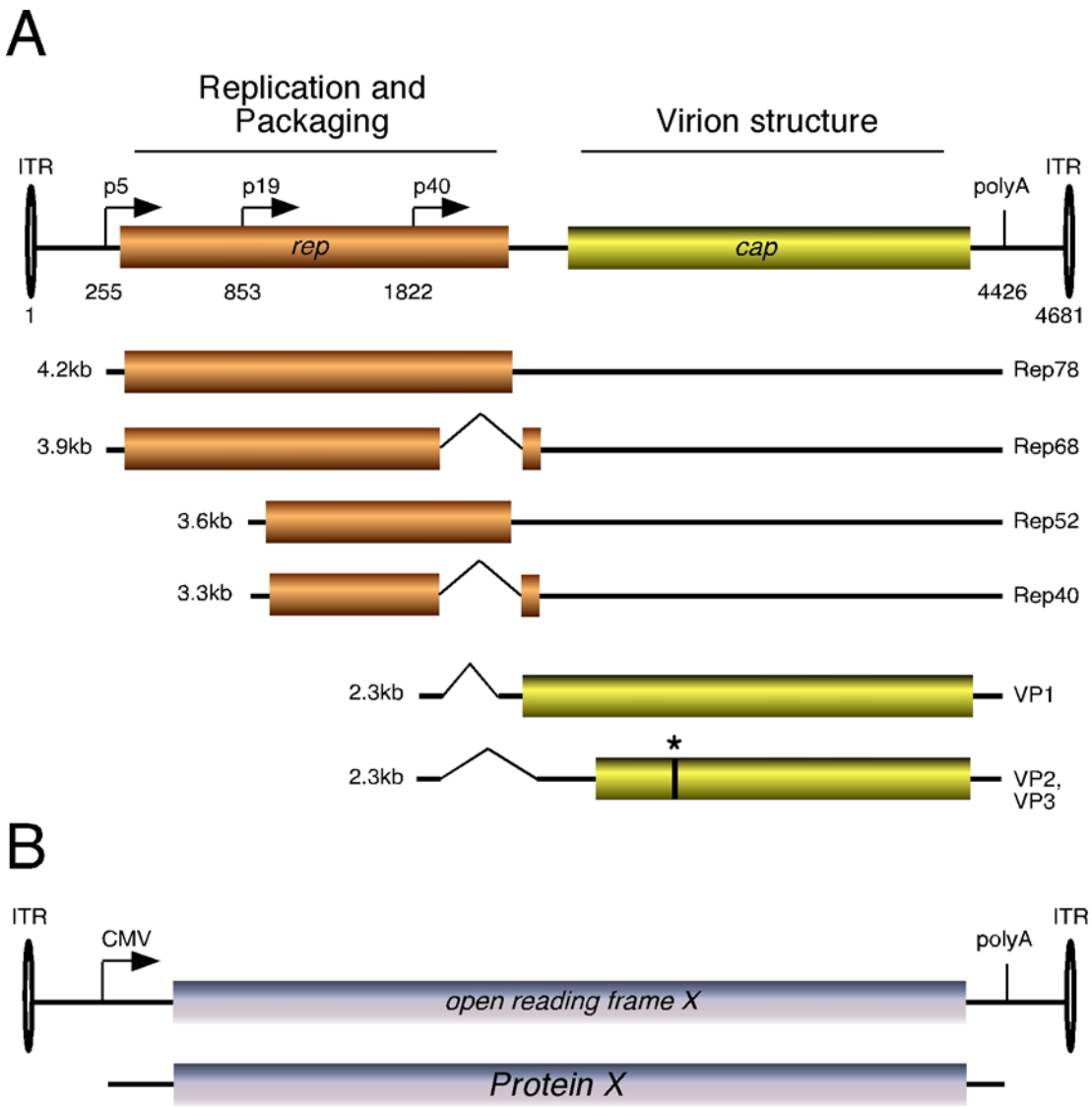

Figure 9. Wild-type and recombinant AAV genomes. (A) Schematic of the wild-type AAV genome illustrating Rep and Cap genes and inverted terminal repeats (ITRs). The promoters p5, p19, and p40 are also listed along with the location of the polyadenylation site (polyA). Below the genome are the Rep and Cap RNA transcripts, sizes, and proteins produced (named to the right). Translation of VP3 begins from an internal AUG start codon (*), while VP2 translation begins from an upstream ACG codon. **(B)** Schematic of a recombinant AAV genome. Rep and Cap genes are replaced by a gene of interest whose transcription is dependent on an alternative promoter, such as CMV depicted here.

defined minimal set of early gene products modulates the host environment rather than directly mediating viral replication. These gene products include E1A, E1b55K, E4orf6, DBP, and the VA RNAs (128, 357) (discussed further in Chapter 5). HSV-1 contributes a disparate set of helpers compared to Ad, including ICP8 and the helicase/primase complex of UL5/8/52 (358, 363), although both viruses commonly provide a ssDNA binding protein (ICP8 from HSV-1 and DBP from Ad), which may facilitate Rep functions (336). However, the mechanisms by which these viral helper proteins act to promote AAV replication are still largely unclear. Unraveling these processes will provide a better understanding of how AAV utilizes the host machinery, and how helper viruses target common cellular pathways.

AAV and the cellular DNA damage response machinery

Like adenovirus, the genome structure of AAV and its replicative intermediates (Figure 10) are potential targets of DNA repair factors. Intriguingly, AAV has a long history with cellular DNA damage response pathways. Genotoxic agents were found to stimulate limited rAAV transduction and WT AAV replication (5, 295, 388) in the absence of helper proteins through unknown mechanisms. Additionally, numerous NHEJ proteins have been shown to process or affect rAAV and scAAV vectors (see Figure 10) (see Chapters 5 and 6 for further detail) in the absence of other viruses. AAV ITRs

Figure 10. Schematic of AAV replication. 1) Incoming single-stranded (ss) virus requires a cellular DNA polymerase and viral helper proteins to undergo efficient second strand synthesis to make a double-stranded (ds) viral genome. This step occurs for both wild-type AAV and recombinant AAV vectors. **2)** For wild-type AAV, Rep proteins are expressed from the ds virus, and Rep78 or Rep 68 cleaves the ds genome at the terminal resolution site (trs) and remains covalently attached to the 5' end. **3)** Helicase activity is required to unwind the inverted terminal repeat (ITR) to allow a DNA polymerase to replicate through it. Terminal resolution is the nicking and replication through the ITR. This results in a dimeric complex of two AAV genomes which refold ITRs to **4)** re-initiate replication **5)** or become packaged into virions with the aid of Rep52 and Rep40. **6)** To produce self-complementary AAV vectors (scAAV), one trs is deleted which allows a ds genome to be packaged, bypassing second-strand synthesis after infection. Rep attached to the incoming viral genome is omitted for simplicity, as are helper proteins. Rfm, replication form monomer and Rfd, replication form dimer.

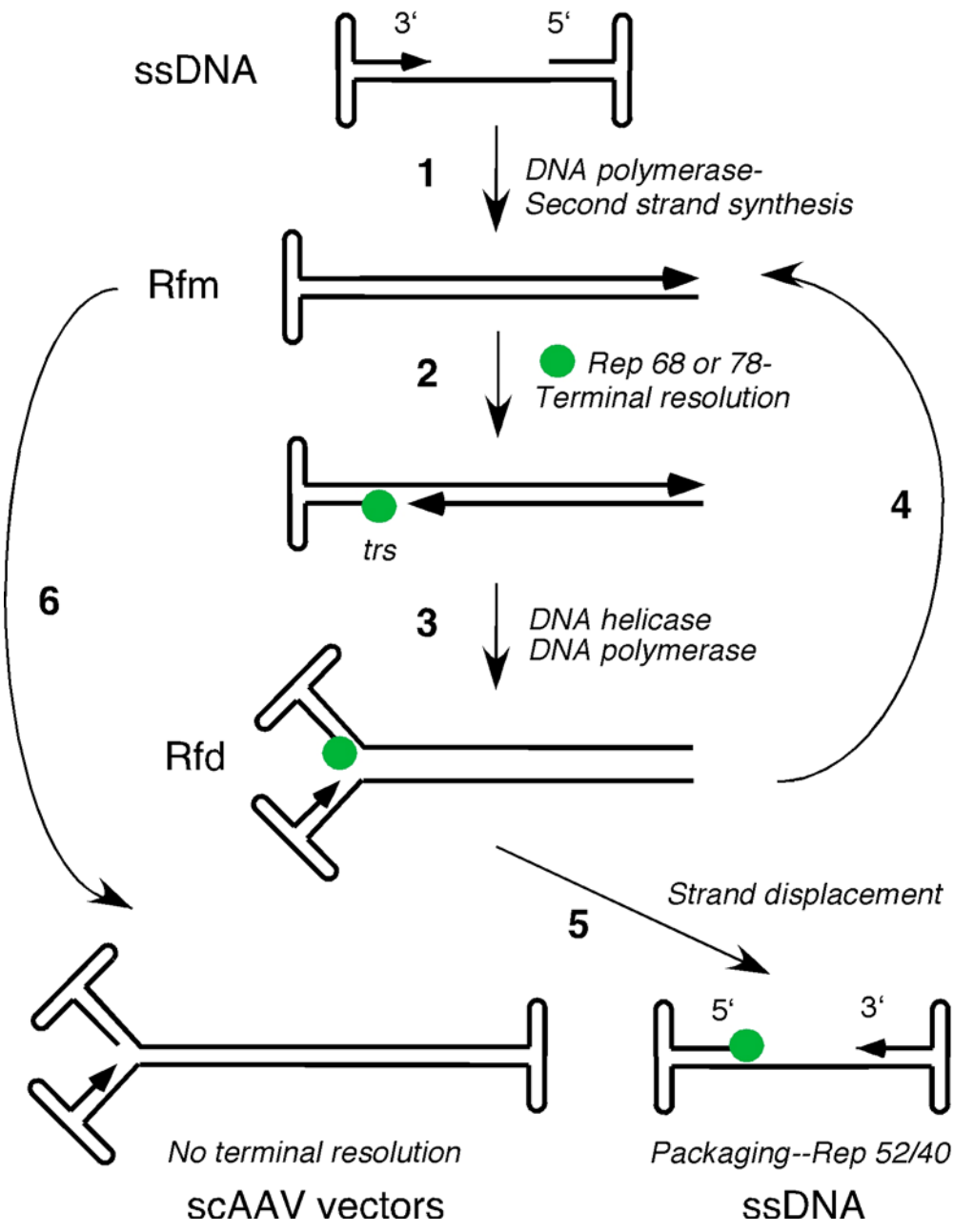
ssDNA
3'
5'
1
DNA polymerase-
Second strand synthesis
Rfm
2
Rep 68 or 78-
Terminal resolution
trs
4
6
3
DNA helicase
DNA polymerase
Rfd
Strand displacement
5
5'
3'
No terminal resolution
scAAV vectors
Packaging--Rep 52/40
ssDNA

(284), genomes (168), and the Rep gene products (21) have all been implicated in inducing ATM and ATR mediated DNA damage responses, although it is not clear how viral replication is affected. Unfortunately, a cohesive model of how the DNA damage response regulates AAV has not emerged from these studies, although these observations suggest that damage signaling has both positive and negative influences. More studies are needed to determine how repair proteins and damage signaling affects steps in the AAV lifecycle. Interestingly, many of the AAV helper viruses and helper proteins have been shown to interact with DNA repair pathways (203). It will be important to determine how viral helper proteins impact these pathways to promote AAV replication.

Thesis overview

This Dissertation focuses on elucidating the relationship between Ad, AAV, and the cellular DNA damage response machinery. The data presented in the first three Chapters uncover mechanistic details behind adenovirus-mediated degradation of cellular substrates, p53, MRN, and DNA Ligase IV. In addition, these experiments address the consequences of E1b55K/E4orf6 expression on cellular responses. The last two Chapters examine the intersection of cellular DNA repair proteins and aspects of the AAV lifecycle. The results from this dissertation provide a better understanding of the roles of

E1b55K and E4orf6 in both the Ad and AAV lifecycles, and the ways in which these adenoviral proteins target host cell factors. Through these studies we have gained a more thorough understanding of how MRN functions during virally-induced damage responses. Additionally, these data provide the basis for viral models that will allow the elucidation of cellular functions of MRN, DNA-PKcs, and ubiquitin ligases.

Figure 7C from this chapter is reprinted from material as it appears in:

Stracker TH, Carson CT, Weitzman MD. Adenovirus oncoproteins inactivate the Mre11-Rad50-NBS1 DNA repair complex. Nature 418:348-352.

This material was published by the dissertation author's advisor and is used as background information in this chapter.

Chapter 2. Effects of the adenoviral E1b55K/E4orf6 protein complex on the cellular DNA damage response and cell cycle checkpoints.

Background

DNA damage elicits a cellular response initiated by the ATM or ATR kinases that includes phosphorylation of a variety of effectors and activation of cell cycle checkpoints (see Chapter 1 for details). In addition, ATM is autophosphorylated on serine 1981, an activity that appears to be required for its activity in mammalian cells (9). These kinases and other DNA repair proteins are found localized to sites of damage (53, 293) to amplify the signal and promote repair. The MRN complex is also important to the DNA damage response, as indicated by studies in yeast and in human cell lines derived from patients with A-TLD and NBS (78) (see also Chapter 1). ATM phosphorylation of Nbs1 after DSBs is necessary for the intra-S phase checkpoint (117, 204, 380, 405). Some evidence at the time also suggested that MRN had a role in damage sensing (235, 350). However, the lethality of null MRN mutations mammalian cells (217, 384, 409) complicated the exact determination of the status of MRN in the DNA damage response hierarchy.

As discussed in Chapter 1, adenovirus is a linear, double-stranded DNA virus that expresses a series of early viral gene products that promote virus production and modulate the host cell environment. Examination of mutant

adenoviruses has shown that E1b and E4 deletion mutants have similar defects in viral DNA replication, viral mRNA transport, host cell shut-off, and viral late protein production (reviewed in (18, 123, 313, 364, 367)). E4orf3 and a complex of E1b55K and E4orf6 act in a partially redundant manner to promote these steps in the viral lifecycle (35, 36, 157, 314), although the mechanisms by which they act are still unclear. The E4 proteins also prevent the concatemerization of viral genomes by the cellular non-homologous end-joining (NHEJ) machinery (see Chapter 1, Figure 7C) (30, 360). This activity is not normally seen during wild-type (WT) Ad infection, and the processing between viral genome junctions suggests that concatemers are not a normal replicative intermediate (360).

In characterizing the mechanism behind concatemer formation, we found that the E1b55K/E4orf6 complex and E4orf3 could independently prevent viral genome concatemerization (335, 360) by targeting the Mre11 complex (MRN). E4orf3 mislocalizes MRN, while the E1b55K/E4orf6 complex promotes its proteasome-mediated degradation (335). The degradation of MRN is consistent with the ability of E1b55K/E4orf6 to destabilize p53 (137, 238, 251, 282, 292, 329). (For further discussion of E1b55K and E4orf6, see Chapters 3 and 4). Although evidence from our concatemer formation studies indicated the importance of MRN and not p53 (335), it was still unclear how

the degradation of these substrates by E1b55K/E4orf6 would impact other cellular responses.

In this Chapter we examined how E1b55K and E4orf6 affect cellular DNA damage signaling and cell cycle checkpoints. We found that an E4-deleted virus induced the phosphorylation of effectors by ATM and ATR, and the accumulation of repair proteins around viral replication centers. In order to assess MRN's contribution to this response, we isolated E1b55K mutants that separated degradation of MRN from p53. Through this analysis, we determined that MRN was critical to damage signaling elicited by mutant virus infection and exogenous DSBs. Finally, we analyzed the effects of E1b55K and E4orf6 on cell cycle progression and checkpoints. While DSB induction of the early G2/M checkpoint required MRN, alteration of S phase progression by E1b55K/E4orf6 did not. At the time of these studies, MRN was implicated as a damage sensor but its role in the early stages of damage detection was elusive. Together, our data indicated that the MRN complex is required for ATM activation and DNA damage signaling stimulated by both DSBs and mutant virus infection (50).

Results

Infection with an E4-deleted mutant adenovirus induces a DNA damage response

Previously, our lab observed a mobility shift of Nbs1 in lysates from cells infected with the E4-deleted adenovirus, *dl*1004, which represented phosphorylation (335). Since this event signified DNA damage signaling, we wanted to further characterize this cellular response. Lysates from cells infected with *dl*1004 were examined over time for protein phosphorylation events, represented by either mobility shifts or phospho-specific antibodies (Figure 1A). Specifically, we noted the early activation of Chk2 and 53BP1, substrates of the ATM kinase. Autophosphorylation of ATM at serine 1981, which had been recently shown at the time to represent activated ATM (9), was also observed. At slightly later time points, we noted the phosphorylation of BRCA1, Nbs1, Chk1, and RPA 32. While we could not exclude antibody affinity differences, these results suggested that ATR mediated phosphorylation might occur at later times during infection.

These data showed that infection with an E4-deleted Ad induced a DNA damage response. When we examined a time course of wild-type (WT) Ad infection, we found that damage-induced phosphorylation events were largely absent (Figure 1B). Slight activation of some substrates appeared at the 24 hour time point, but this was likely due to the onset of cytopathic effects, and was minimal compared to *dl*1004 infection. While members of the MRN complex were degraded over time, consistent with previous results (335), the steady state levels of ATM, ATR, and DNA-PK were unaltered (Figure 1B).

Figure 1. Infection with an E4-deleted adenovirus induces a DNA damage response. HeLa cells were infected with either E4-deleted adenovirus *dl*1004 (MOI 50) **(A)** or wild-type Ad 5 (MOI 50) **(B)**, and harvested at the indicated times post-infection. Lysates were prepared and analyzed by immuno-blotting for the indicated proteins. Phosphorylation events are depicted by mobility shifts of proteins (BRCA1, Nbs1, RPA32) or phospho-specific antibodies (Chk1, Chk2, ATM, 53BP1). Unmodified proteins serve as loading controls. M stands for mock infected cells.

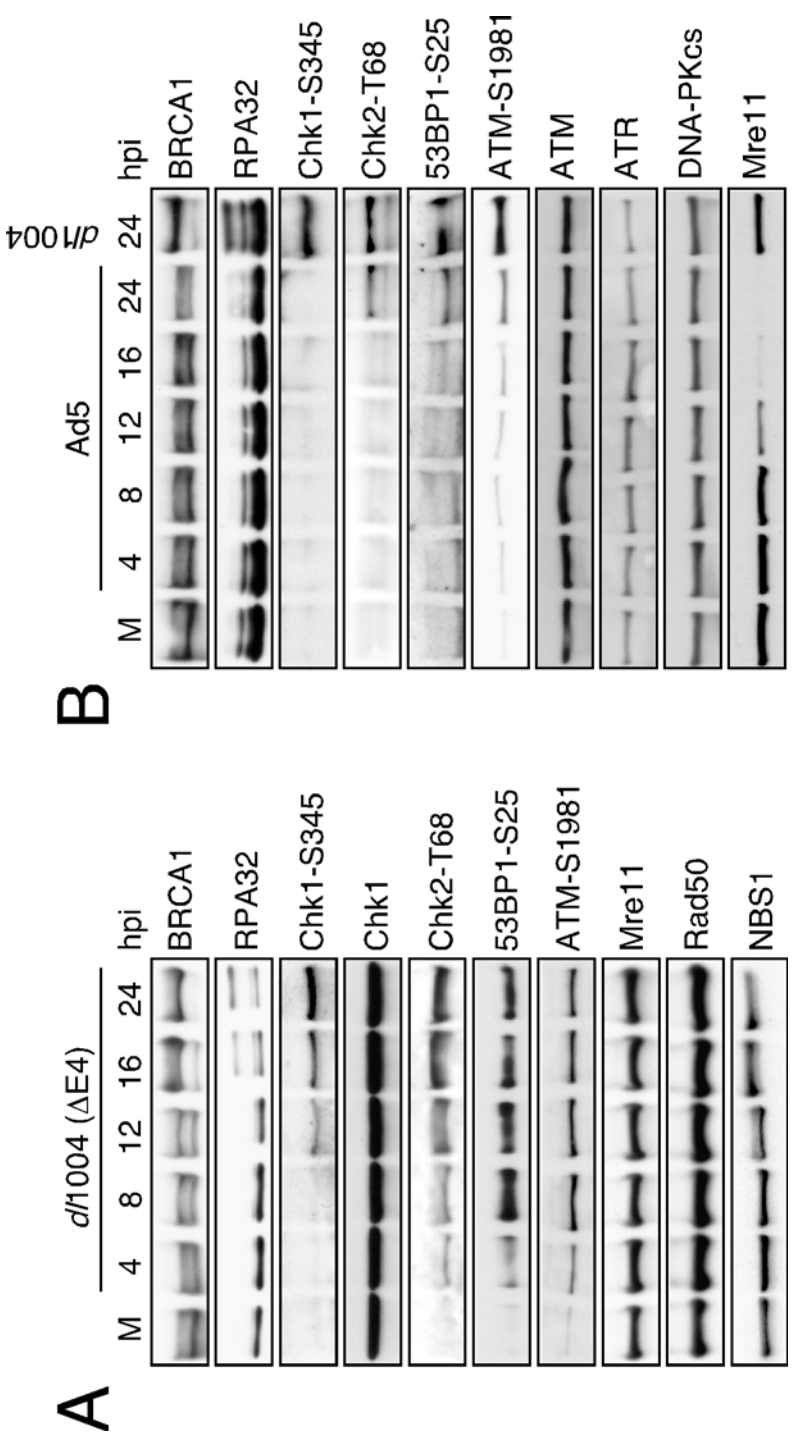
A
dl1004 (ΔE4)
M 4 8 12 16 24 hpi
BRCA1
RPA32
Chk1-S345
Chk1
Chk2-T68
53BP1-S25
ATM-S1981
Mre11
Rad50
NBS1
B
Ad5 dl1004
M 4 8 12 16 24 24 hpi
BRCA1
RPA32
Chk1-S345
Chk2-T68
53BP1-S25
ATM-S1981
ATM
ATR
DNA-PKcs
Mre11

These results suggested that the lack of damage signaling during Ad infection correlated with MRN degradation, and was not due to degradation of PIKKs.

The data from Figure 1 indicated that both ATM and ATR were activated during *dl*1004 infection. To further characterize the roles of these PIKKs in this response, we examined virus-induced damage signaling in cell lines deficient in ATM and ATR kinase activity (Figure 2). Infection of ATM-deficient cells (A-T) (410) with *dl*1004 only prevented the phosphorylation of 53BP1, but treatment with 5mM caffeine abrogated the remaining phosphorylation events (Figure 2A). This dose of caffeine was previously shown to inhibit both ATM and ATR kinase activity (300), and suggested that both kinases mediate signaling in response to *dl*1004. Treatment of infected A-T cells with wortmannin (301) also validated a role for both ATM and ATR in this response. Finally, examining *dl*1004 infection in cells expressing a dominant negative kinase-dead form of ATR (254) revealed that only RPA32 and Chk1 were phosphorylated by ATR (Figure 2B). Together, these results show that an E4-deleted Ad infection induces ATM and ATR kinase activity, and that both PIKKs can phosphorylate substrates redundantly.

DNA repair proteins accumulate at viral replication centers

Since many DNA repair proteins accumulate at sites of DNA damage (53, 293), we wanted to determine if these cellular factors would recognize and localize to Ad replication centers. Ad replication compartments can be

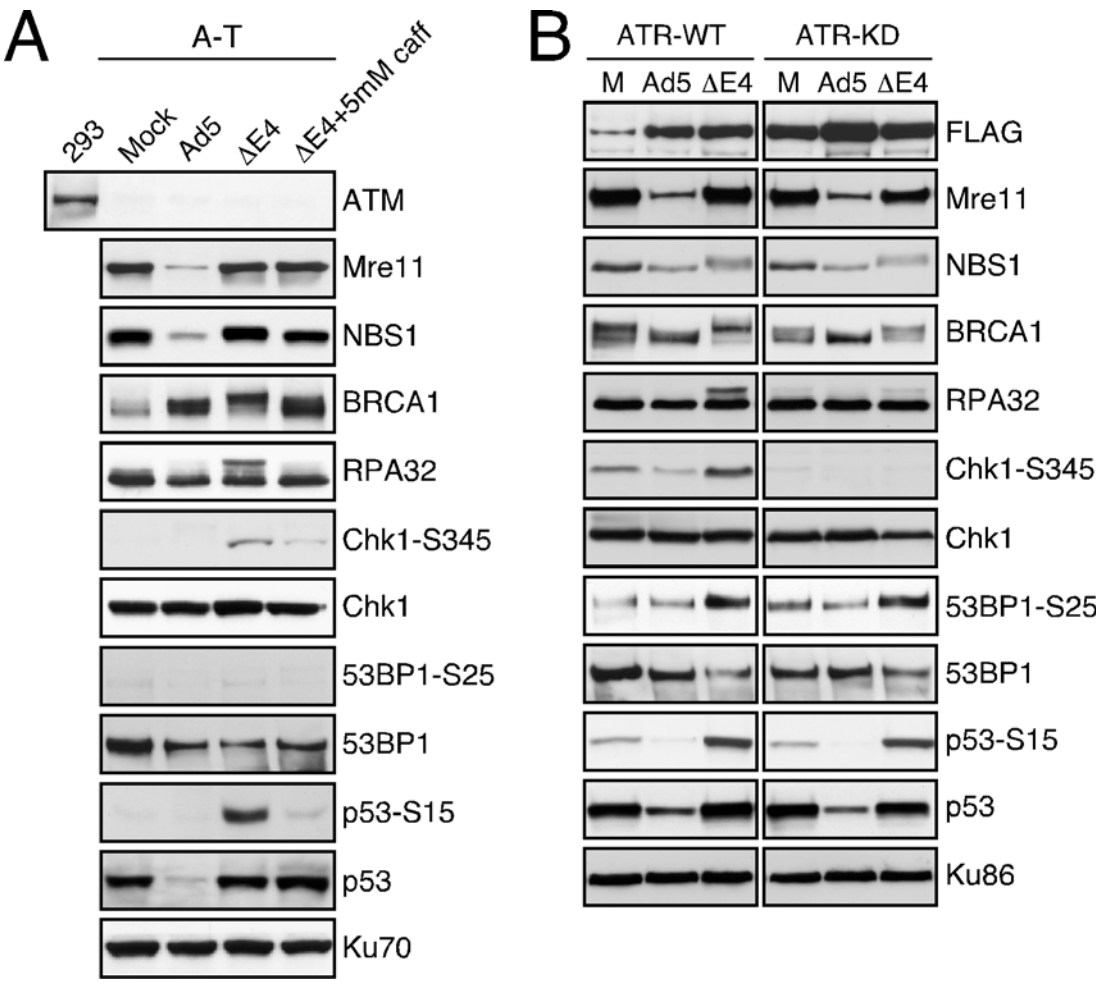

Figure 2. The DNA damage response to mutant adenovirus infection is mediated by ATM and ATR. (A) ATM deficient cells (A-T, GM5849) were infected with Ad5 or *dl*1004 (both at MOI of 50) in the absence or presence of 5mM caffeine for 30 hours before harvesting. **(B)** U2OS-based inducible cell lines expressing wild-type ATR (ATR-WT) or kinase-dead ATR (ATR-KD) were infected for 24 hours with wild-type Ad5 or *dl*1004 (both at MOI of 50) after doxycycline treatment. FLAG shows induced ATR expression. In all experiments, lysates were analyzed for the indicated proteins and Ku70 or Ku86 served as loading controls.

visualized by immunofluorescence by staining for the viral single-stranded DNA binding protein, DBP (276). After infection with *dl*1004, we observed Rad50 localization to viral centers (Figure 3A), consistent with our previous observations (335). Additionally, we found accumulation of BRCA1, 53BP1, autophosphorylated ATM, and phosphorylated H2AX (γH2AX) at *dl*1004 but not WT Ad centers (Figure 3A and data not shown). Interestingly, ATR, ATRIP, and RPA32 were all found at both WT Ad and *dl*1004 centers (Figure 3B and data not shown), likely due to the presence of single-stranded DNA in both locations. The treatment of infected A-T cells with caffeine indicated that Rad50 localization at *dl*1004 centers does not require kinase activity or γH2AX (data not shown and (50)). Similarly, MRN recruitment to DSBs also does not depend on ATM or γH2AX (53, 235). Together, our immunofluorescence and western analysis data imply that MRN functions independently and potentially upstream of ATM and ATR activity.

E1b55K mutants separate p53 and Mre11 complex degradation

Down-regulation of the Mre11 complex during Ad infection correlates with the lack of a DNA damage signaling. However, in order to determine how degradation of MRN impacts the cellular response to mutant viral infection, we needed to separate p53 from MRN down-regulation. A series of E1b55K mutant viruses were screened for those that could degrade either substrate (312, 390). Virus-induced destabilization of targets was compared to both WT

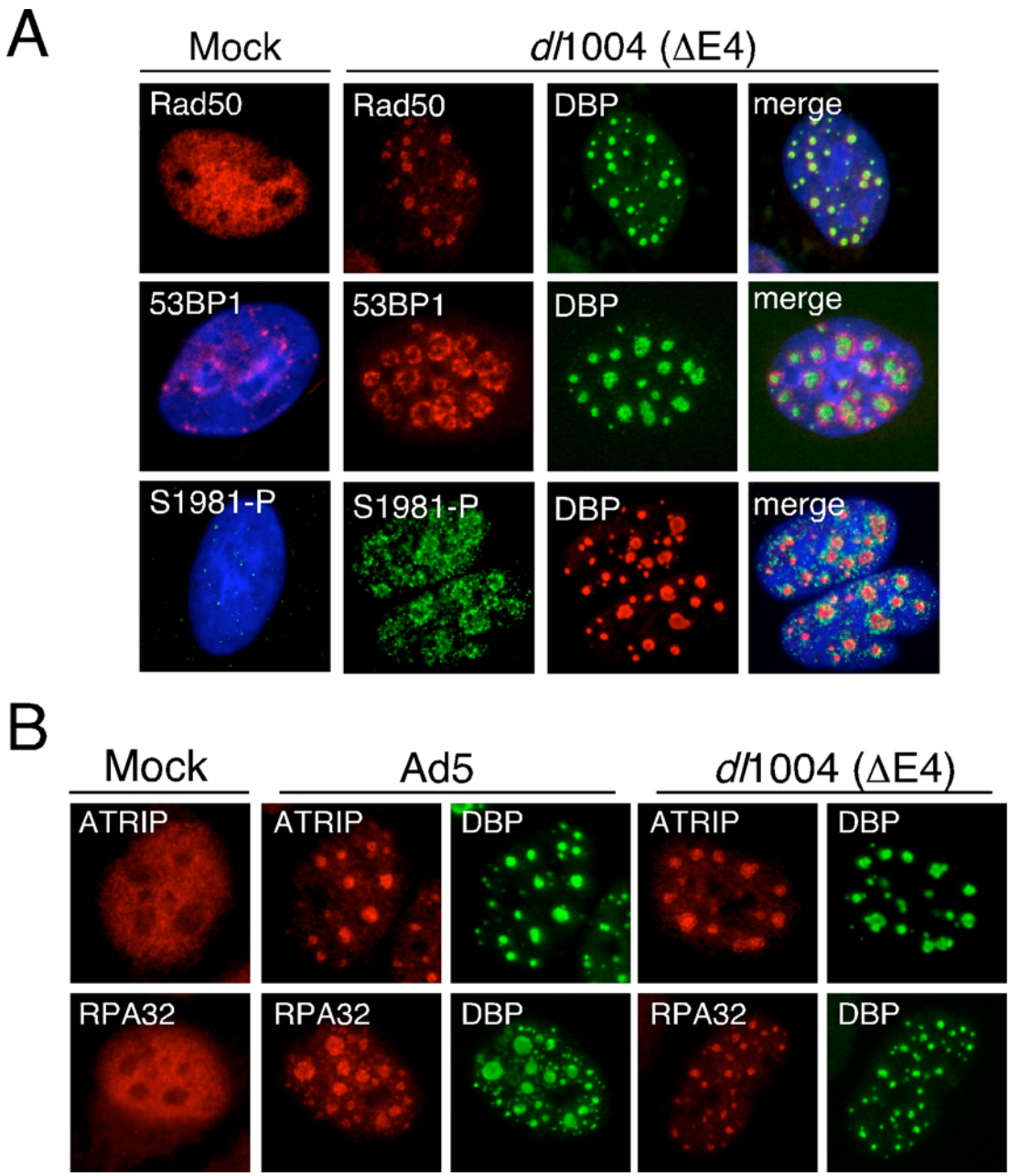

Figure 3. DNA damage response proteins localize to viral replication centers. (A) and **(B)** U2OS cells were untreated (Mock) or infected with either *dl*1004 or Ad5 (both at an MOI 25) for approximately 23 hours before fixing cells. Cells were stained for the indicated proteins by immunofluorescence. DBP marks viral replication compartments while DAPI stains nuclei. (B) shows that ATRIP and RPA proteins localize to viral replication compartments independently of MRN.

Ad infection and infection with the E1b55K-deleted virus, *dl*110. From this screen, we isolated two interesting mutants; H354 (390) exhibited defects in MRN but not p53 degradation, while R240A (312) was defective for p53 but not MRN degradation (Figure 4). These results show that E1b55K mediates substrate recognition of p53 and MRN separately.

In order to analyze substrate degradation in the absence of other viral proteins, we used retroviruses to construct HeLa and U2OS cells lines stably expressing these E1b55K mutants, or WT E1b55K and GFP as controls. E1b55K expression between these cell lines was comparable (Figure 5A). E1b55K localization in these cell lines was assessed by immunofluorescence (Figure 5B). In the absence of E4orf6, E1b55K in all cell lines formed punctate cytoplasmic foci with larger perinuclear aggregates, consistent with other reports (136, 181). The MRN complex, shown by nuclear Nbs1 staining, was unperturbed in these cell lines. Expression of E4orf6 induced nuclear retention of E1b55K in all cell lines, supporting a functional interaction between both viral proteins (294). Additionally, we saw down-regulation of MRN in the WT E1b55K and R240 cell lines, but not the GFP and H354 cell lines (Figure 5B and 5C). Cells expressing WT E1b55K and H354, but not R240A, also degraded p53 as expected (see Chapter 3). These cells lines provide a useful system to study cellular processes in the absence of p53 or MRN.

Figure 4. E1b55K mutants separate degradation of MRN and p53. U2OS cells were infected with the indicated viruses (all at MOI of 25) and harvested at the specified times. Lysates were analyzed by western for degradation of MRN or p53. Ku70 served as a loading control.

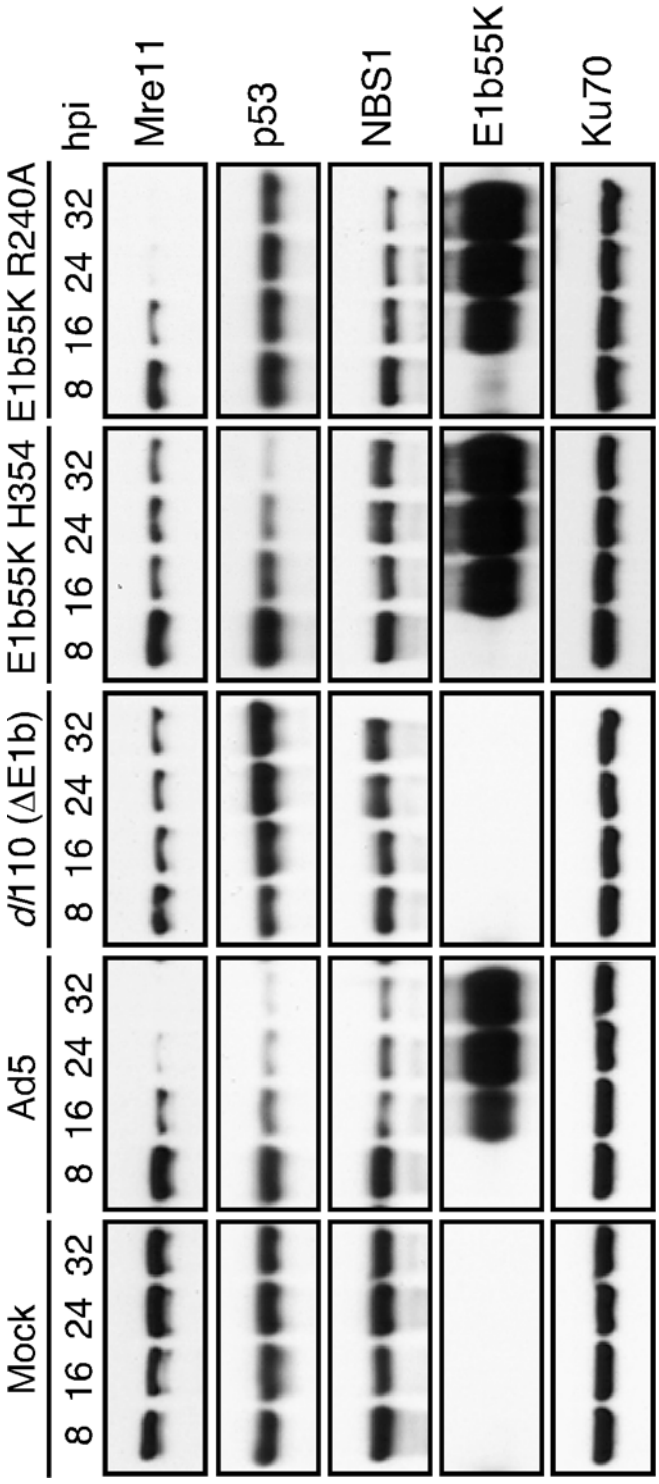
Mock
Ad5
dl110 (ΔE1b)
E1b55K H354
E1b55K R240A
hpi
8 16 24 32
Mre11
p53
NBS1
E1b55K
Ku70

Figure 5. Characterization of stable E1b55K expressing cell lines. (A) Lysates from HeLa and U2OS cells expressing GFP, wtE1b55K, or the E1b55K mutants H354 and R240A were analyzed for E1b55K expression by immunoblotting. Similar levels of E1b55K are observed between stable cell lines. Ku70 is a loading control. **(B)** Stable U2OS cell lines were analyzed by immunofluorescence for localization of E1b55K and Nbs1 in the absence (top panel) and presence (bottom panel) of rAd.E4orf6 (MOI 50). Nbs1 staining is absent from wtE1b55K and R240A expressing cells in the presence of E4orf6 because it is degraded. DAPI staining indicates the nucleus in the merged images. **(C)** Stable HeLa E1b55K expressing cells were infected with rAd.E4orf6 at an (MOI 50) for 24 hours before harvesting. Lysates were analyzed for MRN degradation and E4orf6 expression. GFP expressing cells were also infected with wild-type Ad5 as a control for degradation.

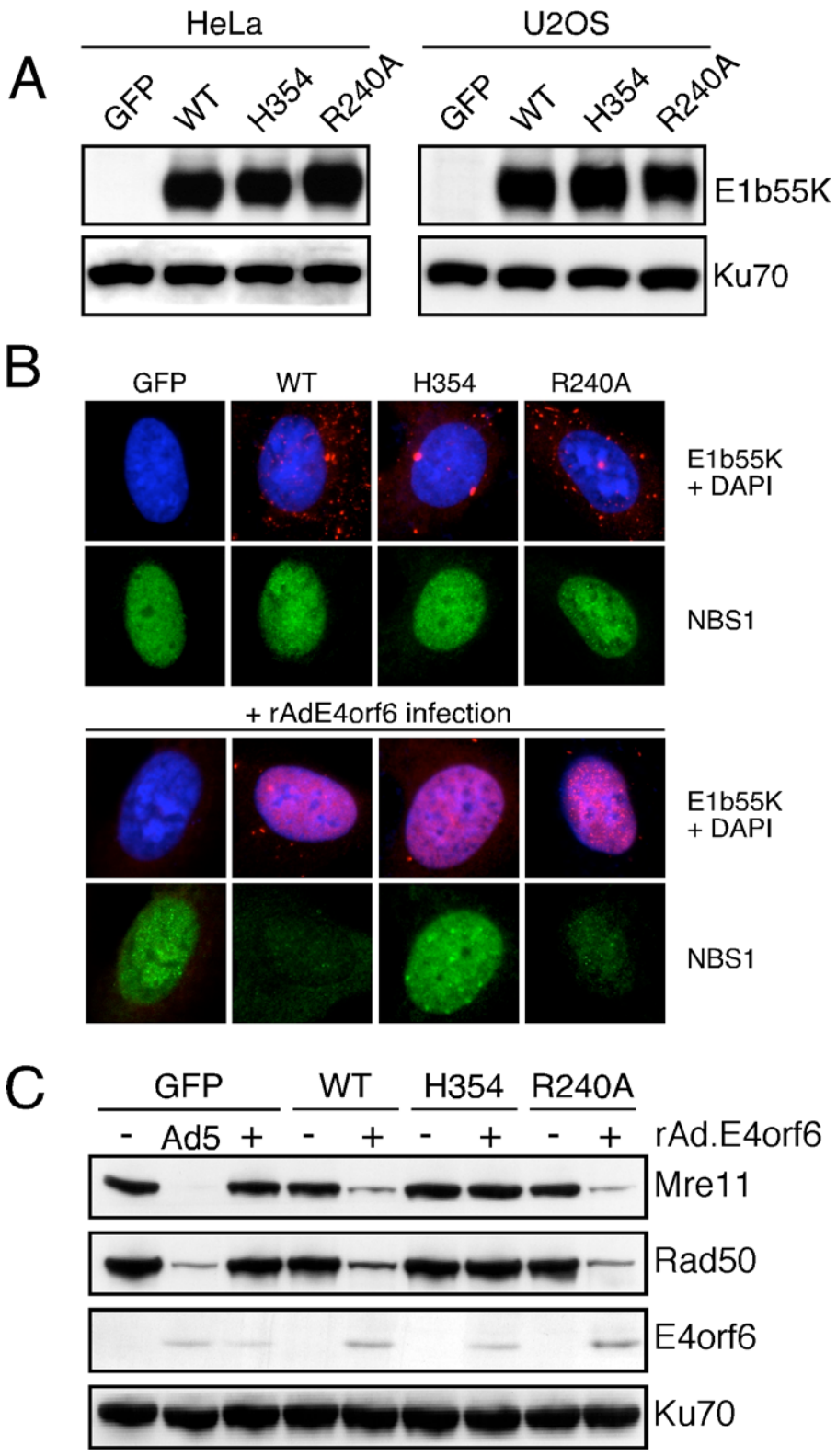
A
HeLa
U2OS
GFP
WT
H354
R240A
E1b55K
Ku70
B
GFP
WT
H354
R240A
E1b55K
+ DAPI
NBS1
+ rAdE4orf6 infection
E1b55K
+ DAPI
NBS1
C
GFP
WT
H354
R240A
- Ad5 + - + - + - +
rAd.E4orf6
Mre11
Rad50
E4orf6
Ku70

Degradation of the Mre11 complex abrogates damage signaling in response to mutant adenovirus infection

Using these E1b55K mutant cell lines, we tested whether degradation of MRN prevented damage signaling in response to mutant viral infection. The U2OS-based E1b55K expressing cell lines were infected with the E1b55K-deleted adenovirus, *dl*1016. This virus was chosen because it is also lacks E4orf3, which can mislocalize MRN proteins (335). Infection of GFP and H354 cells with *dl*1016 resulted in damage signaling, with the activation of ATM (shown by autophosphorylation of serine 1981) and phosphoryation of ATM and ATR substrates (Figure 6A). The MRN complex was present in both of these conditions. Infection of the WT E1b55K and R240A cell lines resulted in MRN degradation and loss of DNA damage signaling, comparable to WT Ad5 infection of GFP cells. Similar data were obtained from the HeLa-derived E1b55K expressing cell lines (Figure 6B). These results imply that MRN degradation, and not p53, is critical to preventing an ATM/ATR mediated damage response to mutant virus infection.

E1b55K mutants can prevent concatemer formation without degrading the Mre11 complex

We previously observed that mutant adenoviruses unable to inactivate MRN are concatemerized by the host cell (335), and this includes the E1b55K/E4orf3-deletion mutant, *dl*1016. We therefore examined whether the

Figure 6. Degradation of MRN prevents DNA damage signaling in response to mutant adenovirus infection. **(A)** U2OS E1b55K expressing cell lines were infected with wild-type Ad5 (MOI 50) or E1b55K/E4orf3 deletion mutant *dl*1016 (MOI 25) for 30 hours before harvesting. Lysates were analyzed for the indicated proteins. **(B)** HeLa E1b55K expressing cell lines were treated as in (A).

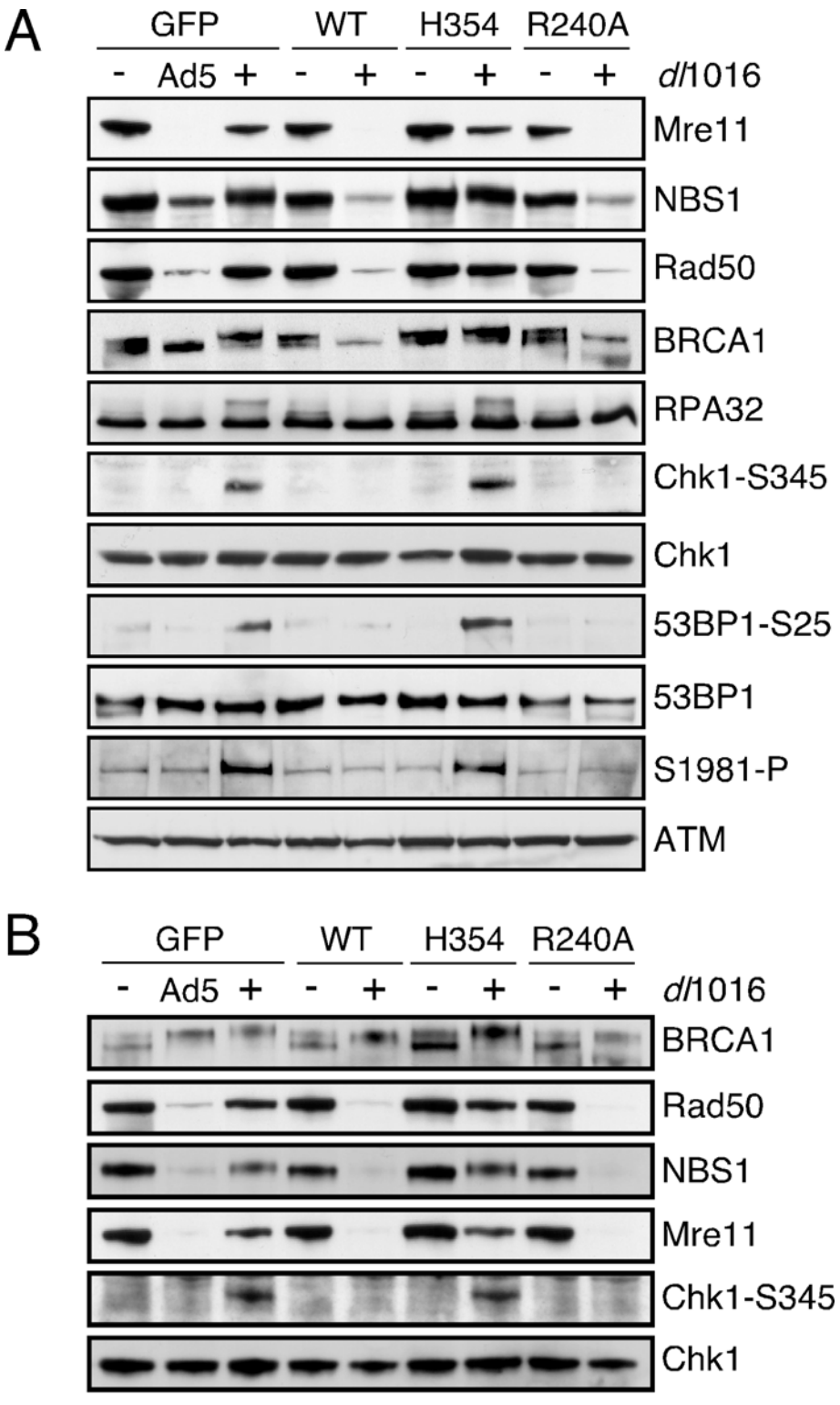
A
GFP
WT
H354
R240A
- Ad5 + - + - + - + d/1016
Mre11
NBS1
Rad50
BRCA1
RPA32
Chk1-S345
Chk1
53BP1-S25
53BP1
S1981-P
ATM
B
GFP
WT
H354
R240A
- Ad5 + - + - + - + d/1016
BRCA1
Rad50
NBS1
Mre11
Chk1-S345
Chk1

E1b55K mutants H354 and R240 could prevent mutant viral genome concatemerization. The U2OS-based cell lines expressing GFP and the E1b55K mutants were infected with *dl*1016 and viral DNA was analyzed for concatemers. Surprisingly, we found that all E1b55K mutant cell lines lacked concatemers, including H354, which does not degrade MRN (Figure 7). Similar results were obtained with HeLa-based cell lines (see Chapter 3). Concatemers still form in the absence of p53 (335), suggesting that p53 down-regulation by E1b55K/E4orf6 is dispensable for preventing concatemers. Therefore, the H354 mutant retains another activity that inhibits mutant viral genome concatemerization (see Discussion and Chapter 3).

MRN degradation prevents ATM activation and damage signaling in response to DNA double-strand breaks

The lethality of null MRN mutations in mammalian cells has precluded exact determination of MRN's role in DNA damage signaling (217, 384). Our E1b55K mutant cell lines allow transient removal of MRN to study its potential functions. Since our data suggested that MRN was required for ATM and ATR signaling in response to mutant virus infection, we wanted to address whether it was also necessary for the damage response to DNA DSBs. We infected the U2OS-based E1b55K cell lines with rAd.E4orf6 for 24 hours to induce degradation of cellular targets before treating cells with 10 Gy of irradiation (IR). Two hours after treatment, cells were analyzed by immunoblotting and

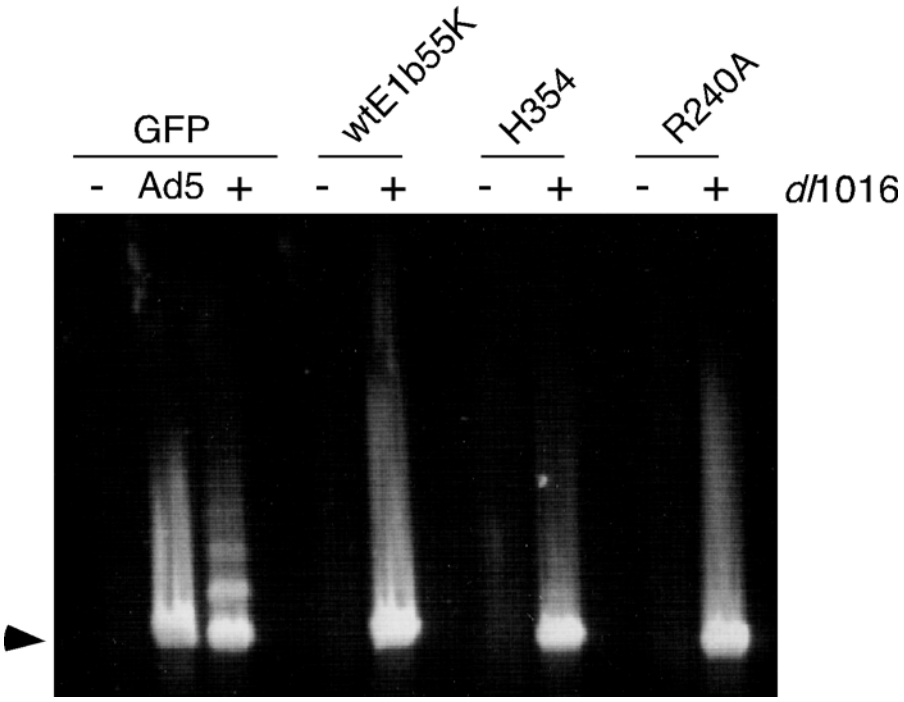

Figure 7. H354 can prevent concatemerization of mutant adenoviral genomes without degrading MRN. U2OS-based E1b55K expressing cells were infected with Ad5 or *dl*1016 (both at an MOI 25) for approximately 30 hours. Cells were harvested and prepared for analysis of viral DNA by pulse-field gel electrophoresis according to Materials and Methods. Arrowhead indicates monomeric adenoviral genome.

immunofluorescence for activation of a DNA damage response (Figure 8A and 8B). Treatment of the GFP and H354 cell lines with IR induced autophosphorylation of ATM and the phosphorylation of Nbs1, BRCA1, Chk2, and 53BP1 (Figure 8A). These events were absent in the WT E1b55K and R240A cell lines where MRN was degraded. Foci of autophosphorylated ATM also failed to form after damage when MRN was down-regulated in the WT E1b55K expressing cell line (Figure 8B). These data suggest that MRN is required for ATM activation and a cellular DNA damage response to DSBs. In support of this, we observed that ATM activation and damage signaling after mutant viral infection or DNA damage were highly abrogated in A-TLD1 cells (50), where the MRN complex is destablilized (330).

E1b55K and E4orf6 affect S phase cell cycle progression in an MRN independent manner

In order to further understand how E1b55K and E4orf6 affect cellular responses, we examined their influence on cell cycle progression and checkpoints. Induced E4orf6 expression in a 293-based cell line (which expresses E1A and E1b proteins) was previously found to disrupt S phase cell cycle progression by stimulating S phase entry and inhibiting S phase exit (139). We wanted to determine whether E1b55K and E4orf6 were sufficient for this effect, and whether MRN degradation was involved. HeLa-based E1b55K expressing cells infected with rAd.E4orf6 were analyzed for their DNA content

Figure 8. Degradation of MRN prevents ATM activation and a DNA damage response to double-strand breaks. (A) U2OS-based E1b55K expressing cells were infected with rAd.E4orf6 (MOI 50) for 24 hours before treating cells with 10Gy of irradiation (IR). Two hours post-IR cells were harvested for analysis of lysates by immunoblotting. **(B)** U2OS E1b55K expressing cells were infected as in (A). One hour after treatment with 10Gy IR, cells were fixed for immunofluorescence and stained for the indicated proteins. DAPI marks cell nuclei.

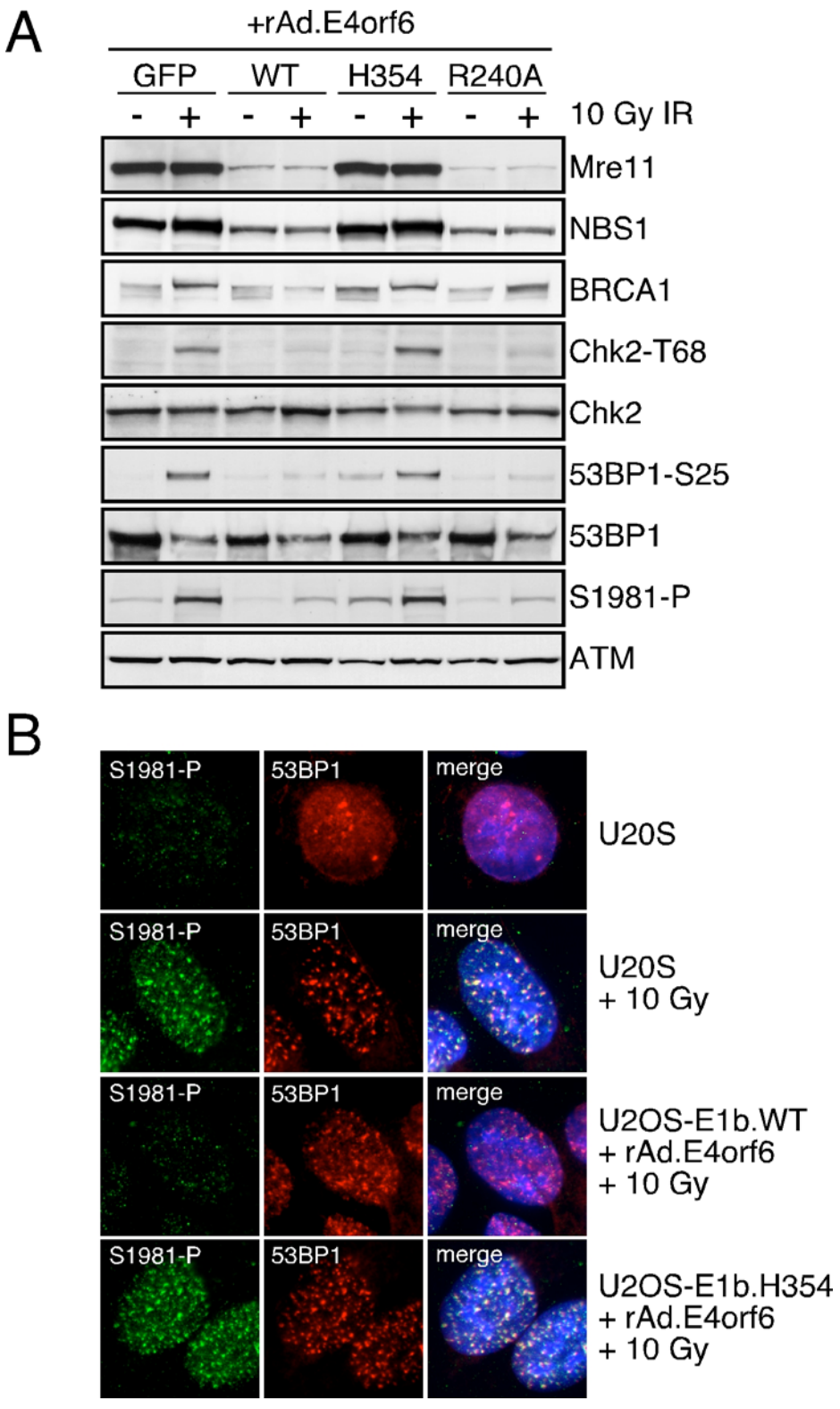
A
+rAd.E4orf6
GFP
WT
H354
R240A
- + - + - + - +
10 Gy IR
Mre11
NBS1
BRCA1
Chk2-T68
Chk2
53BP1-S25
53BP1
S1981-P
ATM
B
S1981-P
53BP1
merge
U20S
U20S
+ 10 Gy
U2OS-E1b.WT
+ rAd.E4orf6
+ 10 Gy
U2OS-E1b.H354
+ rAd.E4orf6
+ 10 Gy

over time (Figure 9A). Cell cycle progression was not affected by E4orf6 or E1b55K alone (Figure 9A and data not shown). However, E4orf6 expression in the WT E1b55K cell line increased the number of S phase cells at 24 hours, implying that E1A is not required. At later times, this population gradually moved through S, and then G2 by 48 hours. Interestingly, H354 and R240A expressing cells with E4orf6 also displayed this phenotype, suggesting that it is independent of MRN and p53 degradation. Addition of a control recombinant Ad (rAd.LacZ) to WT E1b55K expressing cells did not alter S-phase progression (Figure 9B). These cell cycle effects were also seen in the U2OS-based cell lines (data not shown) and IMR90 cells (Figure 9C), indicating that they are independent of cell type.

The perturbed S phase progression in the E4orf6-inducible 293-based cell line was previously associated with post-transcriptional down-regulation of cyclin A (139). We therefore examined the steady state level of cyclin A in the E1b55K cell lines in the presence or absence of E4orf6 (Figure 9D). Intriguingly, we did not observe consistent changes in cyclin A in lysates from any of the E1b55K cell lines with or without E4orf6. This was true for both U2OS and HeLa-based E1b55K expressing cell lines (Figure 9D and data not shown). The cyclin A effects in the 293-based cell line, therefore, might be cell type specific or somehow involve E1A. E4orf6 expression in the 293-based cell line also resulted in inactivation of the cdc2 kinase (139), potentially

Figure 9. E1b55K/E4orf6 alter S phase progression in an MRN and cyclin A independent manner. (A) E1b55K together with E4orf6 alter S phase progression in an MRN independent manner. WT or mutant E1b55K expressing HeLa cells were infected with rAd.E4orf6 (MOI 50) for the indicated time points before harvesting and fixing. Cells were analyzed for DNA content according to Materials and Methods. **(B)** HeLa cells expressing wtE1b55K were mock treated or infected with either rAd.lacZ or rAd.E4orf6 (both MOI 50) for 24 hours before harvesting and fixing. DNA content was analyzed as in (A). **(C)** Cell cycle effects of E1b55K/E4orf6 are not cell type dependent. IMR90 cells were mock treated or infected with rAd.E1b55K (MOI 2), rAd.E4orf6 (MOI 50), or both viruses for 24 hours before harvesting and analysis of cell cycle content. Top panel represents a cell cycle profile from rAd.E1b55K infection, though this result was the same for mock treated cells, and cells infected with rAd.E4orf6. Bottom panel represents the cell cycle profile of IMR90s infected with both viruses. **(D)** Cell cycle effects of E1b55K/E4orf6 are not due to differences in cyclin A levels. U2OS cells, U2OS GFP expressing cells, or U2OS based E1b55K expressing cells were infected with rAd.E4orf6 (MOI 50) for approximately 24 hours before cells were harvested. Lysates were analyzed for cyclin A expression and Ku86 (loading control).

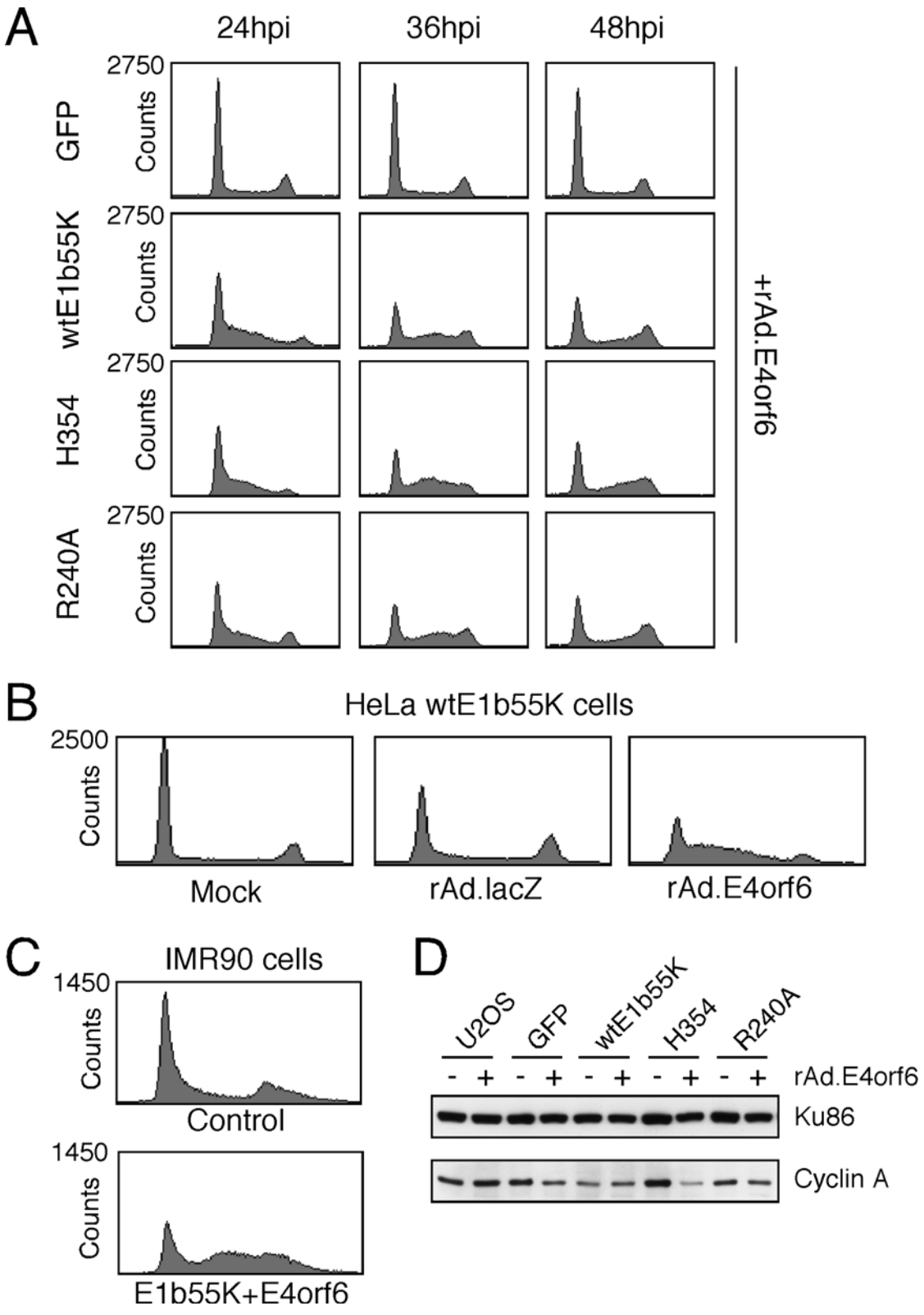
A
24hpi
36hpi
48hpi
2750
Counts
GFP
wtE1b55K
H354
R240A
+rAd.E4orf6
B
HeLa wtE1b55K cells
2500
Counts
Mock
rAd.lacZ
rAd.E4orf6
C
IMR90 cells
1450
Counts
Control
E1b55K+E4orf6
D
U2OS
GFP
wtE1b55K
H354
R240A
- + - + - + - + - +
rAd.E4orf6
Ku86
Cyclin A

delaying S-phase exit. We currently do not know how this kinase is affected in the E1b55K mutant cell lines. More detailed characterization of S phase populations and cell cycle effectors is required to understand these phenotypes.

Degradation of MRN by E1b55K/E4orf6 abrogates the early G2/M checkpoint

MRN has already been implicated in the intra-S phase checkpoint in response to damage (78, 117, 350). The role of MRN in other checkpoints, such as the G2/M checkpoint, has been less clear partly because of the use of hypomorphic cell lines (43, 373, 386, 387). The G2/M checkpoint can be divided into early and late phases (387). Within the first 60-90 minutes following IR, cells in G2 are prevented from entering mitosis. At later times after IR, cells damaged in S phase accumulate in G2 until their damage is repaired or they escape (see below). The early G2/M checkpoint has been shown to be ATM dependent, while later G2 accumulation is not (387), although escape from this later checkpoint appears to require an intact intra-S phase checkpoint (387).

Since our data suggested that MRN was required for ATM activation and a DNA damage response to DSBs, removing MRN should abrogate ATM induction of the early G2/M checkpoint. To test this, HeLa-based E1b55K cell lines were infected with rAd.E4orf6 for approximately 48 hours to degrade

cellular substrates, and were then treated with 10 Gy of IR (see Figure 10A for experimental design). One hour later, cells were harvested, fixed, stained for DNA content and the mitotic marker phospho-histone H3 (386, 387), and analyzed by fluorescence activated cell sorting (Figure 10B and 10C). We noticed that in the presence of E4orf6 (without IR), the E1b55K cell lines displayed lower mitotic index (Figure 10B, top panels), likely due to the effects noted in Figure 9. In the absence of E4orf6, all cell lines demonstrated an intact G2/M checkpoint after IR, indicating that E1b55K alone has no effect on this checkpoint (Figure 10C, left side). However, when E4orf6 was expressed in the WT E1b55K or R240A cell lines where MRN is degraded, the early G2/M checkpoint was abrogated and cells continued to enter mitosis (Figure 10C, right side). GFP and H354 cells infected with E4orf6 still displayed an intact checkpoint, consistent with the presence of MRN. Addition of nocodazole immediately after IR treatment to trap cells in mitosis increased the background number of mitotic cells, but showed the same trend (Figure 11); when the G2/M checkpoint is intact, the 20-30% drop in cells entering mitosis with nocodazole roughly mirrors the ~30% of cells seen entering mitosis in Figure 10C. We also found that abrogation of the early G2/M checkpoint occurred over multiple doses of irradiation (Figure 12) and also occurred in IRM90 cells (Figure 13), indicating that the effects are not specific to HeLa cells. The molecular basis for the difference between R240A and WT

Figure 10. MRN is required for the G2/M checkpoint in response to DNA double-strand breaks. (A) Experimental set-up for analysis of the early G2/M checkpoint in E1b55K expressing cells. **(B)** HeLa-based E1b55K expressing cells were infected for 48 hours with rAd.E4orf6 (MOI 50) before treatment with 10 Gy of irradiation (IR). Cells were treated according to Materials and Methods and analyzed by FACS for DNA content (x-axis) and histone H3 phosphorylation (y-axis), a marker for mitotic cells. A representative FACS experiment is shown with the percent of mitotic cells indicated below the encircled population. **(C)** Graphical representation of the early G2/M assay results. The change in the number of mitotic cells one hour after IR is indicated by the graph. The number of mitotic cells is presented as a percentage of unirradiated mitotic cells. The mean and standard deviation are shown for the results of three independent experiments for each condition.

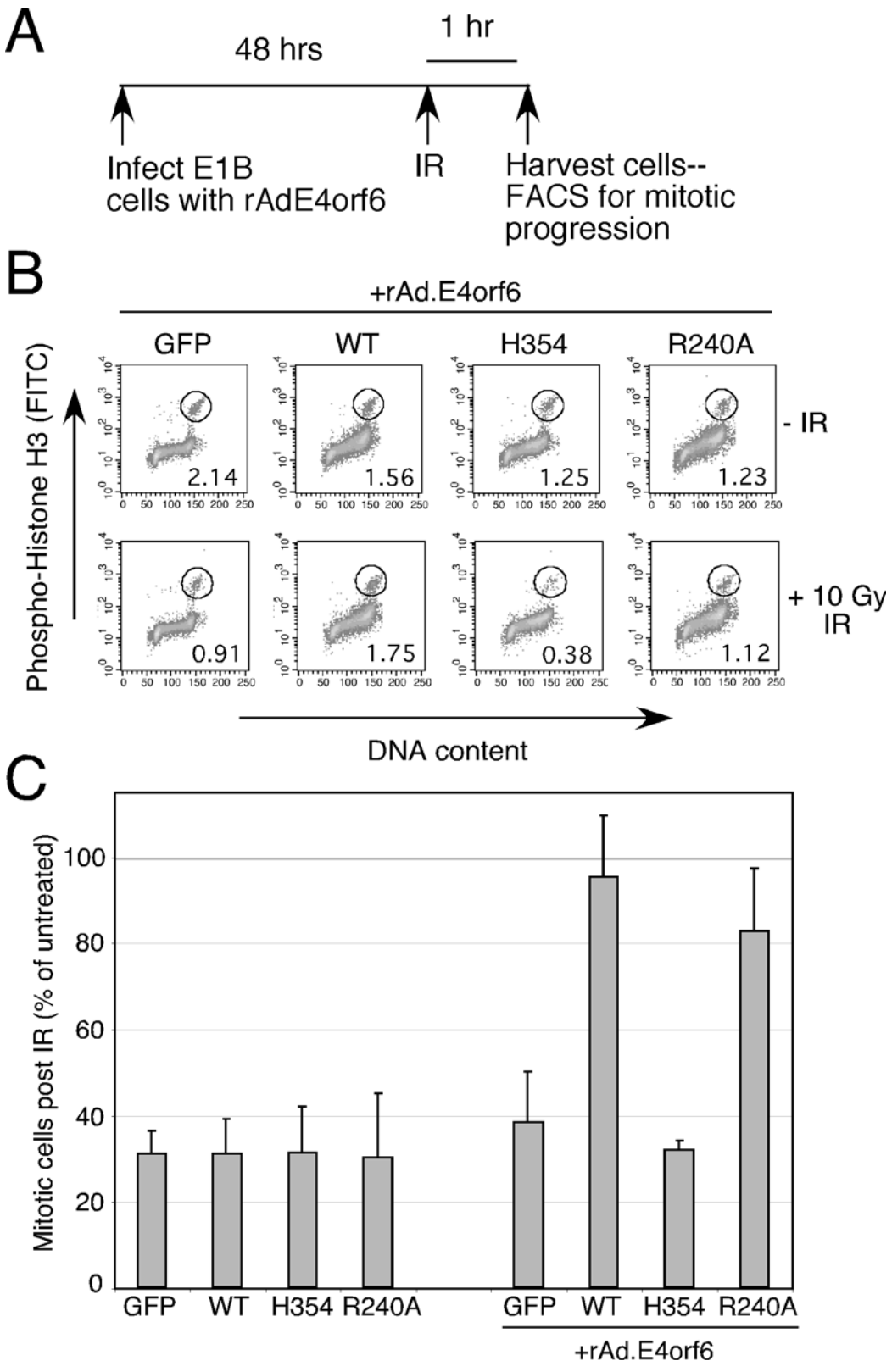
A
48 hrs
1 hr
Infect E1B cells with rAdE4orf6
IR
Harvest cells-- FACS for mitotic progression
B
+rAd.E4orf6
GFP
WT
H354
R240A
- IR
+ 10 Gy IR
2.14
1.56
1.25
1.23
0.91
1.75
0.38
1.12
Phospho-Histone H3 (FITC)
DNA content
C
Mitotic cells post IR (% of untreated)
0
20
40
60
80
100
GFP
WT
H354
R240A
GFP
WT
H354
R240A
+rAd.E4orf6

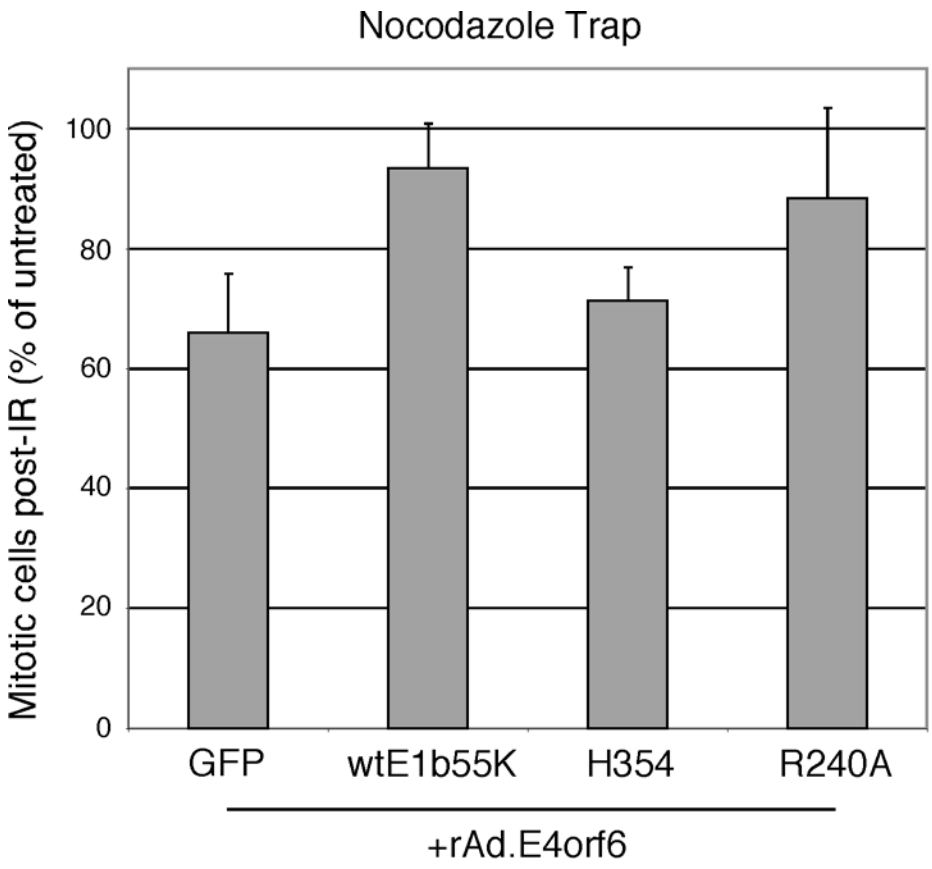

Figure 11. Analysis of the G2/M assay by nocodazole trap. Stable HeLa E1b55K expressing cell lines were infected with rAd.E4orf6 (MOI 50) for 48 hours before treatment with 10Gy IR. Nocodazole (0.2μg/mL) was added immediately after treatment. Cells were harvested and fixed one hour post-IR. Mitotic cells were quantitated by FACS according to Materials and Methods. The graph illustrates mitotic cells after IR as a percentage of untreated mitotic cells. Data represent the mean and standard deviation of three independent experiments, with the exception of R240A, which was analyzed in two independent experiments.

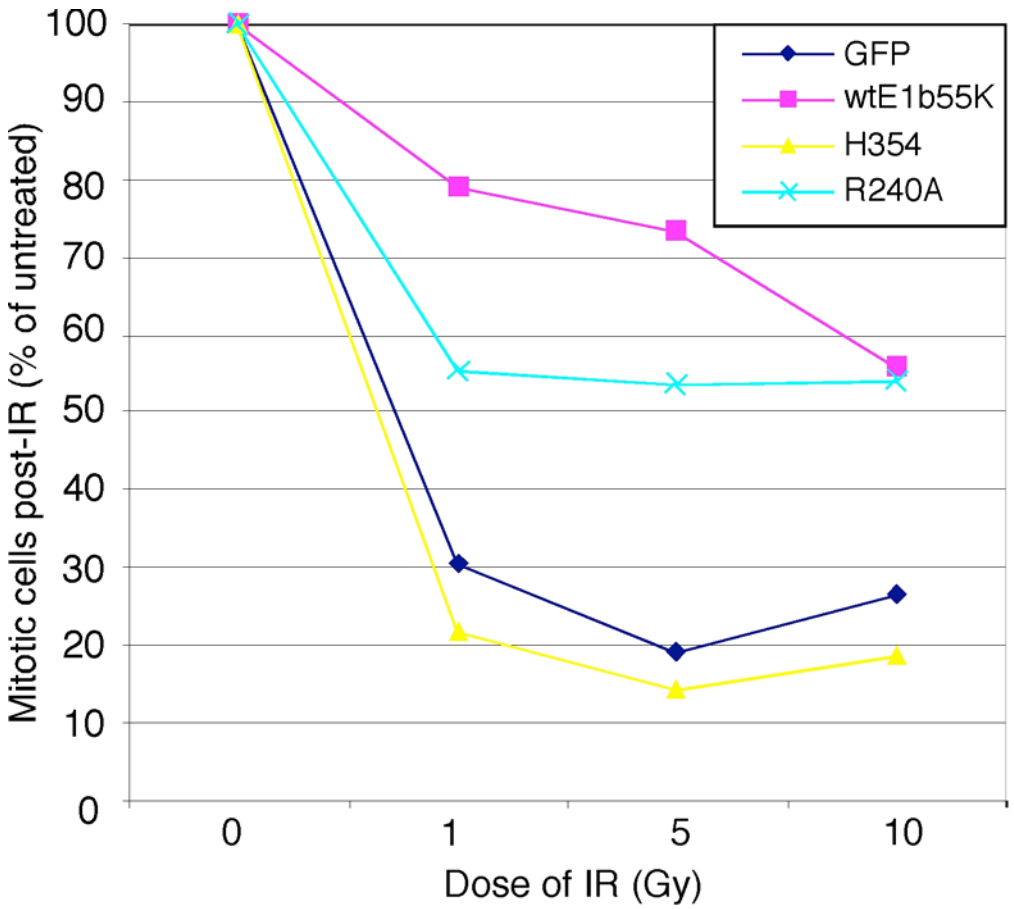

Figure 12. The early G2/M checkpoint is abrogated over multiple doses of irradiation. HeLa E1b55K expressing cell lines were infected with rAd.E4orf6 (MOI 50) for 48 hours before treating with the indicated doses of irradiation (IR). One hour post-treatment, cells were harvested, fixed, and analyzed by FACS according to Materials and Methods. The percent of mitotic cells post-IR is graphed as a function of IR dose.

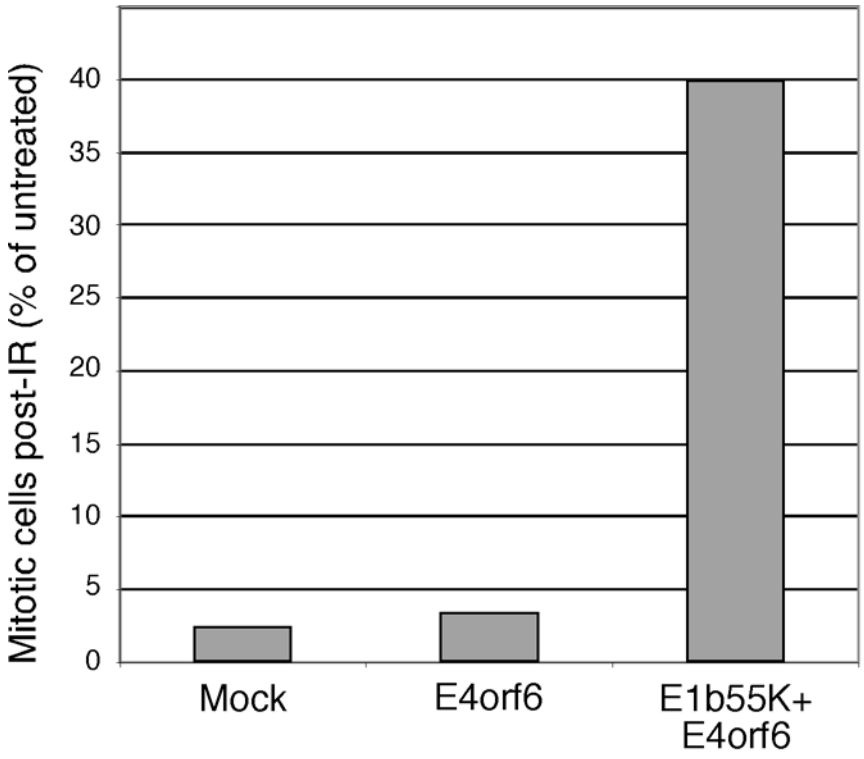

Figure 13. Abrogation of the G2/M checkpoint is cell line independent. IMR90 cells were infected with rAd.E4orf6 (MOI 50) and rAd.E1b55K (MOI 2) for 48 hours before treatment with 10Gy of IR. One hour post-IR, cells were harvested and fixed before staining for FACS analysis according to Materials and Methods. Graph represents mitotic cells after IR as a percent of untreated mitotic cells. Data from one representative experiment is shown.

E1b55K cells in the IR dose response curve (Figure 12) is currently unclear. Finally, analysis of lysates from cells subjected to the early G2/M checkpoint assay also showed that ATM activation and damage signaling was diminished in the absence of MRN (Figure 14), consistent with the results in Figure 6 where MRN had been degraded for 24 hours prior to IR. An increase in the basal level of Chk1 phosphorylation was noted in the E1b55K cell lines with E4orf6, perhaps due to the cell cycle effects shown in Figure 9. Together, these data demonstrate that MRN is required for the ATM dependent early G2/M checkpoint in response to IR.

Effects of E1b55K/E4orf6 on G2 accumulation after damage

We next tried to examine how degradation of cellular substrates might impact G2 accumulation after DNA damage, an ATM independent activity (387). As above, cells irradiated in S phase will accumulate in G2 for longer periods of time until presumably the damage is repaired or they escape (387). Cells with intra-S phase checkpoint defects are particularly sensitive to damage and remain in G2 longer than normal cells (387), perhaps to compensate for lack of the former checkpoint. Since MRN is required for the intra-S phase checkpoint (78, 117, 350), absence of MRN should induce a longer G2 accumulation after damage (387). To test this, E1b55K cell lines were infected with rAd.E4orf6 for 24 hours before treatment with 4 Gy IR (see Figure 15A for experimental design). A lower dose of damage was used to

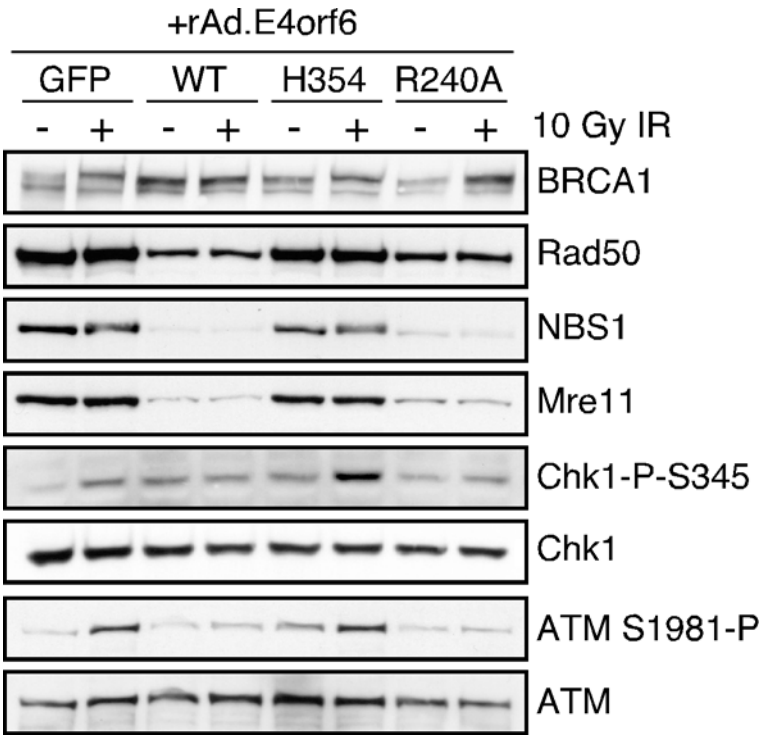

Figure 14. Degradation of MRN prevents ATM activation during the G2/M checkpoint response. Lysates from HeLa E1b55K cell lines used in Figure 17 were analyzed for the indicated proteins by immunoblotting. Phosphorylation is indicated by mobility shifts (BRCA1 and Nbs1) or by phospho-specific antibodies (Chk1 and ATM).

allow for cellular recovery, and DNA content was then analyzed 12-24 hours after treatment. Figure 15B shows that in the absence of E4orf6, WT E1b55K expressing cells exhibit a G2 accumulation 12 hours post-IR, but then recover to a normal cell cycle profile by 24 hours. This was also true for the other E1b55K cell lines, and for GFP expressing cells in the presence of E4orf6. The WT E1b55K and H354 cell lines displayed a different trend in the presence of E4orf6. While control samples at 12 hours post-IR demonstrated a predominant G2 peak, the majority of WT E1b55K and H354 cells were in late S and G2. By 24 hours post-IR when the control cells had recovered, WT E1b55K cells with E4orf6 were still stuck in G2. In contrast, H354 cells began to show some recovery though it was not as complete as control cells. Although these data require follow-up, they support the notion that elimination of cellular factors required for DNA repair and the intra-S phase checkpoint may prevent the cell from recovering from damage. However, the phenotypes seen in these experiments may not be completely related to MRN since H354 cells with E4orf6 still displayed reduced recovery from damage.

Discussion

In this Chapter we examined the relationship between adenovirus and the cellular DNA damage response. Previous work from our lab and others showed that DNA-PKcs, DNA Ligase IV and MRN were required for mutant

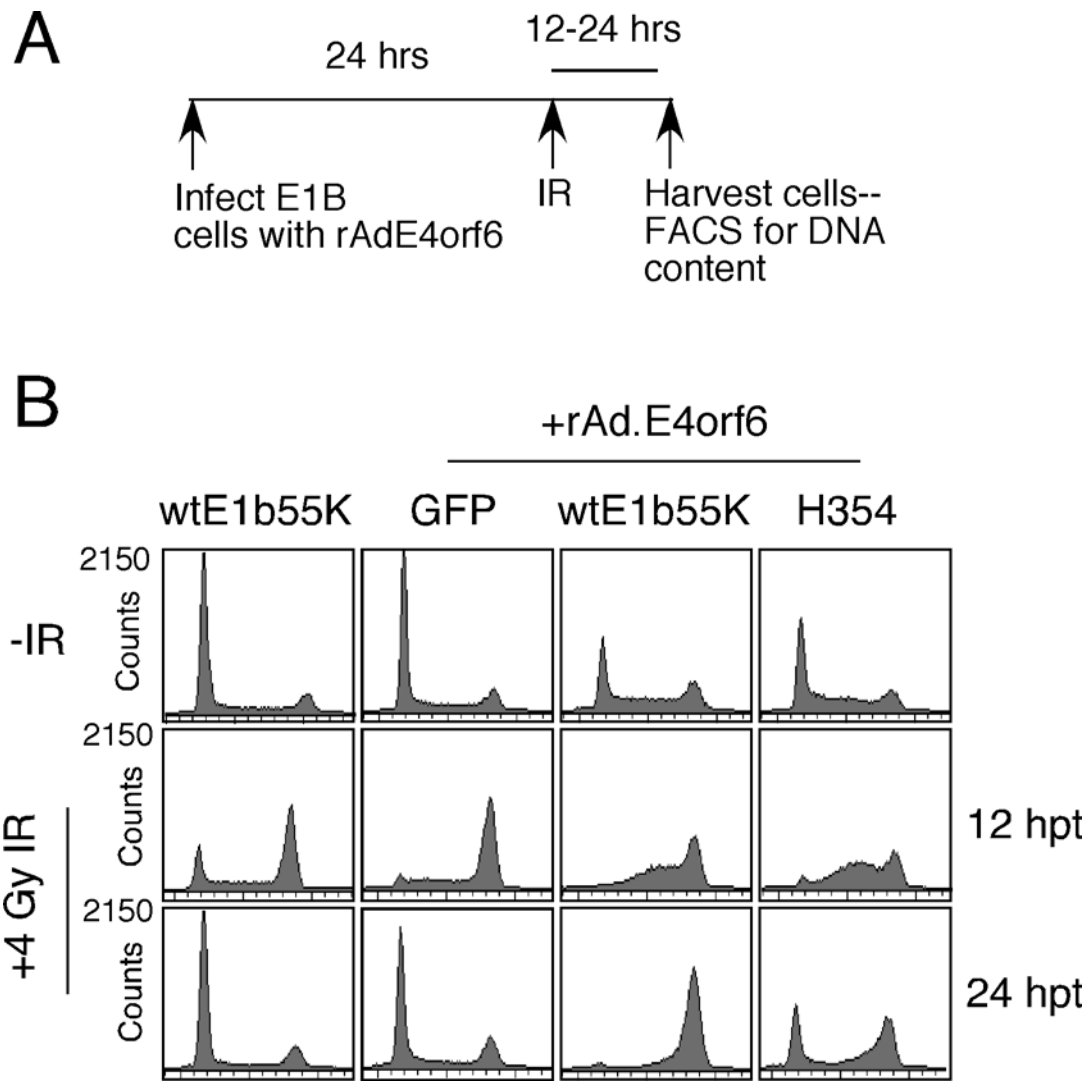

Figure 15. Effects of E1b55K/E4orf6 on G2 accumulation after DNA damage. **(A)** Schematic for experimental set-up for G2 accumulation. **(B)** HeLa based E1b55K expressing cells were infected with rAd.E4orf6 (MOI 50) for 24 hours before treating cells with 4 Gy of irradiation. Cells were then harvested at 12 and 24 hours post-treatment for analysis of DNA content according to Materials and Methods.

adenoviral genome concatemerization (30, 335). Because of this, we postulated that infection with a mutant adenovirus might trigger DNA damage response signaling cascades. Indeed, we observed ATM and ATR kinase activity in response to *dl*1004, and the accumulation of DNA repair proteins at these mutant viral replication compartments. While we noted that disruption of PIKK signaling can prevent mutant viral genome concatemerization (S.S. Lakdawala, *et al.*, submitted), it is currently unclear which events are necessary for this process. However, these data are consistent with a requirement of MRN and ATM in the repair of complicated DNA lesions (286), structures that may somehow resemble Ad genome termini.

Damage signaling and viral genome concatemerization do not normally occur during WT Ad5 infection (50, 335). Since MRN is degraded under these conditions (50, 335), we wished to determine how it affected the cellular response to mutant virus infection. By screening a series of E1b55K mutant viruses, we found mutants that distinguished between p53 and MRN degradation, allowing us to separate these functions (discussed further in Chapter 3). Constructing cell lines expressing these E1b55K mutants allowed us to analyze the effects of MRN degradation on cellular responses. With these tools we showed that MRN down-regulation, but not p53, was required to prevent the ATM and ATR mediated DNA damage response to virus infection. Interestingly, the E1b55K mutant, H354, could still inhibit mutant viral

genome concatemerization despite the presence of MRN and DNA damage signaling. Concatemerization requires DNA Ligase IV (335), and E1b55K/E4orf6 was recently found to degrade this factor (8). Examination of the E1b55K mutants revealed that H354 could degrade DNA Ligase IV (R.A. Schwartz, *et al.*, submitted) (see Chapter 3), providing another mechanism to prevent concatemerization. The fact that E1b55K/E4orf6 employ multiple strategies to prevent this host cell response demonstrates its importance to the viral lifecycle.

E4-deleted adenoviruses have other deficiencies besides concatemer formation. They are defective for viral DNA replication, viral mRNA export, and viral late protein synthesis (reviewed in (123, 313, 343, 364)). How the E1b55K/E4orf6 complex contributes to these other functions is not completely clear, but degradation of MRN may partially explain some phenotypes. Using our separation-of-function E1b55K mutants and deficient cell lines, we have shown that MRN can inhibit viral DNA replication independently of concatemer formation (S.S. Lakdawala, *et al.*, submitted), in agreement with other reports (112, 113, 229). While we postulate that the nuclease activity of Mre11 will inhibit viral DNA replication like it promotes concatemerization (335), perhaps by cleaving the 5' terminal protein primer on Ad genomes (335), it is clear that MRN has additional functions that inhibit viral DNA synthesis without affecting concatemers (S.S. Lakdawala, *et al.*, submitted). Unfortunately, viral DNA

replication defects due to MRN may contribute to down-stream effects on viral mRNA metabolism and late protein synthesis, complicating the analysis of mutants. While it is unclear how viral mRNA export is affected directly, our E1b55K mutants that cannot degrade MRN do not support efficient viral late protein synthesis (Appendix Figure 1 and data not shown).

Using the E1b55K cell lines, we examined the role of MRN in the response to DNA DSBs. Nbs1 is an established target of ATM after damage (78, 195). However, at the time of this research there were indications that MRN may function upstream of ATM (271), although evidence was lacking in the absence of a null mammalian system. By degrading MRN with our viral proteins, we showed that it was required for ATM activation (measured by the autophosphorylation on serine 1981) and signaling in response to IR. We validated our results by examining the damage response in A-TLD1 cells, which express a truncated Mre11 protein unable to stably complex with Rad50 and Nbs1. While A-TLD1 cells are hypomorphic, we saw abrogated damage signaling in response to mutant virus infection and DSBs compared to matched, WT Mre11 expressing cells (50). The requirement of MRN for full ATM activation was also published by another group around the same time (351), and since then, this observation has been validated in a number of systems (195).

Interestingly, our data with mutant viral infection also suggested that MRN was required for ATR signaling. ATR responds to multiple types of lesions within cells, which commonly include single-stranded DNA (411). ATR activation in response to DSBs has now been shown to require MRN (3, 164, 242). The nuclease activities of MRN and CtIP appear to regulate DSB processing to produce ssDNA (164, 205, 243, 303), which RPA, ATRIP, and ATR localize to. Interestingly, we found that during WT Ad5 replication, ATR, ATRIP, and RPA translocated to viral centers independently of MRN, at sites that overlap with viral ssDNA (276). ATR signaling does not occur under these conditions, however, which suggests that another function of MRN stimulates ATR activation. Concatemerization of mutant viral genomes also required Mre11 nuclease activity (335). It will be important to determine if these Mre11 or CtIP functions contribute to ATR activity despite the presence of single-stranded viral DNA.

We also examined the effects of E1b55K/E4orf6 on cell cycle progression and checkpoints. Previous work from our lab implicated the adenoviral E1 proteins and E4orf6 in the perturbation of S phase in the absence of DNA damage (139). Following up on this, we found that E1b55K together with E4orf6 were sufficient for these effects in many cell types. Interestingly, this also occurred independently of p53 or MRN degradation, since S phase progression was altered in all E1b55K mutant cell lines. Cyclin

A down-regulation accounted for some of the effects in the previous work (139), but was not altered in a consistent manner in our experiments. This suggests that E1b55K and E4orf6 employ other mechanisms to alter S phase. We currently do not know whether these are indirect effects of an inability to repair DNA (perhaps from DNA Ligase IV degradation) or whether specifc cell cycle proteins are targeted. It is interesting to note, however, that E1b55K and E4orf6 are required to overcome cell cycle restriction of Ad replication (134, 135). E1b55K was also recently implicated in cyclin E upregulation during adenovirus infection (407). Future studies that ellucidate the mechanism by which E1b55K/E4orf6 disrupt the cell cycle will be important to determining whether these observations are linked.

While MRN is required for the intra-S phase checkpoint (78, 117, 350), a role for MRN in the early ATM-dependent G2/M checkpoint (387) was controversial at the time of our studies (43, 373, 386, 387). Using our degradation system we demonstrated that absence of MRN abrogated this checkpoint, supporting the requirement of MRN for ATM activation. Late G2 accumulation is independent of ATM, occurs is cells damaged during S phase, and is exacerbated in cells deficient of S-phase checkpoints (387). Surprisingly, we found no phenotype for E4orf6 alone in our assays, despite its ability to radiosensitize cells and prevent double-strand break repair (147). Instead, we found pronounced G2 accumulation in damaged cells with both

E1b55K/E4orf6, suggesting defects in S phase checkpoints or repair. Although degradation of MRN may contribute to this phenotype, other E1b55K/E4orf6 functions are also responsible since H354 cells (that do not degrade MRN) did not recover completely. Degradation of p53 is an unlikely candidate since these experiments were performed in HeLa cells and p53 is not required for G2 accumulation (387). Rather, this phenotype might be due to the viral S phase effects (Figure 9), or degradation of other factors such as DNA Ligase IV, which would prevent DNA repair (see Chapter 3). These viral proteins may therefore provide interesting tools to study the intersection between cell cycle checkpoints and DNA repair pathways.

Using our viral system, we have been able to demonstrate a role for MRN in certain signaling and checkpoint functions. In particular, we demonstrated a requirement of MRN in ATM activation. However, we have also made a number of interesting observations with our tools that are likely MRN independent. Future studies focused on how E1b55K/E4orf6 affect cell cycle, cellular DNA replication, and substrate degradation will be required to clarify the molecular basis of some of these phenotypes.

Materials and Methods

Cell lines

HeLa, U2OS, and 293 cells were purchased from the American Tissue Culture Collection. Packaging cells for retroviruses were obtained from I. Verma, W162 cells for growth of the E4-deleted virus were from G. Ketner, and A-T cells (GM02052D and GM5849) were from Y. Shiloh or from the Coriell Institute. The U2OS-derived cells that express inducible wild-type (GW33) and kinase-dead (GK41) ATR proteins were from S. Schreiber and were induced with doxycycline as previously described (254). A-TLD1 cells were from J. Petrini and were immortalized by transduction with retroviruses expressing SV40 T-antigen and hTERT. These cells were then transduced with retrovirus expressing the wild-type Mre11 cDNA cloned into pLPC (309) or the empty vector. Puromycin resistant pools were selected and maintained at 1 μg/ml. All cells were maintained as monolayers in Dulbecco modified Eagle's medium (DMEM) supplemented with 10 or 20% fetal bovine serum (FBS), at 37°C in a humidified atmosphere containing 5% CO_2.

Viruses

Wild-type adenovirus type 5 (Ad5), E1b55K mutant viruses, the double mutant *dl*1016 and E1-deleted recombinant viruses were all propagated in 293 cells. The E4 mutant viruses *dl*1004 and *dl*1016 have previously been described (35), and were obtained from G. Ketner. The *dl*1004 virus was

propagated on W162, a Vero-derived E4-complementing cell line. The mutant E1b55K viruses, H354 and R240A, have been previously described (312, 390) and were obtained from A. Berk and Y. Shen respectively. The recombinant adenoviruses rAd.E4orf6 and rAd.E1b55K have been previously described (281) and were obtained from P. Branton. The rAd.LacZ was provided by provided by J. Wilson. All viruses were purified by two sequential rounds of ultra-centrifugation in cesium chloride gradients and stored in 40% glycerol at -20°C. Infections were performed on monolayers of cultured cells in DMEM supplemented with 2% FBS. After 2 hours at 37°C additional serum was added to a total of 10%.

Pulsed Field Gel Electrophoresis

PFGE was performed essentially as previously described (30, 360). 60-100 cm plates of infected cells were infected as described in the figure legends and text. Cells were washed 2X with PBS, scraped in 1 ml of PBS and transferred to 1.5 ml tubes. Cells were pelleted at low speed and resuspended in 100-350 μl of PBS with 125 mM EDTA. Cells were mixed 1:1 with 1% InCert agarose (BioWhitaker Molecular Applications), which was melted in 50 mM Tris pH 7.4 with 125 mM EDTA, and transferred to a plug mold. Hardened plugs were transferred to proteinase K solution (1.2% SDS, 0.12 mM EDTA, 5 mg/ml pro K) at 50°C overnight. Plugs were washed extensively and stored in 50 mM EDTA. Plugs were loaded into a 1% agarose gel made with 0.5X TBE

and Seakem HGT agarose (BMA). Gels were run at 200V in 0.5X TBE in a Contour Clamped Homogenous Electric Field System (CBS Scientific Co.) chilled to 4°C and controlled by a Programmable Power Inverter (MJ Research). Viral DNA was visualized by staining the gel with ethidium bromide, or by performing a southern for adenoviral DNA (335).

Antibodies

Viral replication centers were visualized by staining for adenovirus DBP with either mouse monoclonal antibody (B6-8) or rabbit polyclonal antisera. Primary antibodies were purchased from Novus Biologicals Inc. (NBS1, NBS1-P-NB100-284, ATM), Genetex (Mre11-12D7, Rad50-13B3), Santa Cruz (Ku70, Ku86, DNA-PKcs, p53, ATR, Chk1), Upstate (Chk2), Cell Signaling (Chk1-S345, Chk2-T68, p53-S15), Oncogene (BRCA1) and Rockland (ATM S1981-P). Antisera to E4orf6 was from P. Branton, antibody to 53BP1 was from T. Halazonetis and the phospho-specific antibody was from P. Carpenter, antibody to RPA32 was from T. Melendy, antibody to phosphorylated H2AX was from W. Bonner, antibodies to DBP and E1b55K were from A. Levine, polyclonal rabbit antisera to DBP was from P. van der Vliet. All secondary antibodies were from Jackson Laboratories.

Generation of E1b55K cell lines

To generate stable expressing E1b55K cell lines, E1b55K was PCR amplified from either wild-type Ad5 or E1b55K mutant viruses. The products

were cloned under control of the CMV promoter in a modified version of the pCLNC retrovirus vector. GFP was also cloned into pCLNC as a control. All constructs were confirmed by DNA sequencing. Retroviruses were generated by transfection of a packaging cell line with the pCLNC E1b55K plasmids and a plasmid expressing the VSV-G envelope protein. HeLa and U2OS cells were infected with retrovirus supernatants and selected in 900 μg/ml G418. Cell lines were maintained in 400μg/ml G418. Expression of E1b55K was assessed by immuno-blotting and immunofluorescence, and pools of resistant clones were used for experiments.

Flow cytometry analysis

The G2M checkpoint assay was performed essentially as previously described (387). Cell lines were uninfected or infected with rAd.E4orf6 (MOI 50) for 48 hours prior to irradiation with 10 Gy, and then analyzed for mitotic index and DNA content at 1 hour post-irradiation. Phosphorylated histone H3 was detected with a phospho-specific polyclonal primary antibody (Upstate Biotechnology) and a FITC-conjugated anti-rabbit secondary antibody (Jackson Laboratories). To measure DNA content, cells were stained with propidium iodide (PI; Sigma). For G2 accumulation, cells were infected with rAd.E4orf6 for 24 hours before irradiation with 4 Gy. 12-24 hours post-treatment, cells were analyzed for DNA content as above. Fluorescence was

measured by flow cytometry using a Becton-Dickson FACScan. For each sample, 20,000 events were analyzed.

Western analysis

Cells were washed and harvested in PBS, pelleted, and incubated with lysis buffer (PBS containing 1% NP40, 0.1% SDS, 0.25% Triton X-100, 1X Complete protease inhibitors (Roche), 1mM PMSF and the phosphatase inhibitors 20 mM NaF, 1 mM Na_3VO_4, and β-glycerophosphate) for 30 min on ice. Lysates were cleared by centrifugation at 14,000g at 4°C and protein concentration was measured by the Lowry assay (Biorad). Proteins were electrophoresed on poly-acrylamide gels and transferred to ECL membrane at 4°C (100V/hr) using Biorad mini-protean II apparatus. Pre-cast 3-8% Tris-Acetate gels (Invitrogen) were used to resolve the phosphorylated forms of ATM, NBS1, BRCA1 and other high molecular weight proteins (ATM, ATR, DNA-PKcs). Novex Mini-cell gel and X-Cell2 transfer apparatus (Invitrogen) was utilized according to manufacturer instructions. Membranes were blocked in PBS-T (PBS with 0.1% Tween-20) with 5% dry milk overnight at 4°C. Blots were rinsed and incubated with the primary antibody in PBS with 3% BSA. After washing with PBS-T, blots were incubated with the secondary antibody (anti-rabbit or mouse conjugated to peroxidase, Jackson) in PBS-T with 5% dry milk for 1 hour at room temperature. After extensive washing with PBS-T, blots were treated with Western Lightning chemiluminescence substrate

(Perkin Elmer) according to manufacturer's instructions and exposed to film (Kodak X-omat) for varying times.

Immuno-fluorescence

Cells were grown on glass coverslips in 24-well dishes and infected with wild-type or mutant viruses according to the figure legends. The cells were washed with phosphate-buffered saline (PBS) and fixed at -20°C for 30 min with ice-cold methanol/acetone (1:1). For detection of ATR, cells were fixed in 3% paraformaldehyde for 20 min and extracted with 0.5% triton-X 100 in PBS for 10 min. In all cases, control staining experiments showed no cross-reaction between the fluorophores, and images obtained by staining with individual antibodies were the same as those shown for double-labeling. Nuclear DNA was stained with 4',6-diamidino-2-phenylindol (DAPI) and coverslips were mounted using Fluoromount-G (Southern Biotechnology Associates). Secondary fluorophore-conjugated antibodies were purchased from Jackson Laboratories. Immuno-reactivity was visualized using a Nikon microscope in conjunction with a CCD camera (Cooke Sensicam). Images were obtained in double or triple excitation mode and processed using SlideBook and Adobe Photoshop.

Acknowledgements

I am grateful to Christian Carson for being a wonderful mentor and guiding much of the research in the publication from this chapter. He was responsible for Figures 1, 2, 3, and 8. We are also grateful to A. Berk, W. Bonner, P. Branton, P. Carpenter, T. Halazonetis, G. Ketner, A. Levine, T. Melendy, J. Petrini, S. Schreiber, Y. Shen, Y. Shiloh, P. van der Vliet, I. Verma and J. Wilson for generous gifts of reagents. We thank J. Karlseder for help with immortalization of A-TLD1 cells.

Some material from this chapter is reprinted in part as it appears in:

Carson CT, Schwartz RA, Stracker TH, Lilley CE, Lee DV, Weitzman MD. The Mre11 complex is required for ATM activation and the G2/M checkpoint. EMBO J. 2003 22:6610-20.

The dissertation author was a researcher and an author of this paper.

Chapter 3. Distinct requirements of the adenovirus E1b55K protein for degradation of cellular substrates.

Background

The linear, double-stranded DNA genome of adenovirus serotype 5 (Ad5) is approximately 36 Kb and encodes five early transcription units whose proteins perform essential functions for efficient infection. Viruses such as adenovirus employ numerous strategies to contend with host cell factors during the course of establishing a productive infection (41, 367). Examining mutant viruses has implicated E1b and E4 proteins in modulation of the host cell environment, promotion of viral DNA replication and viral mRNA export, prevention of viral genome concatemerization, and synthesis of late viral proteins (reviewed in Refs. (18, 343, 364, 367). In Ad-infected cells most of the viral E1b55K protein is complexed with E4orf6 (294, 302). The E1b55K/E4orf6 complex has been implicated in selective modulation of nucleo-cytoplasmic mRNA during the late phase of virus infection (reviewed in Refs. (95, 123). This viral complex also promotes efficient viral replication (36, 144, 157, 362) and prevents the viral genome from being concatemerized by host factors (335, 360). The precise mechanisms by which the E1b55K/E4orf6 complex achieves its many functions remain to be elucidated.

E1b55K displays a complex distribution pattern in infected cells, and requires E4orf6 for nuclear localization (136) and association with viral replication centers (265). The E1b55K protein possesses a leucine rich nuclear export signal (NES), which has been implicated in nucleo-cytoplasmic shuttling via the CRM1-mediated nuclear export receptor (96, 184). Export-deficient mutants of E1b55K accumulate in sub-nuclear aggregates that also contain cellular binding partners (110, 148). In the absence of E4orf6, expression of E1b55K produces cytoplasmic aggregates (93, 136, 181, 210, 263). In transformed cells E1b55K from Ad serotypes 2 or 5 accumulate in a large cytoplasmic body (23, 37, 110, 400) with characteristics of an aggresome (182, 210). Many cellular proteins that interact with E1b55K localize at the aggresome in transfected and transformed cells (23, 37, 110, 122, 210, 221, 400). Therefore, protein aggregation has been proposed as a potential strategy utilized by E1b55K to inactivate cellular proteins (210) and promote transformation (148).

One tactic commonly employed by viruses to inactivate inhibitory host factors is to induce specific down-regulation or degradation of cellular proteins (127, 310). Degradation can be achieved via covalent modification of target proteins with polyubiquitin chains by an E3 ubiquitin ligase, followed by recognition and destruction by the proteasome (reviewed in Ref. (176)). The adenoviral E1b55K and E4orf6 proteins associate with cellular proteins to form

an E3 ligase complex that contains Elongins B and C, Cullin 5, and Rbx1 (28, 146, 281). BC-box motifs in E4orf6 have been identified as important for binding Elongins B and C (24, 61, 218) (see Chapter 4 for further discussion). It has been suggested that all functions of the E1b55K/E4orf6 complex are due to degradation of cellular proteins by the ubiquitin ligase activity (25, 72, 378). Since E1b55K alone can physically associate with p53 (52, 173, 206, 312, 389, 391), DNA Ligase IV (8) and the MRN complex (50), it is believed to mediate substrate recognition, while both E4orf6 and E1b55K are required for proteasome-mediated degradation (50, 52, 281, 282, 312, 370). Not all proteins that interact with E1b55K are down-regulated, but cellular proteins so far identified as degradation substrates of the E1b55K/E4orf6 complex include p53 (52, 146, 238, 251, 281, 282, 292, 329), the Mre11/Rad50/Nbs1 (MRN) DNA repair complex (50, 335), and the DNA Ligase IV protein (8). Exactly which substrates are relevant to specific functions of the E1b55K/E4orf6 complex is unclear. Additionally, the mechanisms for selection and degradation of distinct targets remain to be resolved. Understanding how the E1b55K/E4orf6 viral ubiquitin ligase targets specific cellular substrates is crucial to elucidating how these viral proteins perform their myriad of functions.

In the present study, we characterized some of the cellular and viral requirements for degradation of each target. By examining the steady-state levels of E1b55K/E4orf6 substrates in mutant cells lines, we demonstrate that

degradation of targets can occur independently of each other. Furthermore, our data suggest that Mre11 may be the direct target within the MRN complex. A series of E1b55K mutants were characterized for localization and degradation of the known substrates. We identify regions of E1b55K important for cellular localization, and we demonstrate that there are independent requirements for p53, MRN, and DNA Ligase IV down-regulation. Our results show that affinity for substrates appears to be a major, but not sole, determinant of E1b55K-mediated degradation.

Results

Cellular substrates of the E1b55K/E4orf6 complex are degraded independently of each other

We first analyzed the kinetics of substrate degradation in U2OS cells, which express all currently known targets of the E1b55K/E4orf6 complex. Degradation of cellular proteins was examined by immuno-blotting over a time-course of infection with wild-type (WT) Ad5 (Figure 1). During infection, the E1b55K protein was first detected at 12 hpi. At this time point the total steady-state levels of the Mre11, Rad50, Nbs1, p53 and DNA Ligase IV proteins began to decrease. Nbs1 down-regulation was slightly delayed compared to the other substrates, suggesting that it may not be a direct target. Since many of the cellular DNA repair proteins are part of large protein complexes, we

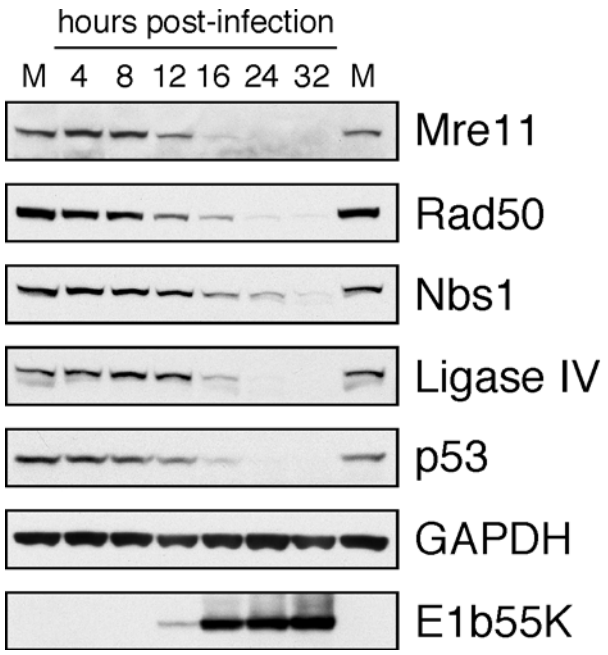

Figure 1. Degradation of cellular substrates over time during wild-type adenovirus infection. U2OS cells were infected with wild-type Ad5 (MOI of 25) and lysates were harvested at the indicated times post-infection for analysis by immuno-blotting with specific antibodies. GAPDH served as a loading control. Proteins levels were compared to those in mock-infected cells (M).

determined whether cellular proteins could be degraded independently of each other using mutant cell lines (Figure 2A). Mre11, Rad50 and DNA Ligase IV were degraded in SAOS2 cells that do not express p53. A-TLD1 cells (330) harbor a mutation in Mre11 that destabilizes the complex. We found that DNA Ligase IV and p53 could still be degraded in these cells, although we noted that p53 levels were not completely diminished. DNA Ligase IV and the MRN complex are critical to DNA repair by non-homologous end-joining (NHEJ). We therefore also examined whether DNA-PKcs, another key NHEJ factor, was required for degradation of substrates. Ad5 infection of FUS9 cells, which lack DNA-PKcs (156), still induced down-regulation of all known substrates. In support of this, we have also previously shown that the ATM and ATR kinases and signaling pathways are not required for degradation of MRN (50). Together, these data demonstrate that virus-induced down-regulation of MRN, p53, and DNA Ligase IV can occur independently of each other and other proteins involved in the DNA damage response.

To address which component of the MRN complex is targeted by E1b55K/E4orf6, we employed mutant NBS and A-TLD cell lines. IMR90 fibroblast cells were infected as a control, and showed degradation of all MRN members (Figure 2B). NBS cells harbor a mutation in the NBS1 gene resulting in a truncated protein defective in complexing with Mre11, and thus, Rad50 (49). Infection of these cells with Ad5 caused degradation of both Mre11 and

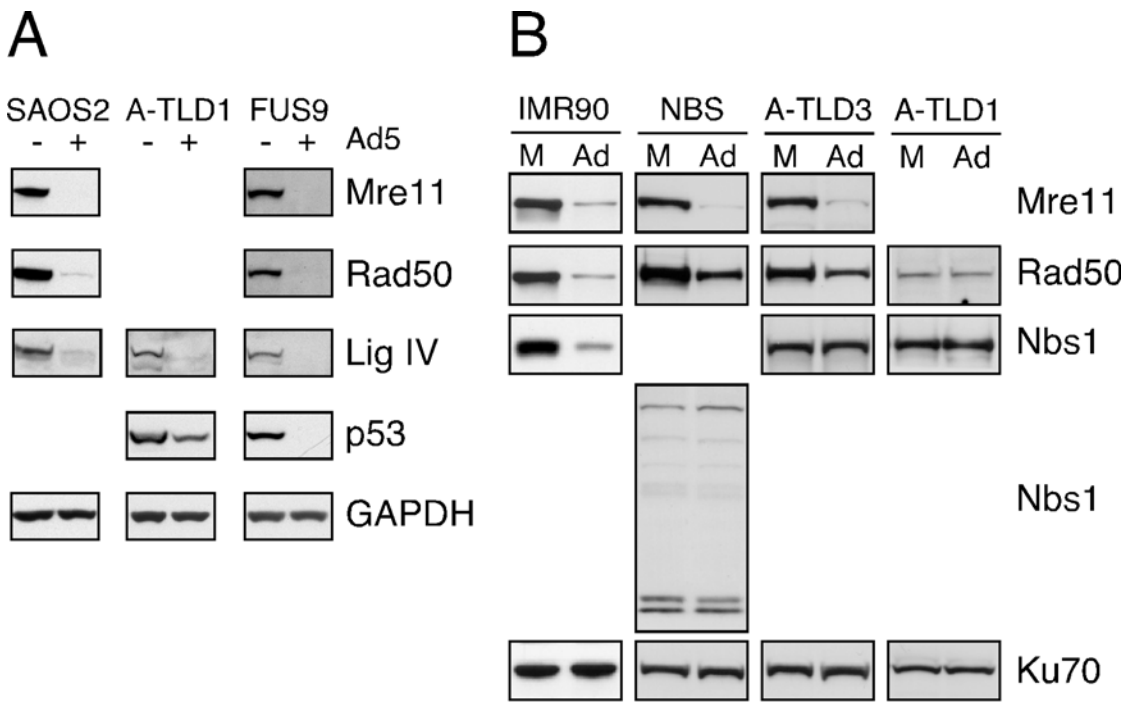

Figure 2. Cellular substrates of the E1b55K/E4orf6 complex are degraded independently of each other during adenovirus infection. (A) Independent degradation of p53, the MRN complex and DNA Ligase IV. Cell lines with mutant p53 (Saos2), Mre11 (A-TLD1), or DNA-PKcs (Fus9) were infected with wild-type Ad5 (MOIs of 25, 100, and 25 respectively). Lysates were prepared at 24-48 hpi and analyzed by immuno-blotting for the indicated proteins. **(B)** Mre11 may be the degradation target within the MRN complex. IMR90, A-TLD3, A-TLD1, or NBS cells were either mock treated (M) or infected with wild-type Ad5 (MOI of 75). Cells were harvested at 24-48 hpi and lysates were analyzed by immuno-blotting for the indicated proteins. Ku70 served as a loading control.

Rad50 (Figure 2B), suggesting that full-length Nbs1 is not required. Smaller sized proteins recognized by the Nbs1 antibody were not altered by Ad5 infection. A-TLD3 cells contain a mis-sense mutation in Mre11 that diminishes its interaction with Nbs1 (330), while A-TLD1 cells express a prematurely truncated Mre11 protein that is unstable and defective for Rad50 and Nbs1 interaction (330). A-TLD3 cells showed reduced levels of both Mre11 and Rad50 during Ad5 infection (Figure 2B). Although we had difficulty visualizing the truncated form of Mre11 in A-TLD1 cells, Rad50 was unaltered (Figure 2B), suggesting that full-length Mre11 is required for destabilization of Rad50 and Nbs1 during Ad5 infection. Together these data imply that the Mre11 protein is the target for degradation. The decreases in Rad50 and Nbs1 proteins are therefore likely indirect consequences of Mre11 removal, consistent with observations from RNAi knockdown experiments in the absence of adenovirus (354, 408).

Identification of additional E1b55K mutants with defects in MRN degradation

Previous studies have described a large number of E1b55K mutants (132, 294, 312, 347, 390), but many of these have not been assessed for degradation of all the known substrates. We previously identified two E1b55K mutants that can distinguish between the degradation targets p53 and MRN (50). In the presence of E4orf6, the R240A mutant degrades the MRN complex

but not p53, whereas the H354 insertion mutant degrades p53 but not MRN. We extended these studies by examining a number of E1b55K mutant viruses (312, 390) with either point mutations or small insertions across the length of E1b55K. A subset of mutants is shown in the schematic in Figure 3. Infections with mutant E1b55K viruses were compared to WT Ad5 and the E1b55K deletion virus *dl*110 for degradation of p53 and MRN over a time-course of infection.

In addition to the previously described H354 and R240A viruses, we found separation-of-function phenotypes for E1b55K mutant viruses R443 (which has a 4 amino acid insertion at residue 443) (390) and Y444A (ONYX85) (312). While both viruses induced degradation of p53 in agreement with previous reports (312, 329), neither virus exhibited complete down-regulation of all three members of the MRN complex (Figure 4A and 4B). The R443 virus also produced more E1b55K compared to WT Ad5. It is interesting to note that the insertion that creates R443, also results in a Y444D mutation (390), which may contribute to a compound phenotype. In the course of our survey we found that the R443A mutation (ONYX84) (312) did not affect degradation of MRN (data not shown), suggesting that this region, rather than the residue itself, is important to MRN degradation.

Given that the MRN complex is required for the DNA damage response to mutant adenoviruses (50), we tested whether these mutants induced

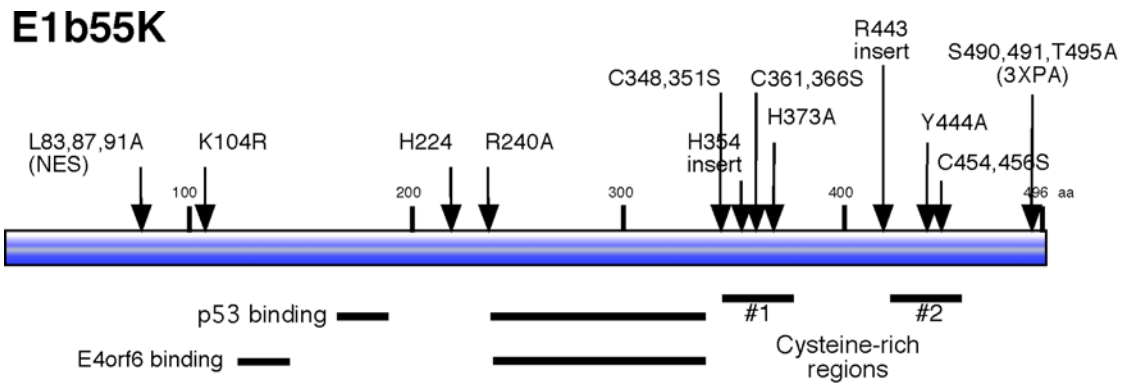

Figure 3. Schematic of E1b55K and mutants. Schematic representation of E1b55K mutants used in this paper and their relative locations within the protein. Relative locations of p53 binding domains (173, 389) and E4orf6 binding domains (294) are underlined. Two cysteine-containing regions important for degradation of substrates are also highlighted.

Figure 4. C-terminal E1b55K mutants have defects in degradation of the MRN complex. U2OS cells were infected (MOI of 50) with wild-type Ad5, the ΔE1b55K mutant *dl*110, or the virus mutants R443 **(A)** and Y444A **(B),** and cells were harvested at the indicated times post-infection. Lysates were analyzed by immuno-blotting with the indicated antibodies and compared to mock infected cells (M). GAPDH served as a loading control.

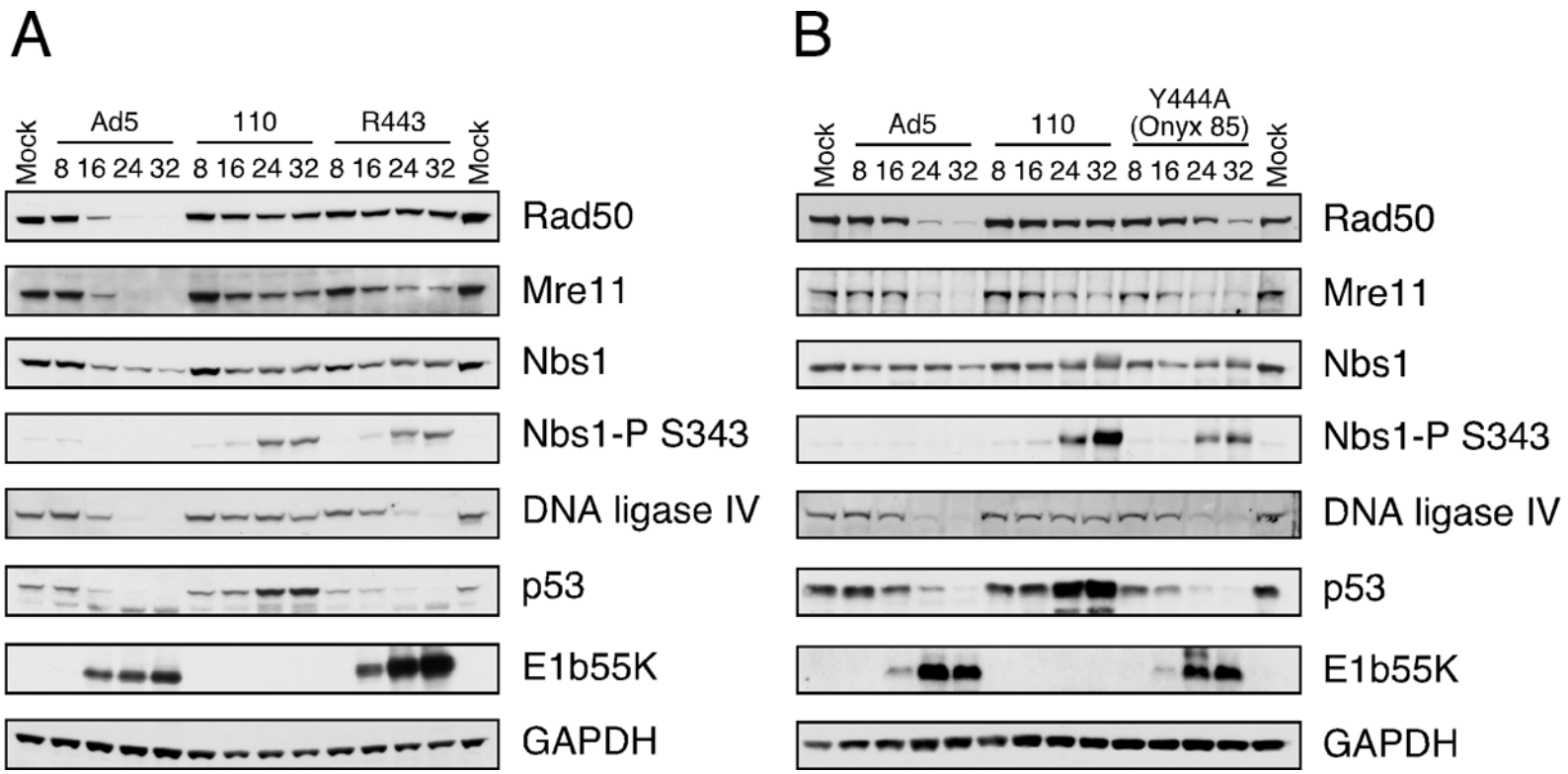
A
Mock
Ad5
110
R443
Mock
8 16 24 32 8 16 24 32 8 16 24 32
Rad50
Mre11
Nbs1
Nbs1-P S343
DNA ligase IV
p53
E1b55K
GAPDH
B
Mock
Ad5
110
Y444A
(Onyx 85)
Mock
8 16 24 32 8 16 24 32 8 16 24 32
Rad50
Mre11
Nbs1
Nbs1-P S343
DNA ligase IV
p53
E1b55K
GAPDH

damage signaling. We observed that partial degradation of MRN by R443 and Y444A was not sufficient to prevent signaling during viral infection (Figure 4A and 4B; data not shown), as indicated by Nbs1 phosphorylation (Nbs1-P S343). This suggests that infection with Ad mutants unable to neutralize MRN completely can induce a DNA damage signaling. Together with our previous observations (50), these data indicate that multiple regions of E1b55K are important for MRN degradation. The complete survey results of mutants are presented in Table 1, together with a summary of observations previously reported in the literature.

Two cysteine-containing regions of E1b55K are important for substrate degradation

The E1b55K mutants we identified as defective for MRN degradation (H354, R443, and Y444A) are located in or near two regions that contain cysteine residues and may resemble zinc-fingers (132). To analyze E1b55K further, we cloned these and other site-specific mutants into retroviral vectors (see Figure 3). Stable cell lines expressing individual E1b55K proteins were generated by retrovirus transduction as previously described (50). Mutants were examined in the presence and absence of E4orf6 for cellular localization and degradation of the MRN complex by immuno-fluorescence. In the absence of E4orf6, WT E1b55K was localized in cytoplasmic aggregates (Figure 5), as previously described (136, 181). In the presence of E4orf6, E1b55K

Table 1. Summary of E1b55K phenotypes from this study and the literature.

E1b55K protein	Substrate degradation[a] (E1b/E4orf6 alone)			Substrate degradation[b] (Virus infection)			Substrate binding[c]		E1b55K aggregate colocalization[d]		E1b55K cyto aggregates[e]	E1b55K nuclear retention by E4orf6[f]	Concate-mers[g]	Additional References[i]
	p53	MRN	Lig4	p53	MRN	Lig4	p53	MRN	p53	MRN				
WT E1b55K	+	+	+	+	+	+	+	+	+	+	+	+	-	
L83,87,89A (NES)	ND	+	ND	+/-	+	ND	+	+	+	+	NA	+	ND	110,148,179,184
K104R	ND	+	ND	+	+	ND	ND	+	ND	+	+	+	ND	111,179
H224 insertion	+	+	+	+	+	+	+	+	+	+/-	+	+/-	-	173,294,390
R240A	-	+	+	-	+	+	-	+	-	+/-	+	+	-	50,312
C348,351S	ND	+	ND	ND	ND	ND	ND	ND	ND	ND	+	+	ND	
H354 insertion	+	-	+	+	-	+	+	-	+	-	+	+	-	50,173,210,389,390
C361,366S	-	-	-	-	-	-	+/-	-	+	-	+	+/-	+	
H373A	+	-	+	+	-	+	+	-	+	-	+	+	-	
R443 insertion	+	-	+	+/-	-	+/-	+	-	+	-	+/diffuse	+/-	+	173,329,389,390
Y444A	+	+	+	+	+/-	+	+	+/-	+	+/-	+	+/-	-	312
C454,456S	-	-	-	-	-	-	+	-	+	-[h]	+	+/-	+	148
S490,491,T495A (3XPA)	-	+	+/-	-	-	-	-	+/-	NA	NA	diffuse	+/-	+	282,346
S490,491,T495D (3XPD)	+	+	+	ND	ND	ND	+	+	+	+/-	+	+	-	

+ proficient, +/- defective, - very defective, ND not determined, NA not applicable

[a] Degradation of endogenous proteins assessed with E1b55K mutants plus rAd.E4orf6 by western or immunofluorescence.

[b] Degradation of endogenous proteins assessed in the context of viruses expressing E1b55K mutants or E1b55K mutant cell lines infected with *dl*3112.

[c] Interaction measured by co-immunoprecipitation experiments.

[d] MRN or p53 colocalization with E1b55K aggregates assessed by immunofluorescence.

[e] E1b55K staining assayed by immuno-fluorescence in the absence of rAdE4orf6. + = presence of E1b55K aggregates, diffuse = diffuse cytoplasmic E1b55K. See Figure 4A for data and details.

[f] E1b55K staining assayed by immuno-fluorescence in the presence of rAdE4orf6. See Figure 4A for data and details.

[g] Concatemer formation of mutant virus *dl*3112 measured in mutant E1b55K expressing cells.

[h] Observation from the present study by E1b55K expression in human cells.

[i] This table summarizes data from this paper in addition to the additional references indicated.

accumulated in a diffuse nuclear pattern with few remaining cytoplasmic foci, and this was accompanied by degradation of Nbs1. The E1b55K mutants exhibited a variety of patterns which are shown in Figure 5 and summarized in Table 1. Those differing from the WT E1b55K pattern included R443, which displayed a predominantly diffuse cytoplasmic staining, and Y444A, which showed more elongated cytoplasmic foci (Figure 5). With the exception of Y444A and C348,351S, the mutants near cysteine regions were unable to degrade MRN in the presence of E4orf6 (Figure 5 and Table 1) regardless of their localization pattern. Many mutants were not retained in the nucleus to the same extent as WT E1b55K in the presence of E4orf6 (Figure 5 and Table 1). However, this phenotype did not correlate completely with lack of MRN degradation, since mutants H224 and Y444A were still able to degrade MRN (Figure 5). This suggests that nuclear retention by E4orf6 is not absolutely required for degradation of cellular substrates.

Using the stable E1b55K expressing cell lines, we also examined E1b55K/E4orf6-mediated degradation of targets by immuno-blotting (Figure 6). The previously characterized cell lines expressing GFP, WT E1b55K, R240A and H354 (50) were included as controls. Immuno-blotting confirmed our initial immuno-fluorescence observations and indicated that, with the exception of Y444A, most of the isolated mutants were defective in MRN degradation (Figure 6 and Table 1). Mutants C361/366S and C454/456S did

Figure 5. Localization of E1b55K mutants in stable cell lines. U2OS cell lines stably expressing wild-type and mutant E1b55K proteins were either mock treated or infected with rAdE4orf6 (MOI of 50) for 24 hours. E1b55K and Nbs1 were detected by immuno-fluorescence. DAPI staining marks the cell nuclei in the top and bottom panels.

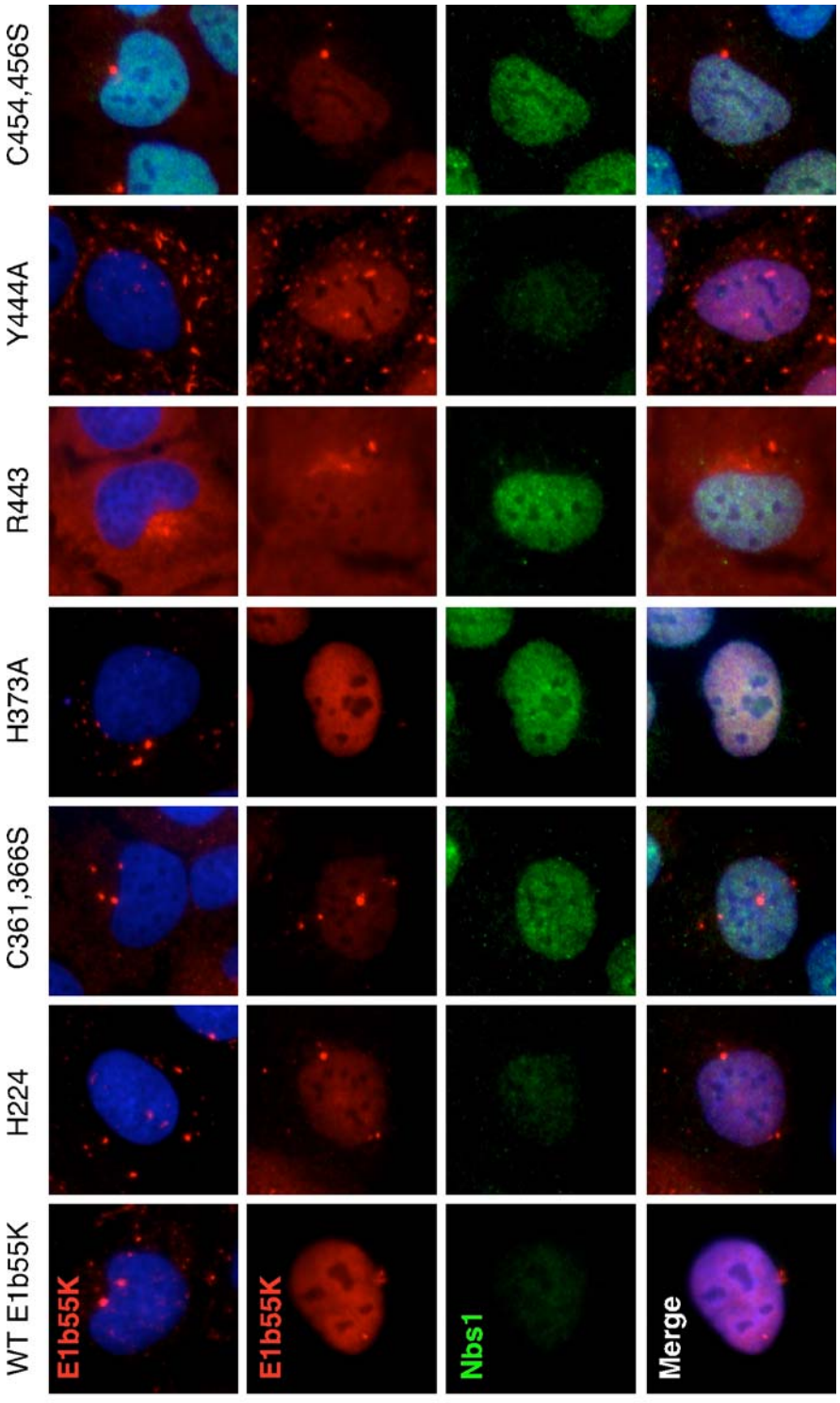
WT E1b55K
H224
C361,366S
H373A
R443
Y444A
C454,456S
E1b55K
E1b55K
Nbs1
Merge
+ rAd.E4orf6

not appear to degrade either p53 or MRN (Figure 6). H373A behaved similarly to H354 (50) in cellular localization and degradation of p53 but not MRN (Figures 5 and 6). R443 also appeared to be a separation-of-function mutant by immuno-blotting, although considering the levels of E1b55K, p53 degradation was not as robust as WT. Together with our previous data (50), these mutants illustrate that requirements for E1b55K-mediated degradation of MRN are distinct from p53, and identify two cysteine regions as critical for proper localization of E1b55K and MRN degradation.

Phosphorylation of E1b55K is required for correct cellular localization and degradation of substrates

Multiple post-translational modifications of E1b55K have been reported, including SUMO-1 conjugation at K104 (111, 179, 199) and phosphorylation at the C-terminus (346, 347). We wanted to address whether these modifications affected E1b55K localization or substrate degradation. E1b55K proteins harboring mutations at the SUMO modification site (K104) (111) and the known phosphorylation sites in the C-terminus (S490, S491, and T495) (346, 347) were expressed from plasmids and first assessed for localization in the absence and presence of E4orf6 (Figure 7 and data not shown). Mutation of the SUMOylation site did not affect E1b55K localization in the absence of E4orf6 (Table 2 and data not shown). However, the triple phosphorylation site mutant, 3XPA, displayed a pattern drastically different from WT E1b55K.

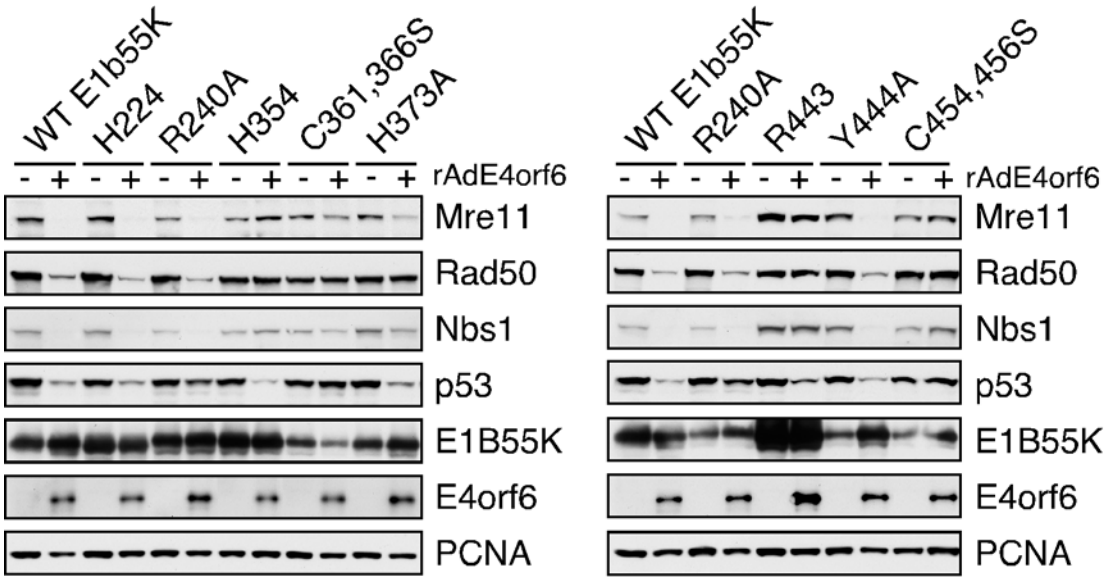

Figure 6. Substrate degradation in cell lines stably expressing E1b55K mutant proteins. Lysates from the infected cells described above were analyzed by immuno-blotting with antibodies to the indicated cellular and viral proteins. PCNA served as a cellular loading control.

Instead of localizing in characteristic cytoplasmic aggregates, 3XPA was found diffusely spread throughout the cytoplasm, somewhat similar to R443 (Figure 7). In some cells, one or two very small E1b55K foci were noted in the cytoplasm, but no larger aggregates were detected. Increased nuclear staining was evident with this mutant in the presence of E4orf6, although a large amount of E1b55K also remained in the cytoplasm (Figure 7). To confirm this localization pattern in the context of virus infection where E4orf6 is also expressed, we infected U2OS cells with viruses expressing phosphorylation site mutants of E1b55K (3XPA in pm490/1/5A and 2XPA in pm490/1A) (346). The expression pattern for E1b55K during infection with the 3XPA mutant virus, pm490/1/5A, was similar to that seen during transfection, while the double-phosphorylation site mutant virus, pm490/1A, displayed a more predominantly nuclear E1b55K stain (Figure 8). To address whether phosphorylation was required for proper localization of E1b55K, we constructed a phospho-mimic mutant in which the amino acids 490, 491, and 495 were changed to aspartic acid (3XPD). After transient transfection of this mutant, we observed a cellular localization pattern more similar to WT E1b55K (Figure 7). However, the cytoplasmic aggregates of E1b55K appeared slightly more elongated, somewhat similar to the Y444A mutant. These results suggest that phosphorylation of E1b55K is critical to proper cellular localization.

Figure 7. Phosphorylation of E1b55K is required for correct cellular localization. U2OS cells were transfected with constructs expressing wild-type E1b55K, mutant E1b55K-3XPA (3XPA), or E1b55K phospho-mimic 3XPD (3XPD). After 16 hours, cells were super-infected with rAdE4orf6 (MOI = 20) for 24 hours before processing for immuno-fluorescence with the indicated antibodies. Cell nuclei are stained with DAPI in the merged image.

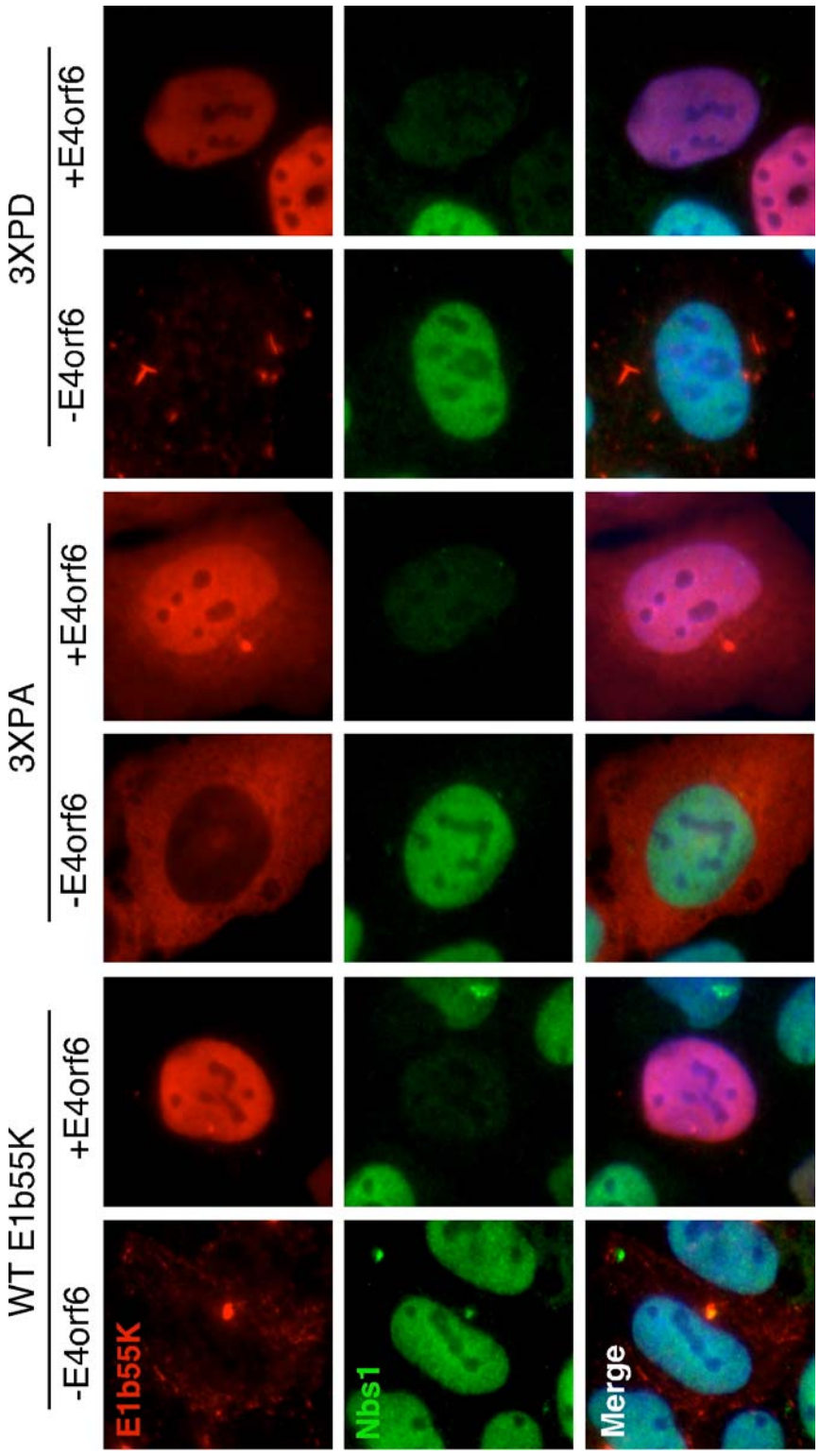
WT E1b55K
3XPA
3XPD
-E4orf6
+E4orf6
-E4orf6
+E4orf6
-E4orf6
+E4orf6
E1b55K
Nbs1
Merge

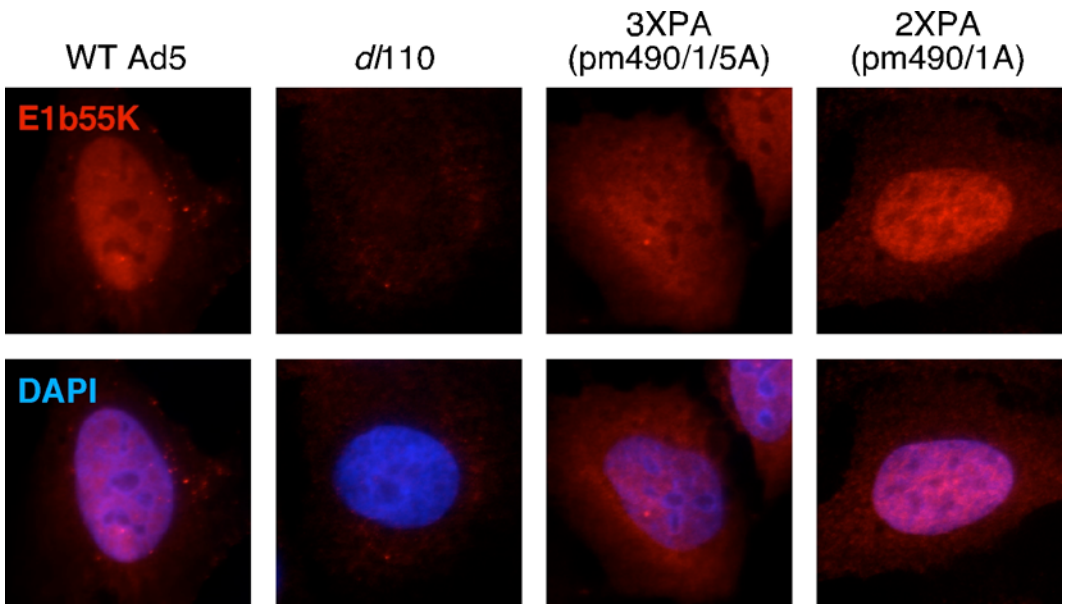

Figure 8. Localization of E1b55K during infection with phosphorylation defective mutant viruses. U2OS cells were infected with wild-type Ad5, the ΔE1b55K mutant *d*/110, or E1b55K mutant viruses pm490/1/5A (3XPA) and pm490/1A (2XPA) for approximately 24 hours. Cells were fixed and analyzed by immuno-fluorescence for E1b55K localization. DAPI indicates cell nuclei in the merged image.

We then examined how these mutants affected substrate down-regulation. Immuno-fluorescence revealed that the SUMO and phosphorylation site mutants were competent to degrade MRN in the presence of E4orf6 (Figure 7 and Table 2). To further analyze the requirement of E1b55K phosphorylation for degradation, we generated stable U2OS cells lines expressing the 3XPA and 3XPD mutants and compared them to the WT E1b55K cell line. The localization pattern in these stable cell lines was similar to that seen with transient transfection, although less nuclear staining was noted in the presence of E4orf6 (data not shown). Degradation of cellular targets was assessed in these cell lines with E4orf6 by immuno-blotting. The MRN complex was degraded in all three E1b55K expressing cell lines (Figure 9), confirming the immuno-fluorescence data (Figure 7). Interestingly, the 3XPA mutant was defective in p53 down-regulation, while the phospho-mimic 3XPD degraded all substrates (Figure 9). To confirm that these phenotypes occurred in the context of virus infection, we infected U2OS cells with either 3XPA or 2XPA mutant viruses (pm490/1/5A and pm490/1A, respectively) and analyzed degradation over time (Figure 10). Although the 2XPA virus was competent to down-regulate substrates and prevent damage signaling, we found that the 3XPA virus was defective for degradation of cellular targets in general (Figure 10). These results agree with previously reported p53 degradation phenotypes (282). Thus, in the context of the virus, there is a

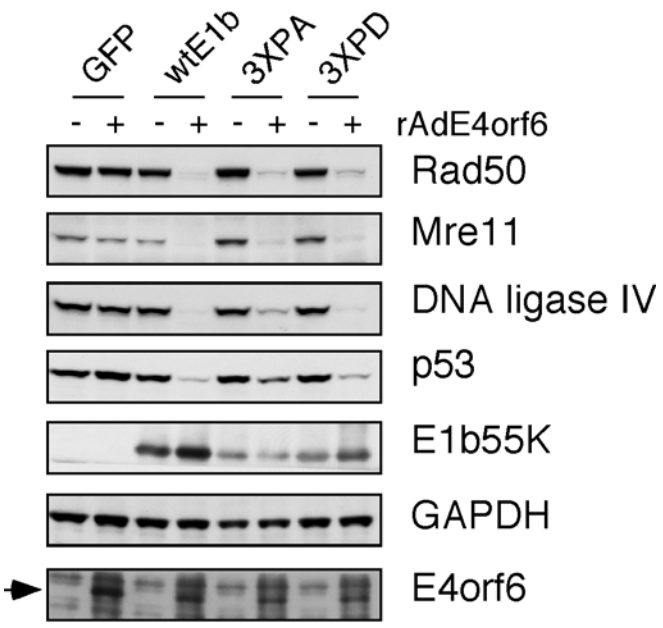

Figure 9. Degradation of substrates in cell lines expressing E1b55K phosphorylation mutants. Cell lines expressing E1b55K mutants were infected with rAdE4orf6 (MOI of 50) for 24 hours. Cells were harvested and lysates were analyzed by immuno-blotting with the indicated antibodies.

Figure 10. Degradation of cellular substrates during infection with phosphorylation defective E1b55K mutant viruses. U2OS cells were infected with wild-type Ad5, the ΔE1b55K mutant *dl*110, or E1b55K phospho-mutant viruses pm490/1/5A (3XPA-left panel) and pm490/1A (2XPA-right panel), all at an MOI of 50. Cells were harvested at the indicated times and processed for immuno-blotting with the indicated antibodies. GAPDH served as a cellular loading control.

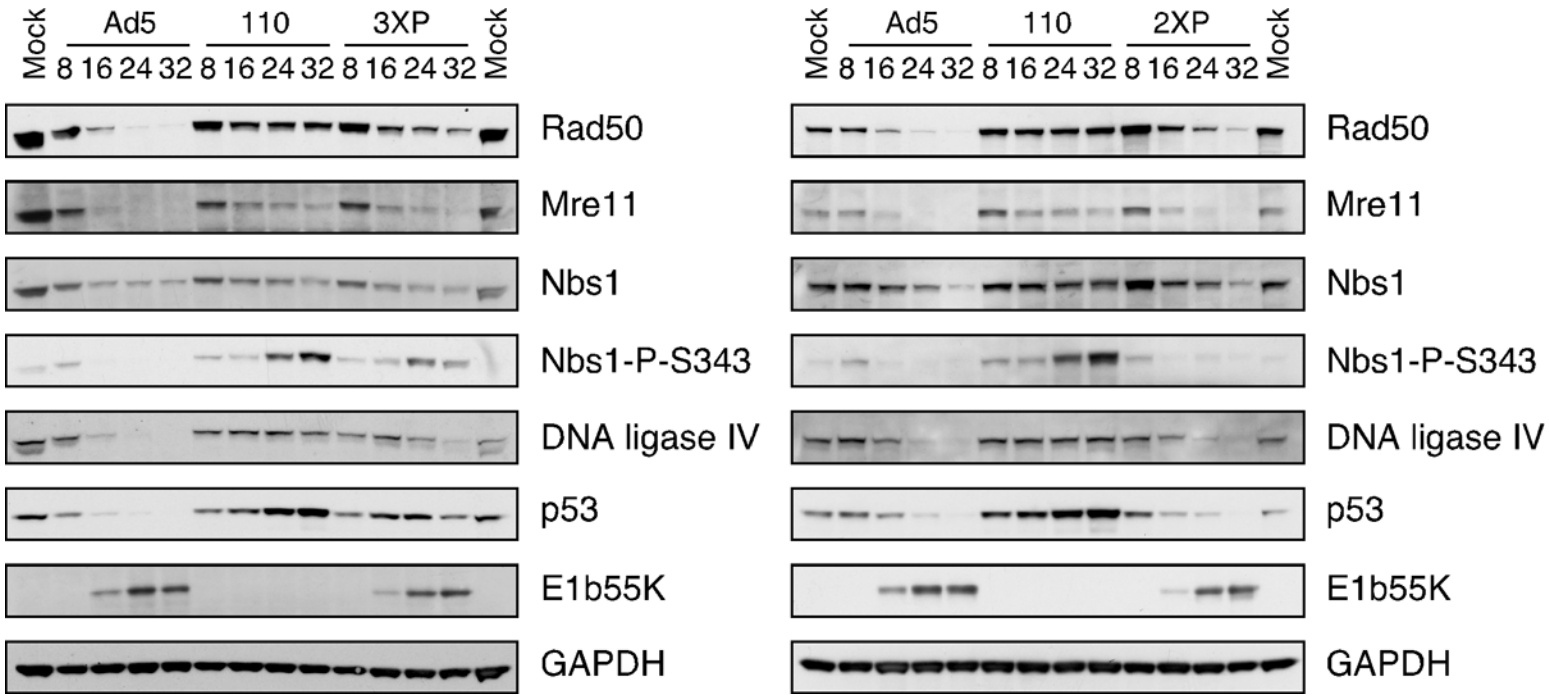
Mock
Ad5
110
3XP
Mock
8 16 24 32 8 16 24 32 8 16 24 32
Rad50
Mre11
Nbs1
Nbs1-P-S343
DNA ligase IV
p53
E1b55K
GAPDH
Mock
Ad5
110
2XP
Mock
8 16 24 32 8 16 24 32 8 16 24 32
Rad50
Mre11
Nbs1
Nbs1-P-S343
DNA ligase IV
p53
E1b55K
GAPDH

more universal requirement of E1b55K phosphorylation for substrate down-regulation.

E1b55K separation-of-function mutants still degrade DNA Ligase IV to prevent concatemer formation

In addition to MRN and p53, DNA Ligase IV was recently described as a degradation substrate of E1b55K/E4orf6 (8). We tested the E1b55K mutant cell lines for down-regulation of this target in the presence of E4orf6. As was observed for MRN and p53 degradation, the mutants C361,366S and C454,456S were also defective for degradation of DNA Ligase IV (Figure 11A). The 3XPA mutant displayed reduced DNA Ligase IV down-regulation (Figures 9, 10, and 11A). Interestingly, we found that the separation-of-function mutants could all degrade DNA Ligase IV, regardless of p53 or MRN specificity (Figure 11A). Similar results were obtained in both U2OS based (Figure 11A) and HeLa based cell lines (Figure 11B). This was also true for most of the E1b55K mutant viruses (Figure 4A, 4B, and Table 1), although the R443 virus had a slight defect (Figure 4A). These data indicate that the requirements of E1b55K for DNA Ligase IV degradation are distinct from both p53 and MRN degradation.

Concatemerization of mutant viral genomes requires both the MRN complex and DNA Ligase IV (335). Therefore, E1b55K proteins unable to degrade MRN may still be able to prevent concatemerization of a mutant virus

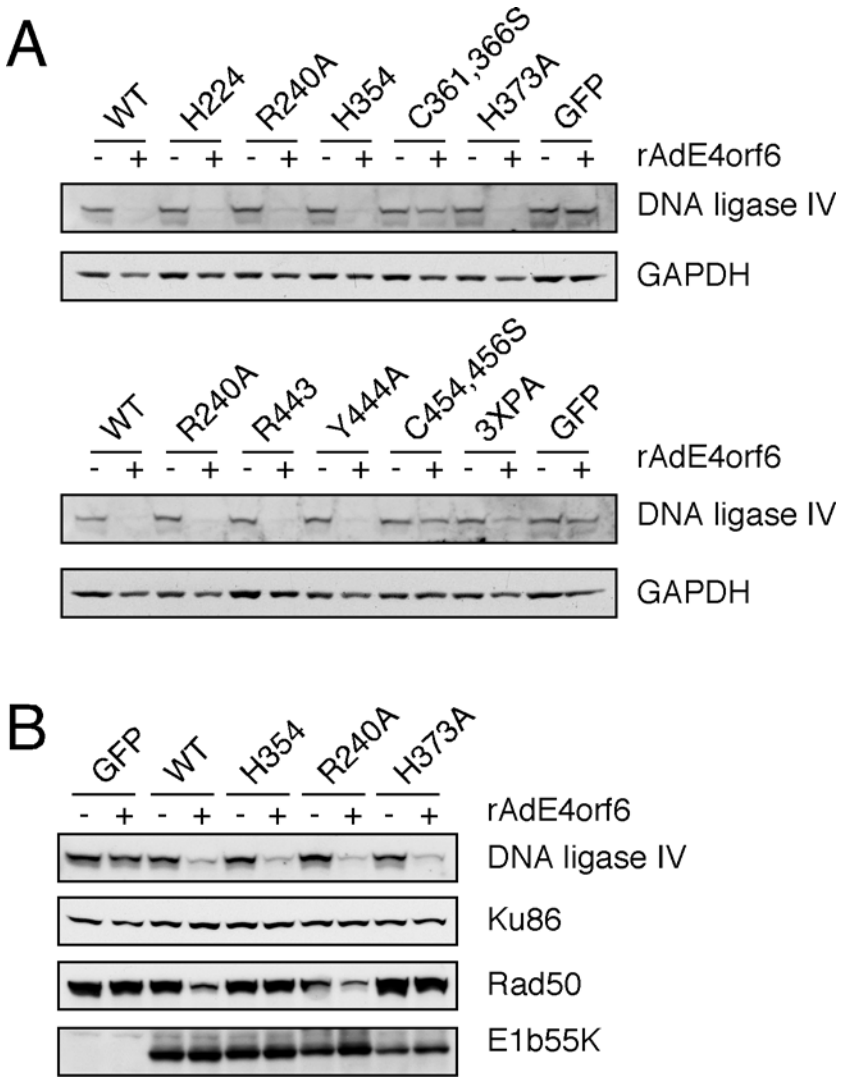

Figure 11. E1b55K separation-of-function mutants degrade DNA Ligase IV. (A) U2OS-based cell lines stably expressing wild-type and mutant E1b55K proteins were either mock treated or infected with rAdE4orf6 (MOI of 50) for 24 hours. Lysates were analyzed by immuno-blotting for DNA Ligase IV and GAPDH (loading control). **(B)** HeLa based cells lines stably expressing E1b55K mutants were infected with rAdE4orf6 (MOI of 50) for 24 hours. Lysates were analyzed as in (A) for the indicated proteins.

if DNA Ligase IV is down-regulated. We examined whether concatemers formed during infection of E1b55K mutant cell lines with the ΔE1b55K/ΔE4orf3 mutant virus, *dl*3112 (Figure 12). As expected, mutant viral genomes were concatemerized during infection of GFP control cells, but not in cells expressing WT E1b55K protein. We also found that concatemers were inhibited in mutant cell lines proficient for degradation of DNA Ligase IV alone (H354, H373A), or in cell lines where both MRN and DNA Ligase IV were degraded (H224, R240A, Y444A, 3XPD) (Figure 12 and Table 1). As expected, the cell lines expressing mutants C361/366S and C454/456S, which were unable to down-regulate any substrates, could not prevent viral genome concatemerization (Figure 12). In these experiments, we found that mutants R443 and 3XPA could not fully complement *dl*3112 to prevent concatemer formation (Figure 12) and degrade MRN or DNA Ligase IV sufficiently (Table 2). These data confirm the requirement of DNA Ligase IV for concatemer formation (335). They also demonstrate that down-regulation of DNA Ligase IV is sufficient to prevent joining of viral genomes even when MRN is not degraded.

E1b55K separation-of-function mutants have defects in substrate binding

We next examined how mutations in E1b55K affect interactions with cellular degradation substrates. Expression of E1b55K in cells can induce a

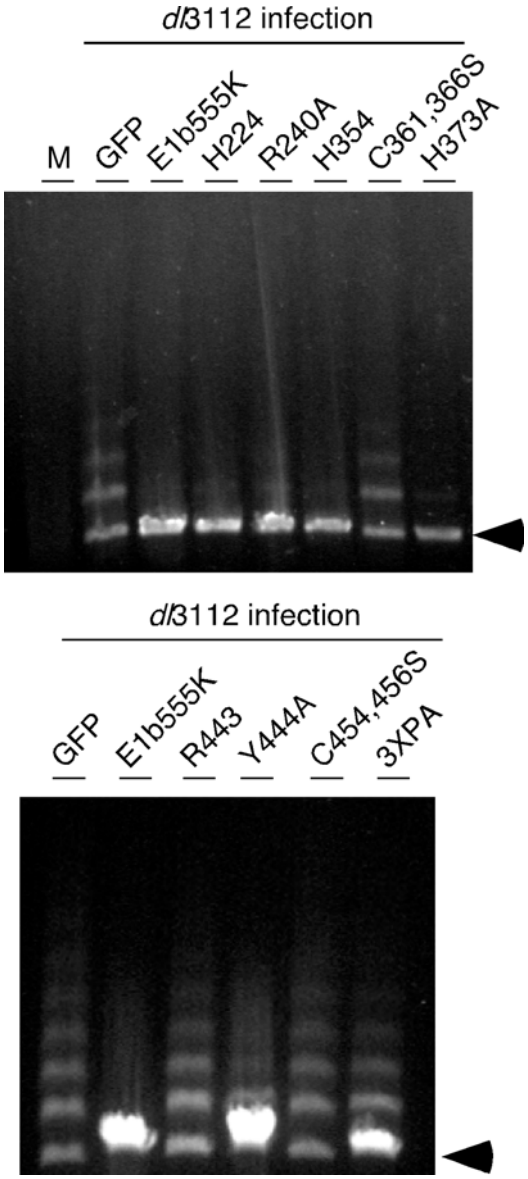

Figure 12. E1b55K mutants that degrade DNA Ligase IV can prevent concatemer formation. E1b55K mutants that cannot degrade MRN still retain the ability to prevent concatemer formation. U2OS cells expressing the indicated E1b55K mutants were infected with *dl*3112 at an MOI of 10, and viral DNA was analyzed at 30 hpi by pulsed-field gel electrophoresis according to Materials and Methods. Controls included a GFP-expressing U2OS cell line that was either mock treated (M) or infected with *dl*3112 to produce concatemers. Arrows indicate the position of the linear viral genome.

large, perinuclear accumulation of the protein with characteristics of an aggresome (210). Many cellular proteins interacting with E1b55K have been observed to colocalize with E1b55K aggresomes (23, 122, 210, 221, 400). We therefore examined the ability of E1b55K mutants to concentrate MRN (Figure 13) and p53 (Figure 14) into cytoplasmic aggregates. Since the E1b55K expression in the stable cell lines did not result in large E1b55K cytoplasmic aggregates, we expressed the E1b55K mutants in U2OS cells by transient transfection. We found that mutants which degrade MRN (H224, R240A, Y444A, and 3XPD) could all relocalize Nbs1 to cytoplasmic aggregates, although some mutants were less efficient than the WT E1b55K protein (Figure 13 and Table 1). Interestingly, we found that all E1b55K mutants concentrated p53 into cytoplasmic aggregates to some extent (Figure 14 and Table 1). Surprisingly, despite their inability to down-regulate the p53 substrate, even the C361/366S and C454/456S mutants relocalized p53. The R240A mutant, however, was extremely defective for this activity (Figure 14), consistent with its diminished capacity to degrade p53 (50, 312).

To confirm our aggresome immuno-fluorescence results we generated mutant E1b55K constructs that also contained a mutation (L83,87,91A) in the nuclear export signal (NES) (184). These E1b55K proteins were expressed by transfection in U2OS cells and analyzed by immuno-fluorescence (Figure 15). Cells expressing E1b55K with a mutated NES displayed nuclear aggregates of

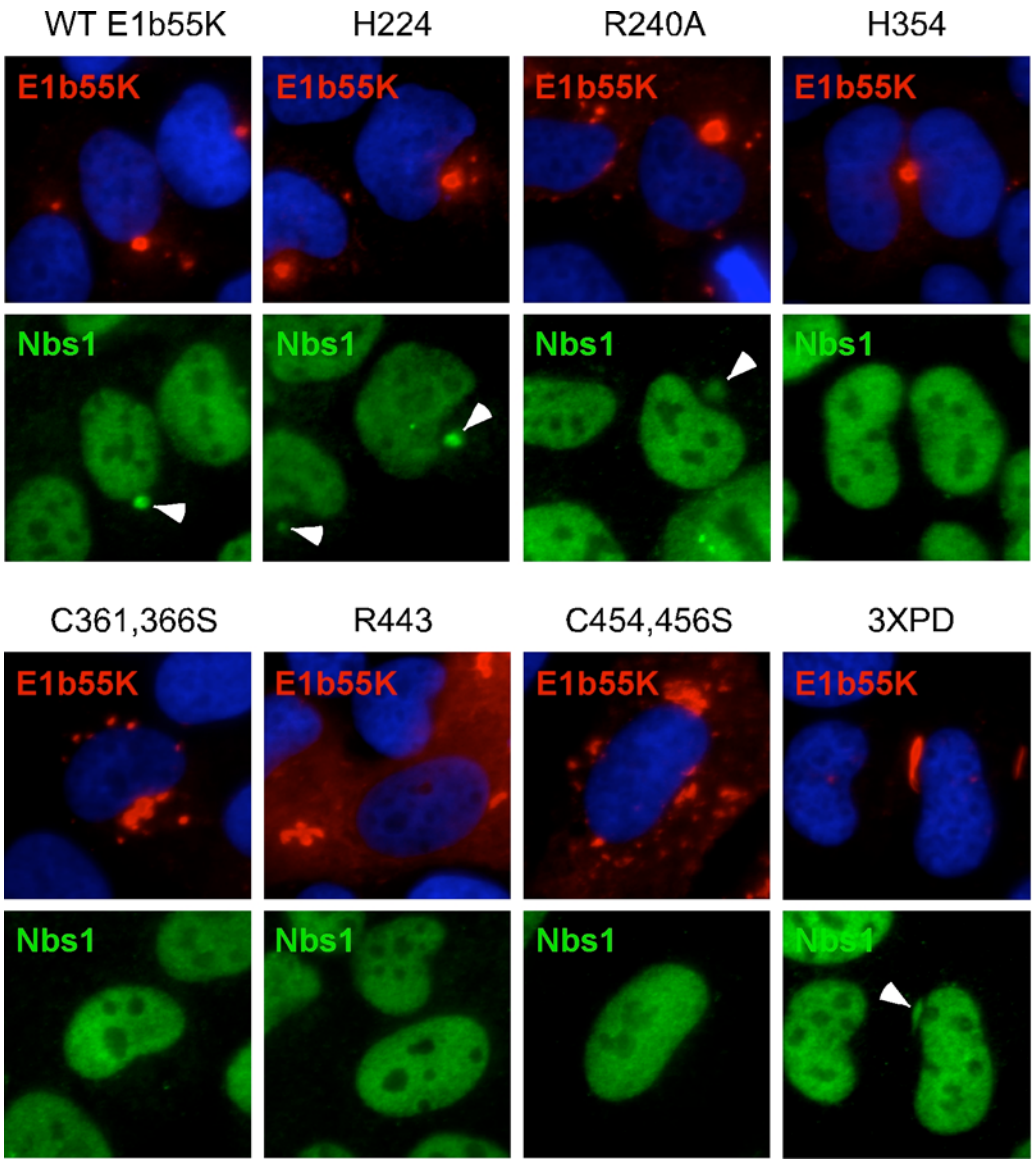

Figure 13. E1b55K mutants colocalize with Nbs1 in cytoplasmic aggregates. E1b55K mutants were transfected into U2OS cells to induce cytoplasmic aggresome/aggregate formation. Cells were processed for immuno-fluorescence after 24-36 hours using E1b55K and Nbs1. DAPI staining marks cell nuclei. White arrows indicate colocalization of substrates with E1b55K in cytoplasmic aggregates.

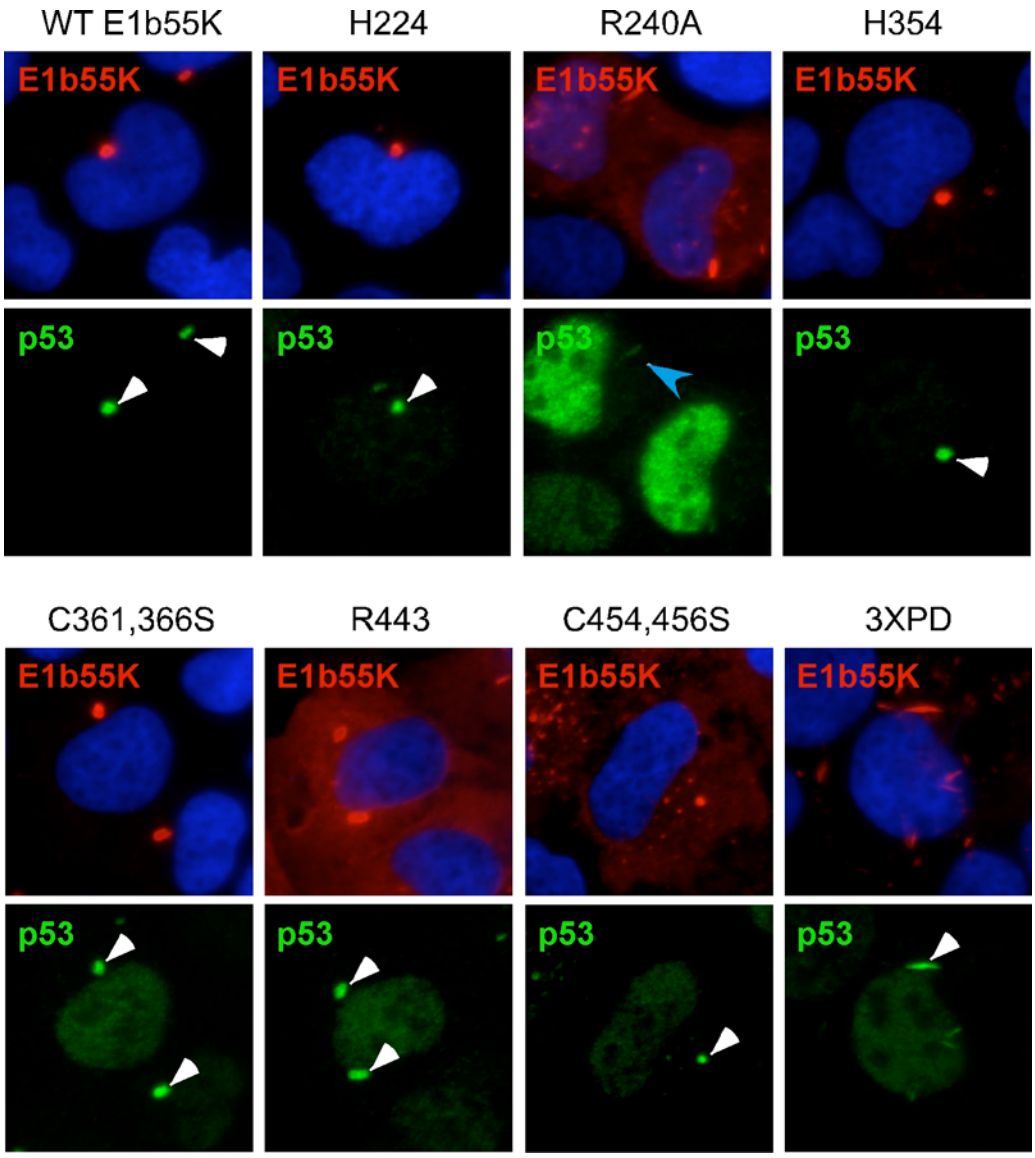

Figure 14. E1b55K mutants colocalize with p53 in cytoplasmic aggregates. E1b55K mutants were transfected into U2OS cells to induce cytoplasmic aggresome/aggregate formation. Cells were processed for immuno-fluorescence after 24-36 hours using antibodies against E1b55K and p53. DAPI staining marks cell nuclei. White arrows indicate colocalization of substrates with E1b55K in cytoplasmic aggregates. Blue arrow indicates weak p53 colocalization with the R240A mutant.

E1b55K staining, as previously reported (110). The endogenous cellular Nbs1 and p53 proteins appeared to colocalize with E1b55K foci, suggesting possible interaction (Figure 15). When our mutants were combined with the NES mutation, all proteins tested formed distinct nuclear foci, but there were differences in their ability to redistribute cellular proteins. Consistent with the degradation data, R240A-NES relocalized Nbs1 efficiently but not p53, whereas H373A-NES and H354-NES recruited p53 efficiently but not Nbs1. Together with the aggresome immuno-fluorescence data, these results suggest that most mutants with defects in degradation also have defects in binding substrates. However, the cysteine mutants (C361,366S and C454,4456S), may have additional defects related to p53 degradation, since they can still bind and relocalize this substrate.

To validate the immuno-fluorescence results, we performed co-immuno-precipitation (IP) experiments with E1b55K mutants in the absence of E4orf6 (Figure 16 and Table 1). E1b55K was immuno-precipitated from lysates of U2OS E1b55K mutant cell lines with the 2A6 antibody, and analyzed for MRN and p53 interaction. Because it was difficult to resolve p53 from the background Ig band in E1b55K immuno-precipitates, we also performed a reverse IP against p53 and probed for E1b55K interaction (Figure 16, bottom panels). Most mutants that failed to degrade specific cellular substrates also failed to interact with these proteins (Figure 16 and Table 1), confirming

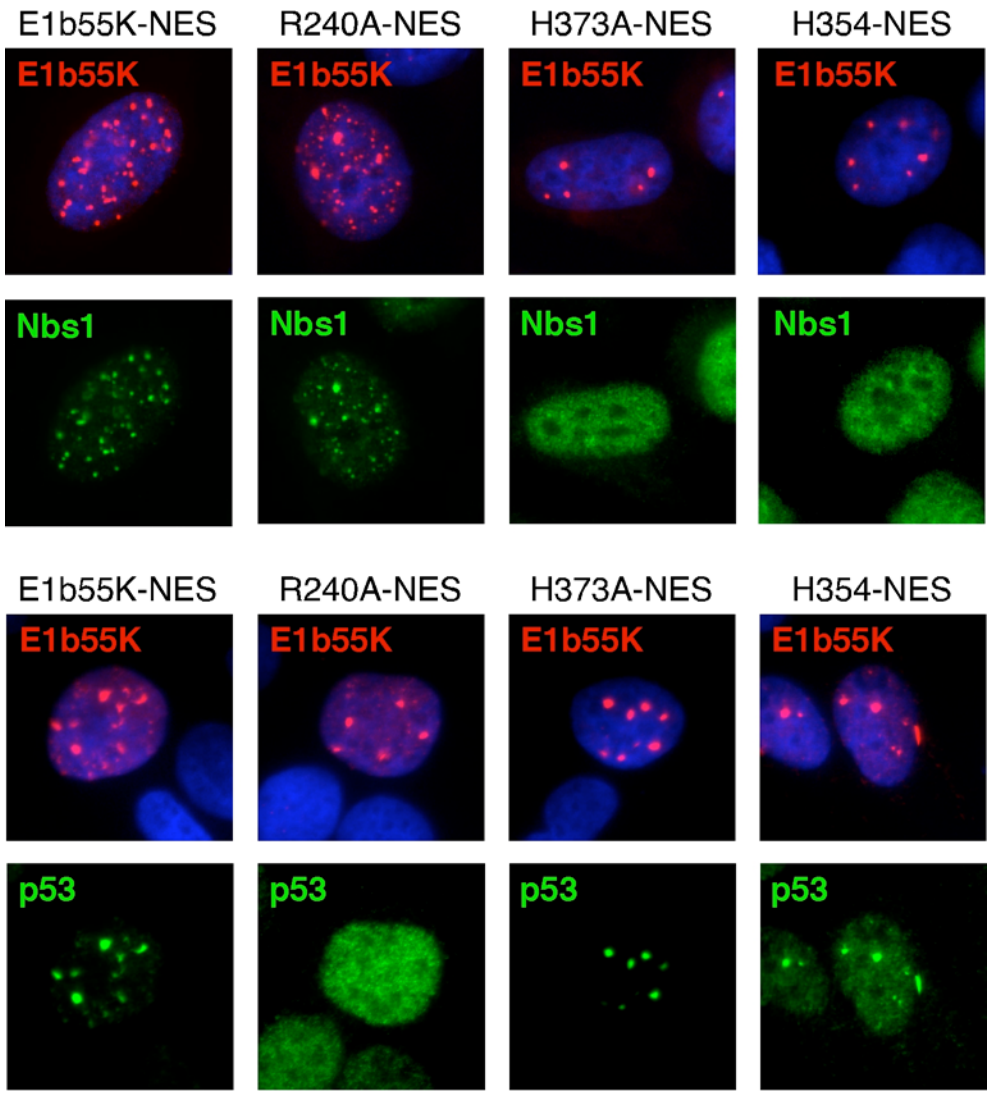

Figure 15. E1b55K-NES mutants relocalize cellular targets into nuclear aggregates. Constructs expressing E1b55K proteins with NES mutations were tranfected into U2OS cells. Cells were processed for immuno-fluorescence after 24 hours using antibodies to the indicated proteins. DAPI staining marks cell nuclei.

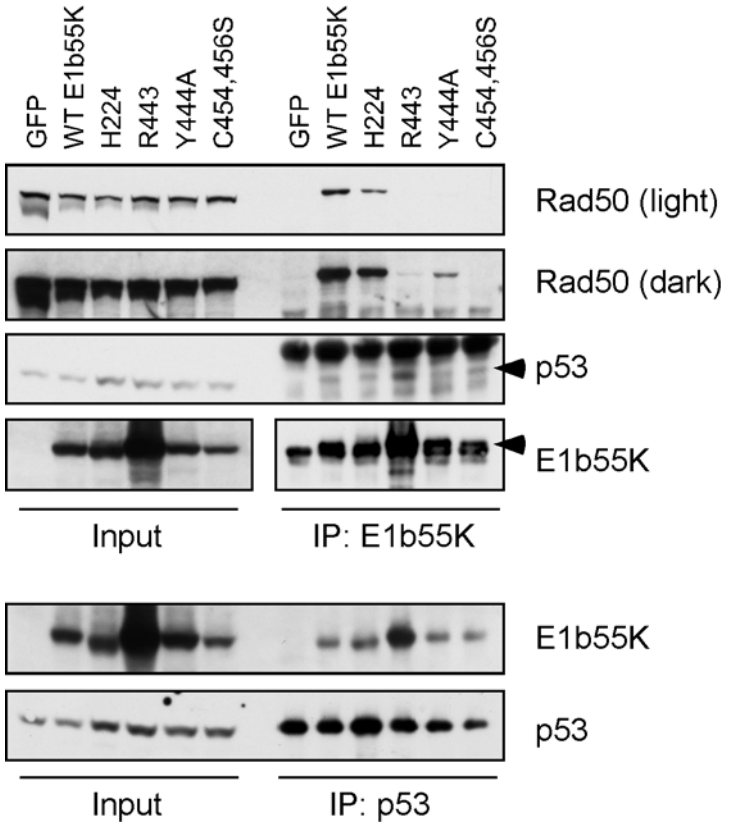

Figure 16. Interaction of cellular substrates with E1b55K mutants by immunoprecipitation. Lysates from mutant E1b55K cell lines were subjected to immuno-precipitation with the 2A6 antibody to E1b55K or a p53 antibody according to Materials and Methods. Approximately half the immuno-precipitate was analyzed by immuno-blotting alongside 5% of the input lysate.

immuno-fluorescence results. In the absence of E4orf6, MRN binding to the Y444A and 3XPA mutants was weaker than WT E1b55K. This interaction, however, is sufficient to induce degradation of MRN in the presence of E4orf6 (see Figures 5, 6, 7, and 9). This suggests that E4orf6 may enhance E1b55K interaction with MRN by relocalizing E1b55K to the nucleus. We also found that the cysteine mutants C361,366S and C454,456S were defective for MRN interaction but still retained the ability to bind p53, although not to the same extent as WT E1b55K (Table 1). Unfortunately, we were unable to examine endogenous DNA Ligase IV by immuno-fluorescence, and could not detect an interaction between E1b55K and endogenous DNA Ligase IV in our immuno-precipitation experiments (data not shown). Together our data suggest that the E1b55K separation-of-function mutants described here are defective in degradation due to diminished substrate binding. The ability of the E1b55K cysteine mutants to bind p53 in the absence of down-regulation suggests that there are additional requirements for substrate degradation.

Discussion

In this study we examined requirements for adenovirus-mediated degradation of the known cellular substrates of the E1b55K/E4orf6 ubiquitin ligase complex: the MRN proteins, p53 and DNA Ligase IV. We first addressed whether degradation of each of these cellular factors required other

proteins in the DNA damage response. While our previous use of E1b55K mutants suggested that MRN and p53 degradation were separable events (50), it was not clear whether the absence of cellular factors would affect degradation of the other substrates. Using mutant cell lines, we found that Ad down-regulates substrates independently from each other, and does not require other DNA damage response proteins (Figure 2A). Additionally, by examining Ad infections in A-TLD and NBS mutant cell lines, we suggest that Mre11 is the degradation target of E1b55K/E4orf6 (Figure 2B). Down-regulation of Rad50 and Nbs1, therefore, may be an indirect consequence of complex destabilization, as noted in other studies using RNAi against particular members of the MRN complex in the absence of virus infection (354, 408).

We analyzed a large collection of E1b55K mutants in order to define further the viral requirements for degradation. We found that down-regulation of the MRN complex is separable from p53 and DNA Ligase IV degradation, as discerned by a number of E1b55K mutants. These mutants suggest that at least two C-terminal cysteine-containing regions are critical to MRN degradation (see Figure 3 and Table 1). These regions include a proposed zinc-finger motif (123) and a transcriptional repression domain (389, 391). In the context of viral infection, mutants with defects in MRN degradation cannot completely prevent DNA damage signaling (Figures 4 and 10; (50)). However,

some of these mutants can still prevent viral genome concatemerization. This appears to occur through degradation of DNA Ligase IV (Figure 11), although we cannot exclude targeting of additional unidentified substrates. Many of the mutants analyzed could degrade DNA Ligase IV independently of p53 and MRN phenotypes, which suggests that there are distinct E1b55K requirements for DNA Ligase IV destabilization.

Further analysis of the panel of E1b55K mutants also identified cysteine mutants (C361,366S and C454,456S) with multiple defects that may affect degradation. In our studies, these mutants were unable to down-regulate any of the known cellular substrates (Figures 6 and 11). This phenotype is unlikely to be due to defective E4orf6 binding since these mutants exhibit an interaction with E4orf6 similar to H224 (Figure 5 and data not shown), a mutant competent to degrade all substrates but previously reported to exhibit reduced interaction with E4orf6 (294). We found that these cysteine mutants were defective in their association with MRN, but not with p53 (Figure 7 and Table 1). This result is consistent with the location of these mutations outside the previously defined p53 interaction domain in E1b55K (389). In contrast to our findings, Hartl *et al*., recently observed that the C454,456S mutant degraded exogenously expressed p53, and mislocalized Rad50 but not Mre11 in transformed baby rat kidney cells (148). The discrepancies may reflect different functions of E1b55K in transformed rodent cells versus human cells,

and the fact that we examined degradation specifically for endogenous proteins. From our data, it appears that the cysteine mutants have an additional defect related to p53 degradation. These amino acids in E1b55K might be important for modifying degradation substrates with ubiquitin or another marker required for ubiquitination and degradation. Unfortunately, we could not detect E1b55K interactions with endogenous DNA Ligase IV, so it is unclear why the cysteine mutants do not down-regulate this substrate. Further insights will come from studies that delineate regions in E1b55K important to binding and degrading DNA Ligase IV.

We examined a number of mutants to address whether post-translational modifications of E1b55K are important for degradation of substrates. We found that the SUMOylation site in E1b55K could be modified without impairing MRN degradation (Table 1), in agreement with a previous report (179). Phosphorylation sites in the C-terminus appeared to be important for both degradation of cellular substrates and correct cellular localization of E1b55K (Figures 7-10). Consistent with our data, a similar Ad12 E1b55K mutant (S476/7A) was also defective in formation of cytoplasmic aggregates (404). Phosphorylation may alter protein conformation, thereby affecting intra-molecular E1b55K interactions or association with partner proteins. Along these lines, we found that the interaction between the 3XPA mutant and p53 was severely defective or unstable by co-immunoprecipitation (Table 1),

consistent with the inability of this mutant to prevent p53-mediated transactivation and promote cellular transformation (346). Phosphorylation of all three amino acids might be required, however, since the 2XPA mutant still degraded p53 (Figure 10; (282)) and other cellular substrates (Figure 10), and retained the ability to bind p53 (347). The interaction between 3XPA and MRN was weaker than WT E1b55K (Table 1), although it was sufficient to induce MRN degradation with rAdE4orf6 (Figures 7 and 9). The phosphorylated amino acids in E1b55K lie within consensus CKI and CKII motifs (346, 347). However, it is still unclear whether these kinases are responsible for the phosphorylation of E1b55K in cells. Identification of kinases that modify E1b55K will provide more insight into the effects of phosphorylation on localization, structure, and protein-protein interactions important to function. It is interesting to note that the R443 mutant also displayed a diffuse cytoplasmic staining pattern in U2OS stable cell lines (Figure 5), although it still formed some small, perinuclear foci. Therefore, the C-terminus of E1b55K may be important to its structure and localization. While we do not know whether phosphorylation is affected in this mutant, R443 retained stable p53 binding (Figure 16; (173, 389)) unlike the 3XPA mutant.

Our analysis of E1b55K mutants illustrated differences when examining degradation by co-expression with E4orf6 alone, compared to the context of virus infection. We noticed a particular difference with mutants in the C-

terminus (Y444A, R443, and 3XPA), where greater defects in degradation of substrates were observed during viral infection (compare Figure 4 to Figure 6, and Figure 10 to Figure 9, see also Table 1). Higher levels of E4orf6 expressed from the recombinant adenovirus might partly contribute to these observations. The experiments with E1b55K mutants and E4orf6 alone are useful in delineating absolute requirements for degradation. For example, phosphorylation of E1b55K might not be absolutely required for MRN degradation, but may contribute more to degradation of p53 and DNA Ligase IV (Figure 9). Interactions between viral proteins are likely to be far more complex in the context of virus infection, and therefore it will be informative to incorporate some of the E1b55K mutants analyzed here into the virus to characterize further their phenotypes. It will also be interesting to examine degradation in primary human cells, in order to determine whether the same requirements hold true.

Although degradation of p53, MRN and DNA Ligase IV induced by E1b55K/E4orf6 appears to be proteasome-mediated, only p53 has been shown to be a direct ubiquitination target. It will be important to determine whether ubiquitination of the MRN complex and DNA Ligase IV by the E1b55K/E4orf6 ubiquitin ligase is directly involved in degradation. This is likely to be the case, since down-regulation of all these substrates is prevented by expression of a trans-dominant Cullin 5 (8, 218, 378) and by siRNA

knockdown of Cullin 5 (see Chapter 4; (218)). Other proteins that interact with E1b55K have been identified by genetic, biochemical and proteomic studies (122, 126, 146, 221, 404), however, not all of these interactors are targets for down-regulation. It will be interesting to ascertain what determines the ubiquitination and degradation of E1b55K associated proteins. Understanding the selective targeting of degradation substrates by E1b55K mutants will help illuminate which cellular proteins are involved in viral replication, late protein production, and cell transformation.

Materials and Methods

E1b55K mutagenesis and cloning, and transfections

Previously described E1b55K mutants were amplified from corresponding viruses (312, 390) with PCR primers RVF (forward primer: 5'-CCGCTCGAGATGGAGCGAAGAAACCCATC-3') and RVR (reverse primer: 5'-CCATCGATTCAATCTGTATCTTCATCGCTAG-3'), and cloned into the Xho1 and Cla1 sites of a modified version of the pCLNC retroviral vector, as previously described (50). Site-directed mutagenesis was performed using QuikChange mutagenesis kit (Stratagene) on E1b55K in either the pDC516 backbone vector (provided by H. Young) or pCLNC using the primers in Table 2. Mutants were screened as described in the text, and interesting mutants in the pDC516 vector were PCR amplified using RVF and RVR primers (or a

Table 2. Summary of E1b55K mutagenesis primers used in this study.

Mutant	Vector backbone	Round of mutagenesis		Primer sequence (5' to 3')*
L83,87,91A (NES)	pDC516	(first round)	Forward	GGCTGAACTGAGACGCATTGCGACAATTACAGAGG
			Reverse	CCTCTGTAATTGTCGCAATGCGTCTCAGTTCAGCC
		(second round)	Forward	GGCTGAACTGTATCCAGAAGCGAGACGCATTGCG
			Reverse	CGCAATGCGTCTCGCTTCTGGATACAGTTCAGCC
		(third round)	Forward	GTACAGGTGGCTGAAGCGTATCCAGAAGCGAGACGC
			Reverse	GCGTCTCGCTTCTGGATACGCTTCAGCCACCTGTAC
K104R	pDC516		Forward	GGGCTAAAGGGGGTGAGGAGGCAGCGGGGGG
			Reverse	CCCCCCGCTGCCTCCTCACCCCCTTTAG
C348,351S	pDC516		Forward	CATAACATGGTAAGTGGCAACAGCGAGGACAGG
			Reverse	CCTGTCCTCGCTGTTGCCACTTACCATGTTATG
C361,366S	pDC516	(first round)	Forward	TCAGATGCTGACCTCCTCGGACGGCAA
			Reverse	TTGCCGTCCGAGGAGGTCAGCATCTGA
		(second round)	Forward	TCGGACGGCAACTCTCACCTGCTGAAG
			Reverse	CTTCAGCAGGTGAGAGTTGCCGTCCGA
H373A	pDC516		Forward	TGCTGAAGACCATTGCCGTAGCCAGCCACT
			Reverse	AGTGGCTGGCTACGGCAATGGTCTTCAGCA
C454,456S	pDC516		Forward	CCAGGTGCAGACCCTCCCGAGTCTGGCGGTAAACATATTAGG
			Reverse	CCTAATATGTTTACCGCCAGACTCGGAGGGTCTGCACCTGG
S490,491,T495A	pDC516	(first round)	Forward	GCTCTAGCGATGAAGATGCAGATTGAGGTACTG
			Reverse	CAGTACCTCAATCTGCATCTTCATCGCTAGAGC
		(second round)	Forward	CGCTGAGTTTGGCGCTGCCGATGAAGATGCAGATTGAGG
			Reverse	CCTCAATCTGCATCTTCATCGGCAGCGCCAAACTCAGCG
S490,491,T495D	pCLNC	(first round)	Forward	GGCTCTAGCGATGAAGATGACGATTGAGGTACTGAA
			Reverse	CAGTACCTCAATCGTCATCTTCATCGCTAGAGC
		(second round)	Forward	CGCTGAGTTTGGCGATGACGATGAAGATGACGATTGAGG
			Reverse	CCTCAATCGTCATCTTCATCGTCATCGCCAAACTCAGCG

*Codons changed in the primer sequence are underlined. Primers were used to introduce changes in E1b55K in backbone pDC516 or pCLNC. Interesting mutants were subcloned into retroviral vector pCLNC to make cell lines with. All mutants were verified by sequencing.

modified RVR primer for 3XPA mutant, 5'-CCATCGATTCAATCTGCATCTTCATCGGCAG-3') and subcloned into Xho1 and Cla1 sites of pCLNC (50). To generate the NES-pDC516 mutants used in Figure 7B, E1b555K mutants R240A and H354 were PCR amplified and replaced WT E1b55K in pDC516 using SmaI and SacI sites. E1b fragments containing mutations were then subcloned as follows: for NES-H373A, the EcoRI-PstI fragment of E1b55K-NES was cloned into H373A-pDC516, and for NES-R240A and NES-H354, the PstI-BglII fragment containing H354 or R240A (in pDC516) was cloned into E1b55K-NES-pDC516. All mutants used in this study were verified by sequencing. Plasmids were transfected into cells with Lipofectamine 2000 (Invitrogen) according to manufacturer's protocol.

Cell lines

HeLa, U2OS, IMR90, Saos2 and 293 cells were purchased from the American Tissue Culture Collection. Stable cell lines derived from HeLa and U2OS that express wild-type (WT) and mutant E1b55K from retrovirus vectors have been described previously in Chapter 2. Immortalized A-TLD3 and A-TLD1 cells were previously described (50, 330, 335). NBS cells were provided by P. Concannon (56). FUS9 cells with mutant DNA-PKcs (156) were provided by T. Melendy. All cells were maintained as monolayers in either Dulbecco modified Eagle's medium (DMEM) supplemented with 10 or 20% fetal bovine serum (FBS) and pen/strep, except FUS9 cells which required 1:1 of DMEM and F10

media supplemented with 10% FBS and pen/strep. All cells were incubated at 37°C in a humidified atmosphere containing 5% CO_2.

Viruses and infections

The mutant virus *dl*3112 (ΔE1b55K/ΔE4orf3) and *dl*110 (ΔE1b55K) have been previously described (6, 314), and were obtained from D. Ornelles and G. Ketner, respectively. The viruses mutated for phosphorylation sites in E1b55K (pm490/1/5A and pm490/1A) have been previously described (346, 347) and were obtained from P. Branton. The H224, H354 and R443 viruses with mutations in E1b55K have been previously described (390) and were obtained from A. Berk. The Y444A (ONYX85) virus has been previously described (312) and was obtained from Y. Shen. The E1-deleted recombinant adenovirus vector expressing E4orf6 was obtained from P. Branton was described in Chapter 2. All virus propagation and infection conditions were also described in Chapter 2.

Antibodies, immunoblotting, and immunofluorescence

Primary antibodies were purchased from Serotech (DNA Ligase IV), Santa Cruz (p53 C-19), Research Diagnostics Inc. (GAPDH), and Calbiochem (PCNA, p53 Ab-6). The E4orf6 mAb RSA#3 was obtained from D. Ornelles. All other primary antibodies were described in Chapter 2. Secondary antibodies were purchased from Jackson Laboratories or Eurogentec. Immuno-blotting and immuno-fluorescence were performed essentially as previously described

(50). For immuno-fluorescence, cells were fixed with 4% PFA before permeablizing with 0.5% Triton-X 100 and processing as previously described (50).

Immuno-precipitations

U2OS E1b55K cell lines were lysed with buffer containing 50 mM Tris (pH 7.5), 150 mM NaCl, 0.5% NP-40, and 1X protease inhibitors without EDTA (Roche) for 30 min on ice. After spinning out cellular debris, 400-500 μg of total protein per reaction (constant between experiments) was pre-cleared with protein A/G beads (Santa Cruz) for 1 hour at 4°C. 25 μL of either the anti-E1b55K antibody (2A6), the anti-DBP antibody (B6) as a control, or 10 μL of the p53 (C-19) antibody was added to the pre-cleared supernatant along with protein A/G beads, and the mixture was rotated overnight at 4°C. Beads were then washed three times for 30 min each in fresh lysis buffer before boiling in SDS loading buffer and running on SDS-polyacrylamide gels for the resolution of interacting proteins by immuno-blotting. To detect interaction of E1b55K mutants with E4orf6, beads were heated at 55°C for 15 min in SDS loading buffer before loading gels.

Analysis of concatemer formation by pulsed-field gel electrophoresis

Cells were infected with wild-type Ad5 or the ΔE1b55K/ΔE4orf3 mutant, *dl*3112, at a multiplicity of infection (MOI) of 10. Cells were harvested at 30 hours post-infection (hpi) and DNA analyzed for concatemer formation as

previously described (335, 360). Briefly, cells were incorporated into agarose plugs that were treated with Proteinase K solution (1.2% SDS, 0.125 M EDTA, and 5 mg/mL Proteinase K) at 50°C overnight, and then washed with 50 mM EDTA solution. Plugs were loaded onto a 1.2% HGT agarose gel and subjected to pulsed-field electrophoresis for 16 hours. DNA was visualized by staining the gel in Sybr Green.

Acknowledgements

I am extremely grateful to Seema Lakdawala, Heather Eshleman, and Matthew Russell for all their contributions in the construction and characterization of E1b55K mutants—this work would not have been possible without their help. I also thank Seema for the analysis of concatemer formation in this Chapter. I am grateful to Christian Carson for the initial characterization of degradation in A-TLD and NBS cell lines in Figure 2B. I thank A. Berk, P. Branton, P. Concannon, G. Ketner, A. Levine, T. Melendy, D. Ornelles, J. Petrini, Y. Shen, and H. Young for generous gifts of reagents. I also thank Daniel Linfesty and Darwin Lee for technical assistance, and members of the Weitzman lab for discussions and critical reading of the manuscript.

Some material from this chapter is reprinted in part as it appears in:

Schwartz RA, Lakdawala SS, Eshleman HD, Russell MR, Carson CT, and Weitzman MD. Distinct requirements of the adenovirus E1b55K protein for degradation of cellular substrates. J Virol, submitted.

The dissertation author was the primary researcher and author of this paper.

Chapter 4. The contribution of E4orf6 and cellular ubiquitin ligase factors to the degradation of cellular targets.

Background

The E4 region of adenovirus (Ad) encodes a series of proteins that modulate the host environment to promote viral replication (313, 343, 364). E4orf6 is a 34kDa protein produced early in infection from this region, and acts with the E1b55K protein (302) in order to overcome cell cycle restrictions, promote viral DNA replication and viral late protein synthesis, prevent viral genome concatemers, and promote host cell shutoff (reviewed in (123, 313, 367)). As mentioned previously, E1b55K/E4orf6 complex association with Cullin 5, Rbx1, and Elongins B and C (Figure 1A) (146, 281) is thought to mediate many of these functions (25, 72, 378), although the mechanisms still remain unclear. E1b55K is believed to recruit cellular targets for degradation, since it can bind substrates without E4orf6 (see Chapter 3). Although E4orf6 can associate with p53 alone (94, 282), ubiquitination and degradation of this target only occurs efficiently with E1b55K (24, 50, 283, 292), further supporting the role of E1b55K in substrate recruitment. E4orf6 is, therefore, primarily responsible for CRL recruitment Rbx1 (146, 281). At the time of these studies, the E1b55K/E4orf6-CRL was believed to degrade p53 (137, 238, 251, 282, 292, 329) and MRN (50, 335), but direct evidence was lacking.

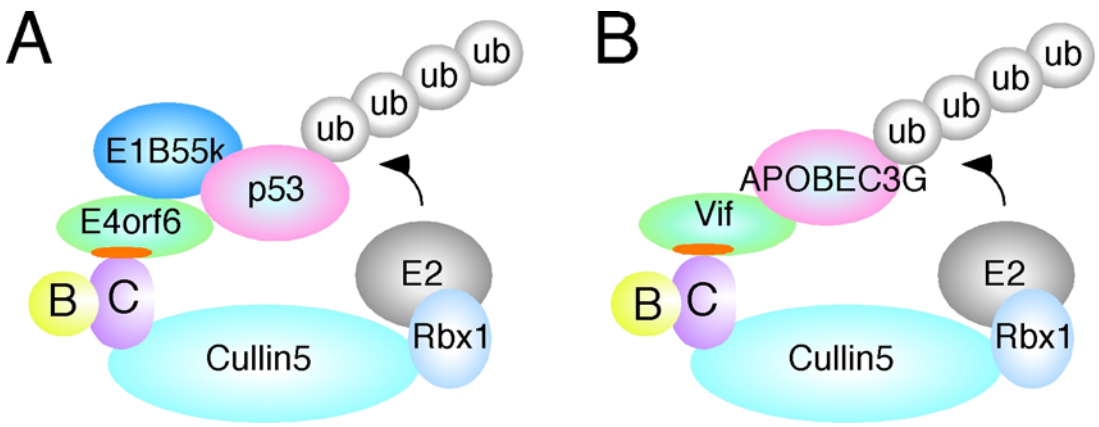

Figure 1. Schematic of viral Cullin-containing ubiquitin ligases. (A) Schematic of the E1b55K/E4orf6 ubiquitin ligase. E1b55K is thought to bind the substrate while E4orf6 recruits the cullin-containing ligase. The orange domain in E4orf6 represents a BC box that binds to Elongin C. The E2 utilized by E1b55K/E4orf6 is currently unknown. **(B)** Schematic representation of the Vif-containing CRL. Cullin 5 links Rbx1 and Elongins B and C. Elongin C binds a divergent BC box in Vif (orange). Vif targets APOBEC family members for ubiquitination and proteasome-mediated degradation.

E4orf6 contains a number of domains crucial to its functions (Figure 2). Its interaction with E1b55K has been mapped to the N-terminus of the protein (283, 294), although E1b55K nuclear retention requires an arginine-rich α-helix near the E4orf6 C-terminus, which is also important to some its functions (Figure 2) (24, 263, 264). E4orf6 also encodes a number of conserved cysteine and histidine residues thought to coordinate zinc (31). Mutation of these amino acids disables E4orf6 for E1b55K interaction, p53 degradation, and E4-deleted adenovirus complementation (31), suggesting that these residues are important structurally. A number of putative BC box sequences have also been identified in E4orf6 (Figure 2) (24, 233). BC box one and two diverge from the traditional consensus motif, and mutations in these sequences disrupt the interaction with both E1b55K and E3 ligase factors, therefore abrogating substrate degradation (24). The third BC box resembles that found in the HIV protein, Vif, which degrades the cellular APOBEC3G protein by hijaking the same CRL composed of Cullin 5, Rbx1, and Elongins B and C (Figure 1B) (233, 399). Despite a body of work describing mutations in many of these E4orf6 domains, it was not completely clear how these regions contributed to degradation of substrates, especially MRN. At the time of these studies, it was also unclear whether MRN and p53 down-regulation proceeded via the same mechanism.

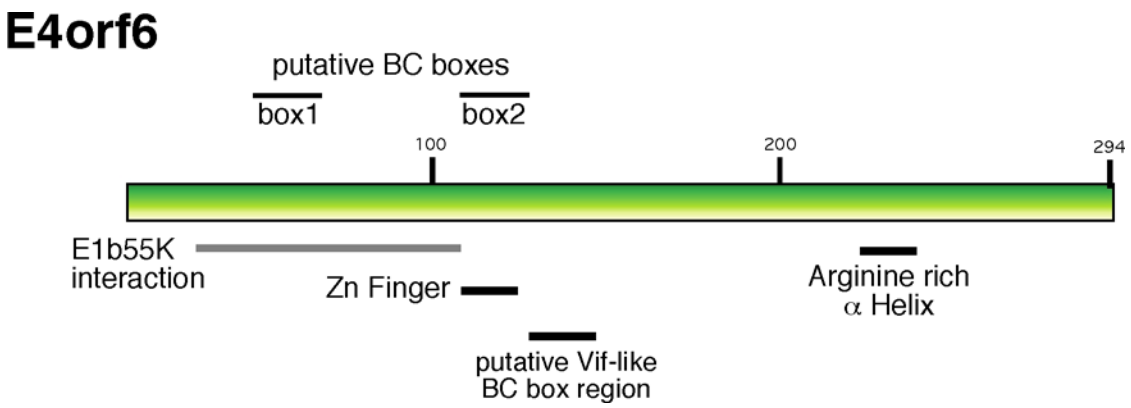

Figure 2. Schematic of E4orf6. Shown above and below E4orf6 are relevant functional domains. Sequences from the putative BC boxes (24) and Vif-like BC box (233) are shown in further detail in Figure 6. The putative zinc finger (31) and arginine rich α-helix (263) are also shown in black below the protein. In gray is the E1b55K interaction domain (283, 294). Numbers indicate the amino acid positions.

In this Chapter we investigated how E4orf6 and E4orf6-recruited E3 ligase components affect degradation of the Mre11 complex. We found that the Vif-like BC box in E4orf6 contributed to efficient substrate down-regulation. However, some E4orf6 mutations in this region were pleiotropic, potentially disrupting association with E1b55K. Despite this, many E4orf6 α-helix mutants down-regulated targets without retaining E1b55K in the nucleus, suggesting that these are separable events. Finally, we examined which ubiquitin ligase factors mediated down-regulation of substrates. While degradation of MRN and p53 both involved Cullin 5, we found surprising evidence that MRN and p53 destabilization may require distinct RING proteins. These results indicate that the E1b55K/E4orf6 complex provides a powerful model to study the assembly and regulation of CRLs.

Results

Effects of E4orf6 mutations in the α-helix on cellular substrate degradation

E4orf6 contains an arginine-rich amphipathic α-helix at its C-terminus (263) (see Figure 2). The net positive charge in this region is required to promote nuclear retention of E1b55K (263, 264), reflecting a functional interaction between E1b55K and E4orf6. Mutations within the α-helix were identified that could complement an E4-deleted adenovirus infection in the

absence of E1b55K nuclear retention (264). Other α-helix mutants were reported to have defects in recruitment of E3 ligase factors (24). Given these phenotypes, we wanted to test how α-helix mutations affected substrate degradation.

A series of E4orf6 α-helix mutants were obtained in which some positively charged arginines were changed to glutamic acid residues or alanines (264). We first transfected these into U2OS cells expressing wild-type (WT) E1b55K to analyze their expression and verify their E1b55K nuclear retention phenotypes. All the arginine mutants displayed a similar expression level and pattern by immunofluorescence, compared to WT E4orf6 (Figure 3 and data not shown). These E4orf6 mutants were also extremely defective in retaining E1b55K in the nucleus, as expected. Figure 4 shows the most robust nuclear E1b55K localization seen for this series of mutants. In our experiments, R241A appeared to retain E1b55K the best. Although this observation was consistent with previous data (264), we found that R243A was as defective as the other arginine mutants, contrasting that report (264). Cell type differences may explain the discrepancy. These results verify the requirement of the positively charged arginine residues in E1b55K nuclear retention (264).

We then addressed whether these E4orf6 arginine mutants could degrade cellular substrates. Degradation of MRN was first examined by

Figure 3. E4orf6 expression is similar between α-helix mutants. U2OS cells expressing wild-type E1b55K were transfected with the indicated E4orf6 mutants for 44 hours. Cells were fixed and processed for immunofluorescence, staining for Rad50 and E4orf6. DAPI shows the nuclei in the merged images. White arrowheads indicate cells in which Rad50 has been degraded.

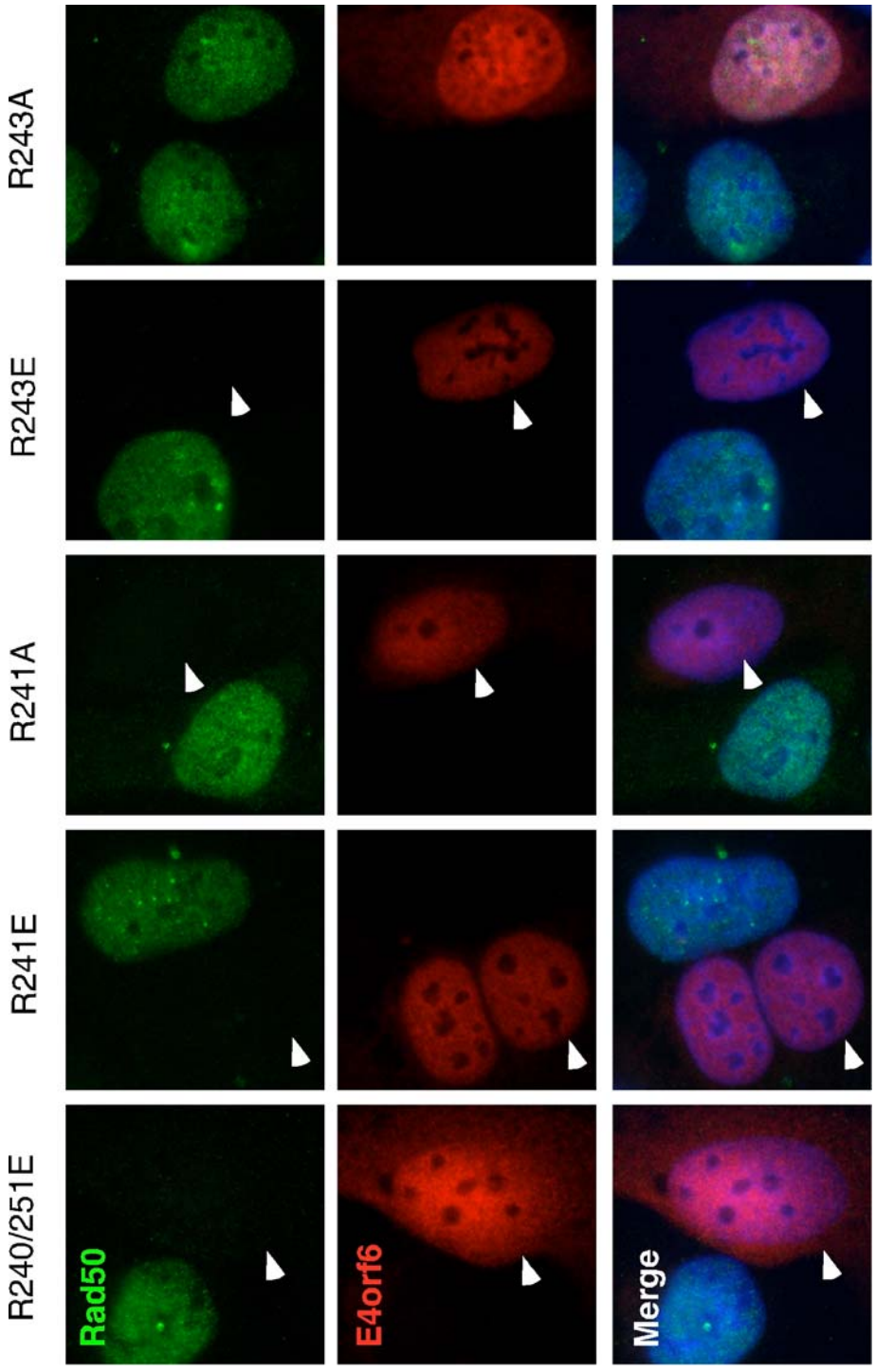
R240/251E
R241E
R241A
R243E
R243A
Rad50
E4orf6
Merge

immunofluorescence (Figure 4). Most mutants could down-regulate MRN despite compromised E1b55K retention. The exceptions to this were L245P, previously reported to be defective for p53 degradation (252), and R243A. The related E4orf6 mutant, AXA (R243A/L245P) (139), was also unable to bind E1b55K and degrade p53 (52). To validate these results, we tested whether the α-helix mutants could complement an E4-deleted adenovirus infection. HeLa cells were transfected with WT E4orf6 or the mutants, before infecting with *dl*1004 (Figure 5). Although transfection efficiency may not have been maximal, we saw a similar trend in the ability of the arginine mutants to degrade MRN and p53 (Figure 5A and data not shown) and prevent concatemer formation (Figure 5B). L245P and R243A were defective in these assays. Although R241A and R241E were barely visible by western analysis (Figure 5A), their expression was comparable by immunofluorescence (Figure 3) and they appeared at least partially functional (Figures 3, 4, and 5). Therefore, antibody recognition during immunoblotting may be obscured by these mutations. More experiments will be required to determine whether the degradation differences in Figure A are real. These results demonstrate that E1b55K nuclear retention is separable from degradation (see also Chapter 3). Interestingly, all mutants except L245P and R243A could complement viral growth of an E4-deleted adenovirus (264) and recruit E3 ubiquitin ligase factors (24), which is consistent with our data. Table 3 summarizes our data

Figure 4. E1b55K nuclear retention by E4orf6 mutants is not required for degradation. U2OS cells expressing wild-type E1b55K were transfected with the indicated E4orf6 constructs for 44 hours before fixing and processing for immunofluorescence. Cells were stained for E1b55K and Nbs1. DAPI indicates the cell nuclei in merged images. White arrowheads indicate cells where Nbs1 has been degraded.

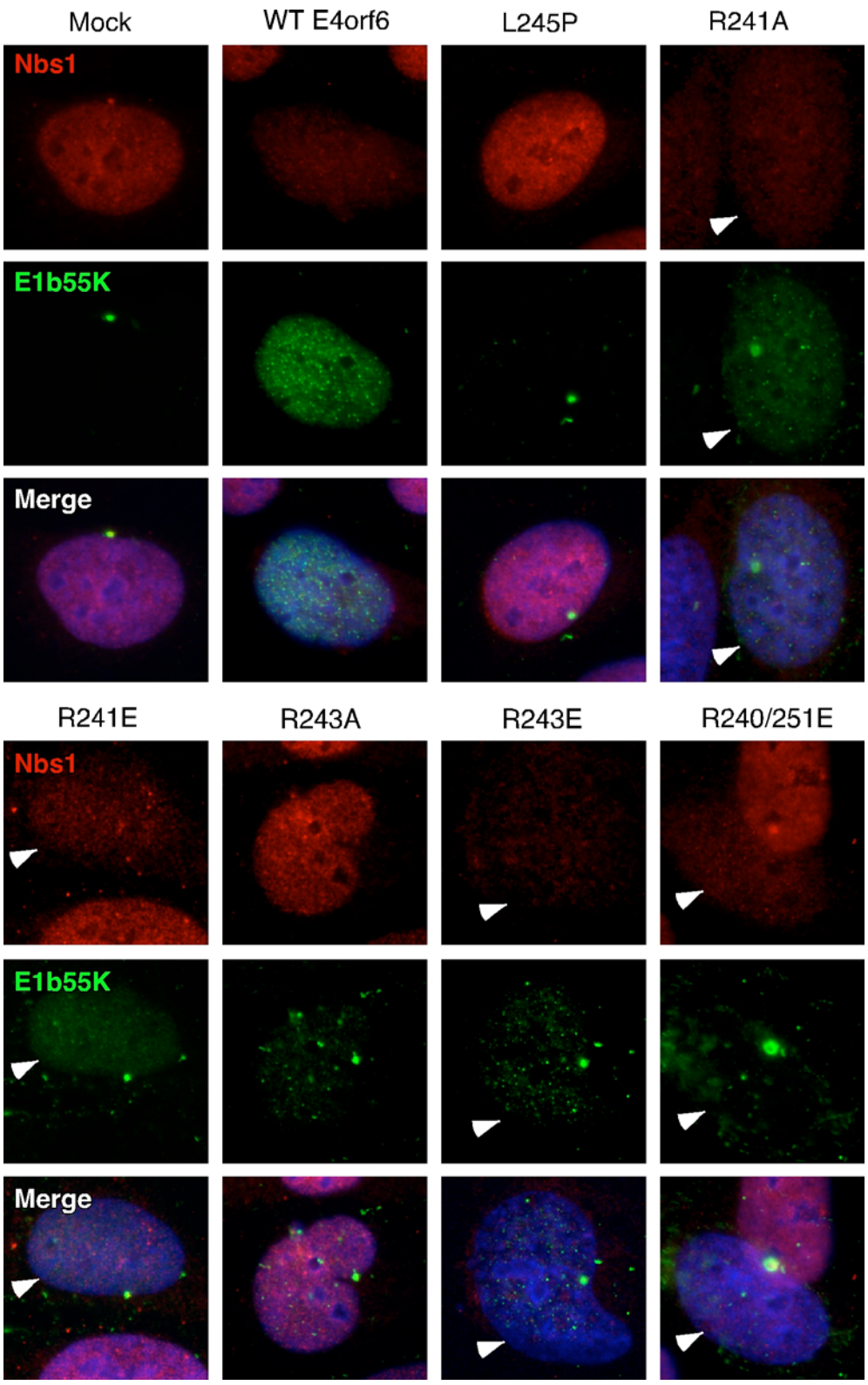
Mock
WT E4orf6
L245P
R241A
Nbs1
E1b55K
Merge
R241E
R243A
R243E
R240/251E
Nbs1
E1b55K
Merge

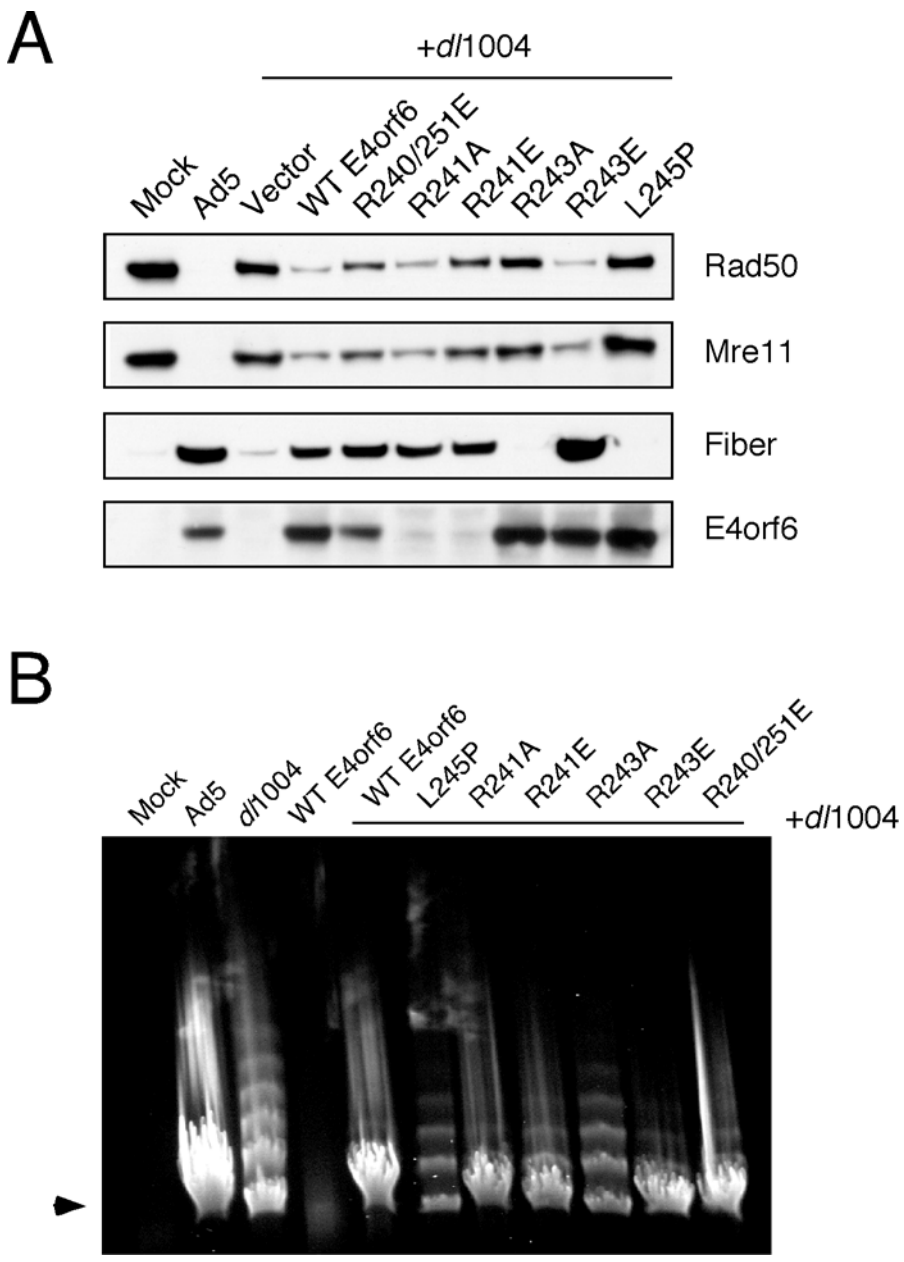

Figure 5. The effects of E4orf6 α-helix mutations on complementation of mutant adenovirus infection. HeLa cells were transfected for 24 hours with the indicated E4orf6 constructs before infecting with Ad5 (MOI of 50) or dl1004 (MOI of 25) for an additional 24 hours. Cells were harvested and processed for immunoblotting **(A)** or pulse-field gel electrophoresis **(B)**. Arrowhead indicates the linear monomeric adenovirus genome in (B).

and published phenotypes of E4orf6 mutants. Given the importance of substrate down-regulation to virus replication, our results likely explain the ability of the arginine mutants to complement mutant virus infection.

Effects of E4orf6 mutations in the Vif-like BC box on substrate degradation

At the time of these studies, two putative BC boxes in E4orf6 were identified, although their sequences diverged from the consensus motif (Figure 6A) (24), and the second BC box was located in the conserved zinc finger region (31). While mutation of key cysteine residues abrogated E3 ligase interaction and substrate degradation, the E1b55K binding was also compromised (24), complicating the interpretation of results. Interestingly, a Vif-like BC box (233, 399) resides nearby the second putative E4orf6 BC box (Figures 2 and 6A). This sequence resembles the consensus motif sequence except that an alanine replaces the cysteine at position 136 (Figure 6A). Mutation of the invariable leucine at position 132 (L132S) and alanine at position 136 to a bulky residue (A136F) resulted in defective E3 ligase association and p53 degradation (X.F. Yu, personal communication). However, mutating A136 to either cysteine or serine retained E4orf6 functionality (X.F. Yu, personal communication), similar to Vif BC box mutants (399), suggesting that these amino acids are functionally equivalent. Given

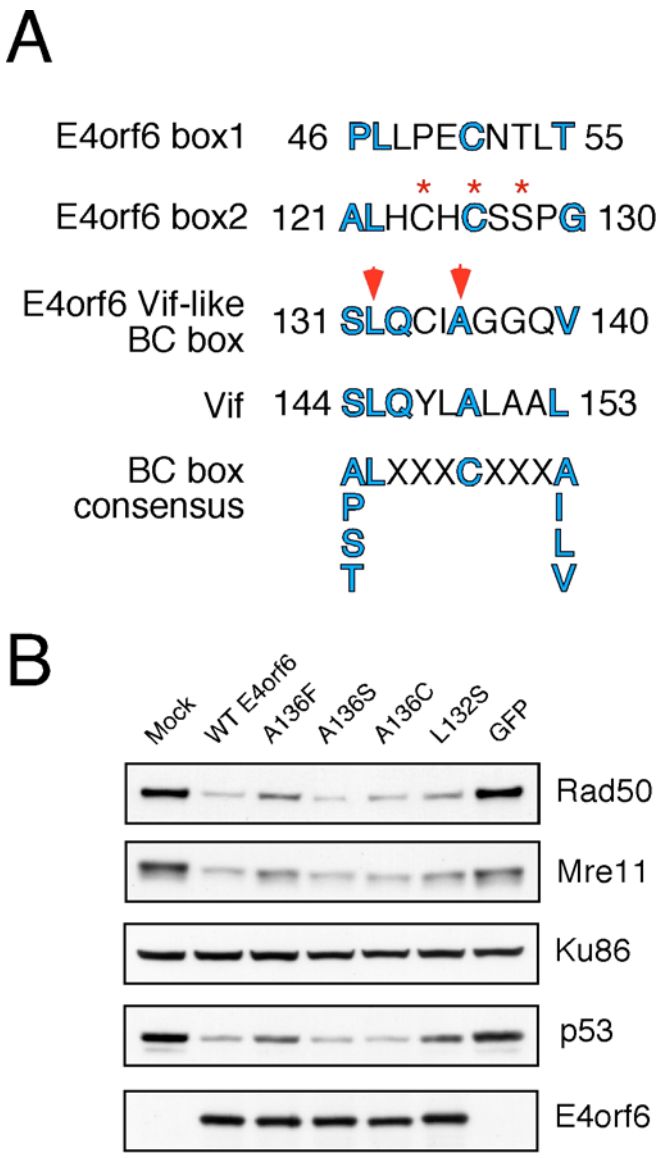

Figure 6. Mutations in the E4orf6 Vif-like BC box region partially abrogate degradation of cellular substrates. (A) Sequences of BC box motifs in E4orf6. Shown are the two putative BC boxes (24), followed by the Vif-like BC box in E4orf6 (233), the Vif BC box (233, 399), and the consensus BC box motif. Highlighted in blue are the critical amino acid positions relative to the consensus BC box motif. E4orf6 mutants in Figures 6-8 are indicated by red arrows. E4orf6 mutants in Figure 9 are highlighted by red asteriks. **(B)** Vif-like BC box mutants partially abrogate degradation. 293Q cells were transfected with wild-type E4orf6 or the indicated mutants for approximately 48 hours before harvesting. Lysates were analyzed for the indicated proteins. Ku86 serves as a loading control.

these phenotypes, we wished to determine how the E4orf6 Vif-like BC box sequence contributed to MRN degradation.

To begin to address this, we first transfected WT E4orf6 or the Vif-like BC box mutants into 293 cells, which already express E1A and E1b proteins (Figure 6B). Expression of WT E4orf6, A136C, or A136S resulted in the down-regulation of p53 and MRN, as expected. However, mutants L132S and A136F, which are defective for E3 ubiquitin ligase recruitment, exhibited partial degradation of substrates. We then tested whether these mutants could complement an E4-deleted adenovirus infection (Figure 7 and Table 3). HeLa cells were transfected with WT E4orf6 or the BC box mutants before infection with *dl*1004. WT E4orf6, A136C, and A136S were all able to degrade MRN, prevent DNA damage signaling (indicated by a shift in Nbs1) (Figure 7A), and prevent concatemer formation (Figure 7B). A few background concatemers were visible in these samples, likely due to incomplete transfection. The defective BC box mutants, L132S and A136F, partially rescued degradation, similar to Figure 6B. Because of this, damage signaling was apparent (Nbs1 was shifted) and concatemers were still obvious. Taken together, our results show that the E4orf6 Vif-like BC box may be required for efficient substrates down-regulation, although the mutants analyzed here are not completely defective, perhaps due to the single amino acid changes.

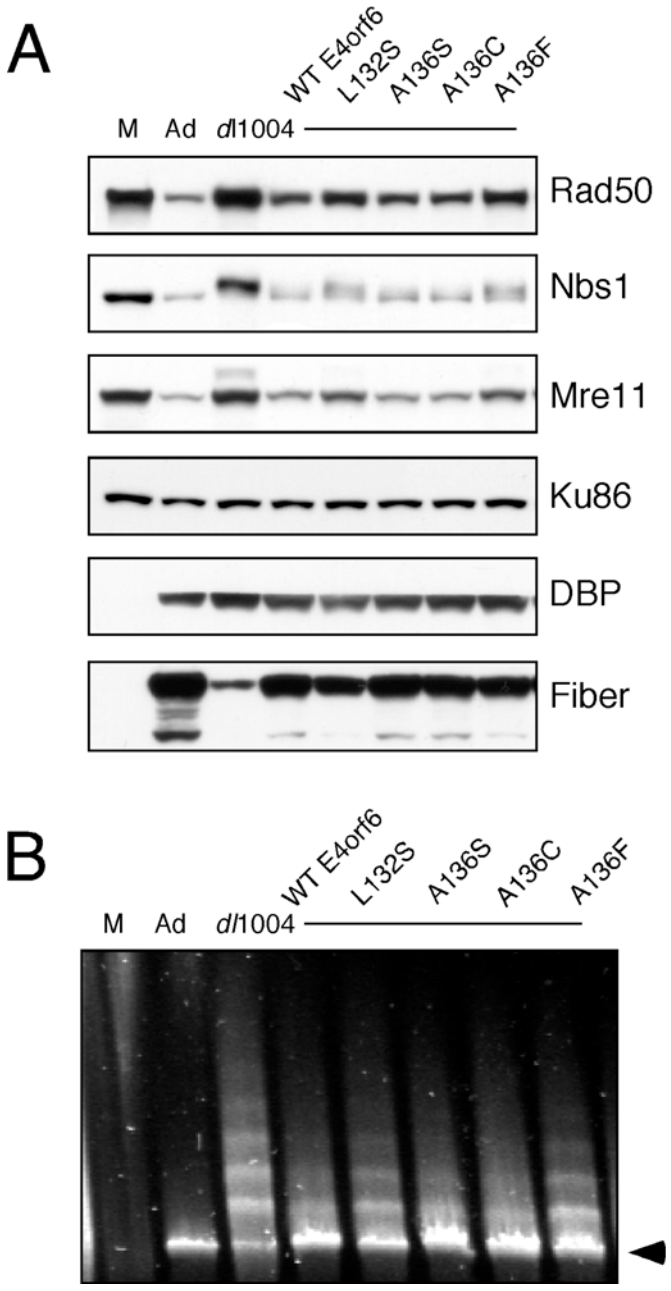

Figure 7. Partial degradation of substrates by E4orf6 BC box mutants does not complement mutant virus infection. HeLa cells were transfected with vector, wild-type E4orf6, or the indicated E4orf6 mutants for 24 hours before infecting with either E4-deleted adenovirus *dl*1004 or wild-type Ad 5 (both at an MOI of 50). Cells were harvested and processed for western analysis **(A)** or pulse-field gel electrophoresis **(B)**. The arrowhead indicates the monomeric Ad genome.

Because mutations in the other E4orf6 putative BC boxes abrogated binding to E1b55K (24), we wanted to determine how the Vif-like BC box mutants interacted with E1b55K. To begin to address this, we examined localization of E1b55K in the presence of the E4orf6 mutants. U2OS cells expressing WT E1b55K were transfected with WT E4orf6, the BC box mutants, or the E4orf6 mutant AXA as a control. As expected, E1b55K was efficiently retained in the nucleus by WT E4orf6, but not by AXA (Figure 8) (52). Mutants A136S and A136C also retained E1b55K in the nucleus, similar to the WT protein. The L132S and A136F mutants induced some E1b55K nuclear retention, but not as much as WT E4orf6. Examination of Nbs1 expression in these experiments revealed some degradation in all transfections (except AXA), consistent with the partial functionality of some mutants. These results suggest that the interaction between L132S or A136F with E1b55K may be slightly compromised or destabilized. Co-immunoprecipitation experiments will be required to validate these observations. However, since E1b55K nuclear retention can be separated from degradation (see above and also Chapter 3), perhaps the defective interaction of L132S and A136F with E3 ligase factors is more important.

The phenotypes of the Vif-like BC box mutants (summarized in Table 3) contrasted those of another E4orf6 mutant, C124/126S (Figure 9) (31). These cysteines reside upstream of the Vif-like BC box within the zinc finger region

Figure 8. E4orf6 Vif-like BC box mutants exhibit defects in nuclear retention of E1b55K. U2OS E1b55K expressing cells were transfected with the indicated E4orf6 constructs for 24 hours before processing for immunofluoresence. Cells were analyzed for E1b55K and Nbs1 localization. DAPI indicates cell nuclei in the merged images.

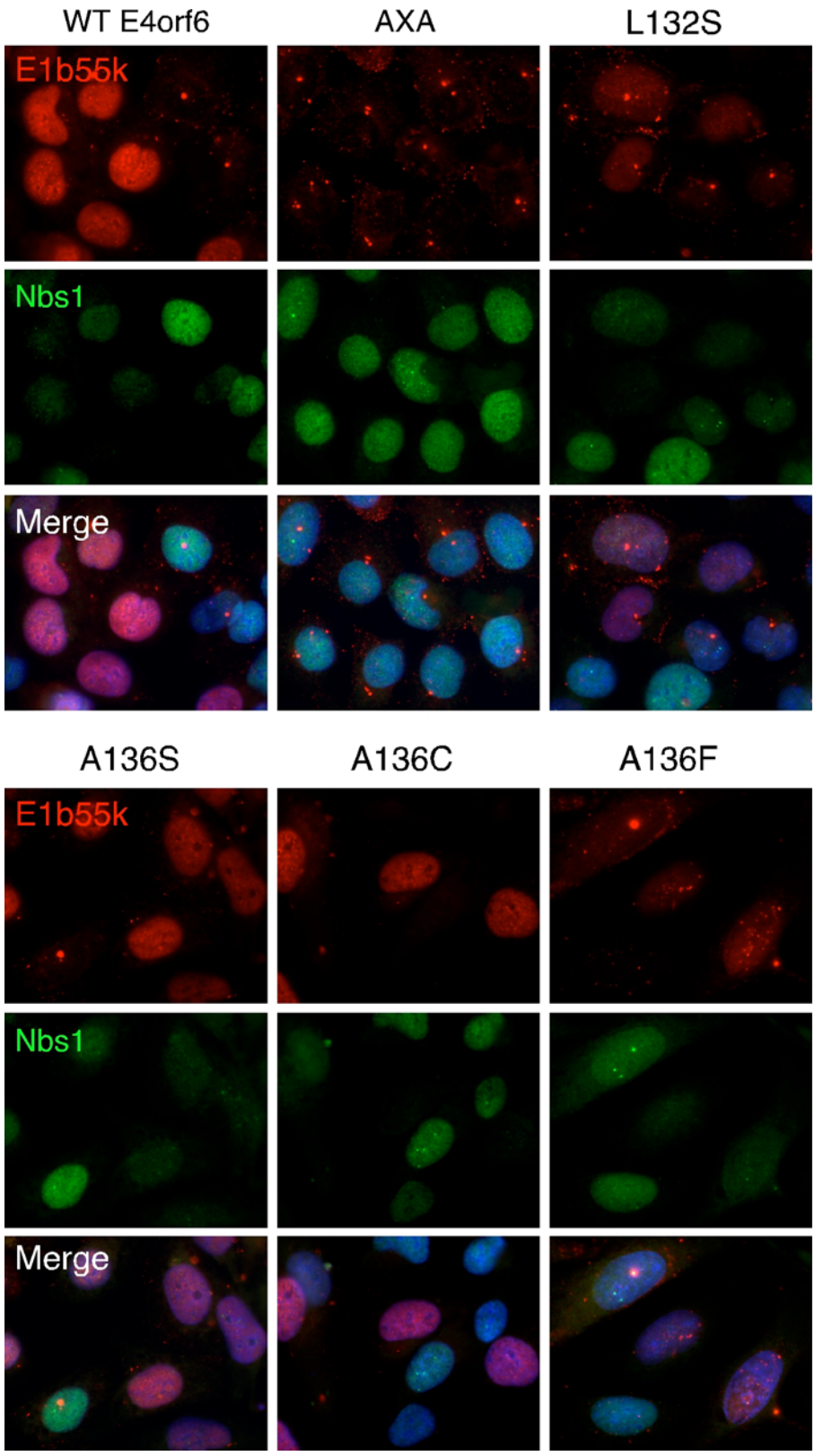
WT E4orf6
AXA
L132S
E1b55k
Nbs1
Merge
A136S
A136C
A136F
E1b55k
Nbs1
Merge

Figure 9. Loss of E4orf6 function by mutation of cysteines 124/126 to serine. U2OS cells expressing wild-type E1b55K were transfected with the indicated E4orf6 constructs for 24 hours before fixing. Cells were processed for immunofluorescence by staining for E1b55K and E4orf6 **(A)** or E1b55K and Nbs1 **(B)**. DAPI indicates cell nuclei in the merged images. **(C)** 293Q cells were transfected with the indicated E4orf6 constructs for approximately 48 hours before harvesting. Lysates were analyzed by immunoblotting for the indicated proteins. PCNA serves as a loading control. In all experiments, S128A serves as a positive control E4orf6 mutant.

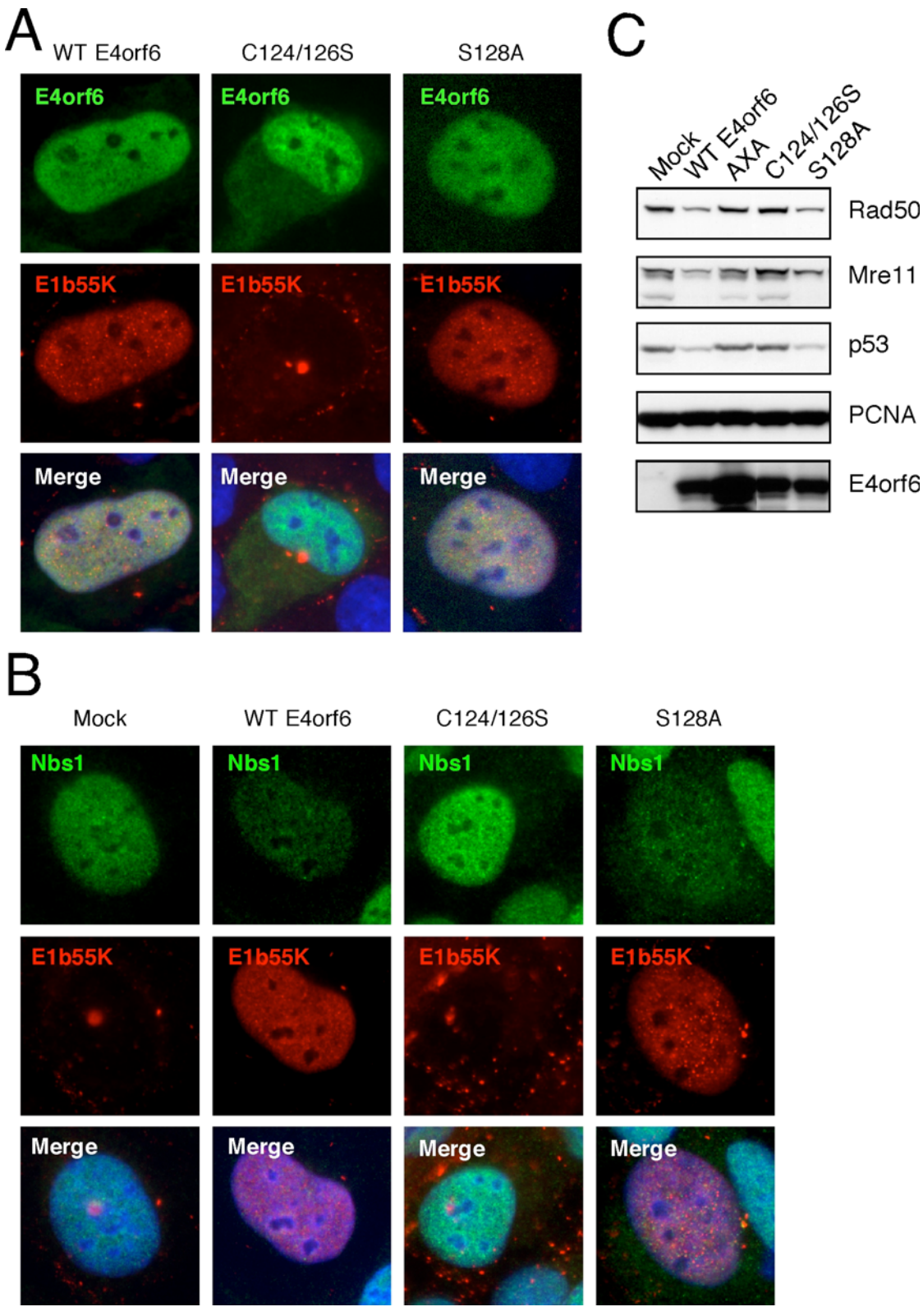
A
WT E4orf6
C124/126S
S128A
E4orf6
E1b55K
Merge
B
Mock
WT E4orf6
C124/126S
S128A
Nbs1
E1b55K
Merge
C
Mock
WT E4orf6
AXA
C124/126S
S128A
Rad50
Mre11
p53
PCNA
E4orf6

Table 1. Summary of E4orf6 mutant phenotypes.

Mutant	E1B nuclear retention	Degradation		Concats	Viral late proteins	ElonginB/ C binding	Viral growth
		MRN	p53				
wt	++	++	++	-	++	++	++
A136S	++	++	++	-	++	+	
A136C	++	++	++	-	++	+	
A136F	+/-	+/-	+/-	+/-	+	-	
L132S	+	+/-	+/-	+/-	+	-	
L245P	-	-	-	+	-	-	-
R241E	-	+	+	-	++	++	+
R241A	+/-	+	+	-	++	++	+
R243E	-	+	+	-	++	+	+
R243A	-	-	-	+	-	-	-
R240,251E	-	+	+	-	++	++	+
AXA	-	-	-	+	-		
S128A	++	++	++	-	++		
C124,126S	-	-	-	+	-	-	-

Table notes: Summary of phenotypes of E4orf6 mutants analyzed in this chapter compared to the wild-type protein. Data is based on results from this chapter and published reports (24, 31, 52, 252, 263, 264). Categories of Elongin B/C binding and Viral growth are solely based on published data. Viral growth refers to viral progeny production. ++ like wild-type, + slightly less than wild-type, +/- partially defective, - severely defective, blank spaces indicate phenotypes not assayed. For the Concats category: + presence of concatemers, - absence of concatemers.

(31) that was assigned to the second putative BC box (see Figure 2) (24). Mutation of these cysteines to serines or alanines completely abrogated the E4orf6 ability to retain E1b55K in the nucleus and degrade cellular substrates (Figure 9) (31, 252). The C to S mutants are also unable to bind E1b55K (31), complement an E4-deleted adenovirus (31), and recruit E3 ubiquitin ligase components (24)(see also Table 3). It is interesting that the C to S/A changes ablated most E4orf6 functions, whereas these changes were tolerated in the Vif-like BC box (Figures 6, 7, and 8) (399). This may suggest that cysteines 124 and 126 have a more important structural role within E4orf6 rather than strictly functioning within a BC box.

Cellular factors required for E1b55K/E4orf6 mediated substrate degradation

Previous reports suggested that the E1b55K/E4orf6 complex was associated with cellular E3 ubiquitin ligase factors Cullin 5 and Rbx1 (146, 281). However, at the time of our studies, it was unclear whether these factors actually mediated p53 and MRN degradation. To test this, we used shRNA constructs to knock-down the levels of Cullin 5 and Rbx1 (170), and asked whether substrate down-regulation by the viral proteins was affected. As controls for our experiments, we also included shRNA constructs against Cullin 2 and Rbx2 (170). We first tested the effectiveness and specificity of these constructs in the absence of virus. Transfection of the shRNA vectors

resulted in visible and specific knock-down of targets and no perturbation of Rad50 (Figure 10). Unfortunately, we did not have a reliable antibody against Rbx2 so we could not analyze this endogenous protein. Interestingly, down-regulation of Rbx1 led to destabilization of Cullin 2 but not Cullin 5. This observation supports data indicating that Cullin 2 and Rbx1 are normally paired in cells (170). The lower levels of Cullin 5 in vector-transfected cells were not seen in other experiments.

Next, we utilized these shRNA constructs to determine which factors were required for substrate degradation by Ad. HeLa cells were transfected with the constructs before infecting with an Ad5 mutant virus lacking E4orf3 (Figure 11A). Immuno-blotting for Rbx1 and Cullin 2 indicated that knock-down was effective with or without virus. Again, we noted the down-regulation of Cullin 2 when Rbx1 was destabilized. We found that virus-induced MRN degradation required Cullin 5, as expected. Surprisingly however, Rbx2 was necessary instead of the predicted Rbx1. While this observation supports data indicating that Cullin 5 and Rbx2 function together in cells (170), it was not consistent with p53 degradation requirements. HeLa cells express the HPV protein E6, which together with E6AP degrades p53 (304, 305), reducing the levels visible by Western analysis. Infecting HeLa cells with an adenovirus mutant lacking either E1b55K or E4orf6 results in p53 stabilization, likely due to E1A (215) and the lack of degradation by E1b55K/E4orf6 (see Chapter 3).

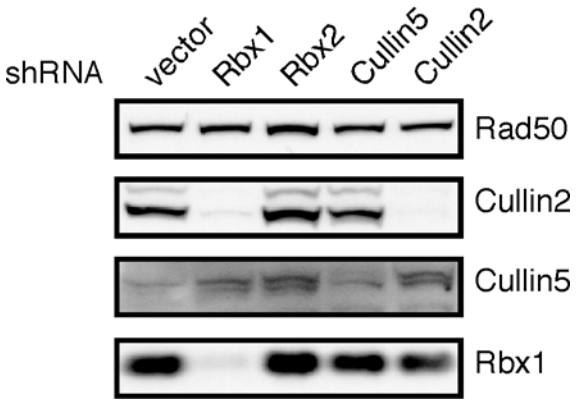

Figure 10. Down-regulation of cellular ubiquitin ligase factors by shRNA constructs. 293 cells were transfected with the indicated shRNA constructs or a puromycin-resistant vector for 24 hours before selecting cells with puromycin (1 μg/mL) for an additional 72 hours. Cells were then harvested and processed for western analysis. Lysates were analyzed for the indicated proteins by immuno-blotting.

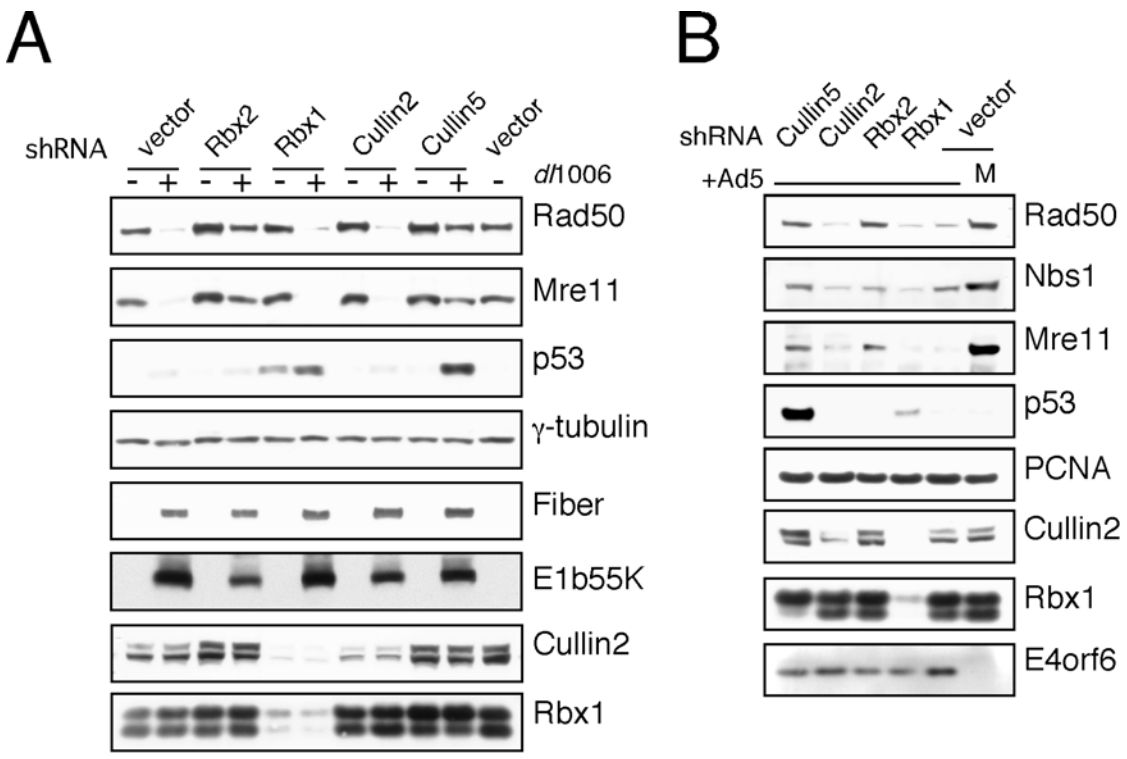

Figure 11. Degradation of MRN requires Cullin 5 and Rbx2. (A) HeLa cells were transfected with the indicated shRNA constructs and selected in puromycin (1 μg/mL) for 72 hours before mock treating or infecting with E4orf3-deleted Ad5 mutant, *dl*1006 (MOI of 50) for an additional 24 hours. Cells were harvested and lysates were analyzed for the indicated proteins by immunoblotting. γ-tubulin serves as a loading control. **(B)** HeLa cells were treated as in (A) except that cells were infected with Ad5 (MOI of 50). PCNA serves as a loading control.

In Figure 11A, we saw that Cullin 5 knock-down stabilized p53 in the presence of this degradation-competent adenovirus. However, it appeared that Rbx1 down-regulation, rather than Rbx2, affected p53 levels. While some p53 was present with the Rbx1 shRNA treatment alone, p53 was further stabilized during infection, suggesting that Rbx1 may be required for p53 degradation. Similar results were also seen during WT Ad5 infection (Figure 11B).

To show that these results were not specific to HeLa cells, we transfected the shRNA constructs into U2OS cells expressing WT E1b55K. These cells express WT p53 and lack additional viral proteins. Infection with rAd.E4orf6 resulted in p53 and MRN degradation with Cullin 2 knock-down but not Cullin 5 knock-down, (Figure 12A and 12B). While down-regulation of ubiquitin ligase factors was not as efficient in these cells (see Rbx1 blot in Figure 13B), MRN degradation appeared to require Rbx2, while p53 degradation needed Rbx1 (Figure 12B). Although these results were not as robust as in the HeLa cells, they support the same trend. Together, these data indicate that E1b55K/E4orf6 may assemble distinct Cullin 5-containing ubiquitin ligases to promote the degradation of MRN and p53. Other cell lines and additional shRNA constructs will be used in future studies to further validate these results.

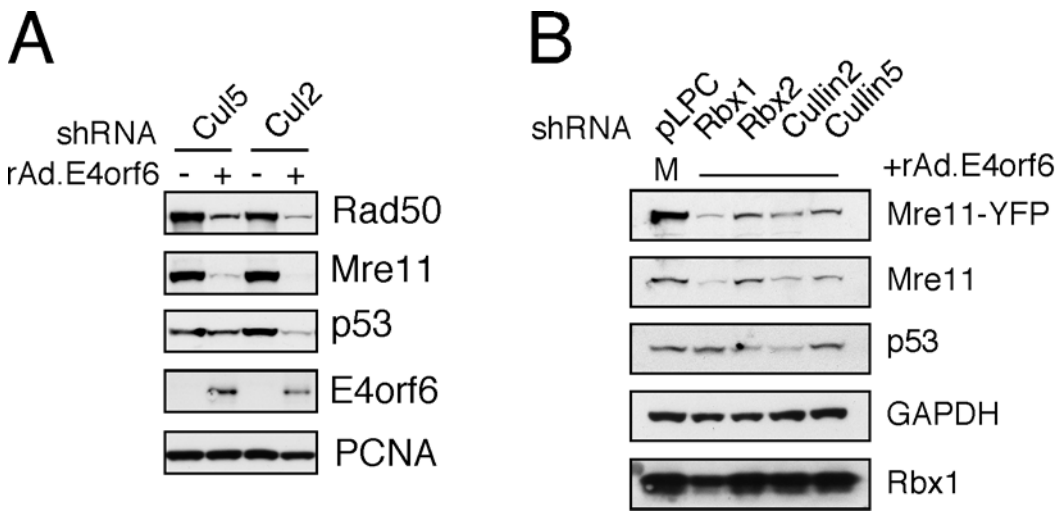

Figure 12. Ubiquitin ligase requirements for degradation of cellular substrates are not cell type specific. (A) U2OS wild-type E1b55K expressing cells were transfected with the indicated shRNA constructs and selected with puromycin as in Figure 11. Cells were then infected with rAd.E4orf6 (MOI of 25) for an additional 24 hours before harvesting. Lysates were analyzed for the indicated proteins. PCNA serves as a loading control. **(B)** U2OS E1b55K expressing cells were transfected with the indicated shRNA constructs and Mre11-YFP and selected as in Figure 11. Selected cells were then infected with rAd.E4orf6 (MOI of 10) for an additional 24 hours before harvesting. Lysates were analyzed for the indicated proteins. GAPDH serves as a loading control.

E4orf6 induces nuclear retention of Rbx2

A previous report showed that E4orf6 could induce nuclear retention of Cullin 5 (281), suggesting the two proteins interact. We therefore wanted to determine if E4orf6 could affect other E3 ligase factors in this manner, especially the RING proteins. Since we do not have a reliable antibody for Rbx2, we utilized flag-tagged versions of Rbx1 and Rbx2 (Figure 13A), and examined their localization by immunofluorescence in the presence and absence of E4orf6. Flag-tagged Rbx1 accumulated primarily in the nuclei of 293 cells diffusely after transfection (Figure 13B), consistent with the endogenous protein pattern (data not shown). E4orf6 co-expression did not appear to alter flag-Rbx1 staining, and resulted in down-regulation of MRN due to the presence of E1b proteins in these cells (Figure 13B). Although we cannot conclude whether E4orf6 binds Rbx1 based on these observations, other reports have validated the interaction using co-immunoprecipitation experiments (146, 281).

We then examined the pattern of flag-Rbx2 in transfected 293 cells (Figure 13C). In contrast to Rbx1, Rbx2 was diffusely present throughout the cell. Upon expression of E4orf6, however, Rbx2 was retained in the nucleus. MRN was also down-regulated, suggesting that the level of flag-Rbx2 over-expression did not interfere with degradation. Since 293 cells also express the adenoviral E1A and E1b proteins, we wanted to determine whether E4orf6

Figure 13. E4orf6 expression retains Rbx2 in the nucleus. (**A)** Expression of Flag-tagged Rbx1 and Rbx2. 293 cells were transfected with empty vector or the flag-tagged constructs for 24 hours before harvesting. Lysates were analyzed for flag expression. Ku86 serves as a loading control. The * indicates a cross-reacting, non-specific band. **(B)** E4orf6 expression does not affect Flag-Rbx1 localization. 293 cells were transfected with flag-Rbx1 in the presence and absence of E4orf6. 24 hours later cells were fixed for immunofluorescence and stained for Flag and Nbs1. DAPI marks cell nuclei in the merged image. Nbs1 is degraded due to the presence of E1b proteins in the 293 cells **(C)** Flag-Rbx2 is retained in the nucleus in the presence of E4orf6. 293 cells were transfected with flag-Rbx2 in the presence or absence of E4orf6 as in (B). After fixing, cells were stained for either flag and Nbs1 (left panels) or flag and E4orf6 (right panels). DAPI stains the nuclei in the merged images. Nbs1 is degraded due to the presence of E1b proteins in the 293 cells.

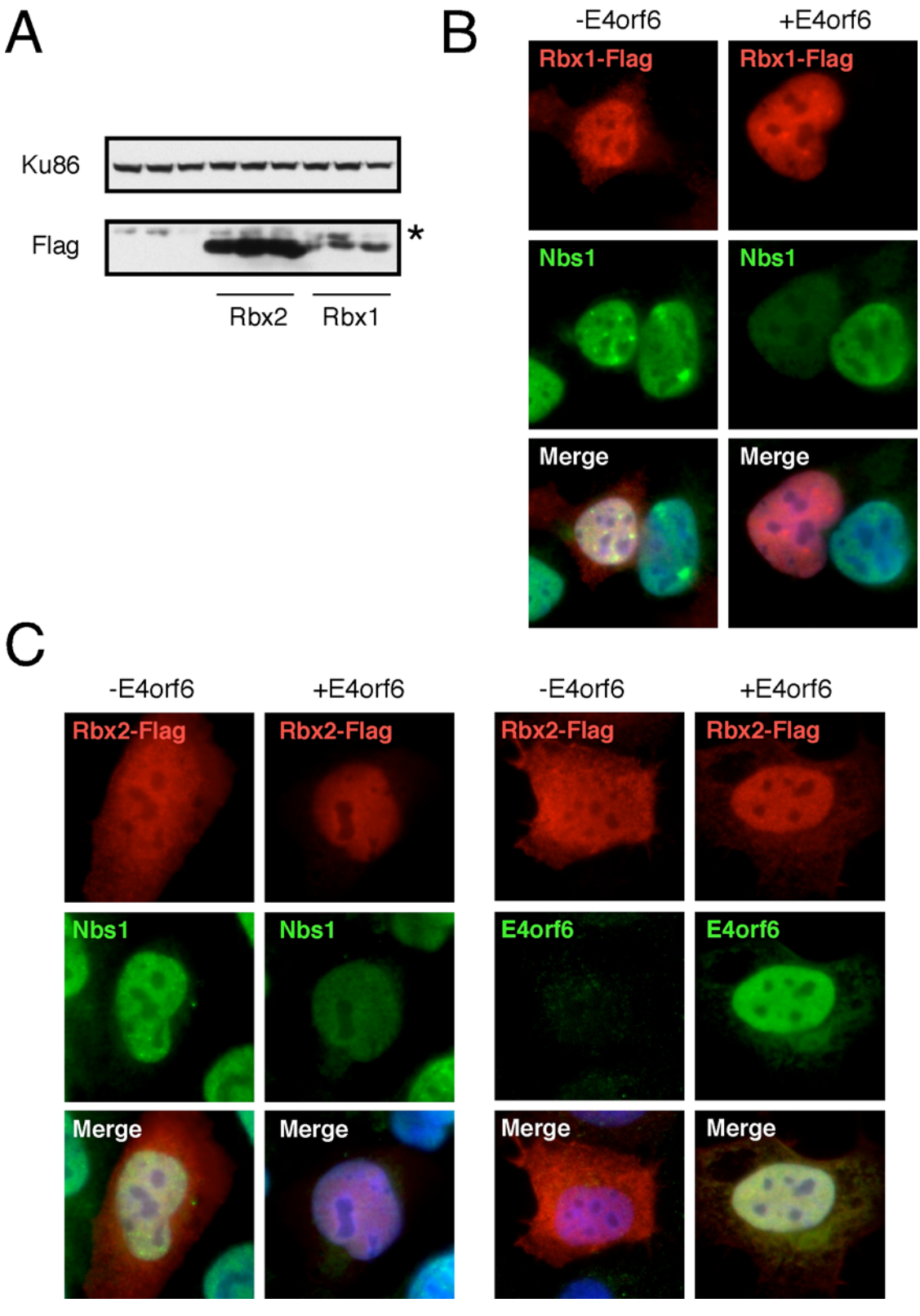
A
Ku86
Flag
*
Rbx2
Rbx1
B
-E4orf6
+E4orf6
Rbx1-Flag
Rbx1-Flag
Nbs1
Nbs1
Merge
Merge
C
-E4orf6
+E4orf6
-E4orf6
+E4orf6
Rbx2-Flag
Rbx2-Flag
Rbx2-Flag
Rbx2-Flag
Nbs1
Nbs1
E4orf6
E4orf6
Merge
Merge
Merge
Merge

alone could mediate these effects. Therefore, we transfected U2OS cells with flag-Rbx2 in the presence and absence of E4orf6. We found the same staining pattern of Rbx2 in these cells, and Rbx2 nuclear retention by E4orf6 alone (Figure 14). Intriguingly, AXA, the E4orf6 mutant that cannot bind E1b55K, could also retain Rbx2 in the nucleus (Figure 14). The related E4orf6 mutants, L245P and R243A (264) were both defective for binding Elongins C and B (24). This may suggest that E4orf6 interacts with multiple E3 ligase factors, however, we need to examine whether Elongins B and C or Cullin 5 are required for E4orf6-mediated Rbx2 localization. It will be interesting to determine if other E4orf6 mutants behave like AXA in this assay, and whether retention of Rbx2 occurs during virus infection. Co-immunoprecipitation experiments with the tagged RING constructs and endogenous proteins will be required to validate these observations. Additionally, future studies will be aimed at dissecting protein-protein interactions between E4orf6 and these cellular factors. These experiments should clarify what associations are necessary for E4orf6 to assemble the E3 ubiquitin ligase.

Discussion

The experiments in this Chapter were aimed at determining how certain domains in E4orf6 contributed to degradation of cellular targets, particularly the Mre11 complex. We first concentrated on an arginine-rich α-helix required

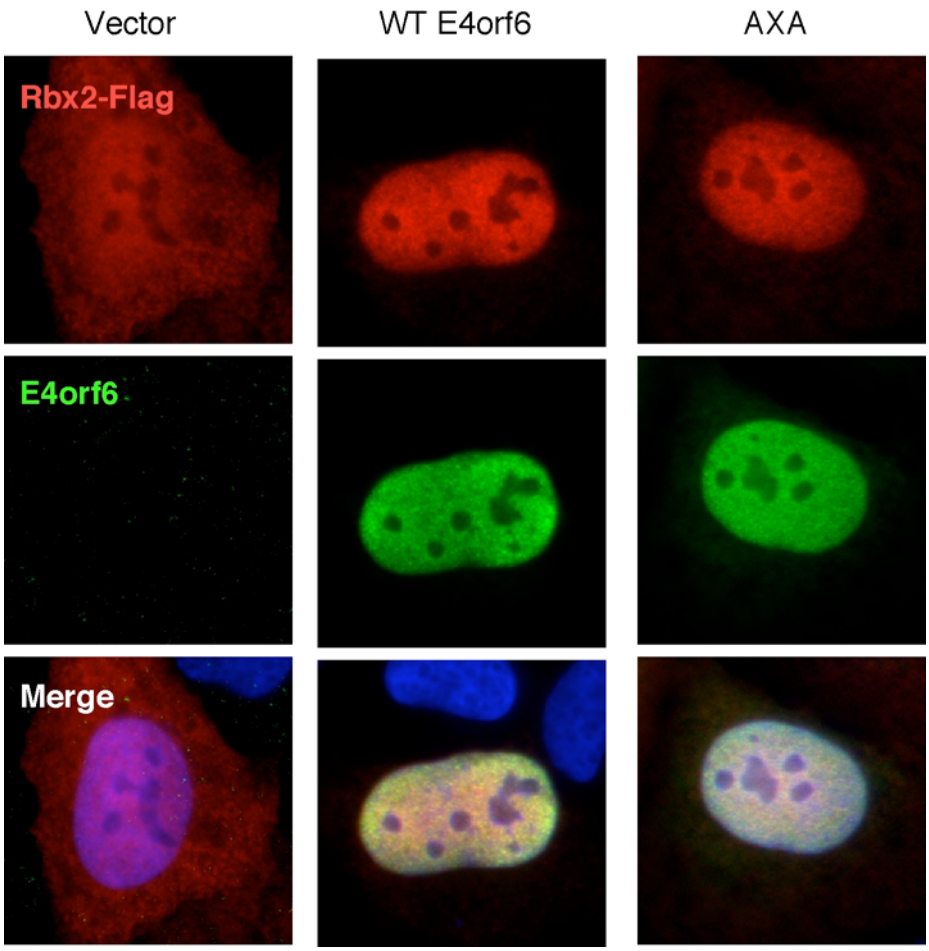

Figure 14. E1b55K is not required for Rbx2 retention in the nucleus. U2OS cells were transfected with flag-Rbx2 and the indicated E4orf6 vectors for 24 hours. Cells were fixed and processed for immunofluorescence, staining for flag and E4orf6. DAPI marks the cell nuclei in the merged images.

for E1b55K nuclear retention (263, 264). Nuclear retention of E1b55K had been used as a read-out for functional E4orf6 interaction, but this may not be an accurate measure in all cases. Indeed, we found that cellular substrate degradation by some E4orf6 mutants was independent of E1b55K retention. Additionally, certain E1b55K mutants exhibiting diminished nuclear presence (see Chapter 3) or unstable E4orf6 binding (312), are still able to degrade cellular factors. The ability to down-regulate substrates by E4orf6 mutants correlated with prevention of mutant genome concatemerization, complementation of mutant viral growth (264), and binding cellular E3 ligase factors (24) (see Table 3 for summary). Some E4orf6 mutants, however, do not retain E1b55K in the nucleus and lose these functions. For example, the L245P, AXA (R243A/L245A), and R243A mutants were unable to degrade cellular substrates and complement mutant virus infection (Table 3), indicating the importance of these amino acids. A complex of E1b55K and E4orf6 is thought to promote substrate degradation, viral replication and late protein synthesis, and prevent viral genome concatemerization (367), so it is unclear how to reconcile some of these data. Perhaps functional E4orf6 mutants can still transiently associate with E1b55K at a level that evades detection by currently utilized assays. Future studies will have to use alternative methods to determine whether binding to E1b55K, even transiently, correlates with E4orf6 functions.

E4orf6 has been shown to recruit Cullin 5, Rbx1, and Elongins B and C to promote degradation of targets (146, 281). Other substrate receptors recruit CRLs through BC boxes motifs, which bind adaptor proteins like Elongin C (272). Identification of similar sequences in E4orf6 has been controversial due to a lack of perfect consensus with the BC box motif and absence of a Cul 5 box (24, 233). The HIV protein Vif was previously shown to recruit a Cullin 5-containing ubiquitin ligase through a novel BC box motif (233, 399). Since E4orf6 contained a similar sequence (233), we wanted to determine its functional relevance to substrate down-regulation. Consistent with Vif (399), mutating A136 to cysteine or serine was tolerated for degradation (Figures 6 and 7). Other mutants in this region also revealed that defective substrate down-regulation correlated with diminished E3 ligase recruitment, a phenotype recently published (218). However, in contrast to the degradation of exogenous p53 (218), we found that down-regulation of endogenous proteins by these E4orf6 mutants was only partially defective (Figures 6 and 7), perhaps due to assay differences. We also noticed that these mutants were somewhat defective for E1b55K nuclear retention. However, as discussed above, this phenotype may be separable from degradation. Therefore, this region likely contributes to efficient degradation of substrates. Analysis of other BC box mutants (218) will help validate this data.

The Branton group had previously implicated two putative E4orf6 BC box sequences in binding Elongins B and C (24). However, these divergent sequences could not tolerate conservative changes of critical cysteine residues to serines or alanines (Figure 9) (31, 218, 252), unlike the Vif BC box mutants described above, suggesting their structural role within the protein. Other putative BC box mutations ablated association with E1b55K (24). Based on this observation, it was argued that E4orf6-E3 ligase interaction is required to stabilize E1b55K binding (24). However, E3 interaction is not sufficient since E4orf6 α-helix mutants can still bind E3 ligase components (24) and degrade factors (Figures 3-5), but lack stable E1b55K association. Recently, the Branton group reported on the Vif-like BC box in E4orf6 (61), but maintained that all three BC boxes mediated E3 ligase recruitment (61). It is unclear why multiple BC boxes would be needed since only one hydrophobic pocket on Elongin C can interact with E4orf6 (24, 218), similarly to the Elongin C-VHL association (328). It is also unclear whether the other BC box mutant defects are truly due to defective E3 ligase recruitment or E1b55K binding.

Since E1b55K appears to mediate substrate specificity (see Chapter 3), mutations in E4orf6 will likely affect degradation of all targets. Indeed, we observed similar MRN and p53 degradation patterns in these experiments. At the time of these studies, DNA Ligase IV had not yet been identified as an E1b55K/E4orf6 substrate. However, we would predict that E4orf6 mutations

abrogating p53 and MRN down-regulation would also inhibit DNA Ligase IV degradation. In our E4orf6 mutant characterization, a tight correlation emerged between substrate degradation, recruitment of E3 ligase components, and complementation of mutant virus (summarized in Table 3). Contributing to virus production, functional E4orf6 mutants were also found to complement viral late protein synthesis (Figures 5A and 7A), and would be assumed to stimulate viral DNA replication since degradation of MRN is required for this (113, 228, 229)(S.S. Lakdawala, *et al.*, submitted). Since E4orf6 mutants do not appear to separate substrate degradation, we cannot determine the relevant targets of various functions. However, E4orf6 mutants illustrate the importance of E3 ligase recruitment and degradation in the viral lifecycle.

At the time of these studies, it was unclear whether the E3 ubiquitin ligase factors recruited by E4orf6 actually mediated substrate degradation. Since that time, other reports have implicated Cullin 5 in the down-regulation of all targets (8, 61, 218, 378), consistent with our shRNA experiments. We also examined the requirement of the RING proteins, Rbx1 and Rbx2, in substrate degradation. Interestingly, our data indicated that distinct RING proteins mediated MRN and p53 degradation (Figures 11 and 12). This surprising result suggests that the E1b55K/E4orf6 complex has requirements beyond a BC box for the selection of ubiquitin ligase factors. Supporting this idea, our immunofluorescence results showed that an E4orf6 mutant unable to

bind Elongins B and C was still able to retain Rbx2 in the nucleus. It is currently unclear what dictates RING protein selection. A study of respiratory syncytial virus-induced STAT2 degradation demonstrated that in certain cell lines, both Rbx1 and Rbx2 were required (107). A report examining RING-mediated degradation in Drosophila suggested that substrates may be involved in the choice (258). We also do not know what regulates E2 selection in cells, and which E2 is utilized by E1b55K/E4orf6. Interestingly, it has been shown that multiple E2s can associate with a ubiquitin ligase to direct the synthesis of distinct ubiquitin chains (67). Therefore, it is possible that the E1b55K/E4orf6 complex could interact with different factors to regulate degradation of individual targets. It will be important to validate our results with binding assays, and determine which factors are required for E3 ligase interactions. While different Cullin-containing ubiquitin ligases have been reported for a number of cellular BC box proteins and viral proteins (12, 170, 222, 272) (see also Chapter 7), our data suggest that E1b55K/E4orf6 form distinct Cullin 5-containing ubiquitin ligases for substrate degradation. It will be interesting to see which ligase factors are required for DNA Ligase IV down-regulation.

Despite the fact that the E1b55K/E4orf6 has been shown to degrade cellular substrates in a manner that requires Cullin5 (8, 218, 378), only p53 has been shown to be ubiquitinated by these viral factors (24, 146, 281).

Given that p53 and MRN down-regulation might require distinct ligase factors, it will be important to examine the ubiquitination of these targets. We have previously noticed the E1b55K/E4orf6-dependent modification of Rad50 in the presence of proteasome inhibitors (Appendix Figure 2A and 2B). While this modification requires E1b55K binding to MRN (Appendix Figure 2B), preliminary experiments suggest it is not ubiquitin dependent (Appendix Figure 2C), indicating that the viral proteins might induce alternative target modifications. Phosphorylation of substrates is often required for their degradation by many ubiquitin ligases (129, 160). Alternatively, SUMOylation of some targets has been recently shown to precede their ubiquitination and degradation (190, 278, 339, 342, 385). E1b55K was recently associated with SUMO ligase activity (A. Berk, personal communication), so the Rad50 modification may represent this. It will be important to determine how E1b55K/E4orf6 recognizes cellular targets for degradation and what protein modifications might be necessary.

While we do not yet have evidence of substrate ubiquitination, E1b55K and E4orf6 may be ubiquitinated (Appendix Figure 2C and 2D). Surprisingly, in these preliminary experiments we also noticed ubiquitination of the E4orf6 mutant, AXA, which should be unable to bind Elongins C and B but can still retain Rbx2 in the nucleus. While it is unclear which cellular interactions induce these modifications, these results suggest that E1b55K and E4orf6 may auto-

ubiquitinate themselves. This activity is reminiscent of another viral ubiquitin ligase, the HSV ICP0 protein, which can also auto-ubiquitinate itself (48). A large number of cellular enzymes harboring de-ubiquitination activity, refered to as DUBs, associate with ubiquitin ligases to regulate their activity, and in some cases, prevent auto-ubiquitination (257). In the case of ICP0, recruitment of the DUB, USP7, prevents this and destabilization of ICP0 (29, 48, 115). The low level of ubiquitinated E1b55K and E4orf6 seen in our pilot studies (Appendix Figure 2C and 2D), and the lack of destabilization during infection or transfection experiments may indicate DUB association. Interestingly, Rbx1 has been shown to interact with USP15 (150), so this may be a candidate DUB for the E1b55K/E4orf6 complex. In the future, it will be important to determine how these viral proteins are modified, and whether regulation of auto-ubiquitination through a cellular DUB is important to E1b55K/E4orf6.

Although much of the data presented in this Chapter is preliminary, we have made a number of interesting observations. Future studies will have to determine which sequences in E4orf6 are required for E3 ligase recruitment, and why certain mutations in E4orf6 abrogate substrate degradation. Additionally, they will have to identify the ubiquitin ligase components needed to degrade substrates. However, the E1b55K/E4orf6 complex should provide a

powerful tool to study the assembly and selection of Cullin-containing ubiquitin ligase factors.

Materials and Methods

Plasmids and transfections

Plasmids encoding mutations in the E4orf6 Vif-like BC box were provided by X.F. Yu and described in (218). The pCMV plasmids used in Figures 3-5, were provided by D. Ornelles (264). The plasmids encoding shRNA constructs against Cullin 5, Cullin 2, Rbx1, or Rbx2 were provided by T. Kamura and K. Nakayama and described in (170). The Mre11-YFP construct used in Figure 13B was previously described (27) and provided by S. Richard. To make the flag-tagged constructs used in Figures 14 and 15, Rbx1 and Rbx2 were PCR amplified from HeLa cDNA and cloned into the SalI and BamHI sites of the pCMX vector provided by R. Evans. Primers used for PCR of Rbx1 were: 5' ACGCGTCGACGCGGCAGCGATGGATGT 3' (forward) and 5' CGCGGATCCCTAGTGCCCATACTTTTGG 3' (reverse). Primers used for PCR of Rbx2 were: 5' ACGCGTCGACGCCGACGTGGAAGACGG 3' (forward) and 5' CGCGGATCCTCATTTGCCGATTCTTTGGA 3' (reverse). Sub-confluent monolayers of cells were transfected with Lipofectamine 2000 (Invitrogen) according to the manufacturer's recommendations. For the shRNA

experiments, 24 hours after transfection, cells were selected with puromycin (1mg/mL) before infections according to the figure legends.

Cell lines and drug treatments

The cell lines used in this Chapter were described in Chapters 2 and 3. For proteasome inhibitor treatment, cells were infected according to the figure legend. Two hours infection, MG132 and epoxomicin (Calbiochem), or DMSO as a control, were added at a final concentration of 10 μM and 2 μM, respectively, for a further 16 hrs.

Viruses and infections

The E4 mutant viruse *dl*1006 has been previously described (36) and was obtained from G. Ketner. Other viruses and infections were described in Chapters 2 and 3.

Antibodies, immunofluorescence and immuoblotting

The commercially available antibodies used in this study were purchased from: Neomarkers (Rbx1), Sigma (Flag), Santa Cruz (Cullin 5) and Oncogene (Cullin 2). All other antibodies were described in Chapters 2 and 3. Immunofluorescence and immunoblotting procedures were also described in Chapters 2 and 3.

Pulse-field gel electrophoresis

Analysis of viral genome concatemers was described in Chapter 2.

Acknowledgements

I thank Seema Lakdawala for help in analyzing E4orf6 mutants and her contribution to Figures 5, 9A, and 9B. I also thank Christian Carson for the data in Appendix Figure 2A. I am grateful to D. Ornelles for providing the E4orf6 α-helix mutants and E4orf6 antibody, and X.F Yu for the E4orf6 Vif-like BC box mutants. I am also thankful for T. Kamura and K. Nakayama for providing the shRNA constructs against the ubiquitin ligase factors. I am grateful to A. Berk, P. Branton, R. Evans, G. Ketner, A. Levine, and S. Richard for generous gifts of reagents.

Chapter 5. The Mre11 complex negatively regulates adeno-associated virus transduction and replication.

Background

The adeno-associated virus (AAV) is a small DNA virus composed of primarily single-stranded DNA with inverted terminal repeats (ITR) at either end (see Chapter 1, Figures 9 and 10) (357). The wild-type (WT) virus minimally encodes two genes, Rep and Cap. The Rep proteins are involved in viral replication and packaging, while the Cap gene products facilitate packaging and form the virion (Chapter 1, Figure 9) (241). The viral Rep and Cap genes are replaced by a transgene in recombinant AAV (rAAV) vectors (Chapter 1, Figure 9). Therefore, gene expression from rAAV vectors (transduction) is regulated solely by host cell factors (130, 138, 299). Both WT AAV and rAAV vectors contain ITRs that prime replication and allow packaging into virion capsids.

Efficient AAV replication requires an unrelated helper virus, such as adenovirus or herpesvirus, and the host replication machinery. Previous studies have delineated a minimal set of Ad proteins required for replication that include E1A, E1b55K, E4orf6 and DBP (128, 357). E1A transactivates viral promoters while establishing an S phase environment in the host cell to facilitate replication (357). The Ad DBP protein promotes AAV replication and

Rep binding to DNA (336, 357), and may protect the single-stranded AAV DNA in cells since it localizes to replication compartments (336, 366). E1b55K and E4orf6 act as a complex to enhance rAAV transduction and WT AAV replication by overcoming barriers to second-strand synthesis of the genome (120, 121), although the mechanism is not understood. E1b55K/E4orf6 has also been shown to form a Cullin-containing ubiquitin ligase to promote degradation of the Mre11 complex, DNA Ligase IV and p53 during Ad infection (Chapters 2 and 3)(8, 146, 281, 335, 378). Degradation of these host cell targets prevents apoptosis, DNA damage signaling, and viral genome processing during Ad infection (50, 282, 335).

Published reports have suggested a relationship between AAV, DNA damage, and components of the cellular damage machinery (64, 168, 284, 298). Genotoxic agents have been observed to stimulate transduction by rAAV and WT AAV replication (5, 295, 388), although the mechanism(s) remain unclear. A number of studies have focused on the molecular fate of rAAV vector genomes and DNA repair proteins that affect transduction. AAV vectors can be converted into circular and concatemeric forms that persist episomally, and this has been correlated with long-term gene expression (101, 102, 306). ATM and other NHEJ factors appear to have a deleterious effect on rAAV transduction and rAAV genome processing (64, 298, 401). DNA-PK, which is another PI-3-kinase related kinase and NHEJ protein, also takes part in rAAV

genome processing *in vivo* (64, 103, 325). UV-inactivated rAAV genomes have been used to study interactions with ATR and downstream effectors (168). Despite increasing research in this area, the connection between these observations remains unclear, and it is not known which specific steps of AAV infection these cellular proteins impact.

Since E1b55K/E4orf6 degrade cellular substrates and provide helper functions for AAV, we wished to determine whether these activities are linked. Here we show that degradation of the Mre11 complex by E1b55K/E4orf6 promotes rAAV transduction, WT AAV replication, and accumulation of high molecular weight viral DNA. We propose that MRN is a direct obstacle to the AAV lifecycle since transduction and replication are enhanced in mutant or shRNA-containing cell lines. Furthermore, we demonstrate that MRN localizes to AAV replication centers, suggesting that viral genomes are recognized as DNA damage. Consistent with this observation, purified proteins bind AAV ITRs *in vitro*, indicating that the ITR may serve as a recognition signal. These results demonstrate that AAV is a target of MRN, and degradation of these cellular factors contributes to the previously described E1b55K/E4orf6-mediated helper function for AAV. Since MRN is required for ATM activity, our data provide biological context for observations that ATM inhibits rAAV transduction. AAV may, therefore, have evolved to rely on Ad proteins to inactivate the Mre11 complex in order to promote a productive infection.

Results

Degradation of MRN enhances rAAV transduction

The Ad E1b55K/E4orf6 protein complex has been shown to enhance rAAV transduction dramatically (120, 121, 139). We wished to determine whether destabilization of a cellular target by E1b55K/E4orf6 is required for this activity. To address this possibility, we first examined the effects of proteasome inhibitors on rAAV transduction in the presence of E1b55K/E4orf6. Stable HeLa-based cell lines (50) expressing either WT E1b55K or GFP as a control, were infected with a rAAV vector expressing β-galactosidase (rAAV.LacZ). E4orf6 was subsequently provided by a recombinant Ad (rAd.E4orf6), and induces proteasome-mediated degradation of cellular substrates in WT E1b55K expressing cells but not GFP expressing cells (50). Proteasome inhibitors were then added approximately 24 hours after rAAV application, to avoid stimulating transduction through modulation of intracellular trafficking (97, 104). Expression of E4orf6 in the WT E1b55K cell line stimulated rAAV transduction, while proteasome inhibitors abrogated this effect (Figure 1). These results argue that E1b55K/E4orf6-mediated degradation of a cellular substrate is critical to helper-dependent enhancement of rAAV transduction.

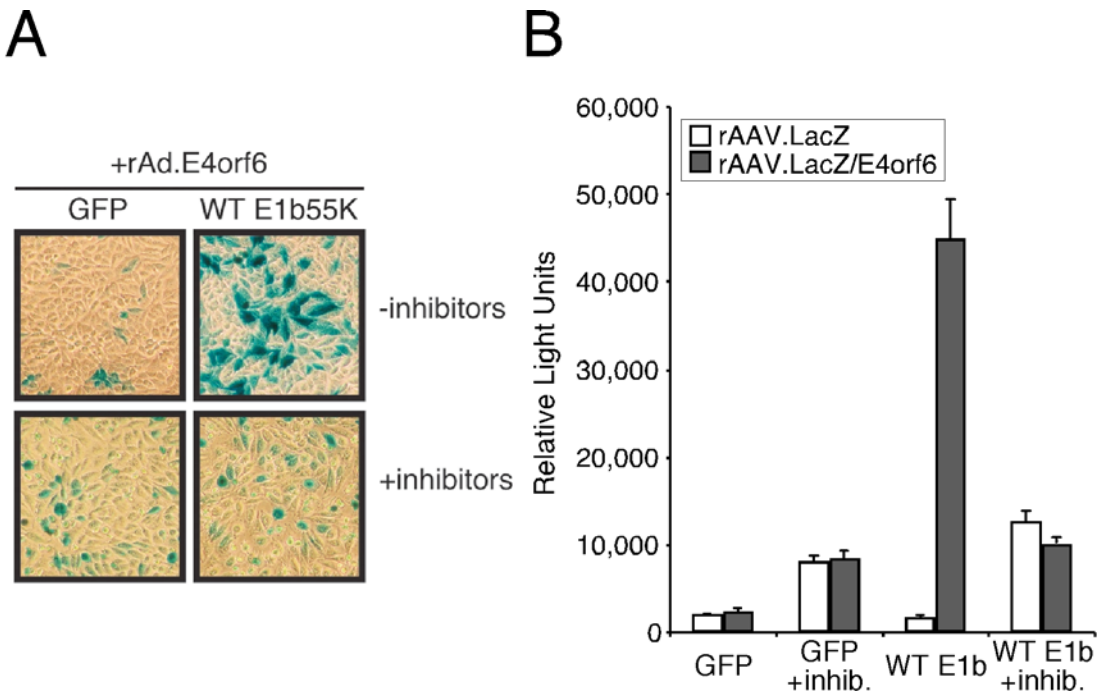

Figure 1. Protein degradation is required for enhancement of rAAV transduction by E1b55K/E4orf6. WT E1b55K or GFP expressing HeLa cells were infected with rAAV.LacZ 24 hours before superinfection with rAd.E4orf6 (MOI 50). MG132 and epoxomicin, or DMSO, were added 2 hours post-infection for another 16 hours. Cells were stained **(A)** or assayed for β-galactosidase enzyme activity **(B)**. Error bars represent SEM from triplicate samples.

To determine which of the known degradation targets are relevant to augmenting rAAV transduction, we used our previously characterized mutant E1b55K-expressing cell lines (50). The R240A mutant expressing cell line can degrade the Mre11 complex but not p53, in the presence of E4orf6. The H354 mutant expressing cell line, however, degrades p53 but not MRN, in the presence of E4orf6. We assayed rAAV.LacZ transduction in these mutant cell lines as well as in the WT E1b55K and GFP expressing cells (Figure 2A and 2B). In the absence of rAd.E4orf6, a similar basal level of β-galactosidase expression was observed in all cell lines. In the presence of rAd.E4orf6, however, we noted a dramatic increase in rAAV transduction only in the cell lines that degrade the Mre11 complex (i.e. in WT E1b55K and R240A expressing cells). Stable E1b55K-expressing U20S cell lines also displayed the same pattern (Figure 2C). This demonstrates that the effect is not cell type specific, and that p53 degradation is not required to augment transduction. To preclude any effects of the recombinant Ad, E4orf6 was transfected into the E1b55K cell lines before rAAV infection, and this yielded similar results (Figure 3). As a control, an E4orf6 mutant unable to bind E1b55K, L245P (52, 263), was transfected into stable E1b55K expressing cells. Consistent with previous results, we found that this mutant was unable to augment rAAV transduction, further confirming the requirement of an E1b55K/E4orf6 complex in this activity (139). Together, these data suggest that degradation of MRN, but not

Figure 2. Enhanced rAAV transduction correlates with MRN degradation. Stable HeLa cell lines expressing GFP, WT E1b55K, or E1b55K mutants were infected with rAAV.LacZ in the presence or absence of rAd.E4orf6 (MOI 50) for 24 hours. Cells were then stained **(A)** or assayed for β-galactosidase enzyme activity **(B)** as in Figure 1. **(C)** Stable U2OS cell lines expressing GFP, WT E1b55K, or E1b55K mutants were infected as above and stained for β-galactosidase as above. A photograph of the experimental plate is shown here instead of pictures as in (A). Enhanced rAAV transduction is only observed with E4orf6 in the WT E1b55K and R240A cell lines, where MRN is degraded.

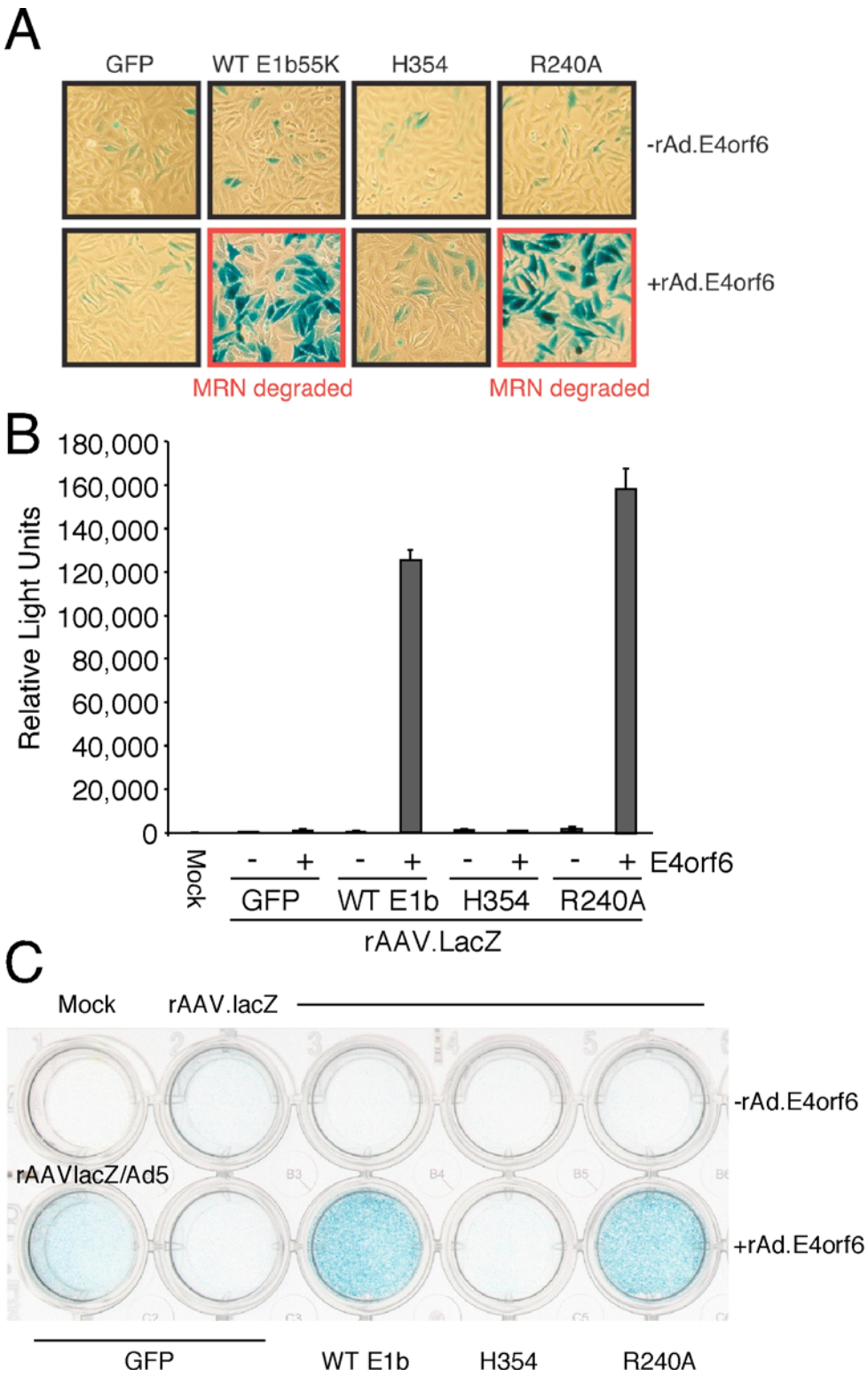
A
GFP
WT E1b55K
H354
R240A
-rAd.E4orf6
+rAd.E4orf6
MRN degraded
MRN degraded
B
Relative Light Units
180,000
160,000
140,000
120,000
100,000
80,000
60,000
40,000
20,000
0
Mock
- + - + - + - + E4orf6
GFP
WT E1b
H354
R240A
rAAV.LacZ
C
Mock
rAAV.lacZ
rAAVlacZ/Ad5
-rAd.E4orf6
+rAd.E4orf6
GFP
WT E1b
H354
R240A

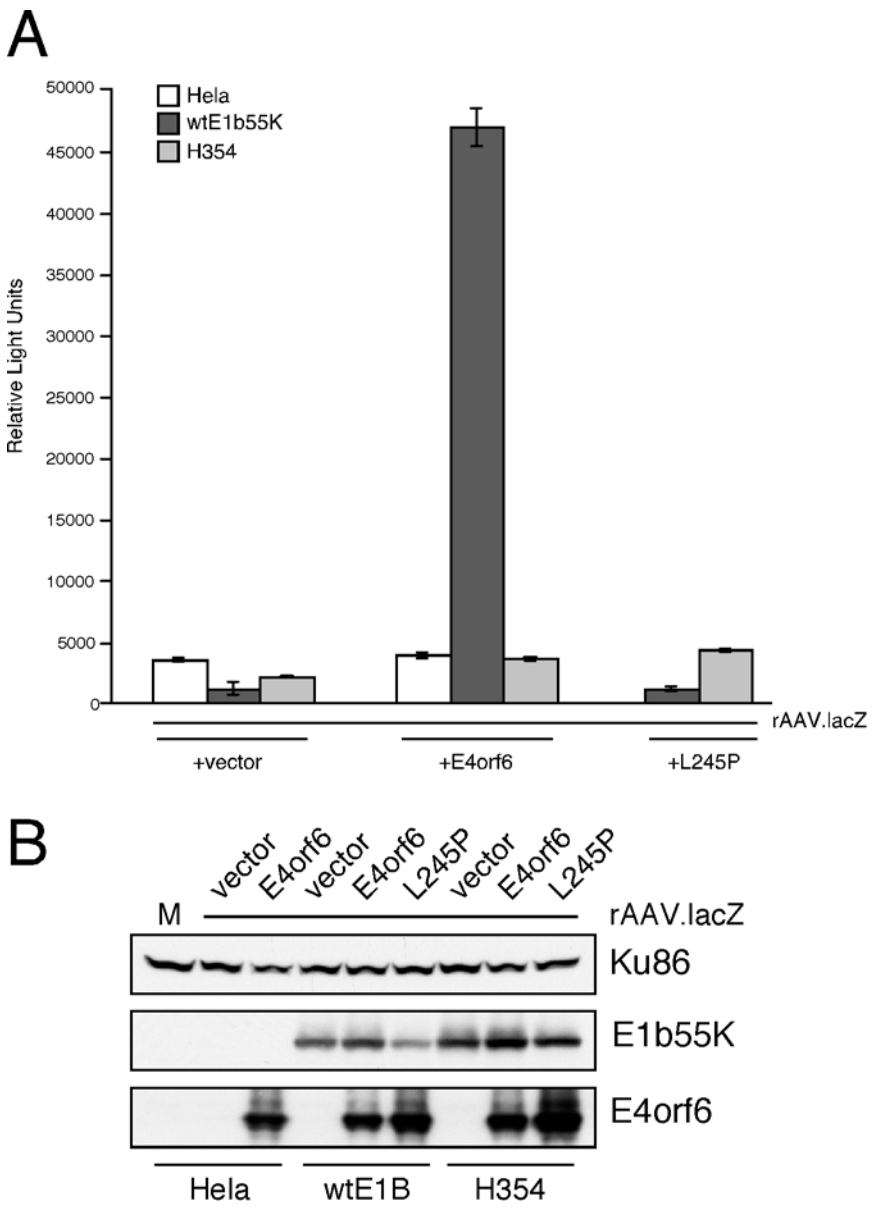

Figure 3. Transfection of E4orf6 into E1b55K expressing cell lines augments rAAV transduction. Stable HeLa cell lines expressing GFP, WT E1b55K or H354 were transfected with empty vector, WT E4orf6, or E4orf6 mutant L245P, which does not bind E1b55K. 24 hours after transfection, cells were superinfected with rAAV.LacZ for another 24 hours. Cells were then harvested and lysates were analyzed for β-galactosidase activity **(A)** and protein expression by immunoblotting **(B)**. Error bars represent SEM from triplicate samples.

p53, by the E1b55K/E4orf6 complex is required to stimulate rAAV transduction.

rAAV DNA accumulation is enhanced by MRN degradation

E1b55K/E4orf6 was previously thought to boost rAAV transduction by promoting second-strand synthesis through an unknown mechanism (120, 121). We examined this process in the E1b55K mutant cell lines by subjecting rAAV DNA to alkaline gel electrophoresis and Southern blot hybridization (Figure 4). In the presence of E4orf6, more double-stranded (ds) rAAV DNA accumulated in cells where the Mre11 complex was degraded (Figure 4A, filled arrowhead) and transduction enhanced (only in WT E1b55K and R240A cells). HeLa parental control cells did not display increased second-strand synthesis regardless of E4orf6 expression. Additionally, U2OS-based E1b55K cell lines yielded similar results (Figure 4B and 4C). These data suggest that MRN degradation is crucial to ds rAAV DNA accumulation.

In order to examine second-strand synthesis in single cells, we recently developed a system to visualize the conversion of rAAV vector genomes from single-stranded to double-stranded DNA in real time. Our approach combines a lactose repressor-GFP fusion protein (GFP-LacR) and a rAAV genome containing 112 lactose repressor binding sites (rAAV.LacO) (57). Only when rAAV.LacO becomes double-stranded does GFP-LacR bind and form fluorescent nuclear foci (Figure 5A). We found that ds rAAV DNA accumulates

Figure 4. Degradation of MRN correlates with increased second strand synthesis. (A) WT or mutant E1b55K expressing HeLa cells were infected with rAAV.GFP in the presence or absence of rAd.E4orf6 (MOI 25) for 24 hours. HIRT extracted viral DNA was analyzed by alkaline gel electrophoresis and Southern blot hybridization with a GFP probe. Filled arrowhead indicates a double-stranded form of rAAV DNA in the WT E1b55K and R240A cells plus E4orf6, where MRN is degraded. ssDNA refers to input rAAV DNA. **(B) and (C)** U2OS WT E1b55K or H354 expressing cells were infected with rAAV.GFP in the presence or absence of rAd.E4orf6 (MOI 25) or Ad5 (MOI 25) for 24 hours. Cells were harvested and HIRT extracted viral DNA was subjected to alkaline gel electrophoresis (B) or neutral gel electrophoresis (C) before Southern blot hybridization with a GFP probe. Filled arrowhead same as above. Open arrowhead indicates a potential dimer of rAAV genomes that have annealed under neutral conditions.

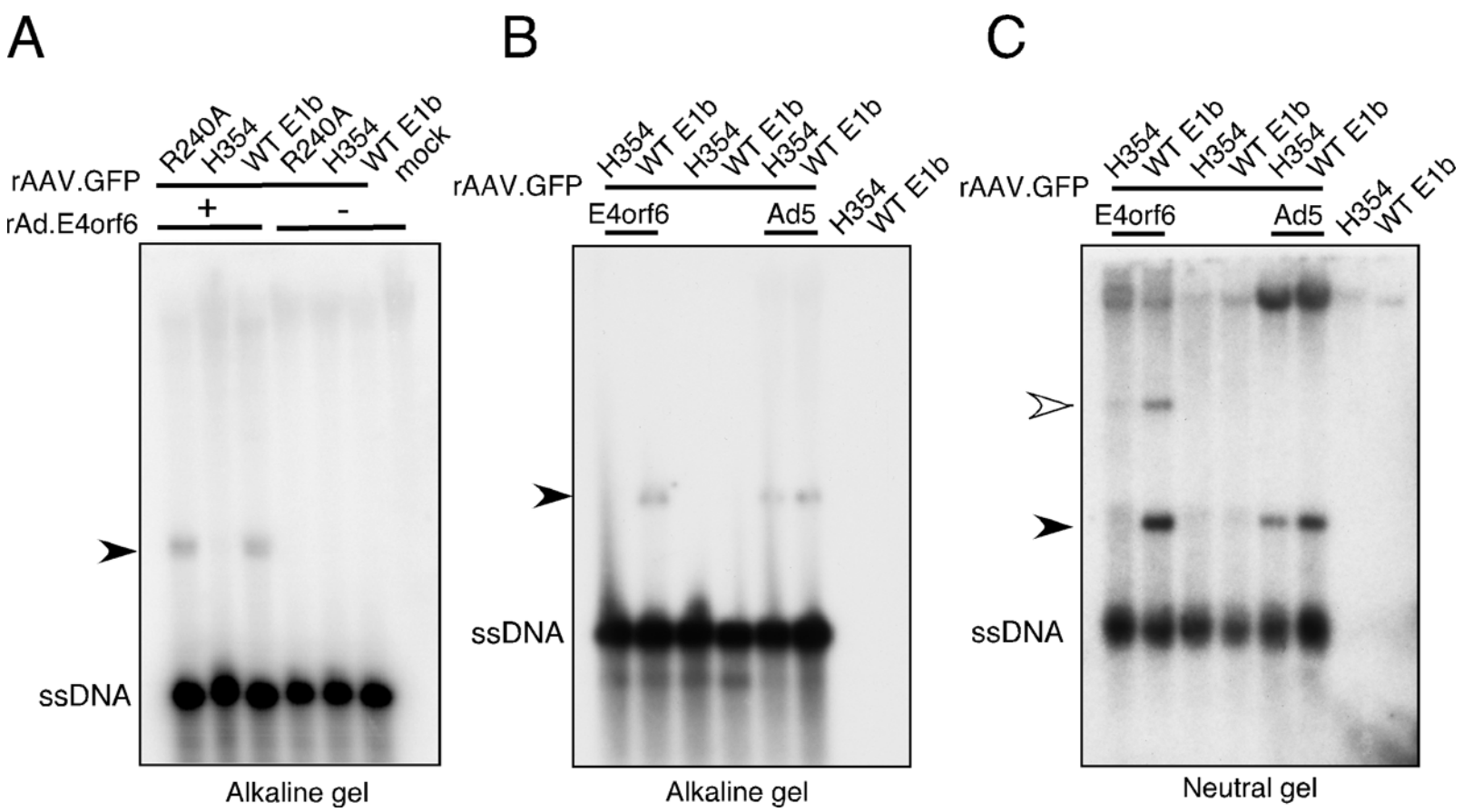
A
R240A
H354
WT E1b
R240A
H354
WT E1b
mock
rAAV.GFP
rAd.E4orf6
+
-
ssDNA
Alkaline gel
B
H354
WT E1b
H354
WT E1b
H354
WT E1b
rAAV.GFP
E4orf6
Ad5
H354
WT E1b
ssDNA
Alkaline gel
C
H354
WT E1b
H354
WT E1b
H354
WT E1b
rAAV.GFP
E4orf6
Ad5
H354
WT E1b
ssDNA
Neutral gel

in discrete foci inside nuclei under conditions of enhanced transduction (57).

We engineered HeLa E1b55K cell lines to express GFP-LacR, and then infected them with the rAAV.LacO vector in the presence or absence of rAd.E4orf6. All cell lines had a similar, small percentage of rAAV.LacO foci after transduction without E4orf6 (Figure 5C and 5D). However, significantly more cells displayed rAAV.LacO foci when MRN was degraded (Figure 5C and 5D), consistent with a greater accumulation of ds rAAV DNA. There was also a small increase in the number of foci per cell, but this was not significant (Figure 5E). Degradation was confirmed by immunoblotting of cell lysates (Figure 5B). No foci were observed in cells without rAAV.LacO infection (data not shown). Although degradation of MRN correlates with the biggest increase in ds rAAV DNA in both assays, H354 cells with E4orf6 displayed a small increase in cells with rAAV.LacO foci. This could reflect increased annealing of rAAV genomes under that condition, which are not detected in the Southern blots in Figure 4A and 4B due to the alkaline electrophoresis conditions. Consistent with this, we did see faint bands and staining under this condition in the Southern blot in Figure 4C, where the gel was run under neutral condtions (both arrowheads). Despite this observation, more ds AAV DNA accumulates in both assays when MRN is degraded. This demonstrates that the previously reported E1b55K/E4orf6-mediated increase in ds AAV DNA may involve disarming of these cellular factors.

Figure 5. Accumulation of rAAV DNA when MRN is degraded. **(A)** Schematic of rAAV.LacO virus and binding of GFP-LacR when virus becomes double-stranded. **(B)** Degradation of MRN in GFP-LacR cell lines. HeLa-derived cell lines expressing GFP-LacR or GFP-LacR with E1b55K proteins were analyzed by immunoblotting for E1b55K expression and degradation of the Mre11 complex in the presence of E4orf6. **(C)** HeLa, WT E1b55K, or H354 cell lines expressing GFP-LacR were infected with rAd.E4orf6 (MOI 25) for 24 hours before super-infecting with rAAV.LacO (MOI 400) for another 16 hours. Cells were fixed and analyzed by confocal microscopy for rAAV.LacO foci. Arrowheads show cells with bright foci. **(D) and (E)** Quantitation of cells with rAAV.LacO foci (D) and number of rAAV.LacO foci per cell (E) in E1b55K cell lines. For each treatment, the average of 3 groups of at least 120 cells each is presented. Error bars represent SEM (D) or SD (E).

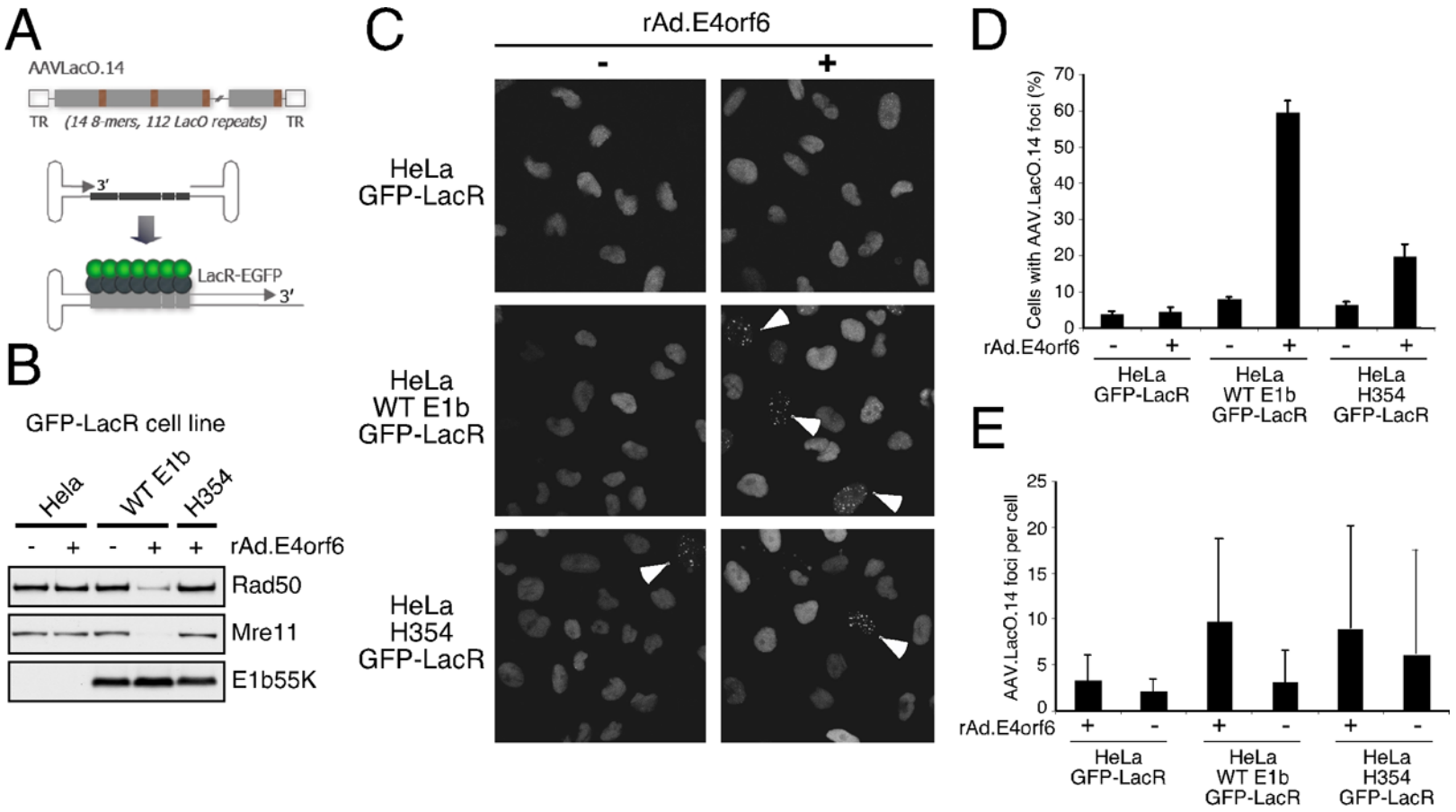
A
AAVLacO.14
TR (14 8-mers, 112 LacO repeats) TR
3′
LacR-EGFP
3′
B
GFP-LacR cell line
Hela
WT E1b
H354
- + - + + rAd.E4orf6
Rad50
Mre11
E1b55K
C
rAd.E4orf6
- +
HeLa GFP-LacR
HeLa WT E1b GFP-LacR
HeLa H354 GFP-LacR
D
Cells with AAV.LacO.14 foci (%)
0 10 20 30 40 50 60 70
rAd.E4orf6
- + - + - +
HeLa GFP-LacR
HeLa WT E1b GFP-LacR
HeLa H354 GFP-LacR
E
AAV.LacO.14 foci per cell
0 5 10 15 20 25
rAd.E4orf6
+ - + - + -
HeLa GFP-LacR
HeLa WT E1b GFP-LacR
HeLa H354 GFP-LacR

Enhanced rAAV transduction in cells lacking MRN

Our data with E1b55K/E4orf6 suggest that degradation of MRN contributes to increased rAAV transduction. We therefore predicted that rAAV transduction should be greater in cells that do not express functional MRN. To test this, we examined rAAV transduction in cell lines from patients with Ataxia-telangiectasia like disorder (A-TLD), in which Mre11 is mutated (330), versus A-TLD cells expressing wild-type Mre11 (335). We observed higher rAAV transgene expression in the mutant cells (Figure 6A), supporting our hypothesis that MRN limits rAAV transduction. This was further evidenced by transduction assays in a cell lines stably expressing shRNA against Rad50 (408) or Mre11 (354) (Figure 6B and 6C). The difference in transduction in these latter systems is less dramatic than in the A-TLD3 cell line likely because the MRN complex was not completely depleted (Figure 6D), and the remaining MRN proteins are fully functional. Both the Rad50 and Mre11 knock-down cells, however, still displayed an increase in transduction over different multiplicities of infection. Importantly, in all systems, we found that when MRN was compromised, rAAV transduction was enhanced, suggesting that this cellular complex poses a barrier to AAV.

Wild-type AAV replication is restricted by MRN

Since E1b55K/E4orf6 provide helper functions for WT AAV replication, we assessed the contribution of MRN degradation during lytic replication with

Figure 6. MRN limits efficient rAAV transduction. (A) A-TLD3 cell lines expressing GFP or WT Mre11 were infected with rAAV.LacZ at the indicated MOIs for 48 hours before processing for quantitative β-galactosidase assay. Infections were performed in triplicate and error bars represent SEM. **(B)** HCT116 cells or HCT116-derived cells containing shRNA to Rad50 (Rad50KD) were infected in triplicate with rAAV.LacZ at the indicated MOIs and harvested after 48 hrs for quantitative β-galactosidase assay and western analysis (D). Error bars represent SEM. Statistical analysis was performed using the unpaired Student's t-test with * representing $p < 0.005$. **(C)** HeLa cells or HeLa-derived cells containing shRNA to Mre11 (shMre11) were infected at the indicated MOIs, harvested, and analyzed as in (B). Error bars represent SEM. **(D)** MRN components are not completely depleted in cell lines expressing shRNA constructs against Rad50 or Mre11. Lysates from (B) and (C) were analyzed by immunoblotting for the indicated proteins. For HCT116/Rad50KD cells, rAAV.LacZ was used at an MOI of 8000.

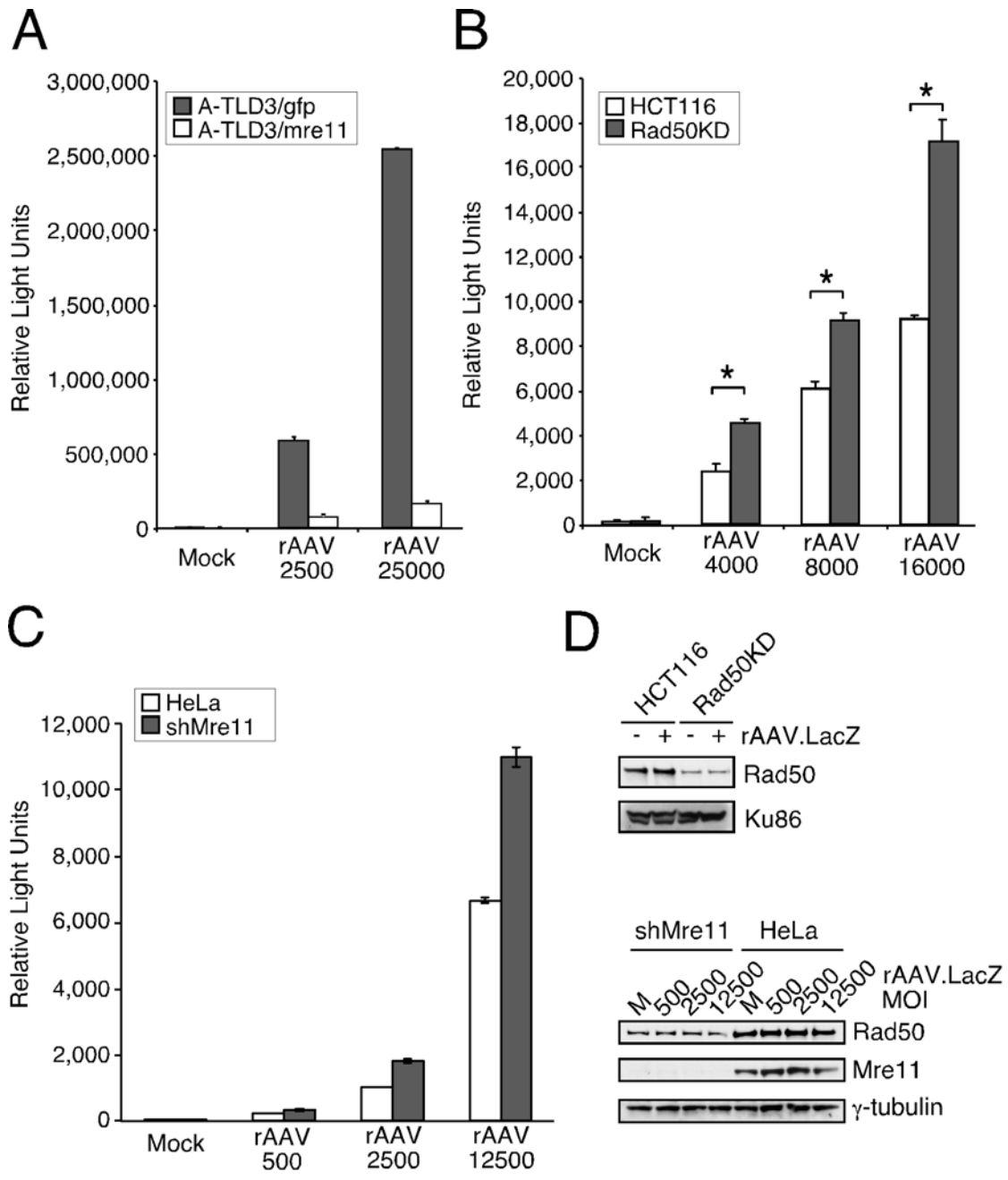
A
A-TLD3/gfp
A-TLD3/mre11
Relative Light Units
3,000,000
2,500,000
2,000,000
1,500,000
1,000,000
500,000
0
Mock
rAAV 2500
rAAV 25000
B
HCT116
Rad50KD
Relative Light Units
20,000
18,000
16,000
14,000
12,000
10,000
8,000
6,000
4,000
2,000
0
*
*
*
Mock
rAAV 4000
rAAV 8000
rAAV 16000
C
HeLa
shMre11
Relative Light Units
12,000
10,000
8,000
6,000
4,000
2,000
0
Mock
rAAV 500
rAAV 2500
rAAV 12500
D
HCT116
Rad50KD
- + - + rAAV.LacZ
Rad50
Ku86
shMre11
HeLa
M 500 2500 12500 M 500 2500 12500
rAAV.LacZ MOI
Rad50
Mre11
γ-tubulin

Ad helper proteins. WT and mutant E1b55K cell lines, or the GFP control cell line, were infected with AAV and an Ad helper virus that cannot down-regulate MRN (*dl*1016, lacking E1b55K and E4orf3). Accumulation of AAV Rep proteins was assessed by imunoblotting, and replicated viral DNA was measured by quantitative PCR (Figure 7A). WT Ad was used a helper control, and AAV replication was quantified relative to an AAV infection with no helper virus. We consistently observed greater Rep expression and viral DNA replication when MRN was degraded (in WT E1b55K and R240A expressing cells), compared to when MRN was present (in H354 and GFP expressing cells). DBP protein levels showed equal *dl*1016 infection between cell lines.

To show that the observed differences were not due to variations in helper virus functions, we assayed WT AAV replication after transfecting an AAV infectious plasmid clone, pNTC244 (60), along with Ad helper proteins E4orf6 and DBP, into the E1b55K cell lines. Viral DNA replication was analyzed by Southern blot hybridization (Figure 7B). Similar to the results obtained above by infection, we observed more AAV replication in the cell lines that degraded the Mre11 complex (WT E1b55K and R240A expressing cell lines). Together, these assays suggest that degradation of MRN is an important AAV helper function provided by E1b55K/E4orf6.

If the Mre11 complex inhibits WT AAV replication, then more AAV DNA should accumulate in cells lacking MRN. To test this, AAV replication was

Figure 7. Degradation of MRN correlates with increased AAV replication. (A) WT or mutant E1b55K expressing HeLa cells were infected with WT AAV with or without Ad mutant *dl*1016 (ΔE1b55K/ΔE4orf3) or Ad5 (both MOI 50) for 24 hours before harvesting for immunoblot analysis or HIRT DNA extraction and quantitative PCR (QPCR) of viral DNA. QPCR levels were normalized to GFP expressing cells infected with AAV alone. Viral replication and Rep accumulation is greatest in E1b55K cells where the MRN complex is degraded (Ad5, or WT E1b55K and R240A cells with *dl*1016). **(B)** AAV replication in E1b55K cell lines by transfection with helper plasmids. HeLa-derived cell lines expressing GFP or E1b55K proteins were transfected with the AAV plasmid pNTC244 in the presence or absence of plasmids expressing E4orf6 and DBP. Infection with Ad5 (MOI 50) served as a positive control. Viral DNA was extracted from cells after 48 hours and analyzed by southern blot hybridization with a Rep probe. Rfd-replication form dimer, Rfm-replication form monomer, and ssDNA-single-stranded DNA.

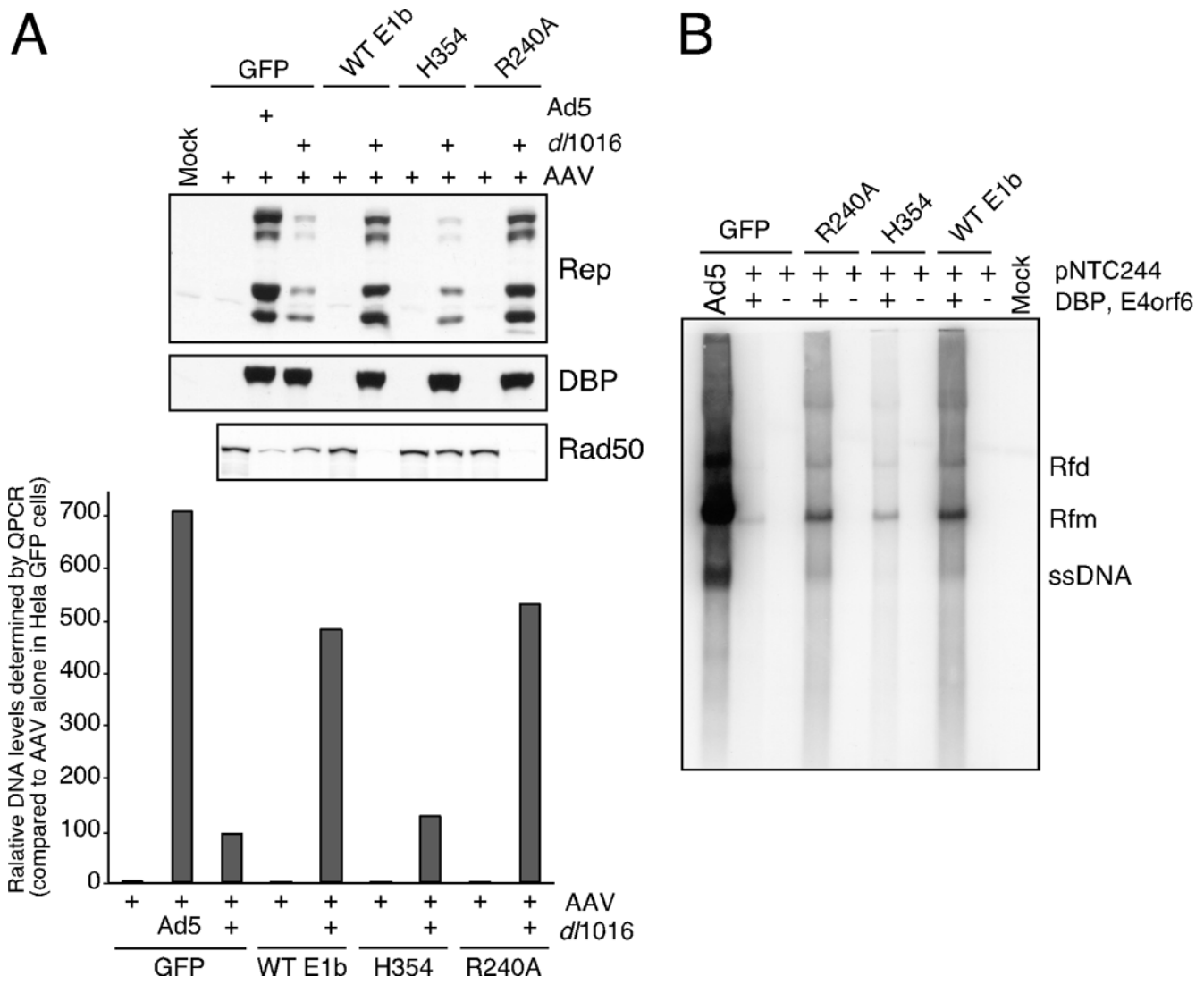
A
GFP
WT E1b
H354
R240A
Ad5
d/1016
AAV
Mock
Rep
DBP
Rad50
Ralative DNA levels determined by QPCR
(compared to AAV alone in Hela GFP cells)
700
600
500
400
300
200
100
0
B
GFP
R240A
H354
WT E1b
Ad5
Mock
pNTC244
DBP, E4orf6
Rfd
Rfm
ssDNA

measured in cells lines harboring mutations in Nbs1 (NBS) (56) and Mre11 (A-TLD3), versus wild-type complemented cells. An E4-deleted Ad that cannot degrade MRN (*dl*1004) was used as a helper virus in these assays. We found that AAV replication was greater in all the mutant cell lines versus their WT protein-expressing counterparts (Figure 8A and 8B), demonstrating that MRN is inhibitory to AAV. Immunoblotting showed levels of viral helper proteins were comparable between NBS mutant and WT-complemented cell lines (Figure 8A), suggesting that this does not account for the observed differences in AAV replication. As a control, we infected both NBS cell lines with WT Ad5, which degrades the remaining MRN members. Similar levels of AAV replication (Figure 8A) were detected between cell lines co-infected with Ad5. This further indicates that the results obtained with *dl*1004 co-infection are due to the MRN mutations in the cell lines. Use of other mutant Ad helper viruses that do not degrade MRN also yielded similar data (Figure 9), suggesting the effects on AAV replication are not helper virus specific. These data demonstrate that MRN limits WT AAV replication, and that suggest E1b55K/E4orf6 provide a helper function to AAV by degrading the complex.

MRN proteins recognize viral replication centers and AAV ITRs

AAV replication centers develop during infection with helper virus (366, 375), or after transfection of the infectious clone pNTC244 with minimal helper virus proteins (336). Since the Mre11 complex localizes to sites of DNA

Figure 8. The Mre11 complex restricts AAV replication. (A) NBS cell lines complemented with empty vector (NBS-) or WT Nbs1 (NBS+) were infected with WT AAV in the presence or absence of Ad5 (MOI 50) or Ad mutant *dl*1004 (MOI 50) for 24 hours. Cells were processed for viral DNA and immunoblotting. DNA was subject to Southern blot hybridization with a Rep probe. Lysates were analyzed by immunoblotting for levels of cellular (MRN) and adenoviral (E1b55K, DBP, and E1A) proteins as shown below. **(B)** A-TLD3 cells complemented with either GFP or WT Mre11 were infected in duplicate with WT AAV at an MOI of 3000, in the presence or absence of *dl*1004 (MOI 25). After 48 hours, cells were processed for viral DNA as above except that a 4kB AAV genome fragment was used as a probe. Rfd, Rfm, and ssDNA as in Figure 7.

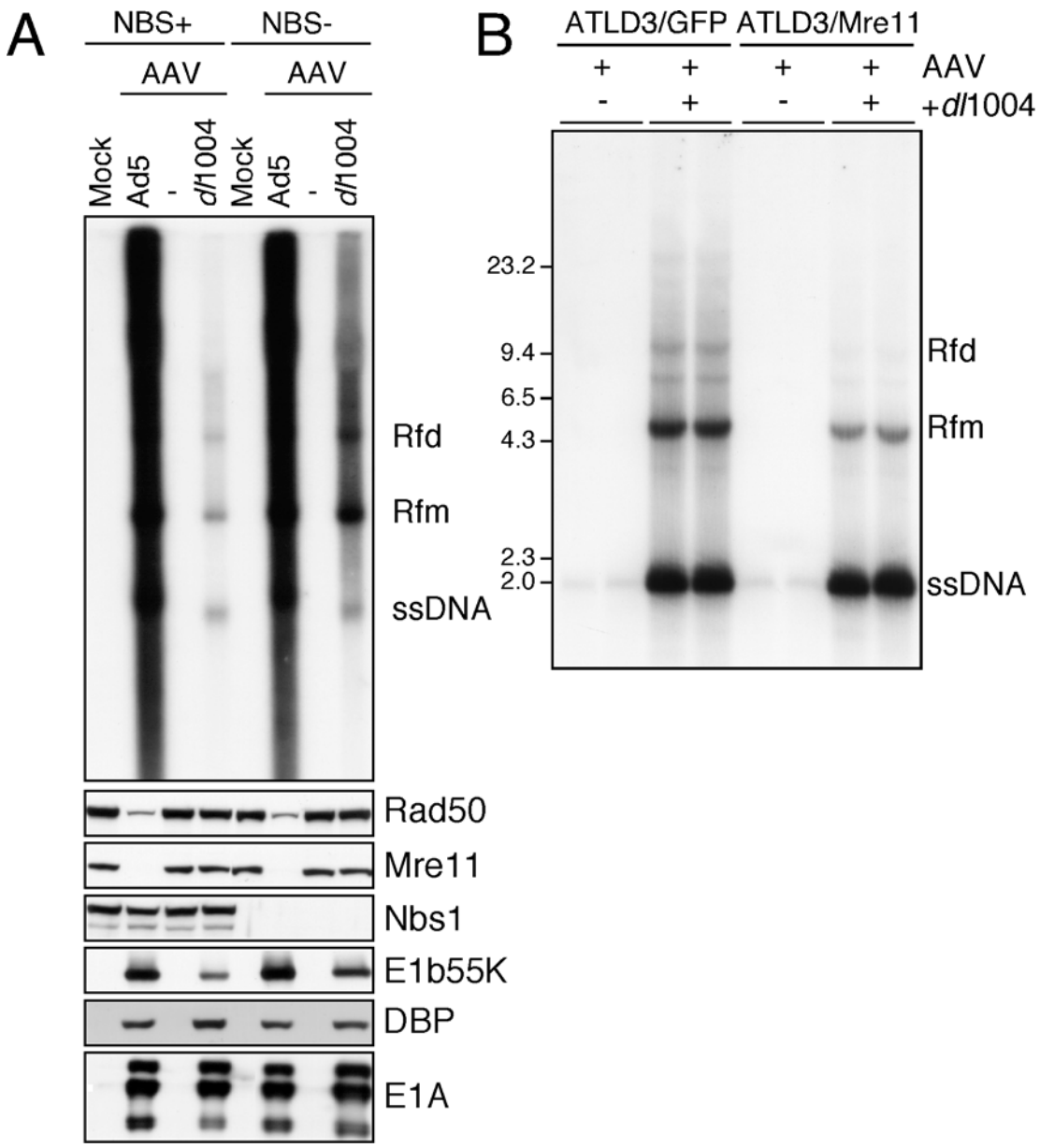
A
NBS+
NBS-
AAV
AAV
Mock
Ad5
-
dl1004
Mock
Ad5
-
dl1004
Rfd
Rfm
ssDNA
Rad50
Mre11
Nbs1
E1b55K
DBP
E1A
B
ATLD3/GFP
ATLD3/Mre11
+
+
+
+
AAV
-
+
-
+
+dl1004
23.2
9.4
6.5
4.3
2.3
2.0
Rfd
Rfm
ssDNA

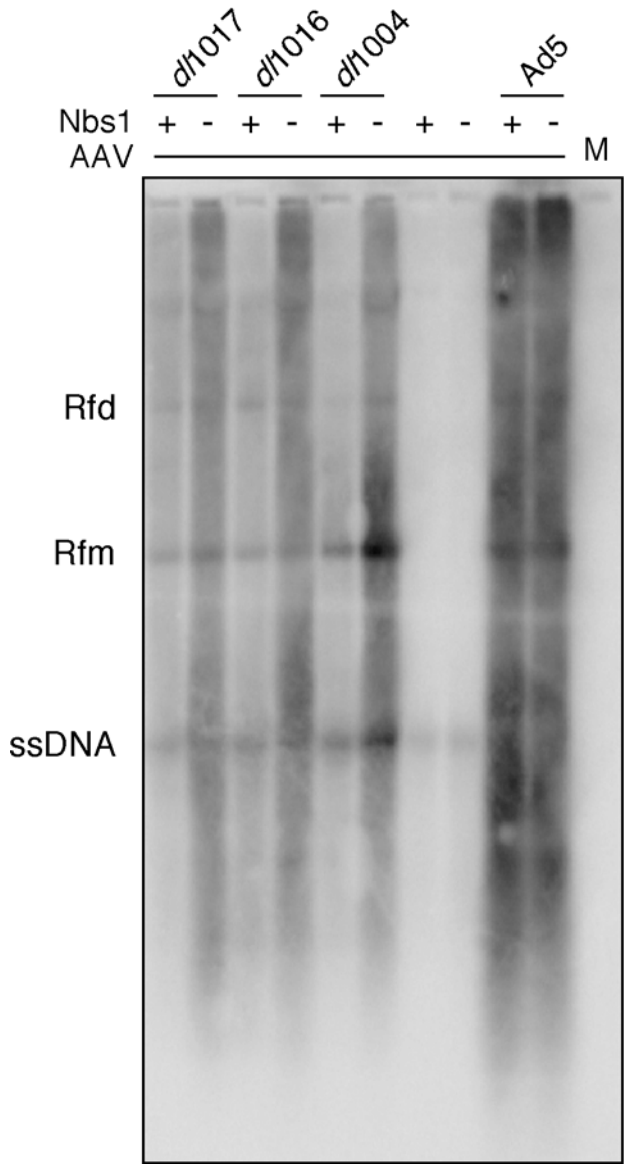

Figure 9. The effects of MRN on AAV replication are not helper virus specific. NBS cell lines complemented with empty vector (-) or WT Nbs1 (+) were infected with WT AAV in the presence or absence of Ad5 or mutant viruses which cannot degrade MRN: *dl*1004 (E4Δ), *dl*1016 (E1bΔ/E4orf3Δ), or *dl*1017 (E1bΔ,E4orf6Δ), all at MOIs of 50. After 24 hours, cells were processed for viral DNA that was analyzed by Southern blot hybridization using a Rep probe. Rfd, Rfm, and ssDNA as in Figure 7.

damage and replication within cells (226, 227, 235, 236), we examined MRN localization and its influence on AAV replication compartment development by immunofluorescence. HeLa cells were transfected with a plasmid that expresses DBP, with or without pNTC244, and cells were stained for members of the Mre11 complex and viral replication centers (Figure 10). In the absence of viral replication centers, DBP and MRN showed a diffuse nuclear staining pattern (Figure 10, DBP only). Transfection of pNTC244 along with DBP induced discrete AAV centers in some cells, where DBP and Rep co-localized. We found MRN accumulated at these viral sites, suggesting that replication compartments may be recognized as DNA damage.

Previous studies (336, 366, 375) have demonstrated that as AAV replication progresses, the Rep pattern changes from small discrete intranuclear foci (early stage), to larger globular structures (middle stage), and eventually to a more diffuse pattern where Rep structures fill much of the nucleoplasm (late stage). To assess further how MRN affects AAV replication compartment progression, we compared AAV centers when MRN was present or absent. The AAV infectious clone pNTC244 was co-transfected with DBP and E4orf6 plasmids into either the WT E1b55K or H354 cell lines, and the relative number of cells at each replication stage was quantitated (Figure 11). We found a larger proportion of late AAV replication centers present in cells where MRN was degraded (the WT E1b55K cells), whereas more early

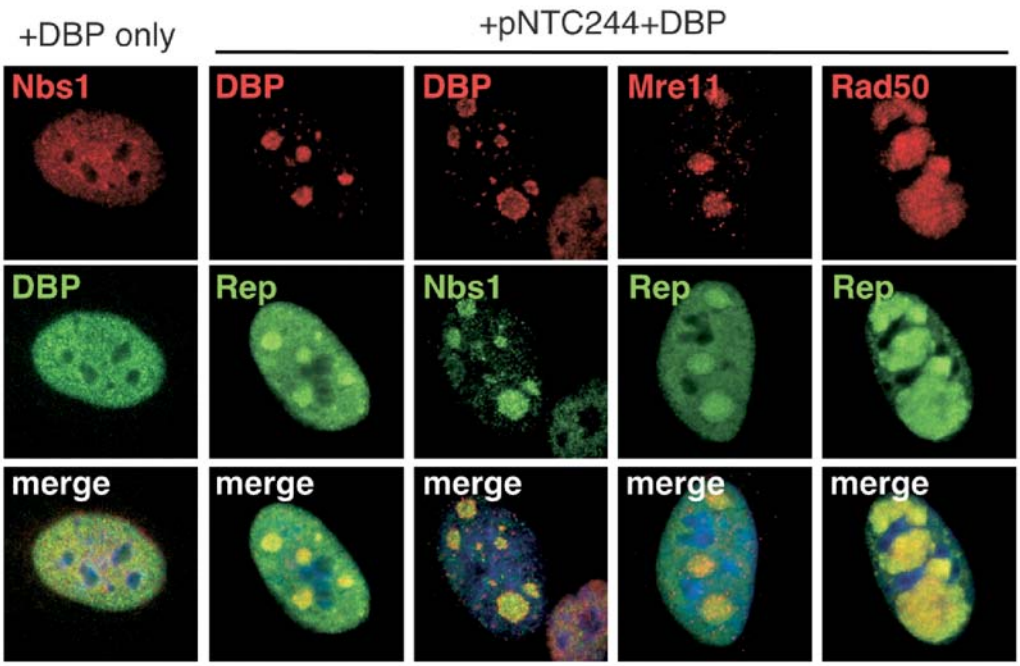

Figure 10. MRN components localize to AAV replication compartments. HeLa cells were transfected with a DBP expression plasmid with or without the AAV infectious clone pNTC244. Cells were fixed and stained for Rep and DBP to mark AAV centers, and for MRN components.

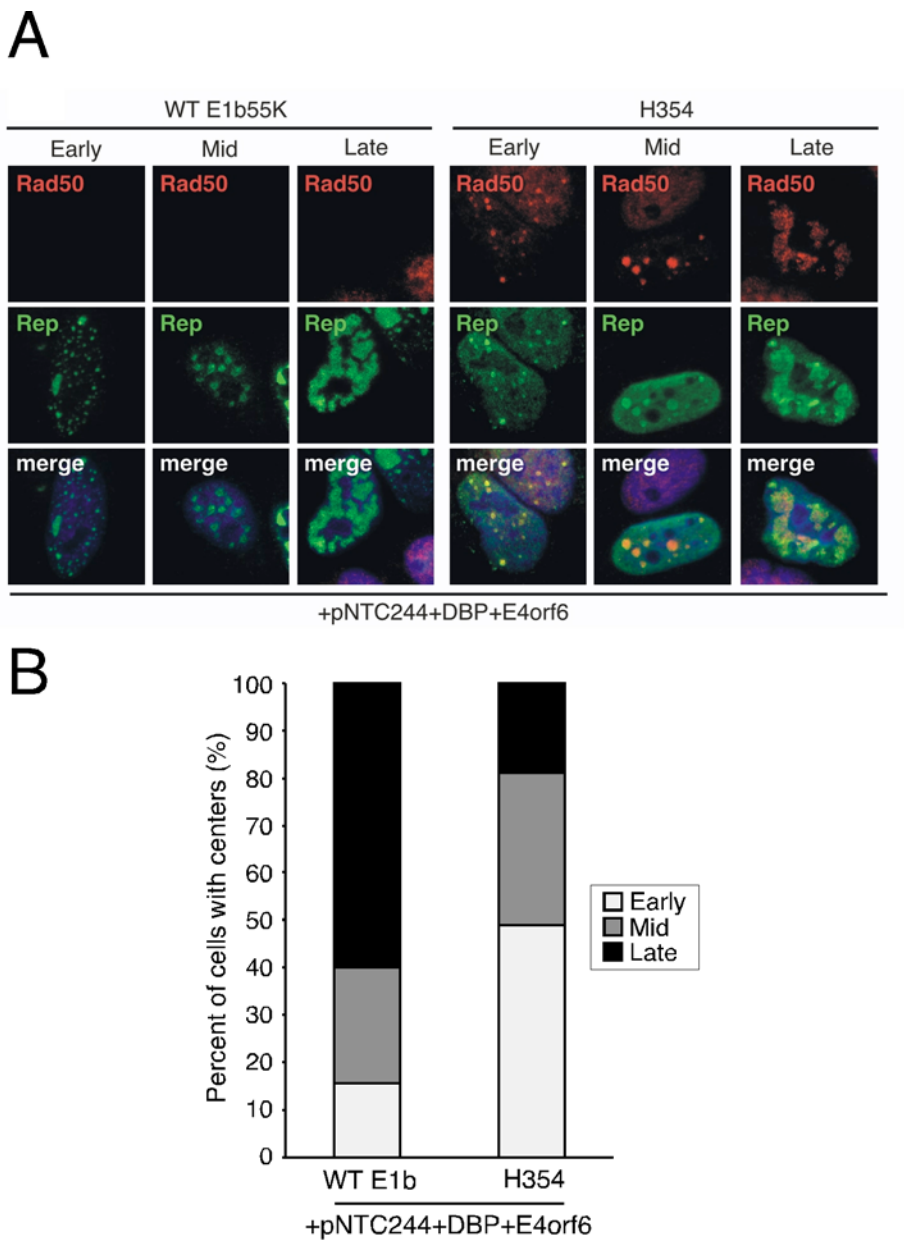

Figure 11. Degradation of MRN results in more advanced AAV replication centers. (A) AAV replication centers formed by plasmid transfection. Examples of stages of replication centers formed when WT E1b55K or H354 cells were transfected with pNTC244, DBP and E4orf6 expression plasmids. Cells were stained for Rep and Rad50. Rad50 staining is absent in WT E1b55K cells as it is degraded with E4orf6. **(B)** WT E1b55K or H354 expressing cell lines were transfected with pNTC244, DBP and E4orf6 expression plasmids. Rep positive cells, 200 per treatment, were quantified for replication center stage and expressed as percent of cells with centers.

centers were visible in cells expressing MRN (the H354 cells). Additionally, during the course of these experiments we found that many more cells displayed replication centers when MRN was degraded (WT E1b55K) versus present (H354). This observation is consistent with the results from Figure 11, further indicating a barrier in the initiation of viral replication. Rad50 localized to viral centers in all H354 cells, whereas MRN was degraded in 95% of transfected WT E1b55K cells. Together, these experiments indicate that MRN may recognize AAV as DNA damage, localizing to AAV centers and limiting the efficiency of viral replication as well as the onset.

Purified Mre11 complex components have been shown to recognize a variety of DNA structures, including hairpins (78). Since the AAV ITR hairpin structures are genetic elements common between WT AAV and rAAV, we wanted to test whether the complex could recognize AAV ITRs directly. Purified Mre11 and Nbs1 proteins were obtained, and tested for association with the ITRs *in vitro*. The electrophoretic mobility shift assay we employed was previously used to study DNA interactions with purified Mre11 and Nbs1 (267). We found that the mobility of the ITR shifted in the presence of Mre11/Nbs1, and was competed efficiently by unlabeled AAV ITR but not by non-specific DNA (Figure 12). These data demonstrate that MRN components can bind AAV ITRs directly, and suggest that ITRs may contribute to MRN recognition in cells.

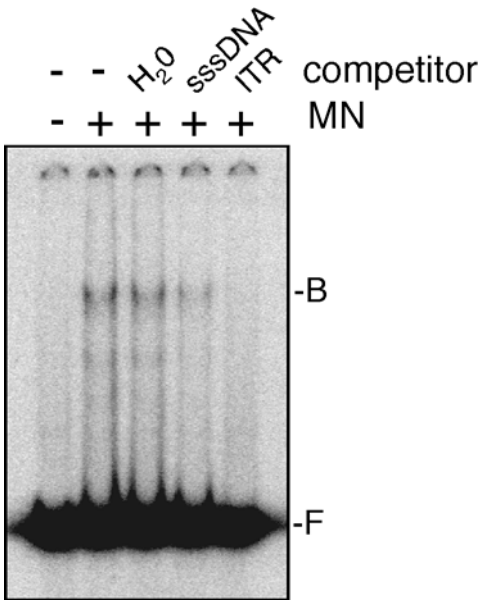

Figure 12. Members of the Mre11 complex bind AAV ITRs. Binding of MRN components to the AAV ITR. The AAV ITR was 5' end-labeled, incubated with purified Mre11/Nbs1 proteins (MN), and electrophoresed according to Materials and Methods. Sonicated salmon sperm DNA (sssDNA) or cold ITR were used as competitors. The positions of bound (B) and free (F) ITR are indicated.

The nuclease activity of Mre11 is not required to limit AAV transduction and replication

Mre11 exhibits both exonuclease and endonuclease activity on a variety of DNA substrates (78). Since Mre11 complex members localized to AAV replication centers (Figure 10) and bound AAV ITRs *in vitro* (Figure 12), we wondered whether Mre11 might directly process AAV genomes to inhibit viral transduction and replication. To test this, we examined whether a nuclease-dead version of Mre11 could still inhibit AAV transduction and replication in cells. We chose the *mre11-3* allele since this mutation in the nuclease domain of Mre11 (see Figure 13A) abrogates activity, but does not affect binding to Rad50 or Nbs1 (34). A-TLD1 cells (330) were reconstituted with empty vector, WT Mre11, or Mre11-3, as previously described (50), and assayed for rAAV transduction (Figure 13A) and WT AAV replication (Figure 13B). Surprisingly, both rAAV transduction and AAV replication were inhibited to a similar extent between the nuclease-dead Mre11 expressing cells and the WT Mre11 expressing cells. This suggests that the nuclease activity does not contribute to limiting AAV transduction and replication, and that another activity of MRN is required.

The C-terminus of Nbs1 is sufficient to limit AAV replication

Nbs1 has a variety of domains important to its protein-protein interactions and functions in the DNA damage response (Figure 14A). We

Figure 13. The nuclease activity of Mre11 is not required to limit AAV transduction and replication. (A) Schematic of the Mre11 protein (see Chapter 1, Figure 3 for further details) illustrating the locations of the mutation in A-TLD1 cells (black arrowhead) and the 11-3 mutation (red arrowhead) that abrogates nuclease activity. **(B)** A-TLD1 cells or cells complemented with WT Mre11 or Mre11-3 were infected with rAAV.lacZ at an MOI of 25,000 for 48 hours before fixing and processing for β-galactosidase activity. Error bars represent the SEM of triplicate samples. **(C)** A-TLD1 cells or cells complemented with WT Mre11 or Mre11-3 were infected with WT AAV (MOI 3000) in the presence or absence of Ad5 or Ad mutant *dl*1004 (E4Δ) (both at MOI 50) for 48 hours before processing for viral DNA. Viral DNA was analyzed by Southern blot hybridization with a probe against Rep. Rfd, Rfm, and ssDNA as in Figure 7.

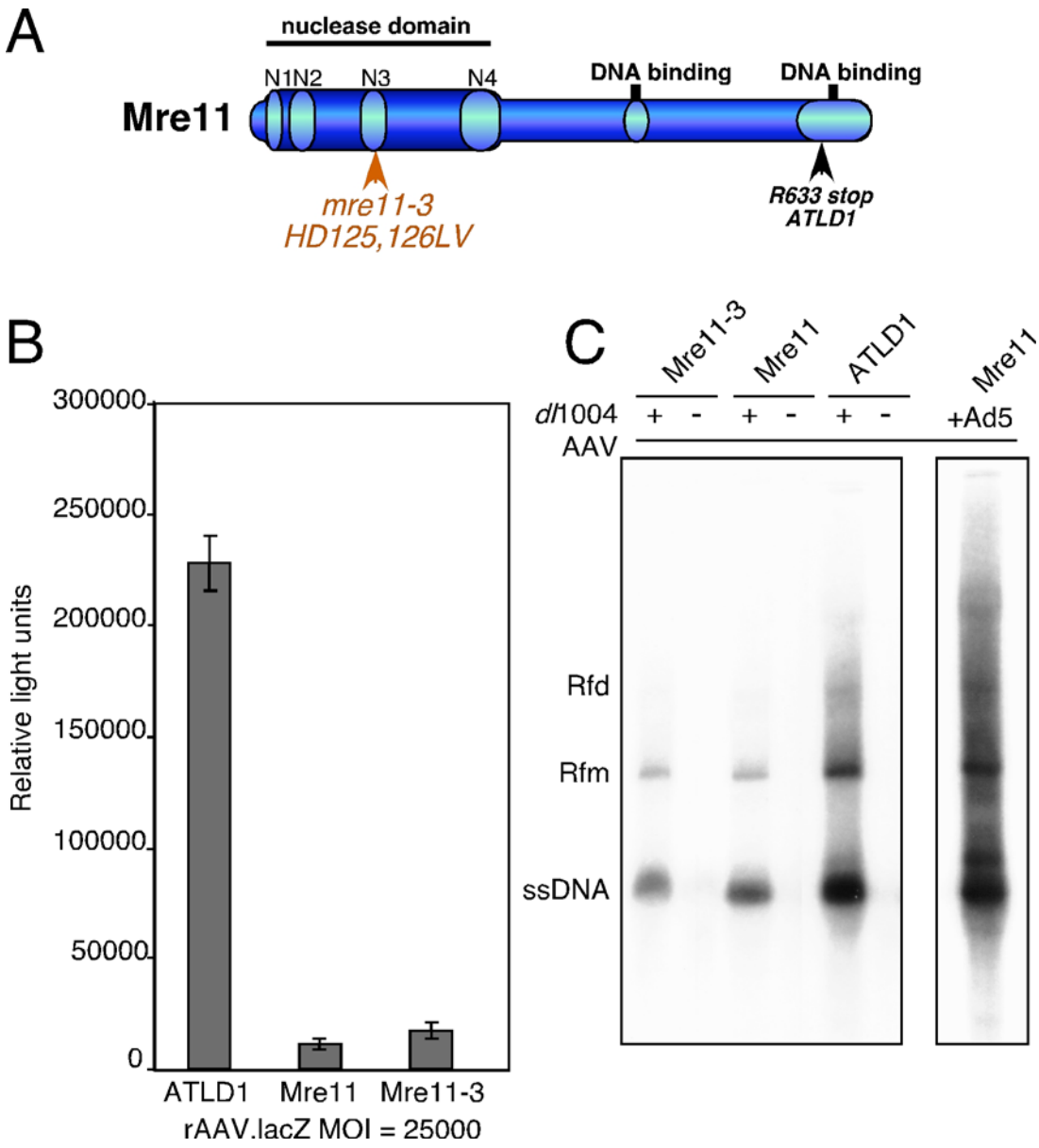
A
nuclease domain
N1N2
N3
N4
DNA binding
DNA binding
Mre11
mre11-3
HD125,126LV
R633 stop
ATLD1
B
Relative light units
300000
250000
200000
150000
100000
50000
0
ATLD1
Mre11
Mre11-3
rAAV.lacZ MOI = 25000
C
Mre11-3
Mre11
ATLD1
Mre11
dl1004
AAV
+ - + - + -
+Ad5
Rfd
Rfm
ssDNA

wanted to determine which regions were required for AAV inhibition to further understand how MRN affects the virus. To address this, we analyzed WT AAV replication in NBS cell lines reconstituted with mutant forms of Nbs1 (54, 86) lacking the N-terminal FHA and BRCT domains (FR5), or the C-terminal Mre11 and ATM binding domains (652). NBS cells expressing the 652 fragment showed increased AAV replication, but not to the level observed with Nbs1 deficient cells (Figure 14B). This result was not due to protein expression since all Nbs1 mutants were expressed similarly (Figure 14C). Instead, the N-terminal Nbs1 domains may contribute marginally to inhibiting AAV replication. However, mutation of the Nbs1 phosphorylation sites, serine 278 and serine 343, did not affect replication (data not shown), indicating that these sites are not involved. Importantly, we found that the C-terminal fragment, FR5, was sufficient to inhibit AAV replication, similarly to WT Nbs1 containing cells (Figure 14B). This suggests that the Mre11 binding domain and/or the ATM binding domain are required to block efficient AAV replication. NBS cell lines expressing mutant Nbs1 proteins lacking these domains separately can be used in future experiments to determine how they impact AAV replication.

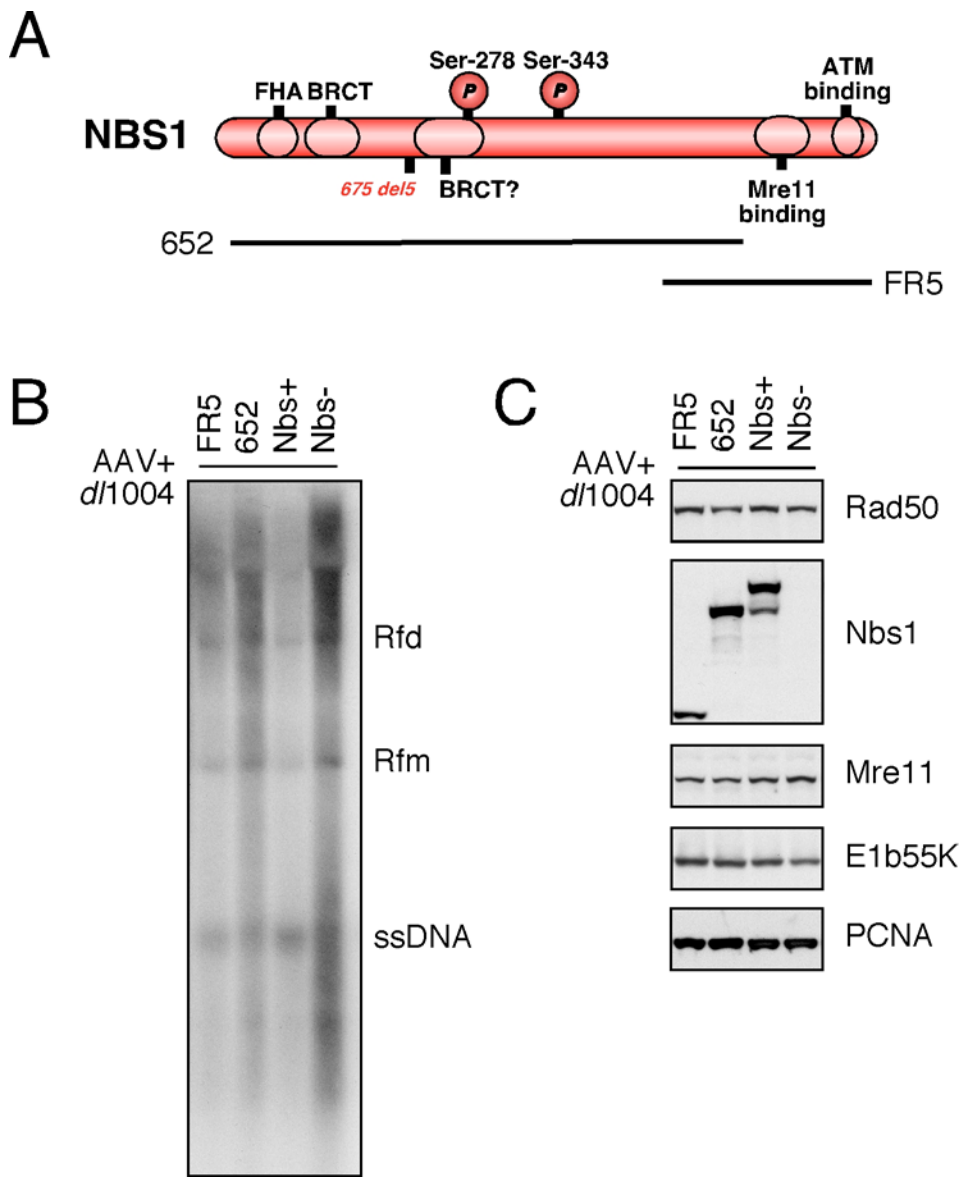

Figure 14. The C-terminus of Nbs1 is sufficient to limit AAV replication. **(A)** Schematic of the Nbs1 protein illustrating the domains (see Chapter 1, Figure 3 for further details), the mutation in NBS cells (675del5), and the regions encompassed by two Nbs1 fragments, 652 and FR5, expressed in NBS mutant cell lines. NBS cells or those complemented with the indicated Nbs1 mutants were infected with WT AAV and Ad mutant *dl*1004 (E4Δ) (MOI 25) for approximately 24 hours. Cells were harvested and processed for Southern blotting of viral DNA **(B)** and immunoblotting **(C)**. E1b55K serves as an infection control and PCNA is a loading control for (C). Rfm, Rfd, and ssDNA as in Figure 7. See text for definitions.

Discussion

Recent research has established links between DNA viruses and the cellular DNA damage response machinery (203, 365). The Mre11 complex is implicated as a major sensor of DNA damage in the cell, recognizing structures such as double-strand DNA ends, single-strand DNA, and hairpins (78, 338). Viral genomes contain such structures and, therefore, some viruses have evolved strategies to inactivate MRN. In the case of Ad, E1b55K/E4orf6 degrade MRN to prevent viral genome processing and damage signaling (50, 335) (see Chapter 2). Given that these viral proteins provide helper functions to promote AAV transduction and replication, we examined whether the Mre11 complex impedes aspects of the AAV lifecycle, and if the E1b55K/E4orf6-mediated helper function involves degradation of these cellular proteins.

Here we have shown that degradation of the MRN complex by E1b55K/E4orf6 creates a more permissive state for both WT AAV replication and rAAV transduction. Use of the E1b55K mutants and HeLa-based cell lines in these assays rules out a role for p53 in inhibiting AAV, in agreement with other reports (64, 139). Cyclin A degradation was previously observed in an E4orf6-inducible 293-based cell line, and suggested to contribute to enhancement of rAAV transduction (139). While this activity may be relevant to the particular 293-based cell line used in that study, we did not observe cyclin A degradation in the E1b55K expressing cell lines used in this work

(Chapter 2, Figure 9). Additionally, the E1b55K expressing cell lines used in these experiments display similar cell cycle profiles in the presence of E4orf6 (Chapter 2, Figure 9), suggesting that the cell cycles effects of these mutant viral proteins may not be limiting to rAAV transduction.

E1b55K/E4orf6 was also recently shown to degrade DNA Ligase IV, a cellular protein involved in NHEJ (8). However, all the E1b55K mutants utilized here degrade DNA Ligase IV in conjunction with E4orf6 (Chapter 3, Figure 11), suggesting little contribution of this activity towards AAV helper function. E1b55K/E4orf6 also appear to down-regulate AAV5 de-novo expressed Cap proteins and Rep52, and AAV2 Rep 52 (249, 250). This activity, though, only occurred under certain conditions (249), and did not appear to affect our replication assay results. By using mutant and shRNA-containing cell lines, we directly demonstrated that MRN proteins negatively regulate viral transduction and replication. This further highlights degradation of MRN as a critical AAV helper function provided by E1b55K/E4orf6. We cannot, however, rule out additional activities of E1b55K/E4orf6 that also contribute to AAV helper function. This may include degradation of unknown relevant substrates by the E1b55K/E4orf6 ubiquitin ligase complex, or a role in RNA processing and transport (296).

AAV has evolved to exploit helper viruses such as Ad to establish a cellular environment conducive to its replication. Other viruses such as herpes

simplex virus 1 (HSV-1) also facilitate aspects of the AAV lifecycle (363). Minimal HSV-1 helper proteins do not promote robust second-strand synthesis and transduction from rAAV vectors (T.H. Stracker and M.D. Weitzman, unpublished data), and this may be due to an inability to neutralize MRN. During WT AAV and HSV-1 co-infection, utilization of the HSV-1 polymerase for AAV replication (358) could bypass the inhibitory effects of MRN on AAV, although the HSV-1 polymerase is not absolutely required (363). Alternatively, since HSV-1 can sequester MRN (202, 345, 372), this may compete the complex away from AAV genomes allowing second-strand synthesis and replication to occur. This latter possibility is consistent with the ability of genotoxic agents to promote limited AAV replication and transduction (5, 295, 388) by potentially recruiting MRN to sites of cellular damage (57). More research will be required to determine how other helper viruses and helper stimuli contend with MRN in facilitating AAV production.

We have used Southern blot hybridization, rAAV.LacO foci formation, and progression of AAV replication centers to demonstrate that the Mre11 complex restricts the accumulation of AAV DNA. In localizing to AAV replication centers and rAAV foci (57), MRN may recognize viral genomes as DNA damage. Our *in vitro* data support a role for the ITRs in this recognition, although we cannot rule out the contribution of other viral structures. For example, replicative forms of the AAV genome (Chapter 1, Figure 10) produce

a variety of structures such as double-strand ends and single-strand overhangs, which may be recognized by MRN (78). In addition, incoming genomes also have Rep covalently bound to the 5' end of the genome (357), and this might resemble a meiotic substrate for MRN (270, 338). However, the targeting of the AAV ITRs would be consistent with other published data showing binding and cleavage of hairpin structures by the Mre11 complex (213, 267, 268). We hypothesized that MRN was restricting AAV DNA accumulation in a similar manner by processing or degrading viral genomes directly via its nuclease activity (267, 268). Interestingly, even though we found that purified MN proteins could cleave AAV ITRs *in vitro* (G.Cassell and M.D. Weitzman, unpublished data), the Mre11 nuclease activity was dispensable in cells for limiting AAV transduction and replication in preliminary experiments.

In trying to determine which functions of MRN are required to inhibit AAV, we found that the Nbs1 C-terminus was sufficient to limit viral replication. This region contains the binding sites for Mre11 and ATM (86, 116, 244, 396). Recruitment of both proteins may be important to inhibiting AAV, since ATM negatively regulates AAV (298, 401), and full activation of ATM requires MRN complex formation and ATM-Nbs1 interaction (55, 116, 196, 396). Nbs1 may therefore utilize ATM and/or ATM signaling to recruit factors that process AAV DNA, or to inhibit cellular proteins and/or polymerases required to synthesize viral DNA. These hypotheses would be consistent with the observation that

knock-down of Nbs1 has no additional effect on rAAV transduction in ATM-deficient cells (57). E1b55K/E4orf6-mediated degradation of MRN would suppress the impact of ATM on AAV, providing an important link between helper function and ATM activity. Although the mechanism by which MRN inhibits AAV is currently unclear, examining AAV replication in NBS cell lines expressing Nbs1 fragments with Mre11 or ATM recruitment domain mutations will further support the involvement of ATM. Additionally, since the major cellular replication factors utilized during AAV replication have been identified (247, 248, 255), we can now begin to examine how MRN and damage signaling affect these and other factors (280) important to virus propagation (see Chapter 6 for further discussion).

An expanding body of work has demonstrated that viruses must contend with the cellular DNA damage response machinery (203, 365). Vectors based on these viruses will, therefore, likely face similar challenges. Here we have shown that the Mre11 complex limits rAAV transduction, similarly to other proteins involved in DNA double-strand break repair (64, 298, 401). Our observation that Mre11 binds to AAV ITRs is consistent with previous reports showing that vector circularization involves MRN (64) and is decreased by E4orf6 (101). Vector design and structure, however, may alter the recognition and outcome of vector-host interactions (299). For example, UV-inactivated AAV genomes, which contain cross-linked viral DNA, were

recognized by a number of DNA damage response proteins in the ATR pathway (168). A self-complementary AAV vector (see Chapter 1, Figure 10), which is already double-stranded, was also recently shown to require certain DNA repair proteins, including the Mre11 complex, for circularization (64). When we analyzed scAAV transduction, we found that MRN was inhibitory (Appendix Figure 4). However, we did not examine the processing or circularization of these vectors, a step that occurs after our transduction readout, and this could explain the apparent discrepancy. The outcome of vector-host interactions may also be impacted by the DNA damage response capacity of certain tissues *in vivo*, which may be altered after differentiation. It will be interesting to see how DNA damage signaling pathways are affected in tissues that display efficient rAAV transduction, and the differences between the dividing cells used in our studies and the non-dividing cells found *in vivo*. Clearly, further research is needed to clarify the relationship of viral vectors to cellular DNA repair proteins and pathways.

Materials and Methods

Plasmids and transfections

The wild-type full-length AAV type 2 genome was supplied by the plasmid pNTC244 (60). For production of recombinant AAV vectors 293T cells were transfected with three plasmids: pXX2 which supplied Rep and Cap

proteins (383); pXX6 which contained the adenovirus helper functions (383); and the vector plasmids pAAV.LacZ or pAAV.GFP which consist of transgenes under the control of the CMV promoter cloned between viral inverted terminal repeats. The transgene expressing the lactose repressor fused to GFP (GFP-LacR) with a nuclear localization signal was isolated from the plasmid p3'ssdEGFP, kindly provided by A.S. Belmont (University of Illinois at Urbana-Champaign), and cloned into the pLPC retrovirus vector under a CMV promoter (309). To make the rAAV.LacO.14 vector, a 292-bp LacO repeat was isolated from pSV2dhfr 8.32 (a plasmid provided by A.S. Belmont that contains 10 kb of 292-bp lac operator repeats) by digestion with Eco RI and cloned into the Eco RI site of pMCS3' (a modified version of the pCMV-MCS plasmid, Stratagene, La Jolla, CA, USA). The 8-mer repeat was then amplified by directional cloning (288) to obtain a vector containing 14 LacO repeats, for a total of 112 LacR binding sites. The 14 LacO repeats were cloned into the Not I site of pAAV-MCS to generate pAAV.LacO.14. The adenovirus helper genes Ad-DBP and E4orf6 were expressed from the CMV promoter in expression vectors pRK5 or pcDNA3.1 (Clontech). The pCMV plasmids used in Figure 3, including the L245P E4orf6 mutant that does not bind E1b55K, were provided by D. Ornelles (263). Sub-confluent monolayers of cells were transfected by calcium phosphate precipitation according to standard protocols or with

Lipofectamine 2000 (Invitrogen) according to the manufacturer's recommendations.

Cell lines and drug treatments

HeLa, U2OS, and 293 cells were purchased from the American Tissue Culture Collection. W162 cells for the growth of E4-deleted viruses were obtained from G. Ketner (361). Stable cell lines derived from HeLa and U2OS that express wild-type (WT) and mutant E1b55K from retrovirus vectors have been described previously (50). NBS cells and complemented counterparts were from P. Concannon (54, 55, 86). HCT116 cells stably expressing shRNA against Rad50 were from D. Ferguson and were previously described (408). HeLa-derived cells expressing an shRNA construct against Mre11 were previously described (354) and provided by C. Her. A-TLD1 and A-TLD3 cells and complemented counterparts were also previously described (50, 335). To generate cell lines expressing GFP-LacR, HeLa E1b55K expressing cells were transduced with retrovirus containing GFP-LacR. Puromycin resistant clones were selected and maintained with 1 mg/mL. HeLa WT E1b55K and H354 GFP-LacR clones were maintained in puromycin and G418 (400 mg/mL). All cells were cultured in Dulbecco's modified Eagle's medium (DMEM) supplemented with 10 or 20% fetal bovine serum (FBS), pen/strep, and appropriate selection at 37°C in a humidified atmosphere containing 5% CO_2. For proteasome inhibitor treatment, cells were infected with rAAV.LacZ for 24

hrs before superinfection with rAd.E4orf6 or Ad5. Two hours post-superinfection, MG132 and epoxomicin (Calbiochem), or DMSO as a control, were added to a final concentration of 10 μM and 2 μM, respectively, for a further 16 hrs.

Viruses and infections

The E4 mutant viruses *dl*1004 and *dl*1016 have previously been described (35, 36) and were obtained from G. Ketner. The recombinant adenovirus rAd.E4orf6, deleted of E1a and E1b and expressing E4orf6 under the CMV promoter, has been previously described (281) and was obtained from P. Branton. Mutant viruses with deletions in E4 were grown on the complementing cell line W162 (361), and all other adenoviruses were propagated on 293 cells. All adenovirus propagation, purification, and titration was previously described (50). Recombinant AAV vectors rAAV.LacZ and rAAV.GFP, description, propagation, and purification have been previously described (121, 336). The self-complementary AAV vector expressing GFP (scAAV.GFP) was provided by R.J. Samulski and propagated like other rAAV vectors. Recombinant AAV with LacO binding sites were generated in 293 cells, using dual plasmid cotransfection procedure with pDG as packaging helper plasmid (kindly provided by J.A. Kleinschmidt, Heidelberg, Germany) as previously described (401). The titers of rAAV.LacO.14 were measured by Southern blotting using serial dilutions of the input pMCS3'lacO.14 plasmid as

a standard. All other AAV titers were determined by quantitative PCR using SYBR Green I double-stranded DNA binding dye and an ABI Prism 7700 Sequence detection system (PE Biosystems). All infections were performed on monolayers of cultured cells in DMEM supplemented with 2% FBS. After 2 hrs at 37°C, DMEM with 10% or 20% FBS was supplemented. All AAV infections were performed at an MOI of 1000 unless otherwise stated.

Antibodies, immunofluorescence and immuoblotting

The primary viral antibodies used in this study were: Rep (rabbit polyclonal, gift of J. Trempe), Ad-DBP (mouse monoclonal B-6, a gift from A. Levine), E4orf6 (rabbit polyclonal, gift from P. Branton), E1b55K (mouse monoclonal 2A6, gift from A. Levine). Commercially available antibodies used in this study were purchased from Calbiochem (E1A, PCNA), Novus (Nbs1), Genetex (Mre11-12D7, Rad50-13B3), Santa Cruz (Ku86), and American Research Products, Inc. (Rep clone 303.9). Secondary antibodies for immuno-fluorescence were coupled to Alexa fluorophores (Invitrogen). 4',6-diamidino-2-phenylindole (DAPI) was used to stain DNA. Cells grown on coverslips in 24-well plates were processed for immunofluorescence for viral replication centers as previously described (50). Images were obtained on a Nikon microscope in conjunction with a CCD camera (Cooke Sensicam) in double or triple excitation mode, and processed using SlideBook and Adobe Photoshop. Western analysis was performed as previously described (50, 335).

Visualization and quantitation of rAAV.LacO foci

The HeLa GFP-LacR, GFP-LacR WT E1b55K, and GFP-LacR H354 cells were plated on 8-well chamber slides before infections described in the figure legend. After infections, cells were fixed with 3.7% paraformaldehyde in PBS and then analyzed by confocal microscopy (Axiovert 100M, Carl Zeiss, Germany). Three groups, a minimum of 120 cells each, per treatment were selected randomly and acquired (optical slice of 0.9 μm). The number of cells with clearly visible rAAV.LacO foci and the number of foci per cell were counted manually.

Reporter Assays for transduction

For β-galactosidase staining, infected cells were washed with 1X PBS before fixing with 2% formaldehyde/0.2% glutaraldehyde in PBS for 10 min at room temperature. After washing, cells were stained with 1 mg/ml X-gal in staining solution (5 mM potassium ferricyanide, 5 mM potassium ferrocyanide, and 2 mM magnesium chloride in PBS) for 2-4 hrs at 37°C. For quantitative β-galactosidase assays, cells were lysed with 1X lysis buffer (Promega). After one freeze/thaw cycle, lysates were spun down and analyzed for β-galactosidase activity using the Tropix Galacto-light Plus kit (Applied Biosystems) according to manufacturer's recommendations. To analyze rAAV.GFP transduction, cells were trypsinized, harvested, and fixed in 2% paraformaldehyde before analyzing the percent of GFP expressing cells by

fluorescence activated cell sorting (FACS) with a Becton Dickinson FACScan. 20,000 events per treatement were analyzed. Alternatively, fluorescent or phase contrast photomicrographs of GFP expressing live cells were captured on a Axiovert 200 (Carl Zeiss, Germany).

HIRT extracts, Southern analysis, and QPCR

To analyze viral DNA, HIRT extracts from infected cells were made as previously described (120). For alkaline gel electrophoresis, HIRT DNA was electrophoresed on a neutral 1% agarose gel (with TAE buffer) or a 1% agarose gel (with 1 mM EDTA and 50 mM NaCl) equilibrated with alkaline running buffer (50 mM NaOH, 1 mM EDTA). Gels were run overnight at 20V for ~18 hrs before processing for Southern blotting as previously described (335). Viral DNA was visualized by hybridization with a probe for GFP. Alternatively, HIRT DNA was run on a neutral 1% agarose overnight and processed accordingly with a probe to Rep (for WT AAV) or a probe to GFP (for rAAV.GFP). HIRT DNA was also subjected to quantitative PCR with primers to the Rep gene as described above.

Purified proteins and electrophoretic mobility shift assay

Mre11 and Nbs1 proteins were purified as in (267) and provided by T.T. Paull. EMSA reaction conditions were adapted from (267). Briefly, reactions were performed in 25 mM MOPS pH 7, 100 mM NaCl, 0.1% Triton X-100, 100 ng/mL BSA, 2 mM DTT, and 100 ng/mL poly dI/dC. AAV ITR was digested

from pSub201 with Xba1 and PvuII, radioactively 5' end-labeled with [γ-^{32}P]ATP and T4 polynucleotide kinase, filled-in with Klenow, and gel-isolated. To form the secondary structure, the ITR was boiled and snap-cooled before filling in with Klenow. The blunt ITR was used at a final range of 0.05 to 0.1 pmol. Approximately 150 ng purified MN was added, and the reactions were incubated at room temperature for ~30 min. Competition experiments used the same unlabeled ITR, sonicated salmon sperm DNA, or water, added after 30 min for an additional 15 min at 10X concentration. Upon completion, 1 mL 50% glycerol was added to each reaction before loading on a 5% native polyacylamide gel. Gels were electrophoresed at 4°C, 100 V for 6 hrs and dried. Analysis was performed with a Molecular Dynamics PhosphorImager.

Acknowledgements

I thank Geoffrey Cassell who performed the EMSA assay in Figure 12 and Sara Adam who performed the rAAV transduction assay in Figure 6A and AAV replication assay in Figure 8B. I also thank Mauro Giacca and Jose Alejandro Palacios for collaborating on this paper and providing the rAAV.LacO data in Figure 5. I am grateful to A. Berk, P. Branton, P. Concannon, D. Ferguson, C. Her, J. Karlseder, G. Ketner, A. Levine, J. Petrini, R.J. Samulski, Y. Shen, J. Trempe and T. Paull for generous gifts of reagents and I. Verma for use of their microscope. I also thank Claudia Hetzer for

cloning LacR-GFP into pLPC, Darwin Lee for propagation of viruses, and members of the Weitzman lab for critical reading of the manuscript.

This chapter in part is a reprint of material as it appears in:

Schwartz RA, Palacios, JA, Adam, SA, Cassell, GC, Giacca, M, Weitzman MD. The Mre11/Rad50/Nbs1 complex limits adeno-associated virus transduction and replication. J Virol. 2007 81(23):12936-12945.

The dissertation author was the primary researcher and author of this paper.

Chapter 6. Effects of the DNA-dependent protein kinase on steps in the adeno-associated virus lifecycle.

Introduction

Adeno-associated virus (AAV) is a small single-stranded DNA virus that relies on helper viruses for propagation (see Chapter 5 for discussion). In the absence of helpers, AAV undergoes latent infection and can site-specifically integrate into a region of chromosome 19 (105, 241). The AAV genome only encodes two genes (see Chapter 1, Figure 9). The Cap gene produces three proteins that compose the virion, and the Rep gene produces four non-structural proteins involved in replication, packaging, and integration. Recombinant AAV vectors (rAAV) are deleted of all viral genes, with Rep and Cap provided in trans to support production of rAAV vectors. Additionally, rAAV vectors still contain the hairpin-containing ITR structures that are required for second strand synthesis (see Chapter 1 Figures 9 and 10).

The larger Rep proteins, Rep78 and Rep68, differ only at the C-terminus (see Chapter 1, Figure 9). These proteins have DNA binding, ATPase, helicase, and DNA nicking activities critical to AAV replication and site-specific integration (62, 241). The smaller Rep proteins, Rep52 and Rep40, only share the C-terminal regions of the larger proteins. Because of this, they lack the DNA binding and nicking activities, but still retain helicase

activity thought to be important in packaging viral DNA (62, 241). The Rep proteins also modulate their own expression in a complex manner during lytic and latent infections (62, 241). Phosphorylation (70, 145, 246) and SUMOylation (359) of the Rep proteins has been reported. Rep phosphorylation may negatively impact DNA binding and AAV replication (145, 246), but it is not clear which kinases are involved.

Since AAV does not encode its own polymerase, it must rely on the host cell machinery for replication (241). Studies examining AAV replication in cells and in vitro have shown that DNA polymerase delta, RPA, RFC, PCNA and MCMs are required (247, 248, 255), and some of these accumulate at AAV centers (168, 336) (see below). Rep and RPA have been shown to interact directly and this stimulates Rep binding to AAV DNA (336). In the presence of helper viruses, AAV does not use the adenovirus polymerase (241), likely due to the different priming mechanism of Ad (see Chapter 2, Figure 7). However, AAV can use the HSV polymerase (358) even though it is not essential to HSV helper function (363).

As mentioned in Chapter 5, a number of reports suggest a relationship between AAV and the cellular DNA damage response machinery. We have shown that the Mre11 complex (MRN) poses a barrier to both rAAV transduction and wild-type (WT) AAV replication (57, 308) (see also Chapter 5). ATM also appears to negatively regulate rAAV transduction (64, 298, 401),

likely acting in the same pathway as MRN (57). Others have suggested that the AAV ITRs (284) or Rep proteins (21) can induce an ATM-dependent damage response in cells. Additionally, UV-inactivated AAV genomes have been shown to accumulate ATR and other DNA repair factors in a manner similar to a stalled replication fork (168). It is currently unclear how these damage response factors intersect to regulate the AAV lifecycle.

Adding to a growing list of DNA repair proteins that affect AAV is DNA-PK, the holoenzyme composed of the PIKK DNA-PKcs, and the Ku70 and Ku86 DNA binding heterodimer (see Chapter 1 for further discussion). DNA-PKcs was found to mediate rAAV processing in certain tissues of animal models (64, 103, 161, 245, 298, 325, 326). DNA-PKcs and Artemis (240) were required to cleave open the AAV ITRs in certain tissues to prevent accumulation of linear double-stranded vectors with covalently closed ends (161), which are substrates unable to circularize. DNA-PKcs and Artemis similarly process DNA hairpin structures during VDJ recombination (220), and repair a subset of complex DSBs (286). Despite these effects of DNA-PKcs and Artemis on rAAV vectors, transduction was not actually affected unless gene expression required vector circularization (64). The effects of DNA-PK on AAV vectors are less clear in cultured cells. Transduction from a self-complementary vector (see Chapter 1, Figure 10) was not altered in DNA-PKcs deficient human cells (64), while rAAV transduction was improved in

Ku80-deficient hamster cells (401). It is difficult to reconcile these results; however, variation in the assays, vectors, and systems utilized may explain the differences. The contribution of DNA-PK to rAAV transduction and WT AAV replication in human cells remains to be determined.

Previously, our lab found that Ad and AAV co-infection induced DNA damage signaling that was not seen with either virus alone (Figure 1A). Similar to an E4-deleted adenovirus infection, we saw autophosphorylation of ATM and phosphorylation of substrates RPA, 53BP1, and Chk2 (Figure 1A). This result was surprising since damage signaling would presumably stall the cellular replication machinery required for viral DNA production. In contrast to mutant adenovirus (Ad) infection that requires MRN for signaling (see Chapter 2), this response occurred despite MRN degradation by Ad. Rep had been previously reported to induce DNA damage signaling (21). However, in our hands, Rep expression did not trigger damage signaling on its own or in combination with Ad or rAAV (Figure 1B). We only observed a DNA damage response under conditions where AAV was replicating (Ad and WT AAV or Ad, Rep, and rAAV in Figure 1B, and data not shown; C.T. Carson, unpublished). The reason for this discrepancy is unclear, but it is possible that Rep induces a low level of signaling that is obscured in these experiments.

We also previously utilized deficient cell lines and small molecule inhibitors to determine which PIKK mediated AAV-induced damage signaling

Figure 1. AAV and Ad co-infection induces a DNA damage response that is Rep independent. (A) U2OS cells were infected with Ad5 (MOI of 50) and AAV (MOI=1000) for 30 hours. Lysates were analyzed by immuno-blotting for the indicated proteins. **(B)** Cells were either uninfected (Mock), infected with Ad5 (MOI of 50), rAAV-GFP (MOI=1000), or a combination of both viruses. At 6 hours post-infection cells were transfected with plasmids encoding GFP or Rep 78 and harvested 30 hours later. rAAV only replicates in the presence of both Rep and Ad. As a positive control, lysate from cells co-infected with Ad5 (MOI of 50) and AAV (MOI of 1000) (24 h infection) was included. Whole cell lysates were analyzed by immuno-blotting for the indicated proteins.

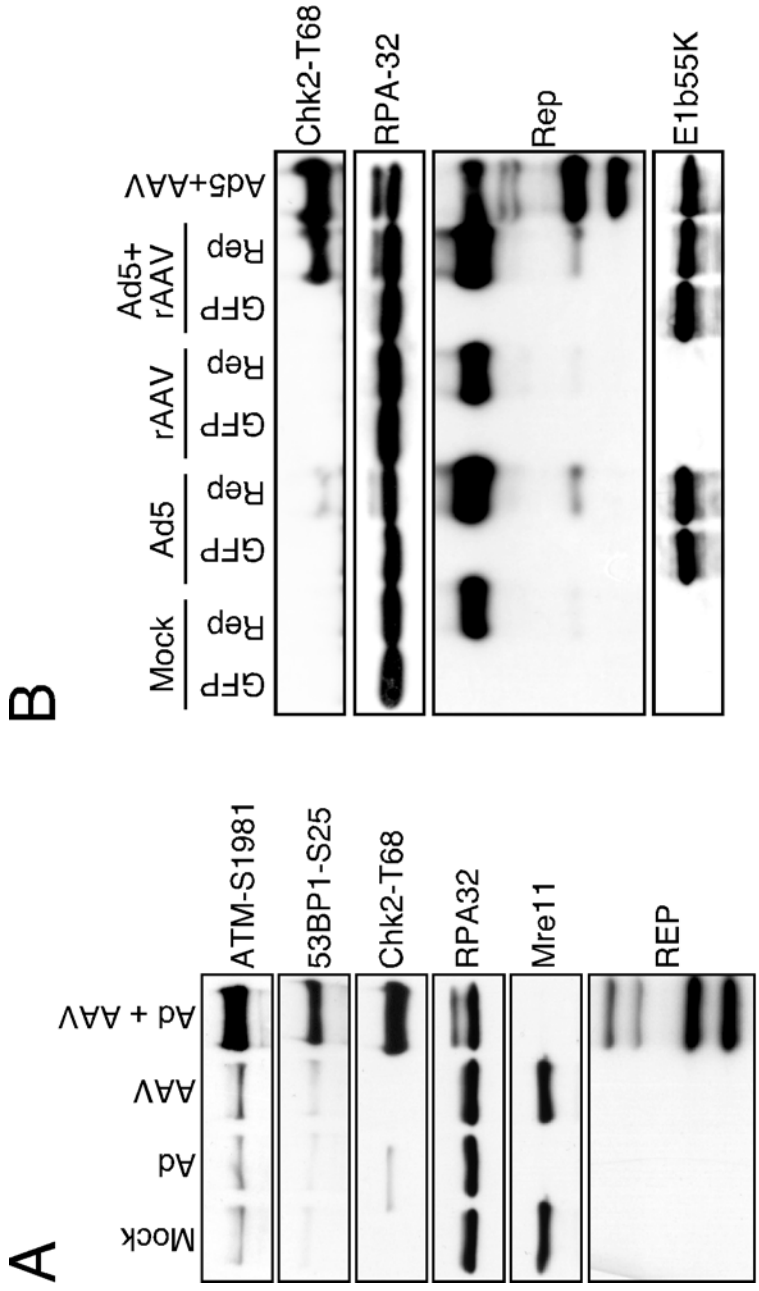
A
Mock
Ad
AAV
Ad + AAV
ATM-S1981
53BP1-S25
Chk2-T68
RPA32
Mre11
REP
B
Mock
GFP
Rep
Ad5
GFP
Rep
rAAV
GFP
Rep
Ad5+ rAAV
GFP
Rep
Ad5+AAV
Chk2-T68
RPA-32
Rep
E1b55K

(Figure 2A-2C). Interestingly, caffeine treatment of A-T cells during Ad/AAV co-infection did not prevent the phosphorylation of substrates (Figure 2A), suggesting that ATM and ATR were not responsible. However, infection of DNA-PKcs deficient cells (Figure 2B), or treatment of infected cells a small molecule inhibitor of DNA-PKcs (353) (Figure 2C) abrogated the DNA damage response. Together, these results indicated that AAV replication could induce robust DNA damage signaling by DNA-PKcs in the absence of MRN.

To better understand how DNA-PK affects the cellular response to AAV, we further characterized damage signaling induced by this PIKK. Using DNA-PKcs deficient cells to assay rAAV transduction and WT AAV replication, we found a requirement for the kinase, although this might be independent of its role in signaling. We also observed localization of DNA-PK components at AAV replication centers. Interestingly, accumulation of Ku70 and Ku86 at AAV centers may be regulated differently compared to DNA-PKcs. Together, our results suggest that DNA-PK impacts AAV and the damage response to AAV, but this kinase may be influenced by other factors.

Figure 2. DNA-PK may mediate DNA damage signaling induced by AAV and Ad co-infection. (A) A-T cells (GM05849) were uninfected (mock) or infected with Ad5 (MOI of 50), AAV (MOI of 1000) or both viruses for 30 hours. The Ad5/AAV co-infection was also performed in the presence and absence of 5mM caffeine. Lysates were analyzed for the indicated proteins by immuno-blotting. **(B)** Fus1 (+DNA-PK) or Fus9 (-DNA-PK) cells were uninfected (mock), infected with Ad5 (MOI of 50), AAV (MOI of 1000) or both viruses for 30 hours. Immuno-blotting was performed on whole cell lysates. **(C)** U2OS cells were uninfected (M) or infected with Ad5 (MOI of 50) and AAV (MOI of 1000) for 30 hours in the presence or absence of the DNA-PK inhibitor, NU7026 (DNA-PKi) according to Materials and Methods. Lysates were analyzed for the indicated proteins by immuno-blotting.

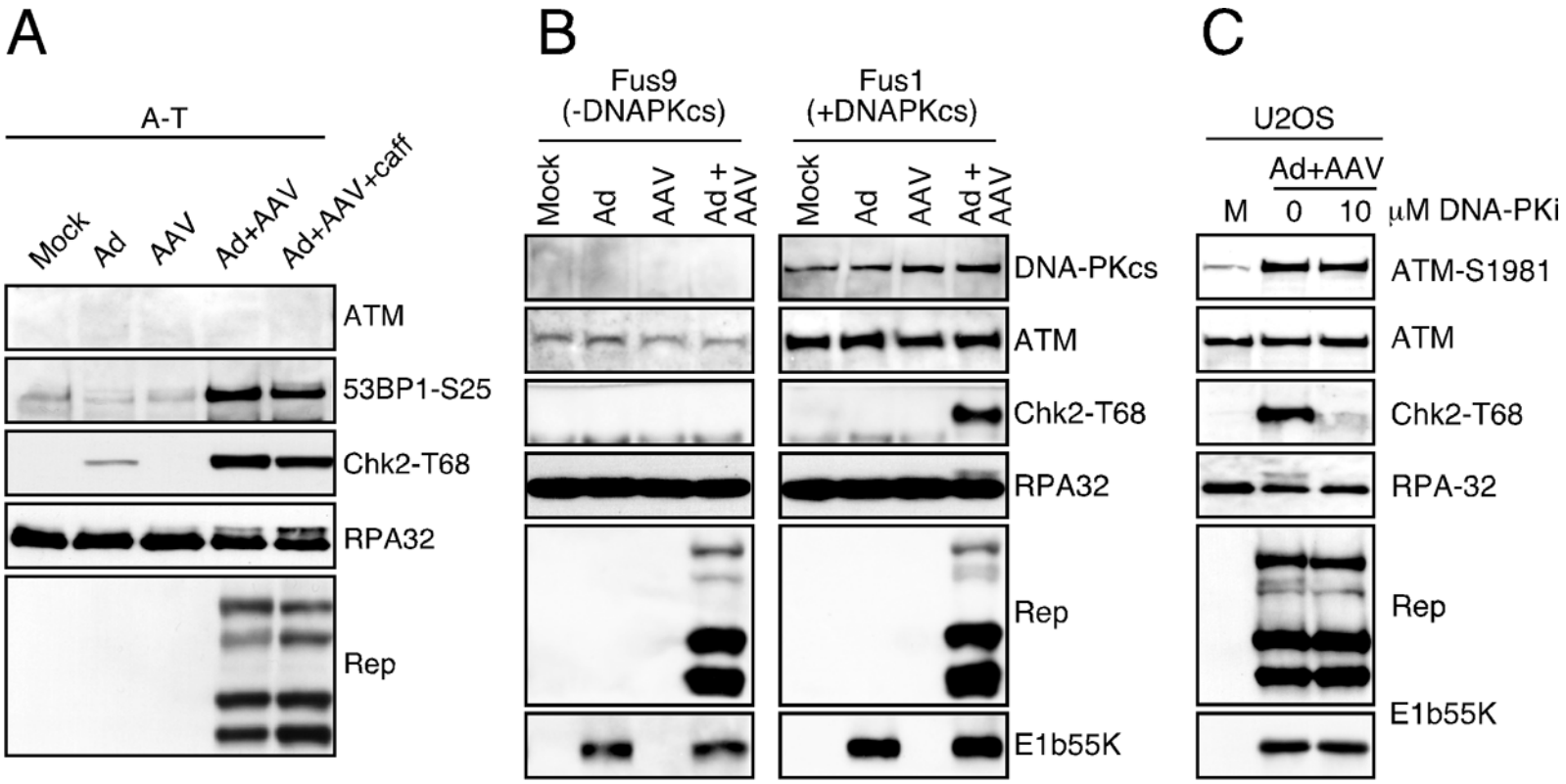
A
A-T
Mock
Ad
AAV
Ad+AAV
Ad+AAV+caff
ATM
53BP1-S25
Chk2-T68
RPA32
Rep
B
Fus9
(-DNAPKcs)
Fus1
(+DNAPKcs)
Mock
Ad
AAV
Ad + AAV
DNA-PKcs
ATM
Chk2-T68
RPA32
Rep
E1b55K
C
U2OS
Ad+AAV
M
0
10
μM DNA-PKi
ATM-S1981
ATM
Chk2-T68
RPA-32
Rep
E1b55K

Results

DNA-PK mediates phosphorylation of damage response proteins during AAV and Ad co-infection

Previous experiments with Ad/AAV co-infection demonstrated autophosphorylation of ATM (S1981), along with phosphorylation of 53BP1, Chk2, and RPA32 (indicated by a mobility shift) by western analysis (Figure 1A). We wanted to extend these observations by characterizing other cellular effectors activated during the AAV/Ad damage response. HeLa cells were infected with both viruses and lysates were examined by western analysis for damage signaling over time (Figure 3). Consistent with previous results, we found that ATM, Chk2, and RPA32 were all phosphorylated (Figure 3 and data not shown). We also noted the phosphorylation of specific a number of specific residues on Chk1, SMC1, and RPA32. Consistent with their phosphorylation, XRCC4 and Artemis also exhibited mobility shifts (230, 286, 402). Additionally, the larger Rep proteins, Rep68 and Rep78, appeared to be migrating as doublets in many experiments, suggesting their potential modification (Figures 1B, 2C, 3, and 4, arrowheads). These events correlated with MRN degradation and the greatest levels of Rep protein expression (24 hours). We did notice some effector phosphorylation at the latest time point in Ad infection (Figure 3A). This might be due to cytopathic effects, since these observations were largely absent from other experiments (Figures 1, 2, 3A, and data not shown)

Figure 3. Phosphorylation of DNA damage response proteins during Ad and AAV co-infection. HeLa cells were infected for the indicated times with AAV (MOI of 500), Ad (MOI of 15) or both viruses. Cells were harvested and lysates were subjected to Western analysis for the indicated proteins. Phosphorylation events and post-translational modifications are shown with phospho-specific antibodies or mobility shifts (arrowheads). M stands for mock-infected cells.

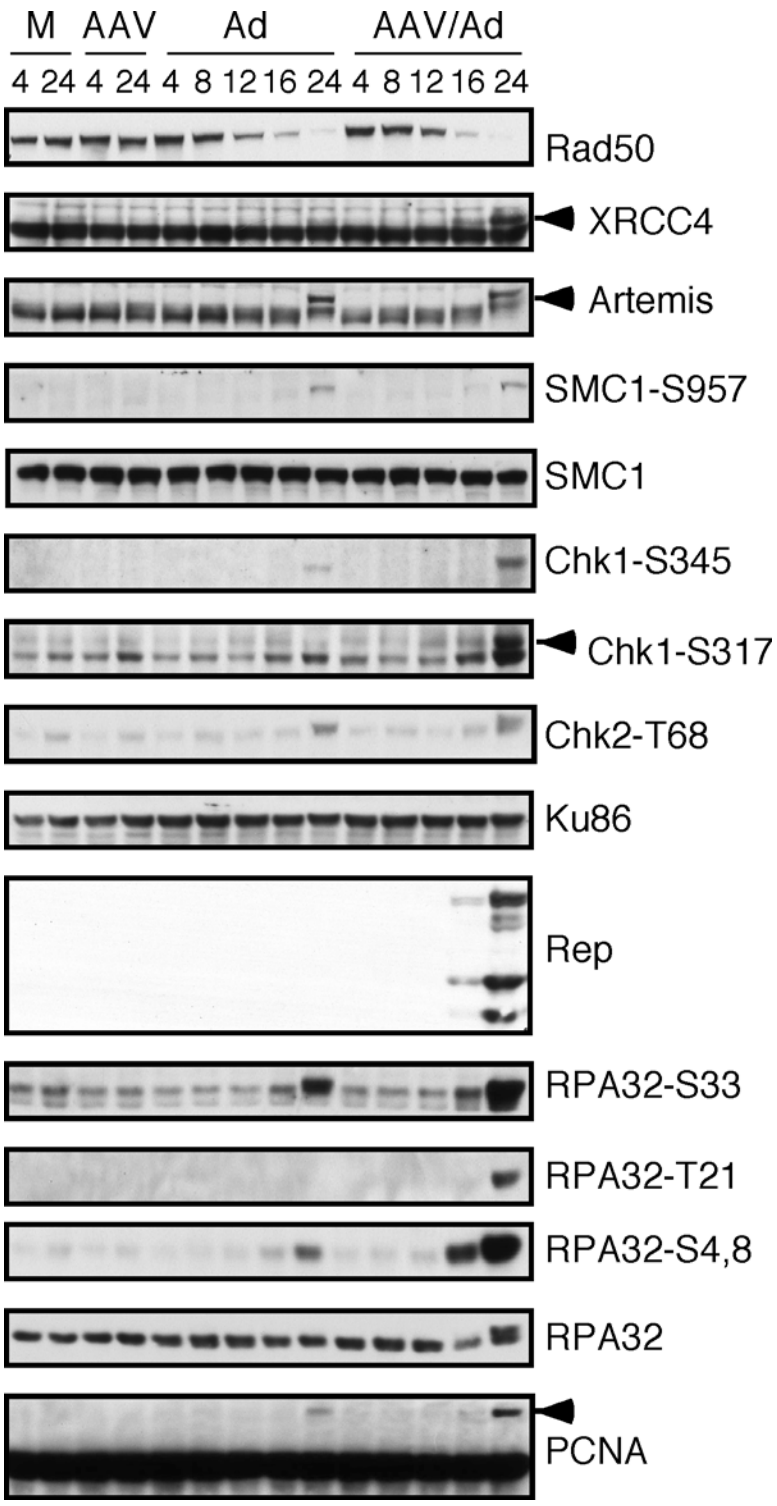
M
AAV
Ad
AAV/Ad
4 24 4 24 4 8 12 16 24 4 8 12 16 24
Rad50
XRCC4
Artemis
SMC1-S957
SMC1
Chk1-S345
Chk1-S317
Chk2-T68
Ku86
Rep
RPA32-S33
RPA32-T21
RPA32-S4,8
RPA32
PCNA

(see also Chapter 2). Most phosphorylation events were also stronger with co-infection than with Ad alone (Figures 1A, 2A, and 3A). Future time courses will be repeated under conditions that produce a better dose-dependent increase in Rep expression and lack Ad signaling.

We next wanted to determine which events were DNA-PKcs dependent, since previous work implicated this kinase in AAV/Ad signaling. To test this, we treated AAV and Ad co-infected cells with inhibitors against DNA-PK (174, 353) (Figure 4A), or infected DNA-PKcs deficient cells (156) (Figure 4B), and analyzed signaling by western. In both experiments, we found some events required DNA-PKcs activity while others did not. Chk1, SMC1, and RPA32 S33 phosphorylation were unaffected when DNA-PKcs was inhibited, suggesting that other kinases may compensate. ATM autophosphorylation was also not altered in these experiments (Figure 2C and data not shown), supporting the independent regulation of this kinase. DNA-PKcs did appear to induce phosphorylation of RPA S4,8, RPA T21, and XRCC4, and shift the mobility of the large Rep proteins (see arrowheads in Figure 4A and 4B), since these events were absent in the deficient cells and cells treated with DNA-PKcs inhibitors. Because phosphorylated Chk2 exhibited altered mobility in some experiments (Figure 3A and Figure 4B), we could not determine whether DNA-PKcs regulated this protein, although previous data suggested it did (Figure 2). Artemis and 53BP1 were not included in these studies due to

Figure 4. Some phosphorylation events during AAV and Ad co-infection are mediated by DNA-PK. (A) HeLa cells were infected with AAV (MOI of 1000), Ad (MOI of 25), or both viruses for approximately 24 hours. DNA-PK inhibitors or DMSO were used at the indicated concentrations according to Materials and Methods. Lysates were analyzed for the indicated proteins. Arrowheads denote mobility shifts due to post-translational modifications. **(B)** Fus1 (+DNA-PK) or Fus9 (-DNA-PK) cells were infected with AAV (MOI of 1000) or AAV and Ad (MOI of 50) for approximately 24 hours before preparing lysates for western analysis. Arrowheads are the same as in (A).

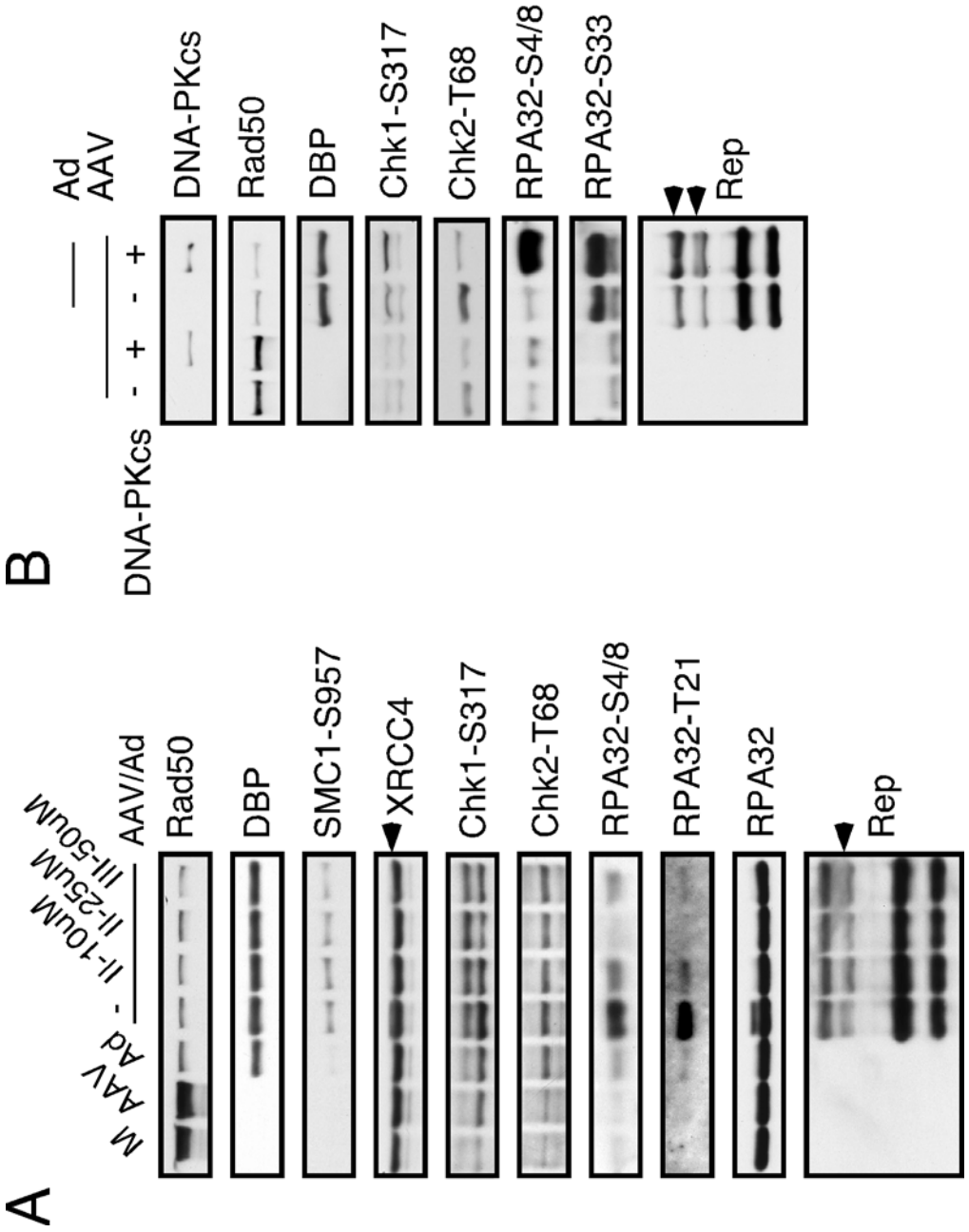
A
M
AAV
Ad
-
II-10uM
II-25uM
III-50uM
AAV/Ad
Rad50
DBP
SMC1-S957
XRCC4
Chk1-S317
Chk2-T68
RPA32-S4/8
RPA32-T21
RPA32
Rep
B
DNA-PKcs
- + - +
Ad
AAV
DNA-PKcs
Rad50
DBP
Chk1-S317
Chk2-T68
RPA32-S4/8
RPA32-S33
Rep

limiting amounts of these antibodies, but will be analyzed in future work. These results indicate that DNA-PKcs mediates many but not all signaling events during the response to AAV and Ad co-infection, including the modification of the viral Rep proteins. Future experiments with phosphatase treatment should validate whether the modification of Rep is indeed phosphorylation.

PCNA is modified during AAV and Ad co-infection

The DNA replication processivity factor, PCNA, is required for AAV replication (247, 255). We also found that PCNA accumulates at AAV replication compartments (Figure 5A and T.H. Stracker, unpublished) when we examined viral centers by immunofluorescence using the infectious AAV plasmid, pNTC244, and minimal adenoviral helper proteins (336) (see Chapter 5 for details). During western analysis of AAV/Ad co-infection, we found that a small amount of PCNA exhibited a mobility shift in darker film exposures (Figure 3A). PCNA can be ubiquitinated in mammalian cells under certain DNA damaging conditions to promote bypass of lesions at replication forks (82, 237), so the shift could reflect this PCNA species. We examined PCNA mobility in the HeLa cell lines used in Chapter 5, Figure 7B, which express mutant E1b55K proteins. These cells were infected with AAV and a mutant Ad, *dl*1016, which cannot degrade MRN. We observed that more PCNA shifted with increased AAV replication and MRN degradation (WT and R240A cells plus *dl*1016) (Figure 5B). Although some PCNA was modified during the Ad

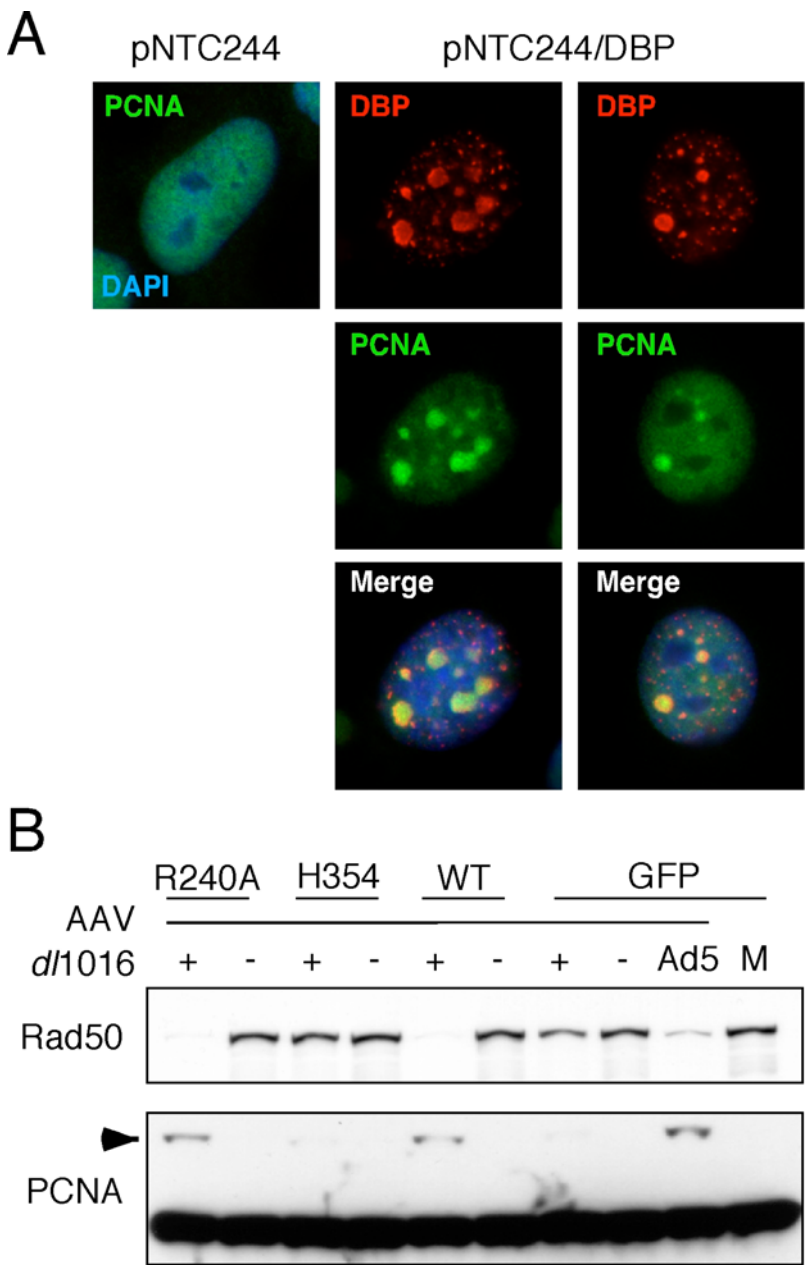

Figure 5. PCNA is modified during AAV and Ad co-infection. (A) HeLa cells were transfected with pNTC244 alone or with a plasmid expressing Ad5 DBP. 24-36 hours after transfection, cells were fixed and processed for immunofluorescence for DBP and PCNA. Nuclei are marked by DAPI stain. **(B)** WT or mutant E1b55K expressing HeLa cells were infected with AAV (MOI of 1000) with or without Ad mutant *dl*1016 (ΔE1b55K/ΔE4orf3) or Ad5 (both MOI of 50) for 24 hours before harvesting for immunoblot analysis for Rad50 and PCNA. Lysates are from the same experiment in Chapter 5, Figure 7B and Rad50 is the same blot used in that figure.

infection in Figure 3A, we did not observe this in most experiments, suggesting that degradation of MRN is not sufficient. Additionally, even though *dl*1016 induces damage signaling (see Chapter 2), we saw little PCNA modification in the H354 and GFP cell lines (Figure 5B). Therefore, the effect on PCNA appears to correlate with increased AAV replication. Future experiments will have to determine whether this modification reflects ubiquitin or another ubiquitin-like protein, and whether modified PCNA associates with AAV DNA or is a byproduct of AAV/Ad induced damage signaling.

DNA-PK is required for rAAV transduction and WT AAV replication

Since DNA-PK regulates part of the response to AAV, we wanted to determine how it affected rAAV transduction and AAV replication. To do this, we assayed these viral processes in DNA-PKcs deficient cells and compared them to cells expressing the WT protein (156) (Figure 6A and 6B). Interestingly, we found that transduction and replication were more efficient in the presence of DNA-PKcs. This result contrasts the negative impact of another PIKK, ATM, on rAAV transduction (298, 401). We also noted that DNA-PKcs was required for AAV replication regardless of the MRN complex (Ad versus E4−deleted mutant, *dl*1004), although replication was better in the absence of MRN, consistent with the findings in Chapter 5. Our previous data showed that DNA-PKcs mediated signaling may not be required for AAV replication, since the small molecule inhibitor used in Figures 2 and 4 had no

Figure 6. DNA-PK is required for rAAV transduction and AAV replication. **(A)** Fus 1 (+DNA-PK) or Fus 9 (-DNA-PK) cells were infected with rAAV.LacZ at the indicated MOIs for 48 hours before harvesting. Lysates were prepared and analyzed for β-galactosidase activity. Error bars represent the SEM from triplicate samples. **(B)** Fus 1 (+DNA-PK) or Fus 9 (-DNA-PK) cells were infected with AAV (MOI of 1000) plus Ad5 (MOI of 50) or *dl*1004 (MOI of 50) for 24 hours before preparing viral DNA for QPCR and southern analysis with a Rep probe. Below the southern are the fold differences in replication between treatments. Rfm-replication form monomer, Rfd-replication form dimer, and ssDNA-single-stranded DNA.

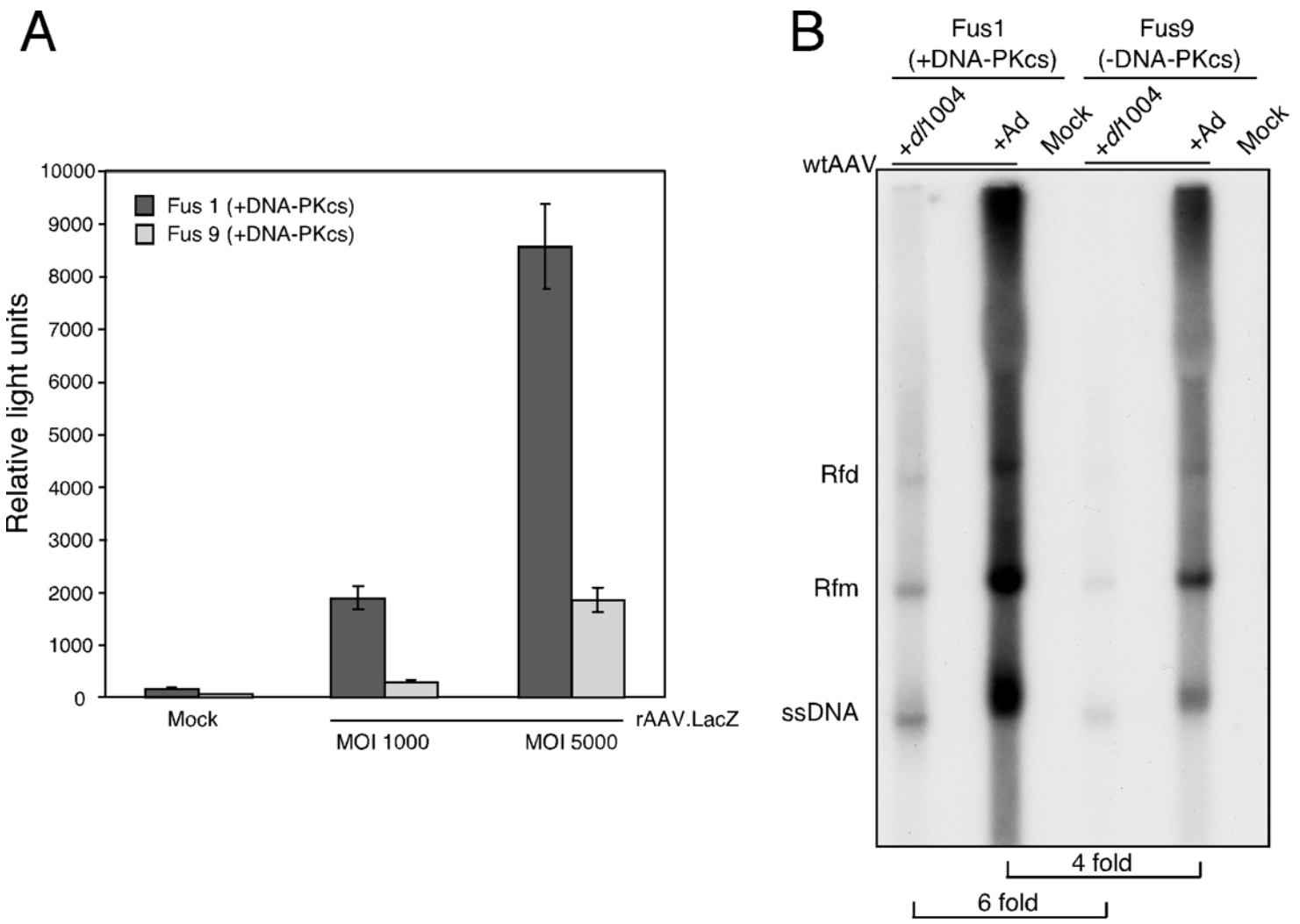
A
Relative light units
10000
9000
8000
7000
6000
5000
4000
3000
2000
1000
0
Fus 1 (+DNA-PKcs)
Fus 9 (+DNA-PKcs)
Mock
MOI 1000
MOI 5000
rAAV.LacZ
B
Fus1
(+DNA-PKcs)
Fus9
(-DNA-PKcs)
+dl1004
+Ad
Mock
+dl1004
+Ad
Mock
wtAAV
Rfd
Rfm
ssDNA
4 fold
6 fold

effect (C.T. Carson, unpublished). Therefore, these data suggest that DNA-PK may promote AAV transduction and replication through a non-signaling mechanism. Further transduction and replication studies using siRNA against individual DNA-PK components should help validate these studies.

DNA-PK localizes to AAV replication centers

Given the effects of DNA-PK on the assays above, we wanted to determine where components of the holoenzyme localized during AAV replication. During AAV and Ad co-infection, viral DNA and proteins localize to the same compartments (366). Because of this, we first examined whether DNA-PK components localized to WT Ad or E4-deleted mutant Ad (*dl*1004) centers like other DNA damage response proteins (see Chapter 2) (50, 335). In mock treated cells, DNA-PKcs, Ku70, and Ku86 exhibited a diffuse nuclear localization (Figures 7 and 8). Interestingly, neither Ad nor *dl*1004 infection changed this pattern. This was unexpected for *dl*1004 infection since many DNA damage response proteins accumulate at viral centers (Chapter 2) (50), and because DNA-PK is implicated in viral genome concatemerization (30, 335). This result might imply that DNA-PK components only transiently associate with adenoviral replication compartments. However to verify our observations, these immunofluorescence experiments should be repeated under conditions where diffuse nucleoplasmic proteins are extracted prior to fixation.

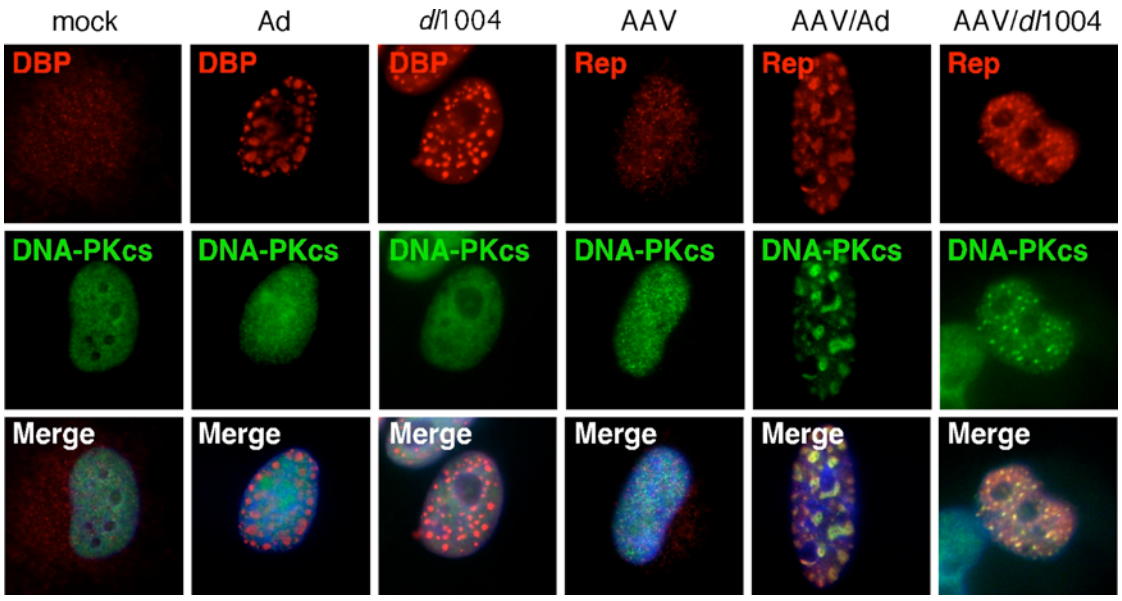

Figure 7. DNA-PKcs localizes to AAV replication centers. (A) HeLa cells were infected with Ad5 (MOI of 25), *dl*1004 (MOI of 50), AAV (MOI of 1000), or a combination of these as indicated. 24 hours after infection cells were fixed and processed for immunofluorescence for DBP, Rep, and DNA-PKcs. Nuclei are stained with DAPI.

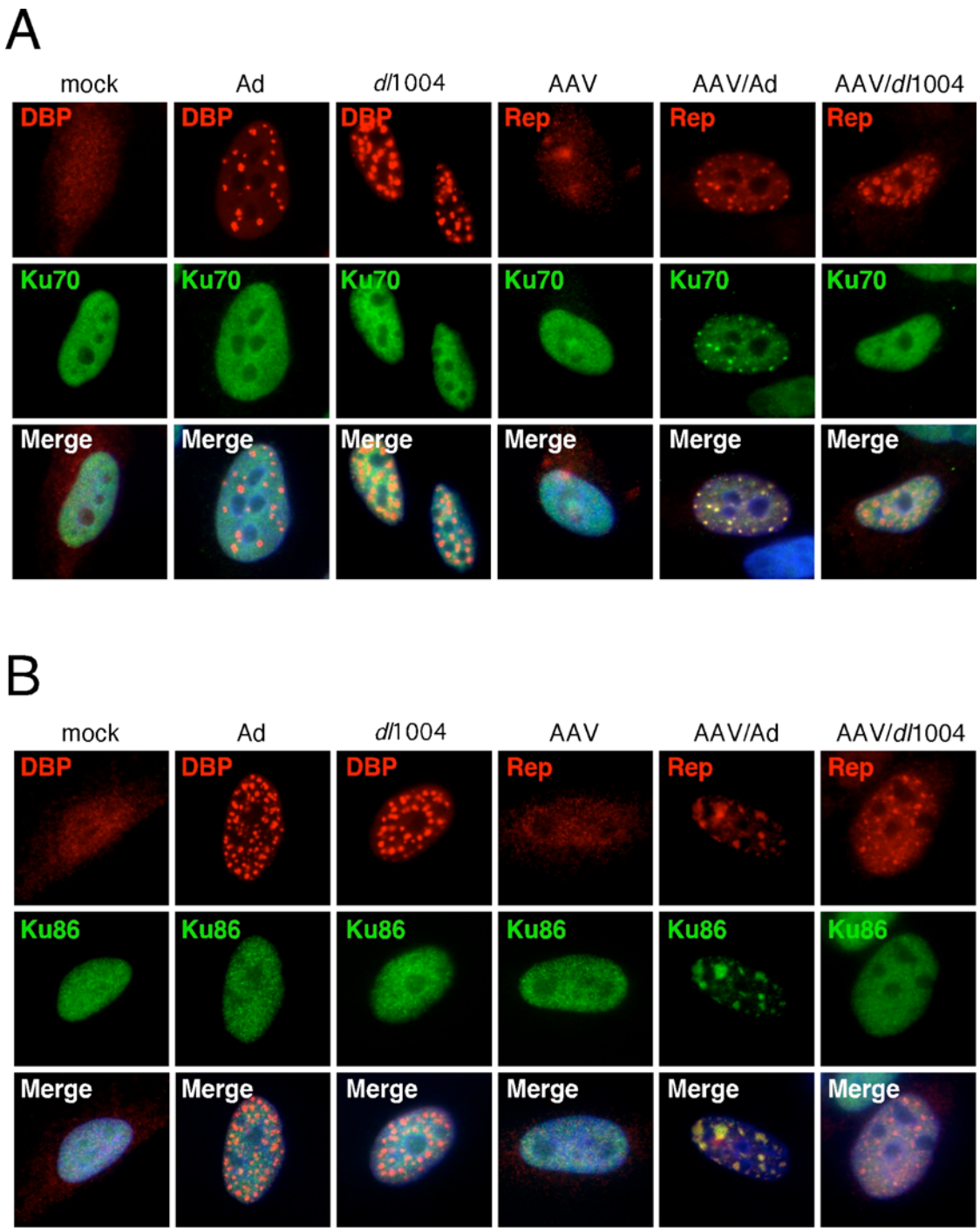

Figure 8. Ku70 and Ku86 both localize differentially to AAV replication centers. Ku70 and Ku86 only localize to sites of AAV replication in the presence of Ad. HeLa cells were infected as in Figure 7 and stained for DBP, Rep and either Ku70 **(A)** or Ku86 **(B).** Nuclei are marked with DAPI.

We then examined whether DNA-PK components localized to AAV replication centers during Ad or *dl*1004 co-infection (Figures 7 and 8). In cells co-infected with Ad, we found that DNA-PKcs, Ku70, and Ku86 were concentrated at Rep-positive compartments, suggesting a role for these proteins in AAV replication. The distribution of these cellular factors, however, changed during AAV and *dl*1004 co-infection. We observed that DNA-PKcs could still co-localize with AAV centers, but Ku70 and Ku86 remained diffusely nuclear (Figures 7 and 8). To avoid potential artifacts induced by Ad and AAV co-infection, we examined DNA-PK component localization under minimal AAV replication conditions using an AAV plasmid and individual adenoviral proteins (336) (see also Chapter 5). WT E1b55K or H354 expressing cells were transfected with plasmids containing the AAV genome (pNTC244) and helper proteins DBP and E4orf6 (Figure 9). The appearance of the AAV centers differed between the two conditions, with H354 cells exhibiting fewer and more round viral compartments (Figure 9). This may be consistent with MRN limiting or altering AAV replication in these cells (see Chapter 5). We found DNA-PKcs staining at AAV replication compartments in both cell lines. However, Ku86 and Ku70 were only concentrated at viral centers in the WT E1b55K cell line (Figure 9 and data not shown), where MRN is degraded. These patterns mirrored the co-infection data in Figures 7 and 8. These results indicate that the two different minimal helper conditions produce qualitatively

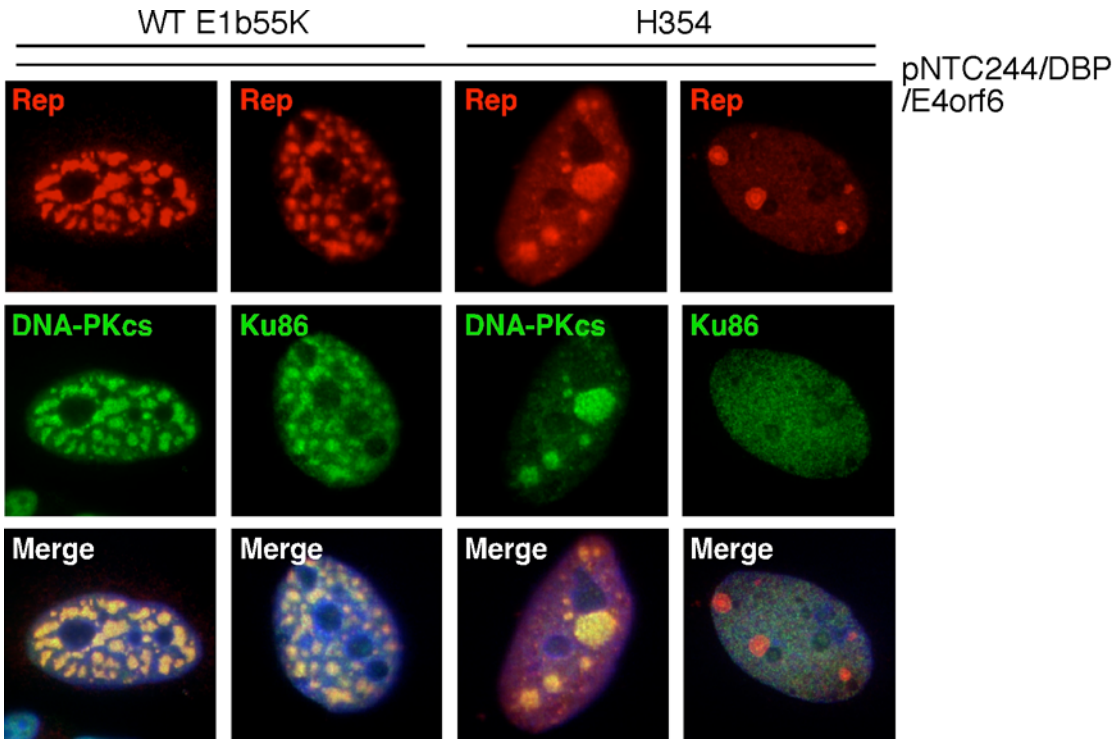

Figure 9. DNA-PK components localize differentially to AAV replication centers under minimal helper conditions. HeLa WT E1b55K or H354 expressing cells were transfected with pNTC244 and plasmids encoding DBP and E4orf6. 24-36 hours after transfection, cells were fixed and processed for immunofluorescence for Rep and DNA-PKcs or Ku86. Nuclei are marked by DAPI stain. Ku86 only localizes to replication centers in the WT E1b55K expressing cells.

distinct AAV replication centers. It is currently unclear what influences these phenotypes. However, since MRN is not degraded in either the *dl*1004 or H354 conditions, it is a prime candidate.

AAV replication induces pan phosphorylation of H2AX

After DNA damage, phosphorylation of the histone variant H2AX (called γH2AX after modification), is observed at DNA DSBs. This modification represents an early marker for damage (290), and is reported to spread up to two megabases either side of a break (289) to amplify the damage signal and provide a scaffold for other repair proteins (53). Depending on the conditions, phosphorylation of H2AX can be mediated by ATM, ATR or DNA-PKcs (116, 119, 332). We previously observed that γH2AX accumulated around mutant Ad replication centers (Figure 10B, see also Chapter 2) (50), where damage signaling is present. Given the robust DNA damage response occurring during AAV replication, we wanted to determine how γH2AX was affected. To avoid artifacts from co-infection of Ad and AAV, we examined γH2AX staining by immunofluorescence with the minimal replication system described above (Figure 10A). Two interesting patterns emerged from these experiments. In all WT E1b55k expressing cells replicating AAV, γH2AX appeared to be pan-activated throughout the cell, regardless of the stage of replication center (Figure 10A). This phenotype was only apparent in H354 expressing cells harboring late AAV centers. H354 cells with early replication compartments

Figure 10. H2AX is phosphorylated during AAV replication. (A) HeLa WT E1b55K or H354 expressing cells were transfected with pNTC244 and plasmids encoding DBP and E4orf6. 24-36 hours after transfection, cells were fixed and processed for immunofluorescence for Rep and γ-H2AX (gH2AX). Arrowheads indicate AAV centers with increased surrounding γH2AX staining. Nuclei are marked by DAPI stain. **(B)** HeLa cells were infected with Ad mutant *dl*1004 (MOI of 50) for 20 hours before fixing and processing for immunoflorescence for DBP and γH2AX. Nuclei are stained with DAPI. **(C)** Approximately 50 HeLa cells in (A) were quantified for γH2AX staining profiles depicted in (A). There was no difference noted between early and late centers in WT E1b55K expressing cells.

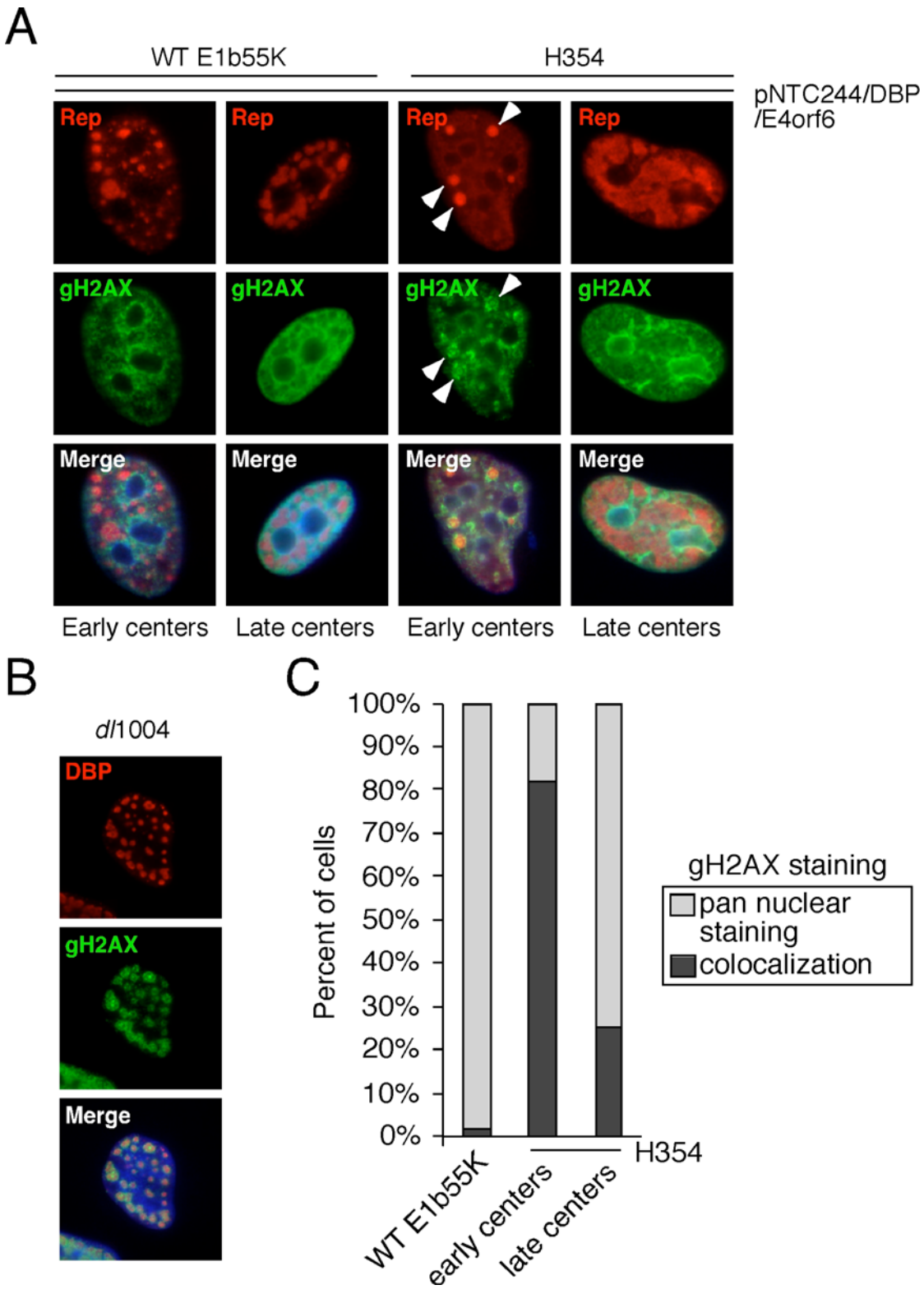
A
WT E1b55K
H354
pNTC244/DBP
/E4orf6
Rep
gH2AX
Merge
Early centers
Late centers
Early centers
Late centers
B
dl1004
DBP
gH2AX
Merge
C
100%
90%
80%
70%
60%
50%
40%
30%
20%
10%
0%
Percent of cells
gH2AX staining
pan nuclear staining
colocalization
H354
WT E1b55K
early centers
late centers

showed pan-activation, but also increased γH2AX staining around the centers (Figure 10A, arrowheads). Quantitation of these phenotypes is shown in Figure 8C. Similar to the results in Figure 9, these observations suggest that the two conditions produce qualitatively different AAV centers. Additionally, these data show that AAV replication affects γH2AX in a distinct manner compared to mutant Ad infection (Figure 10A versus 10B). We do not know whether our results reflect perturbation of cellular chromatin or incorporation of H2AX into "viral chromatin." Determining this and identifying the kinases inducing H2AX phosphorylation will be investigated in the future.

Discussion

Our previous data demonstrated that AAV replication induced a strong DNA damage response. Interestingly, the Mre11 complex was not required for this, since it was degraded by Ad during co-infection with AAV, or by E1b55K/E4orf6 during minimal helper conditions (data not shown; C.T. Carson, unpublished). This observation contrasts the situation where MRN is required for ATM and ATR signaling in response to mutant Ad infection (50) and DNA DSBs (3, 164, 197, 242, 351). A previous study (21) reported that Rep expression alone elicits a damage response, although we did not observe this. The cause for this discrepancy is unclear, but Rep may stimulate a low level of signaling that is obscured in our experiments by the robust AAV/Ad

induced damage response. The results shown in this Chapter indicate that DNA-PKcs may mediate many of these signaling events. This surprising observation has not been seen with the genotoxic agents routinely used to study DNA damage. The exception to this is H2AX, which is phosphorylated by DNA-PKcs only when MRN or ATM is absent (116, 332). While DNA-PKcs contributes to many of the observed signaling events, it may not induce the phosphorylation of Chk1, Chk2 and SMC1. Further characterization of this damage response and identification of responsible kinases will be essential to understanding how the signaling is regulated. Additionally, since DNA-PKcs can autophosphorylate itself and this may regulate its DNA binding, processing, and repair activities (58, 59, 77), it will be important to examine its status in the future.

In analyzing the AAV-induced DNA damage response, we noticed altered migration of the large Rep proteins. Our results are consistent with other reports showing that all Rep proteins are phosphorylated during Ad and AAV co-infection (70, 145, 246). Although the kinases involved and the sites they modify on Rep are largely unknown, Rep phosphorylation has been correlated with decreased DNA binding (145, 246) and AAV replication (246). Our data suggest that DNA-PKcs may at least mediate modification of the large Rep proteins. This result draws an interesting parallel to the SV40 large tumor antigen (LTAg) (see Chapter 7 for further discussion). LTAg has similar

functions to Rep78/68 during SV40 replication and is phosphorylated by ATM during infection (317). PIKKs prefer to phosphorylate SQ or TQ motifs (178). The large Rep proteins share five of these sites, while Rep78 contains one additional C-terminal motif. By mutating these sites, we can determine how DNA-PKcs modifies Rep, and how this affects Rep DNA binding, helicase, and nicking functions. The Rep proteins associate with a number of cellular factors, including PKR and PrKX (63, 87). Therefore, kinases may differentially modify Rep during lytic and latent infection, and this could dictate whether AAV replicates or integrates. Further analysis of Rep 52 and 40 will be required to determine if these proteins are phosphorylated in a DNA-PKcs dependent manner.

During the course of our experiments, we discovered certain damage-induced modifications of replication proteins. These included phosphorylation of many sites on RPA and a mobility shift of PCNA, which is consistent with ubiquitination (82, 171). Phosphorylation of RPA is associated with activation of PIKKs, S-phase checkpoints, replication fork damage, and recombination (118, 413). RPA phosphorylation excludes it from cellular sites of replication (125, 352), and may alter its affinity for certain lengths of DNA to promote repair (118). PCNA can be mono- or poly-ubiquitinated to signal error-prone or error-free damage bypass at replication forks, respectively (237). It is intriguing that AAV replication requires these proteins (247, 255), and damage signaling

does not hinder AAV replication. In fact, phosphorylated RPA localizes to AAV centers (C.T Carson, unpublished). Rep can bind RPA (336), providing another potential mechanism to retain RPA at viral replication centers, although we do not know if modified forms of Rep interact with phosphorylated RPA. Based on this knowledge, it is tempting to speculate that AAV somehow benefits from damage-induced modifications of replication proteins. In support of this, DNA damaging agents can promote limited AAV transduction and replication (5, 295, 388), perhaps by activating certain effectors. AAV ITRs have single-strand/double-strand DNA junctions that may look like stalled replication forks, perhaps requiring the altered activity of DNA replication proteins. Since MRN is inhibitory to early steps of AAV replication (see Chapter 5) (308), the complex may negatively modulate these replication factors. This would be consistent with the presence of MRN at cellular replication forks (226, 236), and the requirement of MRN for the intra-S phase checkpoint (117). We currently do not know how PCNA is ubiquitinated or whether this form localizes to AAV centers. We also do not know if other cellular proteins required for AAV replication are modified; MCMs and RFC2/4 are phosphorylated (73, 163, 316, 393) and ubiquitinated (348), respectively, during DNA damage. It will be important to determine how AAV-induced signaling impacts these replication factors and whether DNA-PKcs is required.

Likewise, we also need to examine how these modifications affect AAV replication.

Our preliminary data suggested that DNA-PKcs was involved in the response to replicating AAV. However, inhibition of kinase activity with a small chemical inhibitor did not affect viral replication (C.T. Carson, unpublished). To further examine the relationship between DNA-PKcs and AAV, we assayed viral replication and transduction in deficient cells. Interestingly, DNA-PKcs appeared to be required for both viral processes, unlike ATM (298, 401). Therefore, DNA-PKcs may affect AAV in a manner independent of its signaling role, although we cannot completely rule out a contribution of other kinases in the DNA-PKcs inhibitor experiment. In vivo studies have implicated DNA-PKcs in rAAV vector processing in certain tissues (64, 103, 161, 298, 325). However, DNA-PKcs did not affect transduction unless gene expression required vector circularization (64). Therefore, the impact of DNA-PKcs may also partially depend on cellular context. Further studies will be required to determine the contribution of DNA-PKcs, Ku86, and Ku70 to AAV transduction and replication.

The involvement of DNA-PK in WT AAV replication was further supported by the dramatic relocalization of its components to viral centers. Surprisingly, despite the involvement of DNA-PKcs in mutant adenoviral genome concatemerization (30, 335), we did not observe its accumulation at

WT or mutant Ad centers. Although pre-extraction before fixation and immunofluorescence should be performed to verify these results, this suggests that distinct elements in AAV centers recruit DNA-PK. The AAV ITRs are prime candidates since DNA-PK is known to recognize and process hairpins with Artemis during VDJ recombination (220). We currently do not know whether Artemis affects WT AAV replication, although it was recently implicated in processing and cleaving rAAV ITRs in vivo (161).

The role of DNA-PK in the AAV lifecycle is likely to be influenced by other repair proteins. We observed that Ku70/Ku86 were absent from AAV centers under certain conditions, despite the presence of DNA-PKcs. This result was surprising since the Ku heterodimer is first required to bind DNA and recruit DNA-PKcs (42, 116). The results above were seen under helper conditions where MRN was present. γH2AX staining was also altered in these experiments. Interestingly, DNA-PK mediated signaling occurs under conditions where MRN is absent, and phosphorylation of H2AX after damage only occurs when MRN or ATM is absent (116, 332). Since MRN negatively affects AAV replication (Chapter 5) (57, 308), it seems likely that MRN influences signaling or recruitment of cellular proteins to AAV centers. MRN, ATM, Artemis, and DNA-PKcs have been implicated in a common pathway to repair a subset of complex DNA lesions (286). Perhaps MRN and ATM dictate the outcome of Artemis and DNA-PK repair activities, and this negatively

affects AAV. Building on these observations, we can begin to examine how MRN influences the accumulation of DNA-PK and other damage proteins (Appendix Figure 4) to AAV centers, and signaling in response to AAV replication.

In this Chapter we extended our understanding of how the DNA damage response is impacted by AAV replication. We made a number of intriguing observations that clearly warrant further investigation. Although these studies are preliminary, they suggest that AAV replication is an excellent model system to understand not only functions of DNA-PK, but also how cellular replication proteins are impacted by the DNA damage response.

Materials and Methods

Cell lines and drug treatments

U2OS cells, HeLa cells and HeLa E1b55K cell lines were described in Chapter 2. MO59J fusion cells, Fus 1 and Fus 9, were previously described (156) and provided by T. Melendy. Fus cells were maintained in a mixture of 1:1 DMEM:F10 media supplemented with 10% FBS. DNA-PK inhibitors II (NU7026) and III (IC86621) were purchased from Calbiochem and previously described (174, 353). For experiments using DNA-PK inhibitors, cells were pre-treated with inhibitors or DMSO for four hours pre-infection. Inhibitors or DMSO were kept in the media throughout the infection.

Plasmids and transfections

Described in Chapter 2, 3, and 5.

Viruses and Infections

All viruses and infections are described in Chapters 2, 3, and 5.

Antibodies, Immunofluorescence, and Immunoblotting

Immunofluorescence and immunoblotting procedures described in Chapters 2, 3, and 5. The Rep mouse monoclonal was a gift from J. Samulski. The 53BP1 antibody was a gift from T. Halazonetes. Commercially available antibodies were purchased from: Upstate (ATRIP), Santa Cruz (Rad17, Ku80), Neomarkers (DNA-PK, Ku70), Serotech (XRCC4), Cytostore (RPA-T21), Abcam (SMC1), Rockland (SMC1-S957), and Bethyl (RPA-S4,8, RPA-S33, Chk1-S317). All other antibodies used were described in Chapters 2, 3, and 5.

HIRT extractions, Southern blotting, QPCR, and reporter assays

Described in Chapter 5.

Acknowledgements

I am grateful to extremely grateful to Christine Schuberth who performed many of the experiments in this Chapter. I am also grateful to Christian Carson who generated the preliminary results in Figures 1 and 2, providing the backbone for this Chapter. I also want to thank J. Trempe and J. Samulski for the Rep antibodies, T. Halazonetes for the 53BP1 antibody and

T. Melendy for the Fus cells and RPA antibody. I am also grateful to Darwin Lee and Daniel Linfesty for propagation of all viruses.

Chapter 7. Discussion

The work in this dissertation utilized two different types of DNA viruses, adenovirus (Ad) and adeno-associated virus (AAV), to study cellular DNA repair and protein degradation pathways. Specifically, we focused on understanding how the adenoviral E1b55K and E4orf6 proteins impact the Ad and AAV lifecycles, and the cellular DNA damage response. These proteins form a complex (302) that promotes the degradation of cellular substrates p53 (52, 146, 238, 251, 281, 282, 292, 329), MRN (335), and DNA Ligase IV (8). These viral proteins were also shown to assemble a ubiquitin ligase with Cullin 5, Rbx1, and Elongins B and C (146, 281). Additionally, E1b55K and E4orf6 were known to facilitate AAV replication and transduction (120, 121). At the onset of these studies, we did not know whether degradation of the different targets proceeded via the same mechanism. It was also unclear how substrate down-regulation affected cellular responses and contributed to the functions of E1b55K/E4orf6. In addressing these questions, we made a number of interesting observations, which are summarized below.

Requirements for substrate degradation by E1b55K/E4orf6

Through our studies, we found that E1b55K/E4orf6 degrade substrates independently, and this occurred at three different levels. Using cell lines deficient in cellular factors, we showed that down-regulation of targets by Ad did not require the presence of each other, or other factors like DNA-PKcs,

ATM, or ATR (Chapter 2 and 3). Interestingly, degradation of MRN by the SV40 Large T Antigen (LTAg) requires ATM kinase activity (406). Perhaps ATM phosphorylation of Nbs1 is necessary for LTAg interaction with Nbs1 (379). Our studies indicate that Mre11 may be the degradation target within the MRN complex (Chapter 3). Therefore, Ad probably has different requirements for MRN association compared to SV40. However, many substrates require prior phosphorylation or SUMOylation before their ubiquitination (160), so it will be interesting to determine if such events are needed for destabilization of targets by Ad.

E1b55K has been shown by us and others to mediate substrate selection, since it can bind p53 (52, 173, 206, 312, 389, 391), MRN (50), and DNA Ligase IV (8) without E4orf6 (see Chapter 3). Because of this, we examined whether E1b55K mutants could separate degradation of targets, and identified a number of mutants with distinct substrate binding capabilities (see Chapters 2 and 3). Additionally, we isolated mutants that retained association with p53, but lost the ability to destabilize it. These data indicate that E1b55K has different requirements for the interaction with and degradation of p53, MRN, and DNA Ligase IV (Chapter 3). Similarly, the KSHV protein, LANA, which also recruits a Cullin-RING ubiquitin ligase (CRL), has distinct domains to bind p53 and VHL and targets them for proteasome-mediated degradation (46). Viral ubiquitin ligases may induce the degradation

of multiple substrates, so the utilization of distinct domains for binding targets is likely to be a common theme.

Finally, we observed that distinct cellular ubiquitin ligase factors facilitated down-regulation of MRN and p53. E4orf6 recruits a complex of Cullin 5, Rbx1, and Elongins B and C (146, 281). While Cullin 5 is required for degradation of all substrates (8, 218, 378) (Chapter 4), we found that Rbx1 mediated p53 degradation and Rbx2 mediated MRN degradation (Chapter 4). Although we do not currently understand what dictates this choice, our observation may reflect a unique viral mechanism to commandeer the cellular degradation machinery. Indeed, a number of other viral proteins have adapted strategies to recruit CRL factors. Vif also associates with Cullin 5 and Rbx1 (397), despite the preferred association of Cullin 2 with Rbx1 and Cullin 5 with Rbx2 (170). RSV mediated degradation of STAT2 in certain cells types requires both Rbx1 and Rbx2 (107). The chicken adenoviral protein, GAM-1, associates with both Cullin 5 and Cullin 2 to degrade SUMO ligase factors Sae1/Sae2 (26), whereas the HIV-1 Vpr protein can interact with both Cullin 1 and Cullin 4 (307). Alternatively, these viral recruitment strategies may simply reflect cellular associations that have not yet been uncovered. Studying the mechanisms behind virus-induced substrate degradation should yield additional insights into the regulation and assembly of CRLs.

Viral and cellular consequences of E1b55K/E4orf6 mediated substrate degradation

In order to analyze how substrate degradation contributed to E1b55K/E4orf6 functions, we utilized E1b55K mutants with separate abilities to bind and destabilize targets. With these tools, we demonstrated that MRN is critical to ATM activation and DNA damage signaling in response to mutant adenovirus infection and exogenous DSBs (50) (Chapter 2). We also showed that E1b55K mutants deficient in MRN degradation can still prevent mutant viral genome concatemerization through DNA Ligase IV destabilization. However, subsequent analysis of the E1b55K mutants revealed that down-regulation of DNA Ligase IV is not sufficient to rescue the replication defect of an E4-deleted mutant adenovirus (Lakdawala et al., submitted), highlighting the impact of MRN on multiple steps in the Ad lifecycle. Finally, we examined the effects of E1b55K/E4orf6 on cell cycle regulation. Our experiments with the E1b55K mutants demonstrated the requirement of MRN in the early G2/M checkpoint (50), and an MRN-independent effect on S phase progression. Therefore, these viral mutants provide useful tools to probe cellular pathways dependent upon the substrates targeted by E1b55K/E4orf6. It still remains to be determined which regions of E1b55K bind DNA Ligase IV and which ubiquitin ligase proteins regulate its destruction. This information will be necessary to fully appreciate how DNA Ligase IV down-regulation contributes

to the Ad lifecycle. It will also be important to identify other E1b55K/E4orf6 targets, since viral mRNA export requires the ubiquitin ligase activity (25, 378) and it is unclear whether degradation of the known substrates contributes.

As mentioned in Chapter 1, adenoviruses can promote transformation of primary cells in culture, particularly with non-permissive rodent cells (109). E1A has long been implicated in this, but requires other Ad proteins such as E1b55K, E4orf6, or E4orf3 for complete transformation (20, 238, 251, 369). Interestingly, E4orf6 or E4orf3 can act synergistically with E1A and E1b55K in this process (238, 251). However, in the absence of E1b55K, viral DNA is not maintained in transformed cells (253), suggesting E4orf6 and E4orf3 can promote transformation by a “hit and run” mechanism where viral genes are only needed only for initiating events (253, 324). Studies examining the requirements of E1b55K in transformation have indicated that neutralization of p53 activity is important (346, 347, 389, 391), a task that E4orf6 can also accomplish (94). However, other data suggest that adenoviral oncoproteins have p53-independent activities important to transformation (109, 148). The targeting of DNA repair pathways (147), or specific DNA repair proteins like MRN (335), DNA Ligase IV (8), and DNA-PKcs (30) by these viral oncogenes may contribute to transformation, especially “hit and run” transformation mediated by E4 proteins. Indeed, one recent report suggests that binding MRN may be relevant (148). Our characterization of E1b55K and E4orf6 mutants

should contribute to a better understanding of which cellular substrates are required in the transformation process.

AAV helper functions of E1b55K/E4orf6

Our studies on the functions of E1b55K/E4orf6 also had implications for the small DNA virus, AAV. AAV utilizes the host replication machinery as well as helper virus functions in order to replicate. While a large amount of research had described the viral requirements for AAV replication, very little was known about how helper proteins facilitated this process. Our data demonstrated that MRN poses a barrier to AAV DNA accumulation, and one helper function of E1b55K/E4orf6 is to degrade this complex (308) (Chapter 5). Although it is still unclear how MRN inhibits AAV, our results and others suggest that ATM may be involved (57, 298, 401) (see also Chapter 5). Since MRN is required for ATM activity (195), our data clarified an important link between ATM and E1b55K/E4orf6 AAV helper function. Other AAV helper viruses also interact with the cellular DNA damage response machinery (203). AAV may, therefore, exploit helpers that can modulate DNA damage response pathways. It will be important to determine how helpers such as HSV-1 and HCMV promote AAV replication, since they activate damage signaling and sequester MRN (202, 219, 345, 372).

AAV and the cellular DNA damage response

Our studies also demonstrated that AAV and Ad co-infection induces a DNA damage response that occurs in the absence of MRN (since it is degraded), and this is mediated in part by DNA-PKcs (Chapter 6). We found an additional requirement for DNA-PKcs in efficient AAV replication and transduction (Chapter 6). Since MRN is a negative regulator of AAV replication, perhaps its presence alters DNA repair pathways involving DNA-PK. MRN can act together with ATM, DNA-PK, and Artemis to repair a subset of complex DSBs (286). Additionally, DNA-PKcs phosphorylation of H2AX only occurs in the absence of MRN or ATM (116, 332). We found robust phosphorylation of H2AX in all cells with AAV replication compartments, but the pattern was altered in both the presence and absence of MRN (Chapter 6). Likewise, there were also differences in DNA-PK component recruitment to AAV centers with or without MRN (Chapter 6). It will be interesting to use AAV as a model system to examine how MRN and ATM regulate DNA-PK activity.

It is currently unclear how AAV triggers signaling through DNA-PKcs and induces relocalization of DNA-PK components to viral centers. However, the AAV ITR hairpins may contribute, since DNA-PK is known to be activated by RAG induced hairpin structures during VDJ recombination (201). It will be informative to determine how DNA-PK and other repair proteins affect other AAV serotypes and more distantly related parvoviruses with different ITR

structures. While we do not know how damage signaling impacts AAV, it is tempting to speculate that it is somehow beneficial, given the localization of DNA repair proteins at AAV centers and the damage induced modification of replication proteins. Genotoxic agents have been previously reported to stimulate limited AAV transduction and replication (5, 295, 388). Perhaps other helper viruses like HSV-1 and HCMV also contribute to AAV replication by activating certain DNA damage signaling proteins. Studying AAV replication should provide important insights into DNA-PK functions, and the relationship between DNA repair and replication pathways.

As shown in Figure 8 in Chapter 1, the AAV lifecycle has a latent component. In the absence of helpers, AAV can site-specifically integrate onto a region of chromosome 19. In the absence of Rep, rAAV vectors also integrate, although this is not site-specific and has been shown to occur at chromosomal breakage sites (234). While the cis elements of the AAV genome and trans Rep functions have been described in some detail for this process (105, 241), cellular factors regulating integration remain to be identified. Retroviruses have been shown to utilize cellular DNA repair factors to promote their integration (323), so it would not be surprising if the same were true for AAV. There may be some differences, however, given the structures of their genomes. We have found that MRN suppresses AAV replication, perhaps through ATM activity. It is possible that in doing so, MRN

may actually promote the establishment of latency. Although the damage signaling occurring in the absence of MRN (due to degradation by Ad) may somehow benefit AAV replication, it could also indicate impending cell death and prevent AAV from establishing latency or promote its reactivation from latency. The damage response induced modification of Rep may serve as the molecular switch to govern AAV lytic and latent phases. Clearly, further research is warranted to determine how DNA repair proteins and damage signaling impact both phases of the AAV lifecycle.

From our studies with AAV, we have learned that the MRN complex negatively regulates viral DNA replication, that AAV replication induces a robust damage response in the absence of MRN, and that the viral Rep proteins appear to be modified in a DNA-PKcs dependent manner (Chapter 6). These results draw some interesting parallels to SV40 replication. SV40 is a small DNA virus that, like AAV, utilizes the host replication machinery to propagate. The SV40 LTAg binds numerous proteins during viral replication, and exhibits both DNA binding, helicase, and multimerization activities (321) like the AAV Rep proteins. Additionally, the N-terminus of Rep shares structural similarity to the DNA binding domain of LTAg (152). Like AAV, MRN has been implicated as an inhibitory factor for SV40, and LTAg appears to neutralize it by binding Nbs1 (89, 192, 379), and promoting MRN degradation later during infection (406). SV40 replication also induces a DNA damage

response, although unlike AAV, it is mediated by ATM (317, 406) and potentially ATR (261). While the function of DNA-PKcs mediated signaling during AAV replication is currently unclear, ATM activity is required for SV40 replication (317, 406). LTAg is phosphorylated by ATM (317), and this may be similar to the DNA-PKcs dependent modification of Rep, although the functional relevance of these events in cells is not understood. It will be interesting to determine how the different DNA damage responses of AAV and SV40 modulate Rep and LTAg functions, and cellular DNA replication factors required for virus production. Studies of both systems may uncover common viral themes and strategies.

Summary

Since viruses have evolved to target key host cell factors to promote their replication, they provide powerful tools to study cellular mechanisms. Viruses have previously contributed to our understanding of RNA splicing (17, 66), DNA replication (376, 377), apoptosis (69, 215, 285), and transformation (109, 141, 191, 207). In recent years, it has become clear that viruses also exhibit complex interactions with the cellular machinery for protein degradation (12, 127, 272) and DNA repair (203, 322, 365). Our work further establishes viruses as valuable model systems that have much to contribute to our knowledge of important cellular pathways.

Appendix

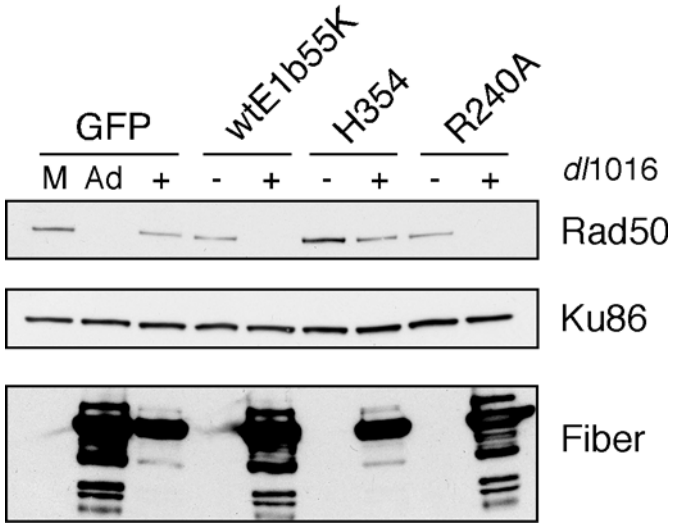

Appendix Figure 1. Degradation of MRN correlates with increased viral late protein synthesis. U2OS E1b55K cell lines were infected with wild-type Ad5 or *dl*1016 (both at MOI of 25) for approximately 24 hours. Lysates were analyzed for degradation of Rad50 and production of late proteins, indicated by Fiber staining. Ku86 serves as a loading control and M refers to mock treated cells.

Appendix Figure 2. E1b55K and E4orf6 may be autoubiquitinated, but Rad50 may be alternatively modified. (A) HeLa cells were mock treated or infected with rAd.E1b55K (MOI of 2) (E1b) or rAd.E1b55K and rAd.E4orf6 (MOI of 50) (E1b+E4orf6) for 24 hours before harvesting. DMSO or proteasome inhibitors MG132 (10μM final) and epoximycin (2μM final) were added 4 hours after infection and kept on during the infection. Lysates were analyzed for Rad50 or Ku70 as a loading control. A ladder of Rad50 seen in the presence of E1b55K/E4orf6 may represent ubiquitin-modified Rad50. **(B)** HeLa E1b55K expressing cells were infected with rAd.E4orf6 (MOI of 20) or mock treated for approximately 20 hours before harvesting. MG132 was added 8 hours post-infection and kept on for the duration. Lysates were analyzed by immunoblotting for the indicated proteins. Darker exposures of MRN are shown in the panel below. A ladder of Rad50 is only seen with wtE1b55K and E4orf6, and not with the H354 mutant that does not bind MRN. **(C)** 293Q cells were transfected with vector or plasmids expressing E4orf6 or E4orf6 mutant AXA in the presence and absence of a his-tagged ubiquitin construct. 24 hours later, cells were treated with the proteasome inhibitor LLnL (50μg/mL) for an additional 6 hours before harvesting. His-ubiquitinated proteins were affinity purified (AP: his) under denaturing conditions and analyzed by immunoblotting for the indicated proteins. 2% input was also analyzed. Both E4orf6 proteins were modified by his-ubiquitin (his-ubiquitin conjugates) but Rad50 was not. Red squares show that Rad50 is still modified. **(D)** E1b55K is modified by ubiquitin. U2OS cells were transfected with empty vector or a his-tagged ubiquitin construct 24 hours before infecting with Ad5 (MOI of 25) for another 20 hours. Six hours post-infection, cells were untreated or treated with LLnL (50μg/mL) for the duration of infection. Cells were harvested and treated as in (C). His affinity purifications (AP: his) and input lysates were analyzed for E1b55K. The ladder represents his-ubiquitin modified forms of E1b55K (his-ubiquitin conjugates).

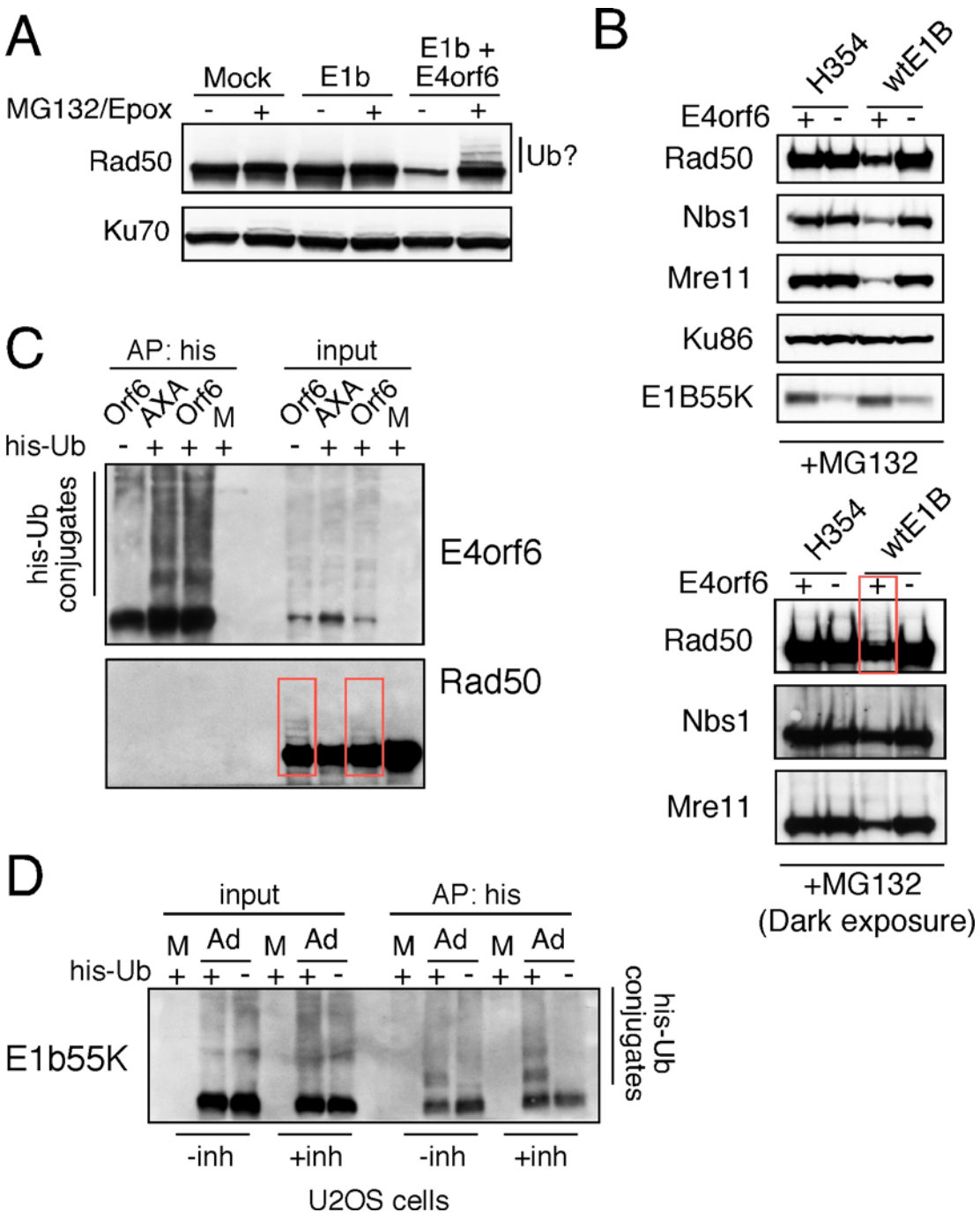
A
Mock
E1b
E1b + E4orf6
MG132/Epox
- + - + - +
Rad50
Ub?
Ku70
B
H354
wtE1B
E4orf6
+ - + -
Rad50
Nbs1
Mre11
Ku86
E1B55K
+MG132
H354
wtE1B
E4orf6
+ - + -
Rad50
Nbs1
Mre11
+MG132
(Dark exposure)
C
AP: his
input
Orf6
AXA Orf6
M
his-Ub
- + + + - + + +
his-Ub conjugates
E4orf6
Rad50
D
input
AP: his
M Ad M Ad M Ad M Ad
his-Ub
+ + - + + - + + - + + -
E1b55K
his-Ub conjugates
-inh
+inh
-inh
+inh
U2OS cells

Appendix Figure 3. The Mre11 complex limits scAAV transduction. (A) HeLa stable cell lines expressing WT E1b55K or mutant H354 were infected at the indicated MOIs with rAAV.GFP or scAAV.GFP in the presence or absence of rAd.E4orf6 (MOI 50). 24 hours after infection cells were fixed and analyzed by fluorescence activated cell sorting to measure viral transduction. Transduction is represented by the percent of cells expressing GFP (y-axis). **(B)** Stable HeLa cell lines expressing GFP, WT E1B55K, H354, or R240A were infected with scAAV.GFP (MOI 25) in the presence and absence of rAdE4orf6 (MOI 25) for 24 hours and treated as in (A). Error bars represent SD of triplicate samples. Enhanced transduction is observed under conditions where MRN is degraded (WT E1b55K and R240A cells plus E4orf6). **(C)** The Mre11 complex inhibits scAAV transduction. A-TLD3 cells were infected with scAAV.GFP (MOI 2000) for 48 hours. Transduced GFP expressing cells are visualized in the fluorescent photomicropgraphs (top panel). Bottom panel depicts phase contrast photomicrographs.

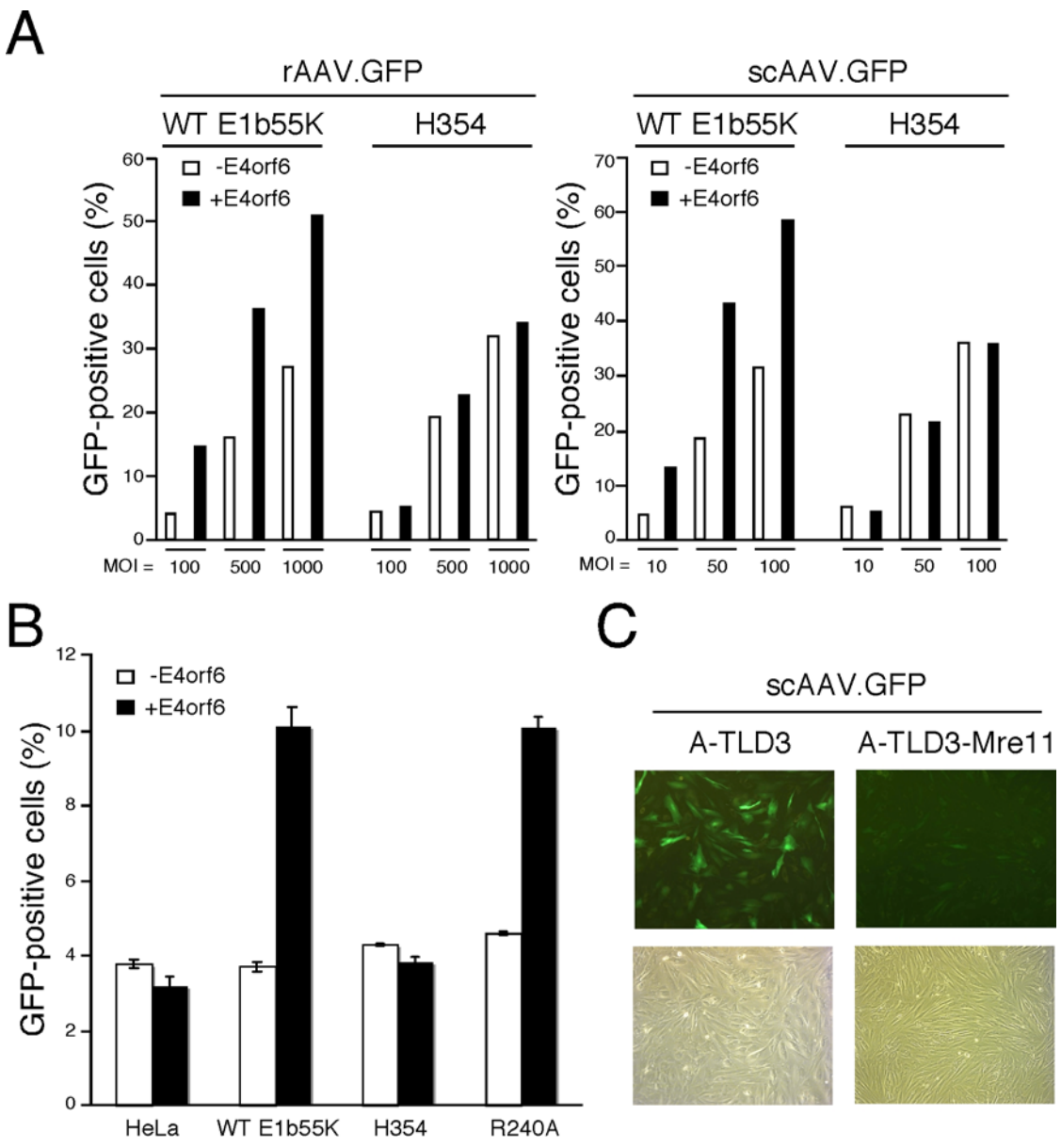
A
rAAV.GFP
scAAV.GFP
WT E1b55K
H354
-E4orf6
+E4orf6
GFP-positive cells (%)
MOI = 100 500 1000 100 500 1000
MOI = 10 50 100 10 50 100
B
GFP-positive cells (%)
HeLa
WT E1b55K
H354
R240A
C
scAAV.GFP
A-TLD3
A-TLD3-Mre11

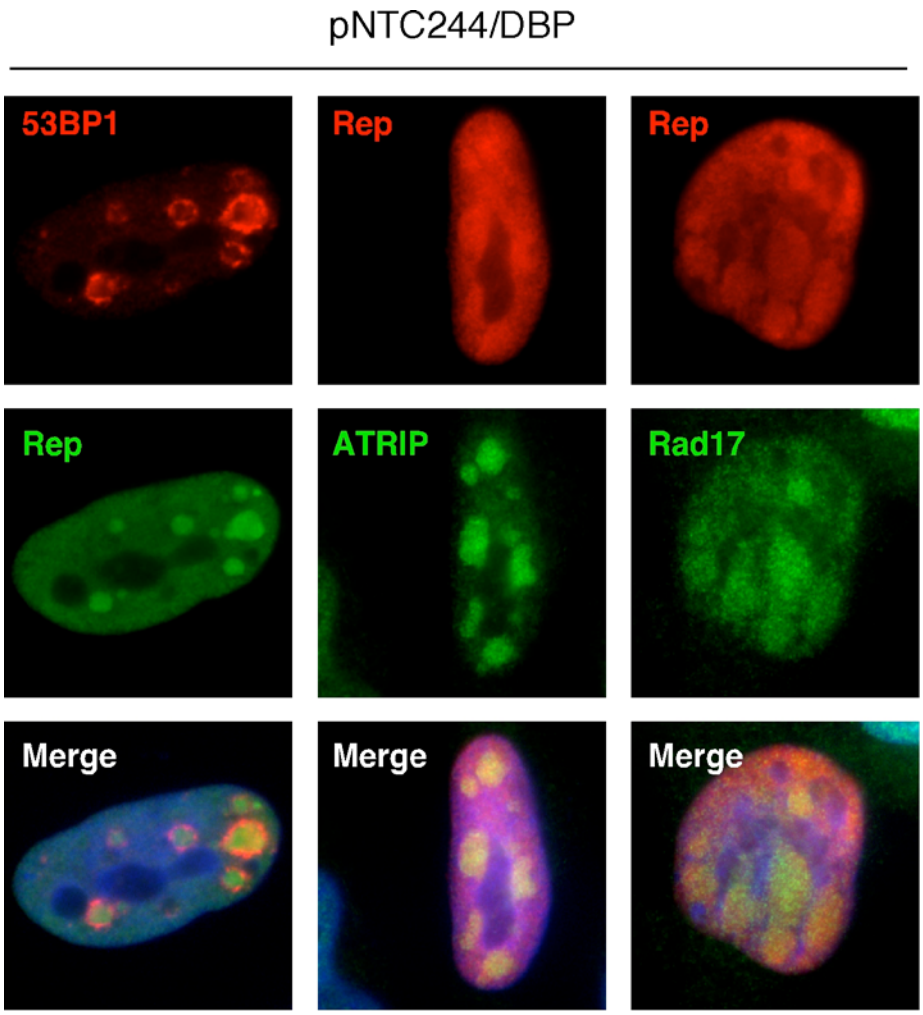

Appendix Figure 4. DNA damage response proteins localize to AAV replication centers. HeLa cells were transfected with pNTC244 and a plasmid encoding DBP for 24-36 hours. Cells were then fixed and processed for immunofluorescence for Rep and the indicated proteins. Nuclei are marked by DAPI stain.

References

1. Abraham, R. T. 2001. Cell cycle checkpoint signaling through the ATM and ATR kinases. Genes Dev 15:2177-96.

2. Abraham, R. T. 2004. PI 3-kinase related kinases: 'big' players in stress-induced signaling pathways. DNA Repair (Amst) 3:883-7.

3. Adams, K. E., A. L. Medhurst, D. A. Dart, and N. D. Lakin. 2006. Recruitment of ATR to sites of ionising radiation-induced DNA damage requires ATM and components of the MRN protein complex. Oncogene 25:3894-904.

4. Ahnesorg, P., P. Smith, and S. P. Jackson. 2006. XLF interacts with the XRCC4-DNA ligase IV complex to promote DNA nonhomologous end-joining. Cell 124:301-13.

5. Alexander, I. E., D. W. Russell, and A. D. Miller. 1994. DNA-damaging agents greatly increase the transduction of non-dividing cells by adeno-associated virus vectors. J. Virol. 68:8282-8287.

6. Babiss, L. E., and H. S. Ginsberg. 1984. Adenovirus type 5 early region 1b gene product is required for efficient shutoff of host protein synthesis. J Virol 50:202-12.

7. Babiss, L. E., H. S. Ginsberg, and J. E. Darnell, Jr. 1985. Adenovirus E1B proteins are required for accumulation of late viral mRNA and for effects on cellular mRNA translation and transport. Mol Cell Biol 5:2552-8.

8. Baker, A., K. J. Rohleder, L. A. Hanakahi, and G. Ketner. 2007. The adenovirus E4 34k and E1b 55k oncoproteins target host DNA ligase IV for proteasomal degradation. J Virol 81:7034-7040.

9. Bakkenist, C. J., and M. B. Kastan. 2003. DNA damage activates ATM through intermolecular autophosphorylation and dimer dissociation. Nature 421:499-506.

10. Bakkenist, C. J., and M. B. Kastan. 2004. Initiating cellular stress responses. Cell 118:9-17.

11. Barlow, J. H., M. Lisby, and R. Rothstein. 2008. Differential regulation of the cellular response to DNA double-strand breaks in G1. Mol Cell 30:73-85.

12. Barry, M., and K. Fruh. 2006. Viral modulators of cullin RING ubiquitin ligases: culling the host defense. Sci STKE 2006:pe21.

13. Bartek, J., C. Lukas, and J. Lukas. 2004. Checking on DNA damage in S phase. Nat Rev Mol Cell Biol 5:792-804.

14. Bekker-Jensen, S., C. Lukas, R. Kitagawa, F. Melander, M. B. Kastan, J. Bartek, and J. Lukas. 2006. Spatial organization of the mammalian genome surveillance machinery in response to DNA strand breaks. J Cell Biol 173:195-206.

15. Bekker-Jensen, S., C. Lukas, F. Melander, J. Bartek, and J. Lukas. 2005. Dynamic assembly and sustained retention of 53BP1 at the sites of DNA damage are controlled by Mdc1/NFBD1. J Cell Biol 170:201-11.

16. Berezutskaya, E., B. Yu, A. Morozov, P. Raychaudhuri, and S. Bagchi. 1997. Differential regulation of the pocket domains of the retinoblastoma family proteins by the HPV16 E7 oncoprotein. Cell Growth Differ 8:1277-86.

17. Berget, S. M., C. Moore, and P. A. Sharp. 1977. Spliced segments at the 5' terminus of adenovirus 2 late mRNA. Proc Natl Acad Sci U S A 74:3171-5.

18. Berk, A. J. 2005. Recent lessons in gene expression, cell cycle control, and cell biology from adenovirus. Oncogene 24:7673-85.

19. Berkovich, E., R. J. Monnat, Jr., and M. B. Kastan. 2007. Roles of ATM and NBS1 in chromatin structure modulation and DNA double-strand break repair. Nat Cell Biol 9:683-90.

20. Bernards, R., M. G. de Leeuw, A. Houweling, and A. J. van der Eb. 1986. Role of the adenovirus early region 1B tumor antigens in transformation and lytic infection. Virology 150:126-39.

21. Berthet, C., K. Raj, P. Saudan, and P. Beard. 2005. How adeno-associated virus Rep78 protein arrests cells completely in S phase. Proc Natl Acad Sci U S A 102:13634-9.

22. Bhaskara, V., A. Dupre, B. Lengsfeld, B. B. Hopkins, A. Chan, J. H. Lee, X. Zhang, J. Gautier, V. Zakian, and T. T. Paull. 2007. Rad50 adenylate kinase activity regulates DNA tethering by Mre11/Rad50 complexes. Mol Cell 25:647-61.

23. Blair Zajdel, M. E., and G. E. Blair. 1988. The intracellular distribution of the transformation-associated protein p53 in adenovirus-transformed rodent cells. Oncogene 2:579-84.

24. Blanchette, P., C. Y. Cheng, Q. Yan, G. Ketner, D. A. Ornelles, T. Dobner, R. C. Conaway, J. W. Conaway, and P. E. Branton. 2004. Both BC-box motifs of adenovirus protein E4orf6 are required to efficiently assemble an E3 ligase complex that degrades p53. Mol Cell Biol 24:9619-29.

25. Blanchette, P., K. Kindsmuller, P. Groitl, F. Dallaire, T. Speiseder, P. E. Branton, and T. Dobner. 2008. Control of mRNA export by adenovirus E4orf6 and E1B55K proteins during productive infection requires E4orf6 ubiquitin ligase activity. J Virol 82:2642-51.

26. Boggio, R., A. Passafaro, and S. Chiocca. 2007. Targeting SUMO E1 to ubiquitin ligases: a viral strategy to counteract sumoylation. J Biol Chem 282:15376-82.

27. Boisvert, F. M., M. J. Hendzel, J. Y. Masson, and S. Richard. 2005. Methylation of MRE11 regulates its nuclear compartmentalization. Cell Cycle 4:981-9.

28. Boivin, D., M. R. Morrison, R. C. Marcellus, E. Querido, and P. E. Branton. 1999. Analysis of synthesis, stability, phosphorylation, and interacting polypeptides of the 34-kilodalton product of open reading frame 6 of the early region 4 protein of human adenovirus type 5. J Virol 73:1245-53.

29. Boutell, C., M. Canning, A. Orr, and R. D. Everett. 2005. Reciprocal activities between herpes simplex virus type 1 regulatory protein ICP0,

a ubiquitin E3 ligase, and ubiquitin-specific protease USP7. J Virol 79:12342-54.

30. Boyer, J., K. Rohleder, and G. Ketner. 1999. Adenovirus E4 34k and E4 11k inhibit double strand break repair and are physically associated with the cellular DNA-dependent protein kinase. Virology 263:307-12.

31. Boyer, J. L., and G. Ketner. 2000. Genetic analysis of a potential zinc-binding domain of the adenovirus E4 34k protein. J. Biol. Chem. 275:14969-14978.

32. Boyer, S. N., D. E. Wazer, and V. Band. 1996. E7 protein of human papilloma virus-16 induces degradation of retinoblastoma protein through the ubiquitin-proteasome pathway. Cancer Res 56:4620-4.

33. Branzei, D., and M. Foiani. 2008. Regulation of DNA repair throughout the cell cycle. Nat Rev Mol Cell Biol 9:297-308.

34. Bressan, D. A., H. A. Olivares, B. E. Nelms, and J. H. Petrini. 1998. Alteration of the N-terminal phosphoesterase signature motifs inactivates *Saccharomyces cerevisiae* Mre11. Genetics 150:592-600.

35. Bridge, E., and G. Ketner. 1990. Interaction of adenoviral E4 and E1b products in late gene expression. Virology 174:345-53.

36. Bridge, E., and G. Ketner. 1989. Redundant control of adenovirus late gene expression by early region 4. J Virol 63:631-638.

37. Brown, C. R., S. J. Doxsey, E. White, and W. J. Welch. 1994. Both viral (adenovirus E1B) and cellular (hsp 70, p53) components interact with centrosomes. J Cell Physiol 160:47-60.

38. Brown, E. J., and D. Baltimore. 2000. ATR disruption leads to chromosomal fragmentation and early embryonic lethality. Genes Dev 14:397-402.

39. Brown, E. J., and D. Baltimore. 2003. Essential and dispensable roles of ATR in cell cycle arrest and genome maintenance. Genes Dev 17:615-28.

40. Buck, D., L. Malivert, R. de Chasseval, A. Barraud, M. C. Fondaneche, O. Sanal, A. Plebani, J. L. Stephan, M. Hufnagel, F. le Deist, A. Fischer, A. Durandy, J. P. de Villartay, and P. Revy. 2006. Cernunnos, a novel nonhomologous end-joining factor, is mutated in human immunodeficiency with microcephaly. Cell 124:287-99.

41. Burgert, H. G., Z. Ruzsics, S. Obermeier, A. Hilgendorf, M. Windheim, and A. Elsing. 2002. Subversion of host defense mechanisms by adenoviruses. Curr Top Microbiol Immunol 269:273-318.

42. Burma, S., and D. J. Chen. 2004. Role of DNA-PK in the cellular response to DNA double-strand breaks. DNA Repair (Amst) 3:909-18.

43. Buscemi, G., C. Savio, L. Zannini, F. Micciche, D. Masnada, M. Nakanishi, H. Tauchi, K. Komatsu, S. Mizutani, K. Khanna, P. Chen, P. Concannon, L. Chessa, and D. Delia. 2001. Chk2 activation dependence on Nbs1 after DNA damage. Mol. Cell Biol. 21:5214-5222.

44. Busino, L., M. Donzelli, M. Chiesa, D. Guardavaccaro, D. Ganoth, N. V. Dorrello, A. Hershko, M. Pagano, and G. F. Draetta. 2003. Degradation of Cdc25A by beta-TrCP during S phase and in response to DNA damage. Nature 426:87-91.

45. Cadwell, K., and L. Coscoy. 2005. Ubiquitination on nonlysine residues by a viral E3 ubiquitin ligase. Science 309:127-30.

46. Cai, Q. L., J. S. Knight, S. C. Verma, P. Zald, and E. S. Robertson. 2006. EC5S ubiquitin complex is recruited by KSHV latent antigen LANA for degradation of the VHL and p53 tumor suppressors. PLoS Pathog 2:e116.

47. Cann, K. L., and G. G. Hicks. 2007. Regulation of the cellular DNA double-strand break response. Biochem Cell Biol 85:663-74.

48. Canning, M., C. Boutell, J. Parkinson, and R. D. Everett. 2004. A RING finger ubiquitin ligase is protected from autocatalyzed ubiquitination and degradation by binding to ubiquitin-specific protease USP7. J Biol Chem 279:38160-8.

49. Carney, J. P., R. S. Maser, H. Olivares, E. M. Davis, M. L. Beau, J. R. Y. III, L. Hays, W. F. Morgan, and J. H. Petrini. 1998. The hMre11/hRad50 protein complex and nijmegen breakage syndrome: Linkage of double-strand break repair to the cellular DNA damage response. Cell 93:477-486.

50. Carson, C. T., R. A. Schwartz, T. H. Stracker, C. E. Lilley, D. V. Lee, and M. D. Weitzman. 2003. The Mre11 complex is required for ATM activation and the G2/M checkpoint. EMBO J 22:6610-20.

51. Carvalho, T., J. S. Seeler, K. Ohman, P. Jordan, U. Pettersson, G. Akusjarvi, M. Carmo-Fonseca, and A. Dejean. 1995. Targeting of adenovirus E1A and E4-ORF3 proteins to nuclear matrix-associated PML bodies. J Cell Biol 131:45-56.

52. Cathomen, T., and M. D. Weitzman. 2000. A functional complex of adenovirus proteins E1B-55K and E4orf6 is necessary to modulate the expression level of p53 but not its transcriptional activity. J. Virol. 74:11407-11412.

53. Celeste, A., O. Fernandez-Capetillo, M. J. Kruhlak, D. R. Pilch, D. W. Staudt, A. Lee, R. F. Bonner, W. M. Bonner, and A. Nussenzweig. 2003. Histone H2AX phosphorylation is dispensable for the initial recognition of DNA breaks. Nat Cell Biol 5:675-9.

54. Cerosaletti, K., and P. Concannon. 2004. Independent roles for nibrin and Mre11-Rad50 in the activation and function of Atm. J Biol Chem 279:38813-9.

55. Cerosaletti, K., J. Wright, and P. Concannon. 2006. Active role for nibrin in the kinetics of atm activation. Mol Cell Biol 26:1691-9.

56. Cerosaletti, K. M., A. Desai-Mehta, T. C. Yeo, M. Kraakman-Van Der Zwet, M. Z. Zdzienicka, and P. Concannon. 2000. Retroviral expression of the NBS1 gene in cultured Nijmegen breakage syndrome cells restores normal radiation sensitivity and nuclear focus formation. Mutagenesis 15:281-6.

57. Cervelli, T., J. A. Palacios, L. Zentilin, M. Mano, R. A. Schwartz, M. D. Weitzman, and M. Giacca. 2008. Processing of recombinant AAV

genomes occurs in specific nuclear structures that overlap with foci of DNA-damage-response proteins. J Cell Sci 121:349-57.

58. Chan, D. W., B. P. C. Chen, S. Prithivirajsingh, A. Kurimasa, M. D. Story, J. Qin, and D. J. Chen. 2002. Autophosphorylation of the DNA-dependent protein kinase catalytic subunit is required for rejoining of DNA double-strand breaks. Genes & Dev. 16:2333-2338.

59. Chan, D. W., and S. P. Lees-Miller. 1996. The DNA-dependent protein kinase is inactivated by autophosphorylation of the catalytic subunit. J Biol Chem 271:8936-41.

60. Chejanovsky, N., and B. J. Carter. 1989. Replication of a human parvovirus nonsense mutant in mammalian cells containing an inducible amber suppressor. Virology 171:239-47.

61. Cheng, C. Y., P. Blanchette, and P. E. Branton. 2007. The adenovirus E4orf6 E3 ubiquitin ligase complex assembles in a novel fashion. Virology 364:36-44.

62. Chiorini, J. A., S. M. Wiener, L. Yang, R. H. Smith, B. Safer, N. P. Kilcoin, Y. Liu, E. Urcelay, and R. M. Kotin. 1996. The roles of AAV Rep proteins in gene expression and targeted integration. Curr Top Microbiol Immunol 218:25-33.

63. Chiorini, J. A., B. Zimmermann, L. Yang, R. H. Smith, A. Ahearn, F. Herberg, and R. M. Kotin. 1998. Inhibition of PrKX, a novel protein kinase, and the cyclic AMP-dependent protein kinase PKA by the regulatory proteins of adeno-associated virus type 2. Mol Cell Biol 18:5921-9.

64. Choi, V. W., D. M. McCarty, and R. J. Samulski. 2006. Host cell DNA repair pathways in adeno-associated viral genome processing. J Virol 80:10346-56.

65. Chou, D. M., and S. J. Elledge. 2006. Tipin and Timeless form a mutually protective complex required for genotoxic stress resistance and checkpoint function. Proc Natl Acad Sci U S A 103:18143-7.

66. Chow, L. T., R. E. Gelinas, T. R. Broker, and R. J. Roberts. 1977. An amazing sequence arrangement at the 5' ends of adenovirus 2 messenger RNA. Cell 12:1-8.

67. Christensen, D. E., P. S. Brzovic, and R. E. Klevit. 2007. E2-BRCA1 RING interactions dictate synthesis of mono- or specific polyubiquitin chain linkages. Nat Struct Mol Biol 14:941-8.

68. Chun, H. H., and R. A. Gatti. 2004. Ataxia-telangiectasia, an evolving phenotype. DNA Repair (Amst) 3:1187-96.

69. Clem, R. J., M. Fechheimer, and L. K. Miller. 1991. Prevention of apoptosis by a baculovirus gene during infection of insect cells. Science 254:1388-90.

70. Collaco, R., K. M. Prasad, and J. P. Trempe. 1997. Phosphorylation of the adeno-associated virus replication proteins. Virology 232:332-6.

71. Collis, S. J., T. L. DeWeese, P. A. Jeggo, and A. R. Parker. 2005. The life and death of DNA-PK. Oncogene 24:949-61.

72. Corbin-Lickfett, K. A., and E. Bridge. 2003. Adenovirus E4-34kDa requires active proteasomes to promote late gene expression. Virology 315:234-44.

73. Cortez, D., G. Glick, and S. J. Elledge. 2004. Minichromosome maintenance proteins are direct targets of the ATM and ATR checkpoint kinases. Proc Natl Acad Sci U S A 101:10078-83.

74. Cortez, D., S. Guntuku, J. Qin, and S. J. Elledge. 2001. ATR and ATRIP: partners in checkpoint signaling. Science 294:1713-6.

75. Costanzo, V., T. Paull, M. Gottesman, and J. Gautier. 2004. Mre11 assembles linear DNA fragments into DNA damage signaling complexes. PLoS Biol 2:E110.

76. Costanzo, V., K. Robertson, M. Bibikova, E. Kim, D. Grieco, M. Gottesman, D. Carroll, and J. Gautier. 2001. Mre11 protein complex prevents double-strand break accumulation during chromosomal DNA replication. Mol Cell 8:137-47.

77. Cui, X., Y. Yu, S. Gupta, Y. M. Cho, S. P. Lees-Miller, and K. Meek. 2005. Autophosphorylation of DNA-dependent protein kinase regulates DNA end processing and may also alter double-strand break repair pathway choice. Mol Cell Biol 25:10842-52.

78. D'Amours, D., and S. P. Jackson. 2002. The Mre11 complex: At the crossroads of DNA repair and checkpoint signalling. Nat. Rev. Mol. Cell Biol. 3:317-327.

79. Dahl, J., J. You, and T. L. Benjamin. 2005. Induction and utilization of an ATM signaling pathway by polyomavirus. J Virol 79:13007-17.

80. Daniel, R., R. A. Katz, and A. M. Skalka. 1999. A role for DNA-PK in retroviral DNA integration. Science 284:644-7.

81. Darbinyan, A., K. M. Siddiqui, D. Slonina, N. Darbinian, S. Amini, M. K. White, and K. Khalili. 2004. Role of JC virus agnoprotein in DNA repair. J Virol 78:8593-600.

82. Davies, A. A., D. Huttner, Y. Daigaku, S. Chen, and H. D. Ulrich. 2008. Activation of ubiquitin-dependent DNA damage bypass is mediated by replication protein a. Mol Cell 29:625-36.

83. de Klein, A., M. Muijtjens, R. van Os, Y. Verhoeven, B. Smit, A. M. Carr, A. R. Lehmann, and J. H. Hoeijmakers. 2000. Targeted disruption of the cell-cycle checkpoint gene ATR leads to early embryonic lethality in mice. Curr Biol 10:479-82.

84. DeFazio, L. G., R. M. Stansel, J. D. Griffith, and G. Chu. 2002. Synapsis of DNA ends by DNA-dependent protein kinase. EMBO J 21:3192-200.

85. Dery, U., and J. Y. Masson. 2007. Twists and turns in the function of DNA damage signaling and repair proteins by post-translational modifications. DNA Repair (Amst) 6:561-77.

86. Desai-Mehta, A., K. M. Cerosaletti, and P. Concannon. 2001. Distinct functional domains of nibrin mediate Mre11 binding, focus formation, and nuclear localization. Mol Cell Biol 21:2184-91.

87. Di Pasquale, G., and S. N. Stacey. 1998. Adeno-associated virus Rep78 protein interacts with protein kinase A and its homolog PRKX and inhibits CREB-dependent transcriptional activation. J Virol 72:7916-25.

88. Difilippantonio, S., A. Celeste, O. Fernandez-Capetillo, H. T. Chen, B. Reina San Martin, F. Van Laethem, Y. P. Yang, G. V. Petukhova, M. Eckhaus, L. Feigenbaum, K. Manova, M. Kruhlak, R. D. Camerini-Otero, S. Sharan, M. Nussenzweig, and A. Nussenzweig. 2005. Role of Nbs1 in the activation of the Atm kinase revealed in humanized mouse models. Nat Cell Biol 7:675-85.

89. Digweed, M., I. Demuth, S. Rothe, R. Scholz, A. Jordan, C. Grotzinger, D. Schindler, M. Grompe, and K. Sperling. 2002. SV40 large T-antigen disturbs the formation of nuclear DNA-repair foci containing MRE11. Oncogene 21:4873-8.

90. Digweed, M., and K. Sperling. 2004. Nijmegen breakage syndrome: clinical manifestation of defective response to DNA double-strand breaks. DNA Repair (Amst) 3:1207-17.

91. Ding, Q., Y. V. R. Reddy, W. Wang, T. Woods, P. Douglas, D. A. Ramsden, S. P. Lees-Miller, and K. Meek. 2003. Autophosphorylation of the catalytic subunit of the DNA-dependen protein kinase is required for efficient end processing during DNA double-strand break repair. Mol. Cell Biol. 23:5836-5848.

92. DiTullio, R. A., Jr., T. A. Mochan, M. Venere, J. Bartkova, M. Sehested, J. Bartek, and T. D. Halazonetis. 2002. 53BP1 functions in an ATM-dependent checkpoint pathway that is constitutively activated in human cancer. Nat Cell Biol 4:998-1002.

93. Dobbelstein, M., J. Roth, W. T. Kimberly, A. J. Levine, and T. Shenk. 1997. Nuclear export of the E1B 55-kDa and E4 34-kDa adenoviral oncoproteins mediated by a rev-like signal sequence. EMBO J 16:4276-84.

94. Dobner, T., N. Horikoshi, S. Rubenwolf, and T. Shenk. 1996. Blockage by adenovirus E4orf6 of transcriptional activation by the p53 tumor suppressor. Science 272:1470-3.

95. Dobner, T., and J. Kzhyshkowska. 2001. Nuclear export of adenovirus RNA. Curr Top Microbiol Immunol 259:25-54.

96. Dosch, T., F. Horn, G. Schneider, F. Kratzer, T. Dobner, J. Hauber, and R. H. Stauber. 2001. The adenovirus type 5 E1B-55K oncoprotein actively shuttles in virus-infected cells, whereas transport of E4orf6 is mediated by a CRM1-independent mechanism. J Virol 75:5677-83.

97. Douar, A. M., K. Poulard, D. Stockholm, and O. Danos. 2001. Intracellular trafficking of adeno-associated virus vectors: routing to the late endosomal compartment and proteasome degradation. J Virol 75:1824-33.

98. Doucas, V., A. M. Ishov, A. Romo, H. Juguilon, M. D. Weitzman, R. M. Evans, and G. G. Maul. 1996. Adenovirus replication is coupled with the dynamic properties of the PML nuclear structure. Genes Dev 10:196-207.

99. Douglas, P., S. Gupta, N. Morrice, K. Meek, and S. P. Lees-Miller. 2005. DNA-PK-dependent phosphorylation of Ku70/80 is not required for non-homologous end joining. DNA Repair (Amst) 4:1006-18.

100. Downs, J. A., and S. P. Jackson. 2004. A means to a DNA end: the many roles of Ku. Nat Rev Mol Cell Biol 5:367-78.

101. Duan, D., P. Sharma, L. Dudus, Y. Zhang, S. Sanlioglu, Z. Yan, Y. Yue, Y. Ye, R. Lester, J. Yang, K. J. Fisher, and J. F. Engelhardt. 1999. Formation of adeno-associated virus circular genomes is differentially regulated by adenovirus E4 ORF6 and E2a gene expression. J Virol 73:161-9.

102. Duan, D., P. Sharma, J. Yang, Y. Yue, L. Dudus, Y. Zhang, K. J. Fisher, and J. F. Engelhardt. 1998. Circular intermediates of recombinant adeno-associated virus have defined structural characteristics responsible for long-term episomal persistence in muscle tissue. J Virol 72:8568-77.

103. Duan, D., Y. Yue, and J. F. Engelhardt. 2003. Consequences of DNA-dependent protein kinase catalytic subunit deficiency on recombinant

adeno-associated virus genome circularization and heterodimerization in muscle tissue. J Virol 77:4751-9.

104. Duan, D., Y. Yue, Z. Yan, J. Yang, and J. F. Engelhardt. 2000. Endosomal processing limits gene transfer to polarized airway epithelia by adeno-associated virus. J Clin Invest 105:1573-87.

105. Dutheil, N., and R. M. Linden. 2006. Site-specific integration by adeno-associated virus, p. 213-236. *In* J. R. Kerr, S. F. Cotmore, M. E. Bloom, R. M. Linden, and C. R. Parrish (ed.), Parvoviruses. Hodder Arnold.

106. Dye, B. T., and B. A. Schulman. 2007. Structural mechanisms underlying posttranslational modification by ubiquitin-like proteins. Annu Rev Biophys Biomol Struct 36:131-50.

107. Elliott, J., O. T. Lynch, Y. Suessmuth, P. Qian, C. R. Boyd, J. F. Burrows, R. Buick, N. J. Stevenson, O. Touzelet, M. Gadina, U. F. Power, and J. A. Johnston. 2007. Respiratory syncytial virus NS1 protein degrades STAT2 by using the Elongin-Cullin E3 ligase. J Virol 81:3428-36.

108. Ellison, V., and B. Stillman. 2003. Biochemical characterization of DNA damage checkpoint complexes: clamp loader and clamp complexes with specificity for 5' recessed DNA. PLoS Biol 1:E33.

109. Endter, C., and T. Dobner. 2004. Cell transformation by human adenoviruses. Curr Top Microbiol Immunol 273:163-214.

110. Endter, C., B. Hartl, T. Spruss, J. Hauber, and T. Dobner. 2005. Blockage of CRM1-dependent nuclear export of the adenovirus type 5 early region 1B 55-kDa protein augments oncogenic transformation of primary rat cells. Oncogene 24:55-64.

111. Endter, C., J. Kzhyshkowska, R. Stauber, and T. Dobner. 2001. SUMO-1 modification required for transformation by adenovirus type 5 early region 1B 55-kDa oncoprotein. Proc Natl Acad Sci U S A 98:11312-7.

112. Evans, J. D., and P. Hearing. 2003. Distinct roles of the Adenovirus E4 ORF3 protein in viral DNA replication and inhibition of genome concatenation. J Virol 77:5295-304.

113. Evans, J. D., and P. Hearing. 2005. Relocalization of the Mre11-Rad50-Nbs1 complex by the adenovirus E4 ORF3 protein is required for viral replication. J Virol 79:6207-15.

114. Everett, R. D. 2006. Interactions between DNA viruses, ND10 and the DNA damage response. Cell Microbiol 8:365-74.

115. Everett, R. D., M. Meredith, A. Orr, A. Cross, M. Kathoria, and J. Parkinson. 1997. A novel ubiquitin-specific protease is dynamically associated with the PML nuclear domain and binds to a herpesvirus regulatory protein. Embo J 16:1519-30.

116. Falck, J., J. Coates, and S. P. Jackson. 2005. Conserved modes of recruitment of ATM, ATR and DNA-PKcs to sites of DNA damage. Nature 434:605-11.

117. Falck, J., J. H. Petrini, B. R. Williams, J. Lukas, and J. Bartek. 2002. The DNA damage-dependent intra-S phase checkpoint is regulated by parallel pathways. Nat Genet 30:290-4.

118. Fanning, E., V. Klimovich, and A. R. Nager. 2006. A dynamic model for replication protein A (RPA) function in DNA processing pathways. Nucleic Acids Res 34:4126-37.

119. Fernandez-Capetillo, O., A. Lee, M. Nussenzweig, and A. Nussenzweig. 2004. H2AX: the histone guardian of the genome. DNA Repair (Amst) 3:959-67.

120. Ferrari, F. K., T. Samulski, T. Shenk, and R. J. Samulski. 1996. Second-strand synthesis is a rate-limiting step for efficient transduction by recombinant adeno-associated virus vectors. J. Virol. 70:3227-3234.

121. Fisher, K. J., G. P. Gao, M. D. Weitzman, R. DeMatteo, J. F. Burda, and J. M. Wilson. 1996. Transduction with recombinant adeno-associated virus for gene therapy is limited by leading-strand synthesis. J. Virol. 70:520-532.

122. Fleisig, H. B., N. I. Orazio, H. Liang, A. F. Tyler, H. P. Adams, M. D. Weitzman, and L. Nagarajan. 2007. Adenoviral E1B55K oncoprotein sequesters candidate leukemia suppressor sequence-specific single-

stranded DNA-binding protein 2 into aggresomes. Oncogene 26:4797-805.

123. Flint, S. J., and R. A. Gonzalez. 2003. Regulation of mRNA production by the adenoviral E1B 55-kDa and E4 Orf6 proteins. Curr Top Microbiol Immunol 272:287-330.

124. Foray, N., D. Marot, A. Gabriel, V. Randrianarison, A. M. Carr, M. Perricaudet, A. Ashworth, and P. Jeggo. 2003. A subset of ATM- and ATR-dependent phosphorylation events requires the BRCA1 protein. EMBO J 22:2860-71.

125. Francon, P., J. M. Lemaitre, C. Dreyer, D. Maiorano, O. Cuvier, and M. Mechali. 2004. A hypophosphorylated form of RPA34 is a specific component of pre-replication centers. J Cell Sci 117:4909-20.

126. Gabler, S., H. Schutt, P. Groitl, H. Wolf, T. Shenk, and T. Dobner. 1998. E1B 55-kilodalton-associated protein: a cellular protein with RNA-binding activity implicated in nucleocytoplasmic transport of adenovirus and cellular mRNAs. J. Virol. 72:7960-7971.

127. Gao, G., and H. Luo. 2006. The ubiquitin-proteasome pathway in viral infections. Can J Physiol Pharmacol 84:5-14.

128. Geoffroy, M. C., and A. Salvetti. 2005. Helper functions required for wild type and recombinant adeno-associated virus growth. Curr Gene Ther 5:265-71.

129. Glickman, M. H., and A. Ciechanover. 2002. The ubiquitin-proteasome proteolytic pathway: destruction for the sake of construction. Physiol Rev 82:373-428.

130. Goncalves, M. A. 2005. Adeno-associated virus: from defective virus to effective vector. Virol J 2:43.

131. Gonzalez, R., W. Huang, R. Finnen, C. Bragg, and S. J. Flint. 2006. Adenovirus E1B 55-kilodalton protein is required for both regulation of mRNA export and efficient entry into the late phase of infection in normal human fibroblasts. J Virol 80:964-74.

132. Gonzalez, R. A., and S. J. Flint. 2002. Effects of mutations in the adenoviral E1B 55-kilodalton protein coding sequence on viral late mRNA metabolism. J. Virol. 76:4507-4519.

133. Goodarzi, A. A., Y. Yu, E. Riballo, P. Douglas, S. A. Walker, R. Ye, C. Harer, C. Marchetti, N. Morrice, P. A. Jeggo, and S. P. Lees-Miller. 2006. DNA-PK autophosphorylation facilitates Artemis endonuclease activity. Embo J 25:3880-9.

134. Goodrum, F. D., and D. A. Ornelles. 1999. Roles for the E4 orf6, orf3, and E1B 55-kilodalton proteins in cell cycle-independent adenovirus replication. J. Virol. 73:7474-7488.

135. Goodrum, F. D., and D. A. Ornelles. 1997. The early region 1B 55-kilodalton oncoprotein of adenovirus relieves growth restrictions imposed on viral replication by the cell cycle. J Virol 71:548-61.

136. Goodrum, F. D., T. Shenk, and D. A. Ornelles. 1996. Adenovirus early region 4 34-kilodalton protein directs the nuclear localization of the early region 1B 55-kilodalton protein in primate cells. J Virol 70:6323-35.

137. Grand, R. J., M. L. Grant, and P. H. Gallimore. 1994. Enhanced expression of p53 in human cells infected with mutant adenoviruses. Virology 203:229-40.

138. Grieger, J. C., and R. J. Samulski. 2005. Adeno-associated virus as a gene therapy vector: vector development, production and clinical applications. Adv Biochem Eng Biotechnol 99:119-45.

139. Grifman, M., N. N. Chen, G. P. Gao, T. Cathomen, J. M. Wilson, and M. D. Weitzman. 1999. Overexpression of cyclin A inhibits augmentation of recombinant adeno-associated virus transduction by the adenovirus E4orf6 protein. J Virol 73:10010-9.

140. Guardavaccaro, D., and M. Pagano. 2004. Oncogenic aberrations of cullin-dependent ubiquitin ligases. Oncogene 23:2037-49.

141. Hahn, W. C., C. M. Counter, A. S. Lundberg, R. L. Beijersbergen, M. W. Brooks, and R. A. Weinberg. 1999. Creation of human tumour cells with defined genetic elements. Nature 400:464-8.

142. Hakem, R. 2008. DNA-damage repair; the good, the bad, and the ugly. EMBO J 27:589-605.

143. Halazonetis, T. D., V. G. Gorgoulis, and J. Bartek. 2008. An oncogene-induced DNA damage model for cancer development. Science 319:1352-5.

144. Halbert, D. N., J. R. Cutt, and T. Shenk. 1985. Adenovirus early region 4 encodes functions required for efficient DNA replication, late gene expression, and host cell shutoff. J Virol 56:250-7.

145. Han, S. I., M. A. Kawano, K. Ishizu, H. Watanabe, M. Hasegawa, S. N. Kanesashi, Y. S. Kim, A. Nakanishi, K. Kataoka, and H. Handa. 2004. Rep68 protein of adeno-associated virus type 2 interacts with 14-3-3 proteins depending on phosphorylation at serine 535. Virology 320:144-55.

146. Harada, J. N., A. Shevchenko, A. Shevchenko, D. C. Pallas, and A. J. Berk. 2002. Analysis of the adenovirus E1B-55K-anchored proteome reveals its link to ubiquitination machinery. J. Virol. 76:9194-9206.

147. Hart, L. S., S. M. Yannone, C. Naczki, J. S. Orlando, S. B. Waters, S. A. Akman, D. J. Chen, D. Ornelles, and C. Koumenis. 2005. The adenovirus E4orf6 protein inhibits DNA double strand break repair and radiosensitizes human tumor cells in an E1B-55K-independent manner. J Biol Chem 280:1474-81.

148. Hartl, B., T. Zeller, P. Blanchette, E. Kremmer, and T. Dobner. 2008. Adenovirus type 5 early region 1B 55-kDa oncoprotein can promote cell transformation by a mechanism independent from blocking p53-activated transcription. Oncogene.

149. Hashimoto, Y., T. Tsujimura, A. Sugino, and H. Takisawa. 2006. The phosphorylated C-terminal domain of Xenopus Cut5 directly mediates ATR-dependent activation of Chk1. Genes Cells 11:993-1007.

150. Hetfeld, B. K., A. Helfrich, B. Kapelari, H. Scheel, K. Hofmann, A. Guterman, M. Glickman, R. Schade, P. M. Kloetzel, and W. Dubiel. 2005. The zinc finger of the CSN-associated deubiquitinating enzyme USP15 is essential to rescue the E3 ligase Rbx1. Curr Biol 15:1217-21.

151. Hicke, L. 2001. Protein regulation by monoubiquitin. Nat Rev Mol Cell Biol 2:195-201.

152. Hickman, A. B., D. R. Ronning, R. M. Kotin, and F. Dyda. 2002. Structural unity among viral origin binding proteins: crystal structure of the nuclease domain of adeno-associated virus Rep. Mol Cell 10:327-37.

153. Hickson, I., Y. Zhao, C. J. Richardson, S. J. Green, N. M. Martin, A. I. Orr, P. M. Reaper, S. P. Jackson, N. J. Curtin, and G. C. Smith. 2004. Identification and characterization of a novel and specific inhibitor of the ataxia-telangiectasia mutated kinase ATM. Cancer Res 64:9152-9.

154. Hoeller, D., C. M. Hecker, and I. Dikic. 2006. Ubiquitin and ubiquitin-like proteins in cancer pathogenesis. Nat Rev Cancer 6:776-88.

155. Hopfner, K. P., L. Craig, G. Moncalian, R. A. Zinkel, T. Usui, B. A. Owen, A. Karcher, B. Henderson, J. L. Bodmer, C. T. McMurray, J. P. Carney, J. H. Petrini, and J. A. Tainer. 2002. The Rad50 zinc-hook is a structure joining Mre11 complexes in DNA recombination and repair. Nature 418:562-6.

156. Hoppe, B. S., R. B. Jensen, and C. U. Kirchgessner. 2000. Complementation of the radiosensitive M059J cell line. Radiat Res 153:125-30.

157. Huang, M. M., and P. Hearing. 1989. Adenovirus early region 4 encodes two gene products with redundant effects in lytic infection. J Virol 63:2605-15.

158. Huen, M. S., and J. Chen. 2008. The DNA damage response pathways: at the crossroad of protein modifications. Cell Res 18:8-16.

159. Huen, M. S., R. Grant, I. Manke, K. Minn, X. Yu, M. B. Yaffe, and J. Chen. 2007. RNF8 transduces the DNA-damage signal via histone ubiquitylation and checkpoint protein assembly. Cell 131:901-14.

160. Hunter, T. 2007. The age of crosstalk: phosphorylation, ubiquitination, and beyond. Mol Cell 28:730-8.

161. Inagaki, K., C. Ma, T. A. Storm, M. A. Kay, and H. Nakai. 2007. The role of DNA-PKcs and artemis in opening viral DNA hairpin termini in various tissues in mice. J Virol 81:11304-21.

162. Ira, G., A. Pellicioli, A. Balijja, X. Wang, S. Fiorani, W. Carotenuto, G. Liberi, D. Bressan, L. Wan, N. M. Hollingsworth, J. E. Haber, and M. Foiani. 2004. DNA end resection, homologous recombination and DNA damage checkpoint activation require CDK1. Nature 431:1011-7.

163. Ishimi, Y., Y. Komamura-Kohno, H. J. Kwon, K. Yamada, and M. Nakanishi. 2003. Identification of MCM4 as a target of the DNA replication block checkpoint system. J Biol Chem 278:24644-50.

164. Jazayeri, A., J. Falck, C. Lukas, J. Bartek, G. C. Smith, J. Lukas, and S. P. Jackson. 2006. ATM- and cell cycle-dependent regulation of ATR in response to DNA double-strand breaks. Nat Cell Biol 8:37-45.

165. Jin, J., X. Li, S. P. Gygi, and J. W. Harper. 2007. Dual E1 activation systems for ubiquitin differentially regulate E2 enzyme charging. Nature 447:1135-8.

166. Jin, J., T. Shirogane, L. Xu, G. Nalepa, J. Qin, S. J. Elledge, and J. W. Harper. 2003. SCFbeta-TRCP links Chk1 signaling to degradation of the Cdc25A protein phosphatase. Genes Dev 17:3062-74.

167. Jones, D. L., and K. Munger. 1997. Analysis of the p53-mediated G1 growth arrest pathway in cells expressing the human papillomavirus type 16 E7 oncoprotein. J Virol 71:2905-12.

168. Jurvansuu, J., K. Raj, A. Stasiak, and P. Beard. 2005. Viral transport of DNA damage that mimics a stalled replication fork. J Virol 79:569-80.

169. Kamura, T., D. M. Koepp, M. N. Conrad, D. Skowyra, R. J. Moreland, O. Iliopoulos, W. S. Lane, W. G. Kaelin, Jr., S. J. Elledge, R. C. Conaway, J. W. Harper, and J. W. Conaway. 1999. Rbx1, a component of the VHL tumor suppressor complex and SCF ubiquitin ligase. Science 284:657-61.

170. Kamura, T., K. Maenaka, S. Kotoshiba, M. Matsumoto, D. Kohda, R. C. Conaway, J. W. Conaway, and K. I. Nakayama. 2004. VHL-box and

SOCS-box domains determine binding specificity for Cul2-Rbx1 and Cul5-Rbx2 modules of ubiquitin ligases. Genes & Dev. 18:3055-3065.

171. Kannouche, P. L., J. Wing, and A. R. Lehmann. 2004. Interaction of the human DNA polymerase eta with monoubiquitinated PCNA: A possible mechanism for the polymerase switch in response to DNA damage. Mol. Cell 14:491-500.

172. Kanu, N., and A. Behrens. 2007. ATMIN defines an NBS1-independent pathway of ATM signalling. EMBO J 26:2933-41.

173. Kao, C. C., P. R. Yew, and A. J. Berk. 1990. Domains required for in vitro association between the cellular p53 and the adenovirus 2 E1B 55K proteins. Virology 179:806-14.

174. Kashishian, A., H. Douangpanya, D. Clark, S. T. Schlachter, C. T. Eary, J. G. Schiro, H. Huang, L. E. Burgess, E. A. Kesicki, and J. Halbrook. 2003. DNA-dependent protein kinase inhibitors as drug candidates for the treatment of cancer. Mol Cancer Ther 2:1257-64.

175. Kastan, M. B., and J. Bartek. 2004. Cell-cycle checkpoints and cancer. Nature 432:316-23.

176. Kerscher, O., R. Felberbaum, and M. Hochstrasser. 2006. Modification of proteins by ubiquitin and ubiquitin-like proteins. Annu Rev Cell Dev Biol 22:159-80.

177. Kim, J. S., T. B. Krasieva, H. Kurumizaka, D. J. Chen, A. M. Taylor, and K. Yokomori. 2005. Independent and sequential recruitment of NHEJ and HR factors to DNA damage sites in mammalian cells. J Cell Biol 170:341-7.

178. Kim, S. T., D. S. Lim, C. E. Canman, and M. B. Kastan. 1999. Substrate specificities and identification of putative substrates of ATM kinase family members. J Biol Chem 274:37538-43.

179. Kindsmuller, K., P. Groitl, B. Hartl, P. Blanchette, J. Hauber, and T. Dobner. 2007. Intranuclear targeting and nuclear export of the adenovirus E1B-55K protein are regulated by SUMO1 conjugation. Proc Natl Acad Sci U S A 104:6684-9.

180. Kolas, N. K., J. R. Chapman, S. Nakada, J. Ylanko, R. Chahwan, F. D. Sweeney, S. Panier, M. Mendez, J. Wildenhain, T. M. Thomson, L. Pelletier, S. P. Jackson, and D. Durocher. 2007. Orchestration of the DNA-damage response by the RNF8 ubiquitin ligase. Science 318:1637-40.

181. Konig, C., J. Roth, and M. Dobbelstein. 1999. Adenovirus type 5 E4orf3 protein relieves p53 inhibition by E1B-55-kilodalton protein. J Virol 73:2253-62.

182. Kopito, R. R. 2000. Aggresomes, inclusion bodies and protein aggregation. Trends Cell Biol 10:524-30.

183. Kozlov, S. V., M. E. Graham, C. Peng, P. Chen, P. J. Robinson, and M. F. Lavin. 2006. Involvement of novel autophosphorylation sites in ATM activation. EMBO J 25:3504-14.

184. Kratzer, F., O. Rosorius, P. Heger, N. Hirschmann, T. Dobner, J. Hauber, and R. H. Stauber. 2000. The adenovirus type 5 E1B-55K oncoprotein is a highly active shuttle protein and shuttling is independent of E4orf6, p53 and Mdm2. Oncogene 19:850-857.

185. Kudoh, A., M. Fujita, L. Zhang, N. Shirata, T. Daikoku, Y. Sugaya, H. Isomura, Y. Nishiyama, and T. Tsurumi. 2005. Epstein-Barr virus lytic replication elicits ATM checkpoint signal transduction while providing an S-phase-like cellular environment. J Biol Chem 280:8156-63.

186. Kumagai, A., and W. G. Dunphy. 2000. Claspin, a novel protein required for the activation of Chk1 during a DNA replication checkpoint response in Xenopus egg extracts. Mol Cell 6:839-49.

187. Kumagai, A., S. M. Kim, and W. G. Dunphy. 2004. Claspin and the activated form of ATR-ATRIP collaborate in the activation of Chk1. J Biol Chem 279:49599-608.

188. Kumagai, A., J. Lee, H. Y. Yoo, and W. G. Dunphy. 2006. TopBP1 activates the ATR-ATRIP complex. Cell 124:943-55.

189. Lai, M., E. S. Zimmerman, V. Planelles, and J. Chen. 2005. Activation of the ATR pathway by human immunodeficiency virus type 1 Vpr involves its direct binding to chromatin in vivo. J Virol 79:15443-51.

190. Lallemand-Breitenbach, V., M. Jeanne, S. Benhenda, R. Nasr, M. Lei, L. Peres, J. Zhou, J. Zhu, B. Raught, and H. de The. 2008. Arsenic degrades PML or PML-RARalpha through a SUMO-triggered RNF4/ubiquitin-mediated pathway. Nat Cell Biol 10:547-55.

191. Lane, D. P., and L. V. Crawford. 1979. T antigen is bound to a host protein in SV40-transformed cells. Nature 278:261-3.

192. Lanson, N. A., Jr., D. B. Egeland, B. A. Royals, and W. C. Claycomb. 2000. The MRE11-NBS1-RAD50 pathway is perturbed in SV40 large T antigen-immortalized AT-1, AT-2 and HL-1 cardiomyocytes. Nucleic Acids Res 28:2882-92.

193. Lau, A., R. Kanaar, S. P. Jackson, and M. J. O'Connor. 2004. Suppression of retroviral infection by the RAD52 DNA repair protein. EMBO J 23:3421-9.

194. Lau, A., K. M. Swinbank, P. S. Ahmed, D. L. Taylor, S. P. Jackson, G. C. Smith, and M. J. O'Connor. 2005. Suppression of HIV-1 infection by a small molecule inhibitor of the ATM kinase. Nat Cell Biol 7:493-500.

195. Lee, J. H., and T. T. Paull. 2007. Activation and regulation of ATM kinase activity in response to DNA double-strand breaks. Oncogene 26:7741-8.

196. Lee, J. H., and T. T. Paull. 2005. ATM activation by DNA double-strand breaks through the Mre11-Rad50-Nbs1 complex. Science 308:551-4.

197. Lee, J. H., and T. T. Paull. 2004. Direct activation of the ATM protein kinase by the Mre11/Rad50/Nbs1 complex. Science 304:93-6.

198. Leppard, K. N., and T. Shenk. 1989. The adenovirus E1B 55 kd protein influences mRNA transport via an intranuclear effect on RNA metabolism. EMBO J 8:2329-36.

199. Lethbridge, K. J., G. E. Scott, and K. N. Leppard. 2003. Nuclear matrix localization and SUMO-1 modification of adenovirus type 5 E1b 55K protein are controlled by E4 Orf6 protein. J Gen Virol 84:259-68.

200. Lieber, M. R. 2008. The mechanism of human nonhomologous DNA end joining. J Biol Chem 283:1-5.

201. Lieber, M. R., Y. Ma, U. Pannicke, and K. Schwarz. 2004. The mechanism of vertebrate nonhomologous DNA end joining and its role in V(D)J recombination. DNA Repair (Amst) 3:817-26.

202. Lilley, C. E., C. T. Carson, A. R. Muotri, F. H. Gage, and M. D. Weitzman. 2005. DNA repair proteins affect the lifecycle of herpes simplex virus 1. Proc. Natl. Acad. Sci. USA 102:5844-5849.

203. Lilley, C. E., R. A. Schwartz, and M. D. Weitzman. 2007. Using or abusing: viruses and the cellular DNA damage response. Trends Microbiol 15:119-26.

204. Lim, D. S., S. T. Kim, B. Xu, R. S. Maser, J. Lin, J. H. Petrini, and M. B. Kastan. 2000. ATM phosphorylates p95/nbs1 in an S-phase checkpoint pathway. Nature 404:613-617.

205. Limbo, O., C. Chahwan, Y. Yamada, R. A. de Bruin, C. Wittenberg, and P. Russell. 2007. Ctp1 is a cell-cycle-regulated protein that functions with Mre11 complex to control double-strand break repair by homologous recombination. Mol Cell 28:134-46.

206. Lin, J., J. Chen, B. Elenbaas, and A. J. Levine. 1994. Several hydrophobic amino acids in the p53 amino-terminal domain are required for transcriptional activation, binding to mdm-2 and the adenovirus 5 E1B 55-kD protein. Genes Dev 8:1235-46.

207. Linzer, D. I., and A. J. Levine. 1979. Characterization of a 54K dalton cellular SV40 tumor antigen present in SV40-transformed cells and uninfected embryonal carcinoma cells. Cell 17:43-52.

208. Liu, B., P. T. Sarkis, K. Luo, Y. Yu, and X. F. Yu. 2005. Regulation of Apobec3F and human immunodeficiency virus type 1 Vif by Vif-Cul5-ElonB/C E3 ubiquitin ligase. J Virol 79:9579-87.

209. Liu, H., J. H. Naismith, and R. T. Hay. 2003. Adenovirus DNA replication. Curr Top Microbiol Immunol 272:131-64.

210. Liu, Y., A. Shevchenko, A. Shevchenko, and A. J. Berk. 2005. Adenovirus exploits the cellular aggresome response to accelerate inactivation of the MRN complex. J Virol 79:14004-16.

211. Llorente, B., and L. S. Symington. 2004. The Mre11 nuclease is not required for 5' to 3' resection at multiple HO-induced double-strand breaks. Mol Cell Biol 24:9682-94.

212. Lobachev, K., E. Vitriol, J. Stemple, M. A. Resnick, and K. Bloom. 2004. Chromosome fragmentation after induction of a double-strand break is an active process prevented by the RMX repair complex. Curr Biol 14:2107-12.

213. Lobachev, K. S., D. A. Gordenin, and M. A. Resnick. 2002. The Mre11 complex is required for repair of hairpin-capped double-strand breaks and prevention of chromosome rearrangements. Cell 108:183-93.

214. Lou, Z., K. Minter-Dykhouse, S. Franco, M. Gostissa, M. A. Rivera, A. Celeste, J. P. Manis, J. van Deursen, A. Nussenzweig, T. T. Paull, F. W. Alt, and J. Chen. 2006. MDC1 maintains genomic stability by participating in the amplification of ATM-dependent DNA damage signals. Mol Cell 21:187-200.

215. Lowe, S. W., and H. E. Ruley. 1993. Stabilization of the p53 tumor suppressor is induced by adenovirus 5 E1A and accompanies apoptosis. Genes Dev 7:535-45.

216. Lukas, C., F. Melander, M. Stucki, J. Falck, S. Bekker-Jensen, M. Goldberg, Y. Lerenthal, S. P. Jackson, J. Bartek, and J. Lukas. 2004. Mdc1 couples DNA double-strand break recognition by Nbs1 with its H2AX-dependent chromatin retention. EMBO J 23:2674-83.

217. Luo, G., M. S. Yao, C. F. Bender, M. Mills, A. R. Bladl, A. Bradley, and J. H. Petrini. 1999. Disruption of *mRad50* causes embryonic stem cell lethality, abnormal embryonic development, and sensitivity to ionizing radiation. Proc. Natl. Acad. Sci. USA 96:7376-7381.

218. Luo, K., E. Ehrlich, Z. Xiao, W. Zhang, G. Ketner, and X. F. Yu. 2007. Adenovirus E4orf6 assembles with Cullin5-ElonginB-ElonginC E3 ubiquitin ligase through an HIV/SIV Vif-like BC-box to regulate p53. Faseb J 21:1742-50.

219. Luo, M. H., K. Rosenke, K. Czornak, and E. A. Fortunato. 2007. Human cytomegalovirus disrupts both ataxia telangiectasia mutated protein (ATM)- and ATM-Rad3-related kinase-mediated DNA damage responses during lytic infection. J Virol 81:1934-50.

220. Ma, Y., U. Pannicke, K. Schwarz, and M. R. Lieber. 2002. Hairpin opening and overhang processing by an artemis/DNA-dependent protein kinase complex in nonhomolgous end joining and V(D)J recombination. Cell 108:781-794.

221. Maheswaran, S., C. Englert, S. B. Lee, R. M. Ezzel, J. Settleman, and D. A. Haber. 1998. E1B 55K sequesters WT1 along with p53 within a cytoplasmic body in adenovirus-transformed kidney cells. Oncogene 16:2041-50.

222. Mahrour, N., W. B. Redwine, L. Florens, S. K. Swanson, S. Martin-Brown, W. D. Bradford, K. Staehling-Hampton, M. P. Washburn, R. C. Conaway, and J. W. Conaway. 2008. Characterization of Cullin-box sequences that direct recruitment of Cul2-Rbx1 and Cul5-Rbx2 modules to Elongin BC-based ubiquitin ligases. J Biol Chem 283:8005-13.

223. Mailand, N., S. Bekker-Jensen, H. Faustrup, F. Melander, J. Bartek, C. Lukas, and J. Lukas. 2007. RNF8 ubiquitylates histones at DNA double-strand breaks and promotes assembly of repair proteins. Cell 131:887-900.

224. Majka, J., S. K. Binz, M. S. Wold, and P. M. Burgers. 2006. Replication protein A directs loading of the DNA damage checkpoint clamp to 5'-DNA junctions. J Biol Chem 281:27855-61.

225. Mari, P. O., B. I. Florea, S. P. Persengiev, N. S. Verkaik, H. T. Bruggenwirth, M. Modesti, G. Giglia-Mari, K. Bezstarosti, J. A. Demmers, T. M. Luider, A. B. Houtsmuller, and D. C. van Gent. 2006. Dynamic assembly of end-joining complexes requires interaction

between Ku70/80 and XRCC4. Proc Natl Acad Sci U S A 103:18597-602.

226. Maser, R. S., O. K. Mirzoeva, J. Wells, H. Olivares, B. R. Williams, R. A. Zinkel, P. J. Farnham, and J. H. Petrini. 2001. Mre11 complex and DNA replication: linkage to E2F and sites of DNA synthesis. Mol Cell Biol 21:6006-16.

227. Maser, R. S., K. J. Monsen, B. E. Nelms, and J. H. Petrini. 1997. hMre11 and hRad50 nuclear foci are induced during the normal cellular response to DNA double-strand breaks. Mol. Cell Biol. 17:6087-6096.

228. Mathew, S. S., and E. Bridge. 2008. Nbs1-dependent binding of Mre11 to adenovirus E4 mutant viral DNA is important for inhibiting DNA replication. Virology 374:11-22.

229. Mathew, S. S., and E. Bridge. 2007. The cellular Mre11 protein interferes with adenovirus E4 mutant DNA replication. Virology 365:346-55.

230. Matsumoto, Y., N. Suzuki, N. Namba, N. Umeda, X. J. Ma, A. Morita, M. Tomita, A. Enomoto, S. Serizawa, K. Hirano, K. Sakaia, H. Yasuda, and Y. Hosoi. 2000. Cleavage and phosphorylation of XRCC4 protein induced by X-irradiation. FEBS Lett 478:67-71.

231. Matsuoka, S., B. A. Ballif, A. Smogorzewska, E. R. McDonald, 3rd, K. E. Hurov, J. Luo, C. E. Bakalarski, Z. Zhao, N. Solimini, Y. Lerenthal, Y. Shiloh, S. P. Gygi, and S. J. Elledge. 2007. ATM and ATR substrate analysis reveals extensive protein networks responsive to DNA damage. Science 316:1160-6.

232. McKee, A. H., and N. Kleckner. 1997. A general method for identifying recessive diploid-specific mutations in Saccharomyces cerevisiae, its application to the isolation of mutants blocked at intermediate stages of meiotic prophase and characterization of a new gene SAE2. Genetics 146:797-816.

233. Mehle, A., J. Goncalves, M. Santa-Maria, M. McPike, and D. Gabduza. 2004. Phophorylation of a novel SOCS-box regulates assembly of the

HIV-1 Vif-Cul5 complex that promotes APOBEC3G degradation. Genes & Dev. 18:2861-2866.

234. Miller, D. G., L. M. Petek, and D. W. Russell. 2004. Adeno-associated virus vectors integrate at chromosome breakage sites. Nat Genet 36:767-73.

235. Mirzoeva, O. K., and J. H. Petrini. 2001. DNA damage-dependent nuclear dynamics of the Mre11 complex. Mol. Cell. Biol. 21:281-288.

236. Mirzoeva, O. K., and J. H. Petrini. 2003. DNA replication-dependent nuclear dynamics of the Mre11 complex. Mol. Cancer Res. 1:207-218.

237. Moldovan, G. L., B. Pfander, and S. Jentsch. 2007. PCNA, the maestro of the replication fork. Cell 129:665-79.

238. Moore, M., N. Horikoshi, and T. Shenk. 1996. Oncogenic potential of the adenovirus E4orf6 protein. Proc Natl Acad Sci U S A 93:11295-301.

239. Moreau, S., J. R. Ferguson, and L. S. Symington. 1999. The nuclease activity of Mre11 is required for meiosis but not for mating type switching, end joining, or telomere maintenance. Mol Cell Biol 19:556-66.

240. Moshous, D., I. Callebaut, R. de Chasseval, B. Corneo, M. Cavazzana-Calvo, F. Le Deist, I. Tezcan, O. Sanal, Y. Bertrand, N. Philippe, A. Fischer, and J. P. de Villartay. 2001. Artemis, a novel DNA double-strand break repair/V(D)J recombination protein, is mutated in human severe combined immune deficiency. Cell 105:177-86.

241. Muzyczka, N., and K. I. Berns. 1997. Parvoviridae: The viruses and their replication, p. 2327-2357. *In* D. M. Knipe, P. M. Howley, and e. al. (ed.), Fields Virology, Fourth Edition. Lippincott Williams and Wilkins.

242. Myers, J. S., and D. Cortez. 2006. Rapid activation of ATR by ionizing radiation requires ATM and Mre11. J Biol Chem 281:9346-50.

243. Nakada, D., Y. Hirano, and K. Sugimoto. 2004. Requirement of the Mre11 complex and exonuclease 1 for activation of the Mec1 signaling pathway. Mol Cell Biol 24:10016-25.

244. Nakada, D., K. Matsumoto, and K. Sugimoto. 2003. ATM-related Tel1 associates with double-strand breaks through an Xrs2-dependent mechanism. Genes Dev 17:1957-62.

245. Nakai, H., T. A. Storm, S. Fuess, and M. A. Kay. 2003. Pathways of removal of free DNA vector ends in normal and DNA-PKcs-deficient SCID mouse hepatocytes transduced with rAAV vectors. Hum Gene Ther 14:871-81.

246. Narasimhan, D., R. Collaco, V. Kalman-Maltese, and J. P. Trempe. 2002. Hyper-phosphorylation of the adeno-associated virus Rep78 protein inhibits terminal repeat binding and helicase activity. Biochim Biophys Acta 1576:298-305.

247. Nash, K., W. Chen, W. F. McDonald, X. Zhou, and N. Muzyczka. 2007. Purification of host cell enzymes involved in adeno-associated virus DNA replication. J Virol 81:5777-87.

248. Nash, K., W. Chen, and N. Muzyczka. 2008. Complete in vitro reconstitution of adeno-associated virus DNA replication requires the minichromosome maintenance complex proteins. J Virol 82:1458-64.

249. Nayak, R., K. D. Farris, and D. J. Pintel. 2008. E4Orf6-E1B-55k-dependent degradation of de novo-generated adeno-associated virus type 5 Rep52 and capsid proteins employs a cullin 5-containing E3 ligase complex. J Virol 82:3803-8.

250. Nayak, R., and D. J. Pintel. 2007. Positive and negative effects of adenovirus type 5 helper functions on adeno-associated virus type 5 (AAV5) protein accumulation govern AAV5 virus production. J Virol 81:2205-12.

251. Nevels, M., S. Rubenwolf, T. Spruss, H. Wolf, and T. Dobner. 1997. The adenovirus E4orf6 protein can promote E1A/E1B-induced focus formation by interfering with p53 tumor suppressor function. Proc Natl Acad Sci U S A 94:1206-11.

252. Nevels, M., S. Rubenwolf, T. Spruss, H. Wolf, and T. Dobner. 2000. Two distinct activities contribute to the oncogenic potential of the adenovirus type 5 E4orf6 protein. J Virol 74:5168-81.

253. Nevels, M., B. Tauber, T. Spruss, H. Wolf, and T. Dobner. 2001. "Hit-and-run" transformation by adenovirus oncogenes. J Virol 75:3089-94.

254. Nghiem, P., P. K. Park, Y. Kim, C. Vaziri, and S. L. Schreiber. 2001. ATR inhibition selectively sensitizes G1 checkpoint-deficient cells to lethal premature chromatin condensation. Proc Natl Acad Sci U S A 98:9092-7.

255. Ni, T. H., W. F. McDonald, I. Zolotukhin, T. Melendy, S. Waga, B. Stillman, and N. Muzyczka. 1998. Cellular proteins required for adeno-associated virus DNA replication in the absence of adenovirus coinfection. J. Virol. 72:2777-2787.

256. Niewolik, D., U. Pannicke, H. Lu, Y. Ma, L. C. Wang, P. Kulesza, E. Zandi, M. R. Lieber, and K. Schwarz. 2006. DNA-PKcs dependence of Artemis endonucleolytic activity, differences between hairpins and 5' or 3' overhangs. J Biol Chem 281:33900-9.

257. Nijman, S. M., M. P. Luna-Vargas, A. Velds, T. R. Brummelkamp, A. M. Dirac, T. K. Sixma, and R. Bernards. 2005. A genomic and functional inventory of deubiquitinating enzymes. Cell 123:773-86.

258. Noureddine, M. A., T. D. Donaldson, S. A. Thacker, and R. J. Duronio. 2002. Drosophila Roc1a encodes a RING-H2 protein with a unique function in processing the Hh signal transducer Ci by the SCF E3 ubiquitin ligase. Dev Cell 2:757-70.

259. O'Driscoll, M., V. L. Ruiz-Perez, C. G. Woods, P. A. Jeggo, and J. A. Goodship. 2003. A splicing mutation affecting expression of ataxia-telangiectasia and Rad3-related protein (ATR) results in Seckel syndrome. Nat Genet 33:497-501.

260. Ohta, T., J. J. Michel, A. J. Schottelius, and Y. Xiong. 1999. ROC1, a homolog of APC11, represents a family of cullin partners with an associated ubiquitin ligase activity. Mol Cell 3:535-41.

261. Okubo, E., J. M. Lehman, and T. D. Friedrich. 2003. Negative regulation of mitotic promoting factor by the checkpoint kinase chk1 in simian virus 40 lytic infection. J Virol 77:1257-67.

262. Olson, E., C. J. Nievera, A. Y. Lee, L. Chen, and X. Wu. 2007. The Mre11-Rad50-Nbs1 complex acts both upstream and downstream of ataxia telangiectasia mutated and Rad3-related protein (ATR) to regulate the S-phase checkpoint following UV treatment. J Biol Chem 282:22939-52.

263. Orlando, J. S., and D. A. Ornelles. 1999. An arginine-faced amphipathic alpha helix is required for adenovirus type 5 e4orf6 protein function. J Virol 73:4600-10.

264. Orlando, J. S., and D. A. Ornelles. 2002. E4orf6 variants with separate abilities to augment adenovirus replication and direct nuclear localization of the E1B 55-kilodalton protein. J Virol 76:1475-87.

265. Ornelles, D. A., and T. Shenk. 1991. Localization of the adenovirus early region 1B 55-kilodalton protein during lytic infection: association with nuclear viral inclusions requires the early region 4 34-kilodalton protein. J Virol 65:424-9.

266. Parkinson, J., S. P. Lees-Miller, and R. D. Everett. 1999. Herpes simplex virus type 1 immediate-early protein vmw110 induces the proteasome-dependent degradation of the catalytic subunit of DNA-dependent protein kinase. J Virol 73:650-7.

267. Paull, T. T., and M. Gellert. 1999. Nbs1 potentiates ATP-driven DNA unwinding and endonuclease cleavage by the Mre11/Rad50 complex. Genes Dev 13:1276-88.

268. Paull, T. T., and M. Gellert. 1998. The 3' to 5' exonuclease activity of Mre 11 facilitates repair of DNA double-strand breaks. Mol Cell 1:969-79.

269. Pellegrini, M., A. Celeste, S. Difilippantonio, R. Guo, W. Wang, L. Feigenbaum, and A. Nussenzweig. 2006. Autophosphorylation at serine 1987 is dispensable for murine Atm activation in vivo. Nature 443:222-5.

270. Petrini, J. H., R. S. Maser, and D. A. Bressan. 2001. The MRE11-RAD50 complex: Diverse functions in the cellular DNA damage response. *In* J. A. Nickoloff and M. F. Hoekstra (ed.), DNA Damage and

Repair, Vol 3: Advances from Phage to Humans, vol. 3. Humana Press Inc.

271. Petrini, J. H., and T. H. Stracker. 2003. The cellular response to DNA double-strand breaks: defining the sensors and mediators. Trends Cell Biol 13:458-62.

272. Petroski, M. D., and R. J. Deshaies. 2005. Function and regulation of cullin-RING ubiquitin ligases. Nat Rev Mol Cell Biol 6:9-20.

273. Pfander, B., G. L. Moldovan, M. Sacher, C. Hoege, and S. Jentsch. 2005. SUMO-modified PCNA recruits Srs2 to prevent recombination during S phase. Nature 436:428-433.

274. Pilder, S., M. Moore, J. Logan, and T. Shenk. 1986. The adenovirus E1B-55K transforming polypeptide modulates transport or cytoplasmic stabilization of viral and host cell mRNAs. Mol Cell Biol 6:470-6.

275. Plans, V., J. Scheper, M. Soler, N. Loukili, Y. Okano, and T. M. Thomson. 2006. The RING finger protein RNF8 recruits UBC13 for lysine 63-based self polyubiquitylation. J Cell Biochem 97:572-82.

276. Pombo, A., J. Ferreira, E. Bridge, and M. Carmo-Fonseca. 1994. Adenovirus replication and transcription sites are spatially separated in the nucleus of infected cells. Embo J 13:5075-85.

277. Prinz, S., A. Amon, and F. Klein. 1997. Isolation of COM1, a new gene required to complete meiotic double-strand break-induced recombination in Saccharomyces cerevisiae. Genetics 146:781-95.

278. Prudden, J., S. Pebernard, G. Raffa, D. A. Slavin, J. J. Perry, J. A. Tainer, C. H. McGowan, and M. N. Boddy. 2007. SUMO-targeted ubiquitin ligases in genome stability. Embo J 26:4089-101.

279. Punga, T., and G. Akusjarvi. 2000. The adenovirus-2 E1B-55K protein interacts with a mSin3A/histone deacetylase 1 complex. FEBS Letters 476:248-252.

280. Qing, K., X. S. Wang, D. M. Kube, S. Ponnazhagan, A. Bajpai, and A. Srivastava. 1997. Role of tyrosine phosphorylation of a cellular protein

in adeno-associated virus 2-mediated transgene expression. Proc. Natl. Acad. Sci. USA 94:10879-10884.

281. Querido, E., P. Blanchette, Q. Yan, T. Kamura, M. Morrison, D. Boivin, W. G. Kaelin, R. C. Conaway, J. W. Conaway, and P. E. Branton. 2001. Degradation of p53 by adenovirus E4orf6 and E1B55K proteins occurs via a novel mechanism involving a cullin-containing complex. Genes & Dev. 15:3104-3117.

282. Querido, E., R. C. Marcellus, A. Lai, R. Charbonneau, J. G. Teodoro, G. Ketner, and P. E. Branton. 1997. Regulation of p53 levels by the E1B 55-kilodalton protein and E4orf6 in adenovirus-infected cells. J. Virol. 71:3788-3798.

283. Querido, E., M. R. Morrison, H. Chu-Pham-Dang, S. W. Thirlwell, D. Boivin, and P. E. Branton. 2001. Identification of three functions of the adenovirus e4orf6 protein that mediate p53 degradation by the E4orf6-E1B55K complex. J Virol 75:699-709.

284. Raj, K., P. Ogston, and P. Beard. 2001. Virus-mediated killing of cells that lack p53 activity. Nature 412:914-7.

285. Rao, L., M. Debbas, P. Sabbatini, D. Hockenbery, S. Korsmeyer, and E. White. 1992. The adenovirus E1A proteins induce apoptosis, which is inhibited by the E1B 19-kDa and Bcl-2 proteins. Proc Natl Acad Sci U S A 89:7742-6.

286. Riballo, E., M. Kuhne, N. Rief, A. Doherty, G. C. Smith, M. J. Recio, C. Reis, K. Dahm, A. Fricke, A. Krempler, A. R. Parker, S. P. Jackson, A. Gennery, P. A. Jeggo, and M. Lobrich. 2004. A pathway of double-strand break rejoining dependent upon ATM, Artemis, and proteins locating to gamma-H2AX foci. Mol Cell 16:715-24.

287. Richardson, C., N. Horikoshi, and T. K. Pandita. 2004. The role of the DNA double-strand break response network in meiosis. DNA Repair (Amst) 3:1149-64.

288. Robinett, C. C., A. Straight, G. Li, C. Willhelm, G. Sudlow, A. Murray, and A. S. Belmont. 1996. In vivo localization of DNA sequences and

visualization of large-scale chromatin organization using lac operator/repressor recognition. J Cell Biol 135:1685-700.

289. Rogakou, E. P., C. Boon, C. Redon, and W. M. Bonner. 1999. Megabase chromatin domains involved in DNA double-strand breaks in vivo. J Cell Biol 146:905-16.

290. Rogakou, E. P., D. R. Pilch, A. H. Orr, V. S. Ivanova, and W. M. Bonner. 1998. DNA double-stranded breaks induce histone H2AX phosphorylation on serine 139. J Biol Chem 273:5858-68.

291. Roshal, M., B. Kim, Y. Zhu, P. Nghiem, and V. Planelles. 2003. Activation of the ATR-mediated DNA damage response by the HIV-1 viral protein R. J Biol Chem 278:25879-86.

292. Roth, J., C. Konig, S. Wienzek, S. Weigel, S. Ristea, and M. Dobbelstein. 1998. Inactivation of p53 but not p73 by adenovirus type 5 E1B 55-kilodalton and E4 34-kilodalton oncoproteins. J Virol 72:8510-6.

293. Rouse, J., and S. P. Jackson. 2002. Interfaces between the detection, signaling, and repair of DNA damage. Science 297:547-51.

294. Rubenwolf, S., H. Schutt, M. Nevels, H. Wolf, and T. Dobner. 1997. Structural analysis of the adenovirus type 5 E1B 55-kilodalton-E4orf6 protein complex. J Virol 71:1115-23.

295. Russell, D. W., I. E. Alexander, and A. D. Miller. 1995. DNA synthesis and topoisomerase inhibitors increase transduction by adeno-associated virus vectors. Proc. Natl. Acad. Sci. USA 92:5719-5723.

296. Samulski, R. J., and T. Shenk. 1988. Adenovirus E1B 55-Mr polypeptide facilitates timely cytoplasmic accumulation of adeno-associated virus mRNAs. J Virol 62:206-10.

297. Sancar, A., L. A. Lindsey-Boltz, K. Unsal-Kacmaz, and S. Linn. 2004. Molecular mechanisms of mammalian DNA repair and the DNA damage checkpoints. Annu Rev Biochem 73:39-85.

298. Sanlioglu, S., P. Benson, and J. F. Engelhardt. 2000. Loss of ATM function enhances recombinant adeno-associated virus transduction

and integration through pathways similar to UV irradiation. Virology 268:68-78.

299. Sanlioglu, S., M. M. Monick, G. Luleci, G. W. Hunninghake, and J. F. Engelhardt. 2001. Rate limiting steps of AAV transduction and implications for human gene therapy. Curr Gene Ther 1:137-47.

300. Sarkaria, J. N., E. C. Busby, R. S. Tibbetts, P. Roos, Y. Taya, L. M. Karnitz, and R. T. Abraham. 1999. Inhibition of ATM and ATR kinase activities by the radiosensitizing agent, caffeine. Cancer Res 59:4375-82.

301. Sarkaria, J. N., R. S. Tibbetts, E. C. Busby, A. P. Kennedy, D. E. Hill, and R. T. Abraham. 1998. Inhibition of phosphoinositide 3-kinase related kinases by the radiosensitizing agent wortmannin. Cancer Res 58:4375-82.

302. Sarnow, P., P. Hearing, C. W. Anderson, D. N. Halbert, T. Shenk, and A. J. Levine. 1984. Adenovirus early region 1B 58,000-dalton tumor antigen is physically associated with an early region 4 25,000-dalton protein in productively infected cells. J Virol 49:692-700.

303. Sartori, A. A., C. Lukas, J. Coates, M. Mistrik, S. Fu, J. Bartek, R. Baer, J. Lukas, and S. P. Jackson. 2007. Human CtIP promotes DNA end resection. Nature 450:509-14.

304. Scheffner, M., J. M. Huibregtse, R. D. Vierstra, and P. M. Howley. 1993. The HPV-16 E6 and E6-AP complex functions as a ubiquitin-protein ligase in the ubiquitination of p53. Cell 75:495-505.

305. Scheffner, M., B. A. Werness, J. M. Huibregtse, A. J. Levine, and P. M. Howley. 1990. The E6 oncoprotein encoded by human papillomavirus types 16 and 18 promotes the degradation of p53. Cell 63:1129-36.

306. Schnepp, B. C., K. R. Clark, D. L. Klemanski, C. A. Pacak, and P. R. Johnson. 2003. Genetic fate of recombinant adeno-associated virus vector genomes in muscle. J Virol 77:3495-504.

307. Schrofelbauer, B., Q. Yu, S. G. Zeitlin, and N. R. Landau. 2005. Human immunodeficiency virus type 1 Vpr induces the degradation of the UNG and SMUG uracil-DNA glycosylases. J Virol 79:10978-87.

308. Schwartz, R. A., J. A. Palacios, G. D. Cassell, S. Adam, M. Giacca, and M. D. Weitzman. 2007. The Mre11/Rad50/Nbs1 complex limits adeno-associated virus transduction and replication. J Virol 81:12936-45.

309. Serrano, M., A. W. Lin, M. E. McCurrach, D. Beach, and S. W. Lowe. 1997. Oncogenic ras provokes premature cell senescence associated with accumulation of p53 and p16INK4a. Cell 88:593-602.

310. Shackelford, J., and J. S. Pagano. 2005. Targeting of host-cell ubiquitin pathways by viruses. Essays Biochem 41:139-56.

311. Shechter, D., V. Costanzo, and J. Gautier. 2004. Regulation of DNA replication by ATR: signaling in response to DNA intermediates. DNA Repair (Amst) 3:901-8.

312. Shen, Y., G. Kitzes, J. A. Nye, A. Fattaey, and T. Hermiston. 2001. Analysis of single-amino-acid substitution mutants of adenovirus type 5 E1B-55K protein. J. Virol. 75:4297-4307.

313. Shenk, T. 1996. Adenoviridae: The viruses and their replication, p. 2111-2147. *In* B. N. Fields, D. M. Knipe, P. M. Howley, and e. al. (ed.), Fields Virology, Third Edition. Lippincott-Raven Publishers.

314. Shepard, R. N., and D. A. Ornelles. 2004. Diverse roles for E4orf3 at late times of infection revealed in an E1B 55-kilodalton protein mutant background. J Virol 78:9924-35.

315. Shepard, R. N., and D. A. Ornelles. 2003. E4orf3 is necessary for enhanced S-phase replication of cell cycle-restricted subgroup C adenoviruses. J Virol 77:8593-5.

316. Shi, Y., G. E. Dodson, P. S. Mukhopadhyay, N. P. Shanware, A. T. Trinh, and R. S. Tibbetts. 2007. Identification of carboxyl-terminal MCM3 phosphorylation sites using polyreactive phosphospecific antibodies. J Biol Chem 282:9236-43.

317. Shi, Y., G. E. Dodson, S. Shaikh, K. Rundell, and R. S. Tibbetts. 2005. Ataxia-telangiectasia-mutated (ATM) is a T-antigen kinase that controls SV40 viral replication in vivo. J Biol Chem 280:40195-200.

318. Shin, D. S., C. Chahwan, J. L. Huffman, and J. A. Tainer. 2004. Structure and function of the double-strand break repair machinery. DNA Repair (Amst) 3:863-73.

319. Shirata, N., A. Kudoh, T. Daikoku, Y. Tatsumi, M. Fujita, T. Kiyono, Y. Sugaya, H. Isomura, K. Ishizaki, and T. Tsurumi. 2005. Activation of ataxia telangiectasia-mutated DNA damage checkpoint signal transduction elicited by herpes simplex virus infection. J Biol Chem 280:30336-41.

320. Shrivastav, M., L. P. De Haro, and J. A. Nickoloff. 2008. Regulation of DNA double-strand break repair pathway choice. Cell Res 18:134-47.

321. Simmons, D. T. 2000. SV40 large T antigen functions in DNA replication and transformation. Adv Virus Res 55:75-134.

322. Sinclair, A., S. Yarranton, and C. Schelcher. 2006. DNA-damage response pathways triggered by viral replication. Expert Rev Mol Med 8:1-11.

323. Skalka, A. M., and R. A. Katz. 2005. Retroviral DNA integration and the DNA damage response. Cell Death Differ 12 Suppl 1:971-8.

324. Skinner, G. R. 1976. Transformation of primary hamster embryo fibroblasts by type 2 simplex virus: evidence for a "hit and run" mechanism. Br J Exp Pathol 57:361-76.

325. Song, S., P. J. Laipis, K. I. Berns, and T. R. Flotte. 2001. Effect of DNA-dependent protein kinase on the molecular fate of the rAAV2 genome in skeletal muscle. Proc Natl Acad Sci U S A 98:4084-8.

326. Song, S., Y. Lu, Y. K. Choi, Y. Han, Q. Tang, G. Zhao, K. I. Berns, and T. R. Flotte. 2004. DNA-dependent PK inhibits adeno-associated virus DNA integration. Proc Natl Acad Sci U S A 101:2112-6.

327. Spagnolo, L., A. Rivera-Calzada, L. H. Pearl, and O. Llorca. 2006. Three-dimensional structure of the human DNA-PKcs/Ku70/Ku80 complex assembled on DNA and its implications for DNA DSB repair. Mol Cell 22:511-9.

328. Stebbins, C. E., W. G. Kaelin, Jr., and N. P. Pavletich. 1999. Structure of the VHL-ElonginC-ElonginB complex: implications for VHL tumor suppressor function. Science 284:455-61.

329. Steegenga, W. T., N. Riteco, A. G. Jochemsen, F. J. Fallaux, and J. L. Bos. 1998. The large E1B protein together with the E4orf6 protein target p53 for active degradation in adenovirus infected cells. Oncogene 16:349-357.

330. Stewart, G. S., R. S. Maser, T. Stankovic, D. A. Bressan, M. I. Kaplan, N. G. Jaspers, A. Raams, P. J. Byrd, J. H. Petrini, and A. M. Taylor. 1999. The DNA double-strand break repair gene hMRE11 is mutated in individuals with an ataxia-telangiectasia-like disorder. Cell 99:577-87.

331. Stewart, G. S., B. Wang, C. R. Bignell, A. M. Taylor, and S. J. Elledge. 2003. MDC1 is a mediator of the mammalian DNA damage checkpoint. Nature 421:961-6.

332. Stiff, T., M. O'Driscoll, N. Rief, K. Iwabuchi, M. Lobrich, and P. A. Jeggo. 2004. ATM and DNA-PK function redundantly to phosphorylate H2AX after exposure to ionizing radiation. Cancer Res 64:2390-6.

333. Stiff, T., C. Reis, G. K. Alderton, L. Woodbine, M. O'Driscoll, and P. A. Jeggo. 2005. Nbs1 is required for ATR-dependent phosphorylation events. EMBO J 24:199-208.

334. Stiff, T., S. A. Walker, K. Cerosaletti, A. A. Goodarzi, E. Petermann, P. Concannon, M. O'Driscoll, and P. A. Jeggo. 2006. ATR-dependent phosphorylation and activation of ATM in response to UV treatment or replication fork stalling. Embo J 25:5775-82.

335. Stracker, T. H., C. T. Carson, and M. D. Weitzman. 2002. Adenovirus oncoproteins inactivate the Mre11-Rad50-NBS1 DNA repair complex. Nature 418:348-52.

336. Stracker, T. H., G. D. Cassell, P. Ward, Y. M. Loo, B. van Breukelen, S. D. Carrington-Lawrence, R. K. Hamatake, P. C. van der Vliet, S. K. Weller, T. Melendy, and M. D. Weitzman. 2004. The Rep protein of adeno-associated virus type 2 interacts with single-stranded DNA-binding proteins that enhance viral replication. J Virol 78:441-53.

337. Stracker, T. H., M. Morales, S. S. Couto, H. Hussein, and J. H. Petrini. 2007. The carboxy terminus of NBS1 is required for induction of apoptosis by the MRE11 complex. Nature 447:218-21.

338. Stracker, T. H., J. W. Theunissen, M. Morales, and J. H. Petrini. 2004. The Mre11 complex and the metabolism of chromosome breaks: the importance of communicating and holding things together. DNA Repair 3:845-854.

339. Sun, H., J. D. Leverson, and T. Hunter. 2007. Conserved function of RNF4 family proteins in eukaryotes: targeting a ubiquitin ligase to SUMOylated proteins. Embo J 26:4102-12.

340. Sung, P., and H. Klein. 2006. Mechanism of homologous recombination: mediators and helicases take on regulatory functions. Nat Rev Mol Cell Biol 7:739-50.

341. Symington, L. S. 2002. Role of *RAD52* epistasis group genes in homologous recombination and double-strand break repair. Microbiol. Mol. Biol. Rev. 66:630-670.

342. Tatham, M. H., M. C. Geoffroy, L. Shen, A. Plechanovova, N. Hattersley, E. G. Jaffray, J. J. Palvimo, and R. T. Hay. 2008. RNF4 is a poly-SUMO-specific E3 ubiquitin ligase required for arsenic-induced PML degradation. Nat Cell Biol 10:538-46.

343. Tauber, B., and T. Dobner. 2001. Molecular regulation and biological function of adenovirus early genes: the E4 ORFs. Gene 278:1-23.

344. Taylor, A. M., A. Groom, and P. J. Byrd. 2004. Ataxia-telangiectasia-like disorder (ATLD)-its clinical presentation and molecular basis. DNA Repair (Amst) 3:1219-25.

345. Taylor, T. J., and D. M. Knipe. 2004. Proteomics of herpes simplex virus replication compartments: association of cellular DNA replication, repair, recombination, and chromatin remodeling proteins with ICP8. J Virol 78:5856-66.

346. Teodoro, J. G., and P. E. Branton. 1997. Regulation of p53-dependent apoptosis, transcriptional repression, and cell transformation by phosphorylation of the 55-kilodalton E1B protein of human adenovirus type 5. J. Virol. 71:3620-3627.

347. Teodoro, J. G., T. Halliday, S. G. Whalen, D. Takayesu, F. L. Graham, and P. E. Branton. 1994. Phosphorylation at the carboxy terminus of the 55-kilodalton adenovirus type 5 E1B protein regulates transforming activity. J Virol 68:776-86.

348. Tomida, J., Y. Masuda, H. Hiroaki, T. Ishikawa, I. Song, T. Tsurimoto, S. Tateishi, T. Shiomi, Y. Kamei, J. Kim, K. Kamiya, C. Vaziri, H. Ohmori, and T. Todo. 2008. DNA Damage-induced Ubiquitylation of RFC2 Subunit of Replication Factor C Complex. J Biol Chem 283:9071-9079.

349. Uematsu, N., E. Weterings, K. Yano, K. Morotomi-Yano, B. Jakob, G. Taucher-Scholz, P. O. Mari, D. C. van Gent, B. P. Chen, and D. J. Chen. 2007. Autophosphorylation of DNA-PKCS regulates its dynamics at DNA double-strand breaks. J Cell Biol 177:219-29.

350. Usui, T., H. Ogawa, and J. H. Petrini. 2001. A DNA damage response pathway controlled by Tel1 and the Mre11 complex. Mol Cell 7:1255-66.

351. Uziel, T., Y. Lerenthal, L. Moyal, Y. Andegeko, L. Mittelman, and Y. Shiloh. 2003. Requirement of the MRN complex for ATM activation by DNA damage. EMBO J. 22:5612-5621.

352. Vassin, V. M., M. S. Wold, and J. A. Borowiec. 2004. Replication protein A (RPA) phosphorylation prevents RPA association with replication centers. Mol Cell Biol 24:1930-43.

353. Veuger, S. J., N. J. Curtin, G. C. Smith, and B. W. Durkacz. 2004. Effects of novel inhibitors of poly(ADP-ribose) polymerase-1 and the

DNA-dependent protein kinase on enzyme activities and DNA repair. Oncogene 23:7322-9.

354. Vo, A. T., F. Zhu, X. Wu, F. Yuan, Y. Gao, L. Gu, G. M. Li, T. H. Lee, and C. Her. 2005. hMRE11 deficiency leads to microsatellite instability and defective DNA mismatch repair. EMBO Rep 6:438-44.

355. Wang, B., and S. J. Elledge. 2007. Ubc13/Rnf8 ubiquitin ligases control foci formation of the Rap80/Abraxas/Brca1/Brcc36 complex in response to DNA damage. Proc Natl Acad Sci U S A 104:20759-63.

356. Wang, B., S. Matsuoka, P. B. Carpenter, and S. J. Elledge. 2002. 53BP1, a mediator of the DNA damage checkpoint. Science 298:1435-8.

357. Ward, P. 2006. Replication of adeno-associated virus DNA, p. 189-210. *In* J. R. Kerr, S. F. Cotmore, M. E. Bloom, L. R.M., and C. R. Parrish (ed.), Parvoviruses. Hodder Arnold.

358. Ward, P., M. Falkenberg, P. Elias, M. D. Weitzman, and R. M. Linden. 2001. Rep-dependent initiation of adeno-associated virus type 2 DNA replication by a herpes simplex virus type 1 replication complex in a reconstituted system. J Virol 75:10250-10258.

359. Weger, S., E. Hammer, and R. Heilbronn. 2004. SUMO-1 modification regulates the protein stability of the large regulatory protein Rep78 of adeno associated virus type 2 (AAV-2). Virology 330:284-94.

360. Weiden, M. D., and H. S. Ginsberg. 1994. Deletion of the E4 region of the genome produces adenovirus DNA concatemers. Proc. Natl. Acad. Sci. USA 91:153-157.

361. Weinberg, D. H., and G. Ketner. 1983. A cell line that supports the growth of a defective early region 4 deletion mutant of human adenovirus type 2. Proc Natl Acad Sci U S A 80:5383-6.

362. Weinberg, D. H., and G. Ketner. 1986. Adenoviral early region 4 is required for efficient viral DNA replication and for late gene expression. J Virol 57:833-8.

363. Weindler, F. W., and R. Heilbronn. 1991. A subset of herpes simplex virus replication genes provides helper function for productive adeno-associated virus replication. J. Virol. 65:2476-2483.

364. Weitzman, M. D. 2005. Functions of the adenovirus E4 proteins and their impact on viral vectors. Front Biosci 10:1106-17.

365. Weitzman, M. D., C. T. Carson, R. A. Schwartz, and C. E. Lilley. 2004. Interactions of viruses with the cellular DNA repair machinery. DNA Repair 3:1165-1173.

366. Weitzman, M. D., K. J. Fisher, and J. M. Wilson. 1996. Recruitment of wild-type and recombinant adeno-associated virus into adenovirus replication centers. J. Virol. 70:1845-1854.

367. Weitzman, M. D., and D. A. Ornelles. 2005. Inactivating intracellular antiviral responses during adenovirus infection. Oncogene 24:7686-96.

368. Weterings, E., and D. J. Chen. 2007. DNA-dependent protein kinase in nonhomologous end joining: a lock with multiple keys? J Cell Biol 179:183-6.

369. White, E., and R. Cipriani. 1990. Role of adenovirus E1B proteins in transformation: altered organization of intermediate filaments in transformed cells that express the 19-kilodalton protein. Mol Cell Biol 10:120-30.

370. Wienzek, S., J. Roth, and M. Dobbelstein. 2000. E1B 55-kilodalton oncoproteins of adenovirus types 5 and 12 inactivate and relocalize p53, but not p51 or p73, and cooperate with E4orf6 proteins to destabilize p53. J Virol 74:193-202.

371. Wilkinson, D. E., and S. K. Weller. 2006. Herpes simplex virus type I disrupts the ATR-dependent DNA-damage response during lytic infection. J Cell Sci 119:2695-703.

372. Wilkinson, D. E., and S. K. Weller. 2004. Recruitment of cellular recombination and repair proteins to sites of herpes simplex virus type 1 DNA replication is dependent on the composition of viral proteins

within prereplicative sites and correlates with the induction of the DNA damage response. J Virol 78:4783-96.

373. Williams, B. R., O. K. Mirzoeva, W. F. Morgan, J. Lin, W. Dunnick, and J. H. Petrini. 2002. A murine model of nijmegen breakage syndrome. Curr. Biol. 12:648-653.

374. Wiltzius, J. J., M. Hohl, J. C. Fleming, and J. H. Petrini. 2005. The Rad50 hook domain is a critical determinant of Mre11 complex functions. Nat Struct Mol Biol 12:403-7.

375. Wistuba, A., A. Kern, S. Weger, D. Grimm, and J. A. Kleinschmidt. 1997. Subcellular compartmentalization of adeno-associated virus type 2 assembly. J Virol 71:1341-52.

376. Wold, M. S., and T. Kelly. 1988. Purification and characterization of replication protein A, a cellular protein required for in vitro replication of simian virus 40 DNA. Proc Natl Acad Sci U S A 85:2523-7.

377. Wold, M. S., D. H. Weinberg, D. M. Virshup, J. J. Li, and T. J. Kelly. 1989. Identification of cellular proteins required for simian virus 40 DNA replication. J Biol Chem 264:2801-9.

378. Woo, J. L., and A. J. Berk. 2007. Adenovirus ubiquitin-protein ligase stimulates viral late mRNA nuclear export. J Virol 81:575-87.

379. Wu, X., D. Avni, T. Chiba, F. Yan, Q. Zhao, Y. Lin, H. Heng, and D. Livingston. 2004. SV40 T antigen interacts with Nbs1 to disrupt DNA replication control. Genes Dev 18:1305-16.

380. Wu, X., V. Ranganathan, D. S. Weisman, W. F. Heine, D. N. Ciccone, T. B. O'Neill, K. E. Crick, K. A. Pierce, W. S. Lane, G. Rathbun, D. M. Livingston, and D. T. Weaver. 2000. ATM phosphorylation of nijmegen breakage syndrome is required in a DNA damage response. Nature 405:477-482.

381. Wyman, C., D. Ristic, and R. Kanaar. 2004. Homologous recombination-mediated double-strand break repair. DNA Repair (Amst) 3:827-33.

382. Wyman, C., D. O. Warmerdam, and R. Kanaar. 2008. From DNA end chemistry to cell-cycle response: the importance of structure, even when it's broken. Mol Cell 30:5-6.

383. Xiao, X., J. Li, and R. J. Samulski. 1998. Production of high-titer recombinant adeno-associated virus vectors in the absence of helper adenovirus. J Virol 72:2224-32.

384. Xiao, Y., and D. T. Weaver. 1997. Conditional gene targeted deletion by cre recombinase demonstrates the requirement for the double-strand break repair Mre11 protein in murine embryonic stem cells. Nuc. Acids Res. 25:2985-2991.

385. Xie, Y., O. Kerscher, M. B. Kroetz, H. F. McConchie, P. Sung, and M. Hochstrasser. 2007. The yeast Hex3.Slx8 heterodimer is a ubiquitin ligase stimulated by substrate sumoylation. J Biol Chem 282:34176-84.

386. Xu, B., S. Kim, and M. B. Kastan. 2001. Involvement of Brca1 in S-phase and G(2)-phase checkpoints after ionizing irradiation. Mol Cell Biol 21:3445-50.

387. Xu, B., S. T. Kim, D. S. Lim, and M. B. Kastan. 2002. Two molecularly distinct G2/M checkpoints are induced by ionizing radiation. Mol. Cell Biol. 22:1049-1059.

388. Yalkinoglu, A. O., R. Heilbronn, A. Burkle, J. R. Schlehofer, and H. z. Hausen. 1988. DNA amplification of adeno-associated virus as a response to cellular genotoxic stress. Cancer Res. 48:3123-3129.

389. Yew, P. R., and A. J. Berk. 1992. Inhibition of p53 transactivation required for transformation by adenovirus early 1B protein. Nature 357:82-5.

390. Yew, P. R., C. C. Cheng, and A. J. Berk. 1990. Dissection of functional domains in the adenovirus 2 early 1B 55k polypeptide by suppressor-linker insertional mutagenesis. Virology 179:795-805.

391. Yew, P. R., X. Liu, and A. J. Berk. 1994. Adenovirus E1B oncoprotein tethers a transcriptional repression domain to p53. Genes Dev 8:190-202.

392. Yondola, M. A., and P. Hearing. 2007. The adenovirus E4 ORF3 protein binds and reorganizes the TRIM family member transcriptional intermediary factor 1 alpha. J Virol 81:4264-71.

393. Yoo, H. Y., A. Shevchenko, A. Shevchenko, and W. G. Dunphy. 2004. Mcm2 is a direct substrate of ATM and ATR during DNA damage and DNA replication checkpoint responses. J Biol Chem 279:53353-64.

394. Yoshizawa-Sugata, N., and H. Masai. 2007. Human Tim/Timeless-interacting protein, Tipin, is required for efficient progression of S phase and DNA replication checkpoint. J Biol Chem 282:2729-40.

395. You, Z., J. M. Bailis, S. A. Johnson, S. M. Dilworth, and T. Hunter. 2007. Rapid activation of ATM on DNA flanking double-strand breaks. Nat Cell Biol 9:1311-8.

396. You, Z., C. Chahwan, J. Bailis, T. Hunter, and P. Russell. 2005. ATM activation and its recruitment to damaged DNA require binding to the C terminus of Nbs1. Mol Cell Biol 25:5363-79.

397. Yu, X., Y. Yu, B. Liu, K. Luo, W. Kong, P. Mao, and X. F. Yu. 2003. Induction of APOBEC3G ubiquitination and degradation by an HIV-1 vif-cul5-SCF complex. Science 302:1056-1060.

398. Yu, Y., W. Wang, Q. Ding, R. Ye, D. Chen, D. Merkle, D. Schriemer, K. Meek, and S. P. Lees-Miller. 2003. DNA-PK phosphorylation sites in XRCC4 are not required for survival after radiation or for V(D)J recombination. DNA Repair (Amst) 2:1239-52.

399. Yu, Y., Z. Xiao, E. S. Ehrlich, X. Yu, and X. F. Yu. 2004. Selective assembly of HIV-1 Vif-Cul5-ElonginB-ElonginC E3 ubiquitin ligase complex through a novel SOCS box and upstream cysteines. Genes Dev 18:2867-72.

400. Zantema, A., J. A. Fransen, A. Davis-Olivier, F. C. Ramaekers, G. P. Vooijs, B. DeLeys, and A. J. Van der Eb. 1985. Localization of the E1B proteins of adenovirus 5 in transformed cells, as revealed by interaction with monoclonal antibodies. Virology 142:44-58.

401. Zentilin, L., A. Marcello, and M. Giacca. 2001. Involvement of cellular double-stranded DNA break binding proteins in processing of the recombinant adeno-associated virus genome. J. Virol. 75:12279-12287.

402. Zhang, X., J. Succi, Z. Feng, S. Prithivirajsingh, M. D. Story, and R. J. Legerski. 2004. Artemis is a phosphorylation target of ATM and ATR and is involved in the G2/M DNA damage checkpoint response. Mol Cell Biol 24:9207-20.

403. Zhang, Y. W., D. M. Otterness, G. G. Chiang, W. Xie, Y. C. Liu, F. Mercurio, and R. T. Abraham. 2005. Genotoxic stress targets human Chk1 for degradation by the ubiquitin-proteasome pathway. Mol Cell 19:607-18.

404. Zhao, L. Y., A. L. Colosimo, Y. Liu, Y. Wan, and D. Liao. 2003. Adenovirus E1B 55-kilodalton oncoprotein binds to Daxx and eliminates enhancement of p53-dependent transcription by Daxx. J. Virol. 77:11809-11821.

405. Zhao, S., Y. C. Weng, S. S. F. Yuan, Y. T. Lin, H. C. Hsu, S. C. J. Lin, E. Gerbino, M. h. Song, M. Z. Zdzienicka, R. A. Gatti, J. W. Shay, Y. Ziv, Y. Shiloh, and E. Y. H. P. Lee. 2000. Functional link between ataxia-telangiectasia and nijmegen breakage syndrome gene products. Nature 405:473-477.

406. Zhao, X., R. J. Madden-Fuentes, B. X. Lou, J. M. Pipas, J. Gerhardt, C. J. Rigell, and E. Fanning. 2008. Ataxia telangiectasia-mutated damage-signaling kinase- and proteasome-dependent destruction of Mre11-Rad50-Nbs1 subunits in Simian virus 40-infected primate cells. J Virol 82:5316-28.

407. Zheng, X., X. M. Rao, J. G. Gomez-Gutierrez, H. Hao, K. M. McMasters, and H. S. Zhou. 2008. Adenovirus E1B55K region is required to enhance cyclin E expression for efficient viral DNA replication. J Virol 82:3415-27.

408. Zhong, H., A. Bryson, M. Eckersdorff, and D. O. Ferguson. 2005. Rad50 depletion impacts upon ATR-dependent DNA damage repsonses. Human Molecular Genetics 14:2685-2693.

409. Zhu, J., S. Petersen, L. Tessarollo, and A. Nussenzweig. 2001. Targeted disruption of the Nijmegen breakage syndrome gene NBS1 leads to early embryonic lethality in mice. Curr Biol 11:105-9.

410. Ziv, Y., A. Bar-Shira, I. Pecker, P. Russell, T. J. Jorgensen, I. Tsarfati, and Y. Shiloh. 1997. Recombinant ATM protein complements the cellular A-T phenotype. Oncogene 15:159-67.

411. Zou, L. 2007. Single- and double-stranded DNA: building a trigger of ATR-mediated DNA damage response. Genes Dev 21:879-85.

412. Zou, L., and S. J. Elledge. 2003. Sensing DNA damage through ATRIP recognition of RPA-ssDNA complexes. Science 300:1542-8.

413. Zou, Y., Y. Liu, X. Wu, and S. M. Shell. 2006. Functions of human replication protein A (RPA): from DNA replication to DNA damage and stress responses. J Cell Physiol 208:267-73.